Probabilistic Seismic Hazard in New Mexico and Bordering Areas

by

Kuo-wan Lin

Submitted in Partial Fulfillment of

the Requirements for the Degree of

Doctor of Philosophy

New Mexico Institute of Mining and Technology

Socorro, New Mexico, 87801

November, 1999

Acknowledgements

I would like to thank my advisor, Allan Sanford, for his professional and private guidance. His extensive knowledge of the seismicity of New Mexico was crucial to the completion of the project. I thank him for patiently assisting my flawed English and sharing his views with me. Suggestions from my other committee members, Rick Aster, Dave Love, Larry Teufel, and Dave Johnson have improved this dissertation. I thank Hans Hartse for the use of his location program SEISMOS, which is the program for locating almost all earthquakes in this study. Special thanks to my wife, I-Ching Tsai. Without her, the completion of my dissertation would have been impossible. I thank my family in Taiwan for their continual support.

Table of Contents

Abstract 1

1. Introduction 3

2. Improving Regional Earthquake Locations Using a Modified G Matrix 6

Common Procedure for Earthquake Location 7

Modified G Matrix 8

Forward Modeling Plus Fuzzy Logic Approach 12

Distinctive Features 12

Quantifying uncertainties 12

Regrouping G matrix 12

Logic operations using fuzzy logic 13

Fuzzy Logic Approach 13

Earthquake Location Procedure for New Mexico 16

Problem Definition 16

Defining Fuzzy Sets 17

P-P travel time interval (PP) 17

S-S travel time interval (SS) 17

S-P travel time interval (SP) 19

Example Earthquakes 19

Felt Earthquake 19

Earthquake Swarm 31

Discussion 35

3. Catalog of Instrumentally Recorded Earthquakes for New Mexico and Bordering Areas 1962-1998 36

Magnitudes 36
Location Program 37
Velocity Model 37
Procedure for Refining Locations of Earthquakes 37
Initial Catalog 38
Final Catalog 38
Geographic Distribution of Earthquakes 40
Quality of Locations of Earthquakes 43
4. Probabilistic Seismic Hazards for New Mexico Using Instrumental Data 1962 - 1998 48
Earthquake Data 1962-1998 49
Magnitudes 49
Completeness of data 49
Temporal variations in activity 51
Removal of dependent events 51
Recurrence Relation 55
Probabilistic Ground Accelerations 59
Expected return intervals 61
Probability of occurrence 61
Ground acceleration footprints 61
Spatial probability of occurrence 63
Overall probability of occurrence 63
Probabilistic Seismic Hazard Maps 65
Seismic Risks 69
Comparisons of Hazard Estimates 72
5. Sensitivity Study of Probabilistic Seismic Hazard Estimates for

New Mexico 78
Completeness of Earthquake Data 1962-1998 79
Removal of Dependent Events 79
Deviations of the Maximum Likelihood Slope β 82
Maximum Magnitude Earthquake 89
Pre-instrumental Earthquake Data 1868-1961 92
Discussion 97
6. Effects of Active Faults on Probabilistic Seismic Hazard Estimates 101
Comparison of Recurrence Rates Based on Faults and Instrumental Data . . . 101
Effects of Active Faults on Estimates of Seismic Hazard- Socorro Seismic Anomaly 102
Identifiable Faults 105
Random Earthquakes on Hidden Faults 109
7. Summary and Conclusions 113
Fuzzy Logic Algorithm 113
Earthquake Catalogs for New Mexico and Bordering Areas 1962-1998 114
Probabilistic Seismic Hazard Map for New Mexico and Bordering Areas . . . 115
References 119
Appendix I Listings of Magnitude Differences Between New Mexico Tech and Contributing Institutes 125
Appendix II Earthquake Catalogs for New Mexico and Bordering Areas: 1962 through 1998; Moment Magnitude ≥ 2.0 136
Appendix III Magnitude - Peak Horizontal Ground Acceleration Relationship in Probabilistic Seismic Hazard Analysis 172
Appendix IV Published Abstracts 185

List of Figures

2.1. Schematic diagram for seismic stations S1 and S2 and the trial epicenter O. . . . 10

2.2. Travel distance curves for S-P, P-P, and S-S travel time intervals. 11

2.3. Comparisons of classic logic and fuzzy logic. 14

2.4. Results of P-P travel time interval between station CPRX and CL7. 15

2.5. Velocity models for mapping uncertainties in calculated wave velocities into logic space. 18

2.6. Geographical location of the Logan earthquake with respect to seismic networks in New Mexico. 21

2.7. Results of (a) P-P and (b) S-S travel time intervals between station CPRX and CL7 after mapping uncertainties in calculated velocities into logic space. . . . 22

2.8. Results of fuzzy logic operation (a) Union and (b) Intersection for P-P and S-S travel time intervals between station CPRX and CL7. 24

2.9. Results of (a) classic and (b) fuzzy logic Union operations for P-P and S-S travel time intervals between station CPRX and CL7. 25

2.10. Results of P-P travel time intervals for all recorded stations (6 stations). . . . 26

2.11. Resolution matrix for determining epicenter. 29

2.12. Resolution matrices with various levels of arrival time errors. 30

2.13. Locations of epicenters derived from SEISMOS and Fuzzy/SEISMOS programs. 32

2.14. Events with discrepant locations of epicenters. 34

3.1. Seismicity of New Mexico and bordering areas; time period 1962-1998, moment magnitudes 2.0 or greater. 41

3.2. Seismicity of New Mexico and bordering areas; time period 1962-1998, moment magnitudes 3.0 or greater. 42

3.3. Quality of earthquake locations for the state of New Mexico and bordering areas; time period 1962 through 1998 and moment magnitudes of 2.0 or greater. 47
4.1. Seismicity of New Mexico from 1962 through 1998 with moment magnitudes greater than or equal to 2.0. 50
4.2. Annual recurrence relations for the SSA with different cut-off magnitudes and time periods. 52
4.3. Annual recurrence relations for the RNM with different cut-off magnitudes and time periods. 53
4.4. Temporal seismicity for the SSA and RNM with magnitude ≥ 2.0 for all recorded events. 54
4.5. Seismicity of New Mexico from 1962 through 1998 with duration magnitudes greater than or equal to 2.0. 56
4.6. Temporal seismicity for the SSA and RNM with magnitude ≥ 2.0 after dependent events were removed. 57
4.7. Annual recurrence relations for the SSA and the RNM with a cut-off magnitude of 2.0 for the time period 1962-1998. 58
4.8. Micro-seismic source zones for seismic hazard analysis. 62
4.9. Examples of areal probability. 64
4.10. Schematic illustration of evaluation of probability-ground acceleration curves. 66
4.11. Probabilistic seismic hazard map (10% and 50 year) for the state of New Mexico and bordering areas. 67
4.12. Probabilistic seismic hazard map (2% and 50 year) for the state of New Mexico and bordering areas. 68
4.13. Probability-ground acceleration curves for six population centers and two

dam sites for a period of 50 years. 70
4.14. Distribution of earthquakes at various magnitudes contributing to the seismic hazard estimate for the Socorro area. 71
4.15. Probabilistic seismic hazard maps generated by NMT and USGS at 10% probability of exceedance in a 50 year period. 73
4.16. Earthquake data sets used by NMT and the USGS for estimating seismic hazards in New Mexico. 75
4.17. Background seismic source zones selected by the USGS. 76
5.1. Annual recurrence relations for SSA and RNM for the time periods 1962-1981 and 19821998. 80
5.2. Annual recurrence relations for both the SSA and the RNM before and after dependent events were removed. 81
5.3. Distribution of β values from recurrence relations for both SSA and RNM based on instrumental data, dependent events removed. 84
5.4. Ratios of the estimated recurrence rates using the average slope β and the two likelihood slope β values from estimates of one standard deviation for the two source zones. 85
5.5. Probabilistic seismic hazard map for the state of New Mexico and bordering areas using slope β values of 1.75, 1.686, and 1.767. 86
5.6. Magnitude contribution curves for the Socorro area at 10% probability of exceedance in a 50 year period using the slope β values of 1.75, 1.686, and 1.767. 90
5.7. Maximum likelihood slope β for both SSA and RNM with respect to selected maximum magnitude. 93

5.8. Probabilistic seismic hazard map for the state of New Mexico and bordering areas using maximum magnitude earthquakes of 6.0, 7.0, 8.0. 94
5.9. Annual recurrence relations for both the instrumental and pre-instrumental earthquake data for the SSA. 99
6.1. Annual recurrence relations for the SSA and the RGR after dependent events were removed. 103
6.2. Peak horizontal ground accelerations at 10% probability of exceedance in a 50 year period for the SSA. 104
6.3. Locations of the La Jencia fault, the Socorro Canyon fault and the Coyote Springs fault. 106
6.4. Horizontal peak ground accelerations at 0.2% and 0.5% probabilities of exceedance in a 50 year period based on the three active faults: the La Jencia fault, the Socorro Canyon fault and the Coyote Springs fault. 107
6.5. Peak horizontal ground accelerations at 10% probability of exceedance in a 50 year period based on (a) instrumental data; (b) both instrumental and fault data. 108
6.6. Peak horizontal ground accelerations at 0.2% and 0.5% probabilities of exceedance in a 50 year period based on the three active faults: the La Jencia fault, the Socorro Canyon fault and the Coyote Springs fault. 110
6.7. Peak horizontal ground accelerations at 10% probability of exceedance in a 50 year period based on (a) instrumental data; (b) both instrumental and fault data. 111
A.1. Magnitude distribution percentile for the city of Socorro for ground acceleration ranging from 0.01g to 0.40g at 0.02g intervals for a 50 year period. 173
A.2. Magnitude distribution percentile for the city of Albuquerque for ground

acceleration ranging from 0.01g to 0.40g at 0.02g intervals for a 50 year period. 174
A.3. Magnitude distribution percentile for the city of Los Alamos for ground acceleration ranging from 0.01g to 0.40g at 0.02g intervals for a 50 year period. 175
A.4. Magnitude distribution percentile for the city of Santa Fe for ground acceleration ranging from 0.01g to 0.40g at 0.02g intervals for a 50 year period. 176
A.5. Magnitude distribution percentile for the city of Carlsbad for ground acceleration ranging from 0.01g to 0.40g at 0.02g intervals for a 50 year period. 177
A.6. Magnitude distribution percentile for the city of Los Cruces for ground acceleration ranging from 0.01g to 0.40g at 0.02g intervals for a 50 year period. 178
A.7. Magnitude distribution percentile for the Elephant Butte Lake for ground acceleration ranging from 0.01g to 0.40g at 0.02g intervals for a 50 year period. 179
A.8. Magnitude distribution percentile for the Navajo Reservoir for ground acceleration ranging from 0.01g to 0.40g at 0.02g intervals for a 50 year period. 180
A.9. Distribution of earthquakes at various magnitudes contributing to the seismic hazard estimates for both the Socorro (0.12g) and the Albuquerque (0.08g) areas at 10% probability of exceedance in a 50 year period. 181
A.10. Distribution of earthquakes at various magnitudes contributing to the seismic hazard estimates for both the Los Alamos (0.07g) and the Santa Fe (0.03g) areas at 10% probability of exceedance in a 50 year period. 182

A.11. Distribution of earthquakes at various magnitudes contributing to the seismic hazard estimates for both the Carlsbad (0.04g) and the Las Cruces (0.04g) areas at 10% probability of exceedance in a 50 year period. 183

A.12. Distribution of earthquakes at various magnitudes contributing to the seismic hazard estimates for both the Elephant Butte Lake (0.03g) and the Navajo Reservoir (0.04g) areas at 10% probability of exceedance in a 50 year period. 184

List of Tables

3.1. Applied Magnitude Adjustments for Events from Collaborated Institutes 39

3.2. Classifications of Quality of Earthquake Locations 45

5.1. List of Pre-instrumental Earthquakes for the SSA for the Time Period 1868 through 1961with Modified Mercalli Intensity Scale V or Greater 98

Abstract

Presented in this dissertation is a catalog of magnitude 2.0 or greater earthquakes for New Mexico and bordering areas for the time period 1962–1998. This catalog contains 925 events (215 inside the Socorro Seismic Anomaly) and covers the region longitude 101° W to 111° W and latitude 31° N to 38° Significant contributions to this catalog came from Los Alamos National Laboratory, the U.S. Geological Survey, University of Texas at El Paso, University of Texas at Austin, and Texas Tech University. The unique features of this catalog include reassignment of magnitudes using a duration scale tailored to the region, and relocation of epicenters using the SEISMOS program. A major factor in improving locations was the development of an innovative subroutine that calculates a reliable first estimate of the epicenter for input into the SEISMOS program. The subroutine is based on a modified *G* matrix and fuzzy logic. Inclusion of it in the location process avoids problems encountered when using data from small aperture networks or when confronted with earthquake phase readings containing large errors; both rather frequent occurrences with the catalog events.

Probabilistic seismic hazards for the region based on the catalog are presented in maps of 10% and 2% probability of exceedance in a 50 year period. The hazard maps show moderate to low seismic hazards for the region; with the highest level of ground acceleration, ~0.18g, inside the Socorro Seismic Anomaly (10% probability of exceedance in a 50 year period). Along the major population corridor of the state from Albuquerque to Santa Fe, the peak ground acceleration is ~0.08g, which generates Modified Mercalli Intensity (MMI) VI effects. The magnitude contribution curves for selected areas show that earthquakes with magnitude 4.5-5.5 contribute the most to seismic hazards. Structural damage is not expected to modern buildings for earthquakes in this strength range but non-structural damage can be significant.

Sensitivity studies for the probabilistic seismic hazard analyses indicate that the hazard estimates for New Mexico are stable. Among controlling factors, the maximum likelihood slope B in the recurrence model is the most important factor for estimating rates for earthquakes in the magnitude range 4.0 to 6.5. A recurrence relationship based on pre-instrumental data 1868-1961 for the Socorro Seismic Anomaly (SSA) is in reasonably good agreement with the rate based on instrumental data 1962-1998. The recurrence rates based on active faults in the Rio Grande rift and the SSA suggest that active faults in these regions do not significantly affect hazard estimates for a short return interval of 500 years.

1. Introduction

New Mexico Tech, in collaboration with Los Alamos National Laboratory, the U.S. Geological Survey, University of Texas - El Paso, and Texas Tech University, has been using instrumental data to map earthquake activity in New Mexico and bordering areas since 1962. Sanford *et al.* (1997) undertook the project of collating data from all organizations into a comprehensive and consistent earthquake catalogs for New Mexico and bordering areas. I was involved in the preparation of the earthquake catalogs and have utilized the catalogs as the input data to generate the first probabilistic seismic hazard map that is specifically designed for New Mexico and bordering areas. In this dissertation I present the following specific results of my research: 1) A procedure for improving regional earthquake locations using a modified *G* matrix, 2) An earthquake catalog of magnitude 2.0 or greater earthquakes in New Mexico and bordering areas for the time period 1962 – 1998, 3) Two probabilistic seismic hazard maps for New Mexico and bordering areas using the instrumental data, 4) Sensitivity studies of probabilistic seismic hazard estimates for New Mexico, and 5) Studies of the effects of active faults on probabilistic seismic hazard estimates for New Mexico. Given below are brief descriptions of these specific studies covered in Chapter 2 through Chapter 6 of this dissertation.

Improving regional earthquake locations using a modified *G* matrix. The distribution of seismicity is pretty much uniform throughout the state of New Mexico. However, the seismic stations have been concentrated along the Rio Grande rift and in the southeastern corner of the state which requires location of regional events with small aperture networks. In order to improve regional earthquake locations, I modified the *G* matrix for solving earthquake locations using a generalized inversion method to accommodate arrival time differences of phase readings. In addition, I solved the modified *G* matrix using a forward method and a fuzzy logic algorithm. In Chapter 2, I describe the modified *G* matrix and the

methodology to solve the *G* matrix. Real world examples are included at the end of the chapter to demonstrate the effectiveness of the method.

Earthquake catalog of magnitude 2.0 or greater for New Mexico and bordering areas for the time period 1962 – 1998. This catalog supercedes a listing of earthquakes submitted for the seismicity map published in conjunction with the Decade of North American Geology volume entitled Neotectonics of North America (Sanford *et al.*, 1991). It also supercedes listings appearing in New Mexico Geophysics Open-File Reports 79 (Sanford *et al.*, 1995) and 83 (Sanford *et al.*, 1997). In Chapter 3 I describe the procedures for generating the catalog and the improvements of this catalog over previous earthquake listings. These improvements include 1) unified measurements of magnitude and 2) relocations using a velocity model and program most appropriate for New Mexico earthquake data. In addition, quality of earthquake locations in the study area is assessed.

Probabilistic seismic hazard map for New Mexico and bordering areas using instrumental data. I evaluated probabilistic seismic hazards for New Mexico and bordering areas using instrumental data from 1962-1998. The hazard estimates are presented in the format of 10% and 2% probability of exceedance in a 50 year period. These seismic hazard maps show that the Socorro area has the highest level of ground accelerations in the region. Along the major population corridor from Albuquerque to Santa Fe, the seismic hazards are moderate. In Chapter 4 I describe the procedure for preparing the earthquake catalog for the purpose of hazard analysis and derive relations between probability and peak horizontal ground acceleration for the area. Similarities and differences between my seismic hazard maps and the 1998 USGS hazard maps are also discussed.

Sensitivity studies of probabilistic seismic hazard estimates of New Mexico. The probabilistic seismic hazard estimates of New Mexico are somewhat subjective depending on the chosen input parameters and methods. In Chapter 5 I discuss the factors that might have affected the hazard estimates. These factors include 1) completeness of the earthquake

catalog, 2) uncertainties in the derived recurrence model including the maximum likelihood slope and the choice of maximum magnitude earthquake, and 3) the recurrence relation based on long-term average of pre-instrumental earthquake data. Though the hazard estimates for the region appear reasonable, it is also difficult to prove that these factors were not biased during the evaluation process.

Effects of active faults on probabilistic seismic hazard estimates of New Mexico. In Chapter 6 I compare the recurrence interval for magnitude 7.0 or greater earthquakes based on active faults (15 ka or younger in age) in the Rio Grande rift with the recurrence interval obtained from an extrapolation of the instrumental data in the same region. To examine effects of individual faults on hazard estimates, I evaluate seismic hazards for the SSA using both instrumental data and data for three of the most active faults inside the SSA. In an additional study, I assume 30 random earthquakes of magnitude 6.5 on hidden faults. A recurrence interval for these earthquakes that produces a level of activity consistent with the instrumental data is calculated.

2. Improving Regional Earthquake Locations Using a Modified *G* Matrix

Typical problems associated with locating regional earthquakes are inaccurate arrival times, an inaccurate velocity model and therefore a less stable *G* matrix. Because epicentral distances are commonly much larger than the distances among stations, unknown parameters in the *G* matrix (hypocenter and origin time of the event) can only be solved for epicenters and origin times with fixed focal depths (e.g., Palvis, 1992; Lienert, 1997). An additional problem arises when using a small aperture array to locate regional earthquakes because parameters of the epicenters become highly dependent on the origin time parameter in the *G* matrix. Common location programs based on the generalized inverse method like HYPO71 (Lee and Lahr, 1975) or SEISMOS (Hartse, 1991), which were originally designed for locating local earthquakes, tend to fail because no clear minima exists.

In this chapter, I approached the problem by using a modified *G* matrix containing only travel time intervals. Thus, no origin time parameter was included in the modified *G* matrix. Furthermore, I solved the modified *G* matrix using a forward method instead of an inverse method. During the process, the *G* matrix was regrouped into two matrices based on the characteristics of travel time differences: the matrix confining the epicentral distance (S-P time interval) and the matrix confining the distribution of azimuth (P-P and S-S time intervals). Individual matrices were mapped into the fuzzy logic space with measured uncertainties in terms of deviations in wave velocities. Locations of epicenters of earthquakes were then evaluated in the logic space.

Two examples of real world earthquakes (a felt earthquake and a swarm) were selected as case studies in this chapter. The location of the epicenters for these events were

evaluated based on both inverse and forward methods. In the case of the felt earthquake, a series of tests on the sensitivity of the location methods to faulty arrival times were conducted to evaluate the fitness of both methods. An earthquake swarm was used in the second case study to demonstrate improvements of quality of locations on smaller magnitude earthquakes using the new earthquake location method.

Common Procedure for Earthquake Location

The generalized linear inversion method is the most commonly used procedure to achieve a high accuracy location of hypocenters for earthquakes. There are four hypocentral parameters (*x, y, z, t*), the spatial coordinates and the origin time, to be solved by this method, and this is usually done by using Geiger's method or its variants.

Typically Geiger's method starts with the time residual Δd_i between the arrival time $d_i^{'}$ at the *i*th station and the trial solution d_i^o

$$\Delta d_i^o = d_i^{'} - d_i^o . \tag{2-1}$$

By assuming the time residual is small, a Taylor expansion of it will give

$$\Delta d_i^o = dt + \frac{\partial d_i}{\partial x} dx + \frac{\partial d_i}{\partial y} dy + \frac{\partial d_i}{\partial z} dz + e_i \cong \sum_j \frac{\partial d_i}{\partial m_i}\Big|_{m^o} \Delta m_j^o \tag{2-2}$$

where *m* is a known model vector composed of the source location and origin time

$$m = m_j = (x, y, z, t). \tag{2-3}$$

Let *G* be equal to the partial derivative matrix

$$G = \frac{\partial d_i}{\partial m_i} \tag{2-4}$$

and the equation becomes

$$\Delta d_i = \sum_j G_{ij} \Delta m_j . \tag{2-5}$$

Since this is often an overdetermined problem it can be solved with the generalized inverse of *G* or G^{-g} so that

$$\Delta m = (G^T G)^{-1} G^T \Delta d = G^{-g} \Delta d . \qquad (2\text{-}6)$$

As a result, this method is iterative and the new model

$$m' = m^o + \Delta m^o \qquad (2\text{-}7)$$

is repeatedly adjusted until the minimum misfit $\sum (\Delta d_i)^2$ is reached.

This procedure works well for local earthquakes occurring within networks. However, for regional earthquakes occurring outside a network and hypocenter-station distances significantly larger than distances between stations, it is more difficult to constrain focal depths. People usually circumvent this problem by using fixed focal depths. Nonetheless, problems still arise when closely spaced stations have little azimuthal constraint on the epicenters of earthquakes. As a result, the epicenters are highly dependent on observed arrival times and initial epicenter estimates. Small errors in observed arrival times often result in huge shifts to epicenters and sometimes the epicenter is placed at a local minima far from the real location.

Modified *G* Matrix

Another approach to solving this problem is to remove the origin time parameter from the equation of the time residual by using only S and P travel time intervals. With little modification of the travel time-distance equation the time residual becomes

$$\Delta d_i^o = \frac{\partial d_i}{\partial x} dx + \frac{\partial d_i}{\partial y} dy + \frac{\partial d_i}{\partial z} dz + e_i \cong \sum_j \frac{\partial d_i}{\partial m_i}\Big|_{m^o} \Delta m_j^o . \qquad (2\text{-}8)$$

The major disadvantage of this approach is that one is unable to incorporate direct P and S arrivals into the *G* matrix, which are crucial losses to an already limited number of recorded seismic parameters.

It is possible to increase input data to equation (2-8) by expanding the partial derivative matrix *G* to accommodate both P-P and S-S travel time intervals. During the process, we assume a one-dimensional crustal model and a small azimuthal distributions of seismic stations. In other words, all P-P and S-S travel time intervals are required to have

similar ray paths in order to be included into the G matrix. Near field variations of crustal structure can be taken into account by using station corrections. As a result, we retain the same forward model as shown in equation (2-8). However, Δd for P-P and S-S travel time intervals become travel time differences between two stations through a specified layer and S-P travel time intervals are travel time differences due to differences in P and S wave velocities along the same ray path to a single station.

Figure 2-1 illustrates a simple example of travel time interval between two stations with respect to a trial epicenter. As shown in the figure, the distances from a trial epicenter to stations S_1 and S_2 are D_1 and D_2, respectively. Both D_1 and D_2 are significantly larger than the spacing between the two stations, $2d$, and have similar ray paths. After station corrections for near field variations in crustal structure, the difference between arrival times can be attributed to the travel time difference through a specified layer with wave velocity V. For a half-space velocity model the travel time interval between two stations can be simply expressed as

$$T_{12} = T_1 - T_2 = \frac{D_1}{V} - \frac{D_2}{V} \tag{2-9}$$

where

$$D_1 = \sqrt{d^2 + D^2 - 2dD\cos\theta} \text{ and } D_1 = \sqrt{d^2 + D^2 + 2dD\cos\theta}\,. \tag{2-10}$$

Note that the origin time term does not appear the equation.

Unlike relationships between travel distances and origin time derived from direct P and direct S arrival times, P-P and S-S travel time intervals result in relationships between D and θ as shown in Figure 2-2. The curve radiates outward approximately from the mid-point between two coupling stations with asymptotes of

$$\theta = \pm\cos^{-1}\left(\frac{VT_{12}}{2d}\right). \tag{2-11}$$

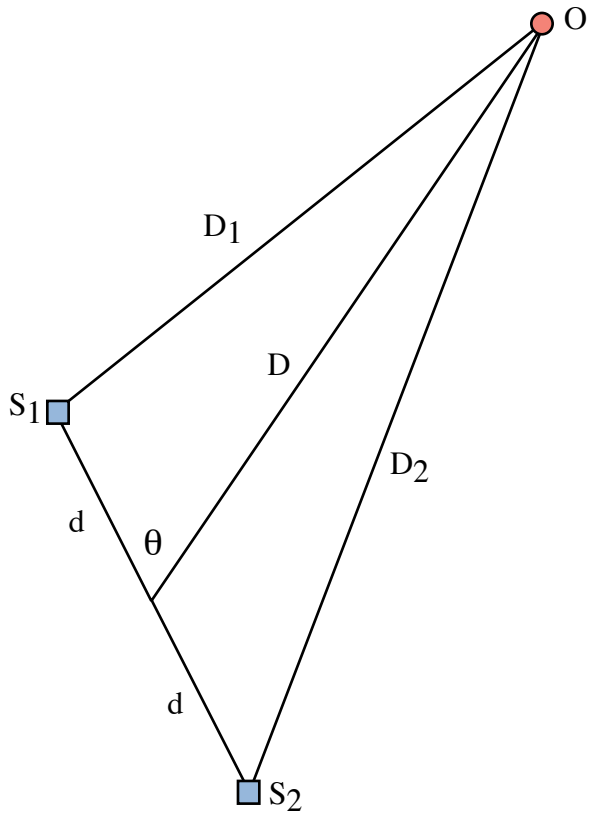

Figure 2-1. Schematic diagram for seismic stations S_1 and S_2 and the trial epicenter O. Epicentral distance D represents the distance from O to the midpoint between the two seismic stations.

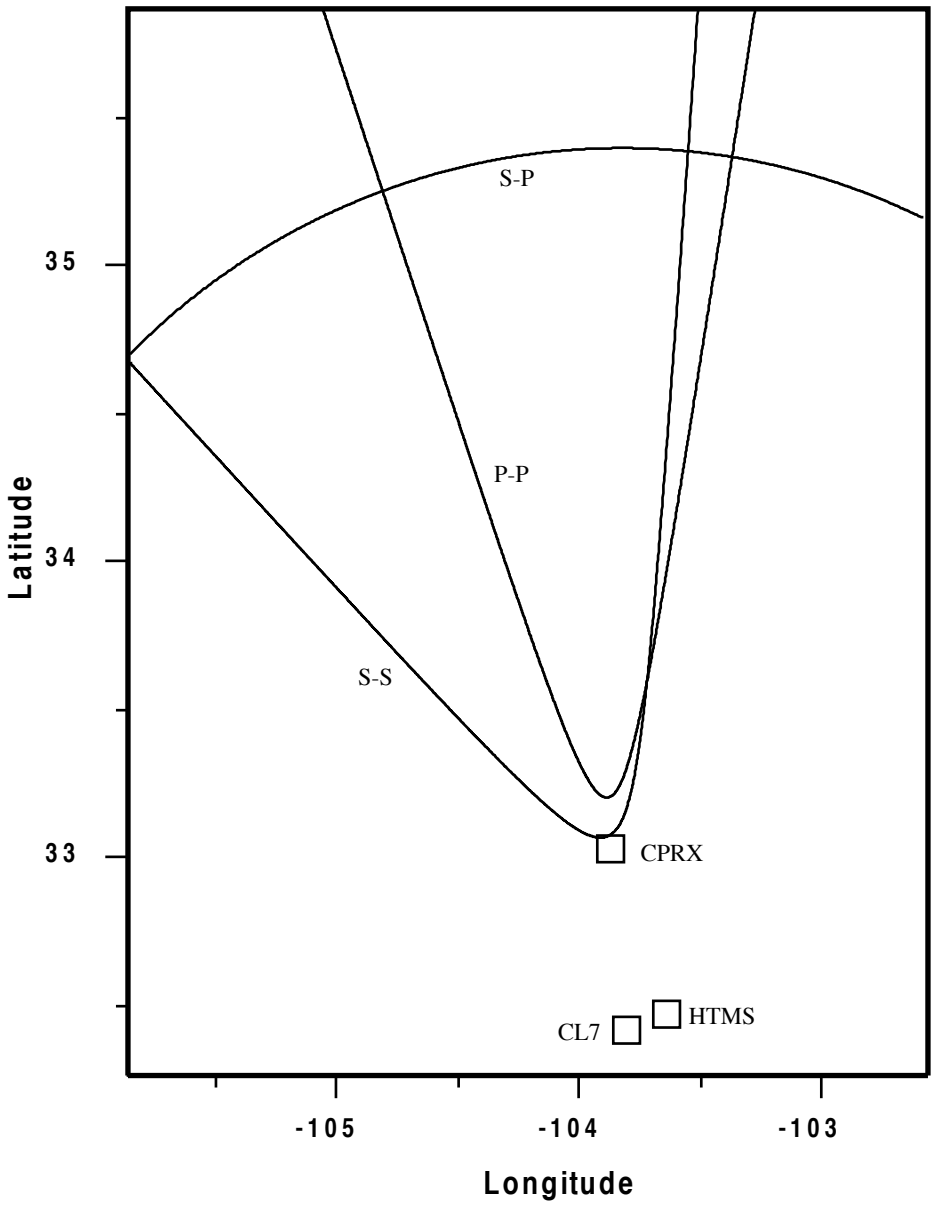

Figure 2-2. Travel distance curves for S-P, P-P, and S-S travel time intervals. Note that the S-P travel time interval produces a circular curve and the P-P and S-S travel time intervals produce hyperbolic-like curves. The S-S curve is for station pair CPRX and HTMS and the P-P curve is for station pair CPRX and CL7.

As distance D increases, changes in azimuthal angle θ with change in location decreases to minimum. Thus, θ is less sensitive to D when D is significantly larger than d. Also, the unconfined nature of the curves makes the G matrix become less stable during the inversion process. Therefore it would not be practical to incorporate P-P and S-S travel time intervals into the G matrix and solve for earthquake locations using an inverse method.

Forward Modeling Plus Fuzzy Logic Approach

Distinctive Features

In this study I solve equation (2-8) using a forward modeling technique. Instead of solving the modified G matrix directly as in an inverse method, I modify the procedure for optimum location of regional earthquakes. Distinctive features of the modified procedure are listed below:

Quantifying uncertainties. Recorded arrival times of regional earthquakes often contain large uncertainties in both arrival times and in the velocity model. Traditional methods usually assume a perfect velocity model and attribute uncertainties of recorded phases to uncertainties in reading arrival times on seismic records. By excluding variations in velocity structure along their ray paths and assigning fixed numbers of uncertainties to phases with respect to the arrival time, earthquake locations are often incorrect. In this study I convert uncertainties in arrival times into uncertainties in the velocity model. With preset upper and lower bound velocities for individual phases, the distance weighing factor is easily taken into account in terms of uncertainties in wave velocities.

Regrouping G matrix. Derived curves from S-P, P-P, and S-S travel time intervals are divided into two groups based on their distinct nature. In other words, circular curves of S-P travel time intervals constrain epicentral distance and hyperbolic-like curves of P-P and S-S travel time intervals constrain azimuth. Joint evaluation of earthquake locations by

combining results from one S-P matrix and one P-P and S-S matrix provide more stable results.

Logic operations using fuzzy logic. Fuzzy logic operation is primarily a forward modeling technique. This method is especially useful for handling data with large uncertainties. Deviations between trial and observed travel times in equation (2-8) for different time intervals can be mapped into the logic space. In the logic space, logic operations can be easily carried out according to relationships between individual G matrices and yield optimal results for earthquake location.

Fuzzy Logic Approach

The theory of fuzzy logic deals with two problems: fuzzy set theory, which deals with the ambiguity found in semantics, and fuzzy measurement theory, which deals with the ambiguous nature of judgements and evaluations.

A fuzzy set may be represented by a mathematical formulation often known as the membership function. This function gives a degree or grade of membership within the set. The membership function of a fuzzy set A, denoted by $\mu_A(x)$, maps the elements of the universe X into a numerical value within the range [0, 1], i.e.,

$$\mu_A(x) \in [0,1] \tag{2-12}$$

$$A = (x, \mu_A(x) | x \in X) \tag{2-13}$$

A simple graphical comparison of classic (or crisp) set theory and fuzzy set theory is shown in Figure 2-3 (Jamshidi *et al.*, 1993).

By adapting fuzzy logic theory, we are able to incorporate uncertainties from measurements of arrival times into variations of velocity structure. Figure 2-4 shows an example of such assessment. Let D_{12} equal the difference in epicentral distances with respect to station 1 and station 2 (Figure 2-1). Thus the uncertainty of travel time difference at these two stations can be expressed as the uncertainty in the velocity model

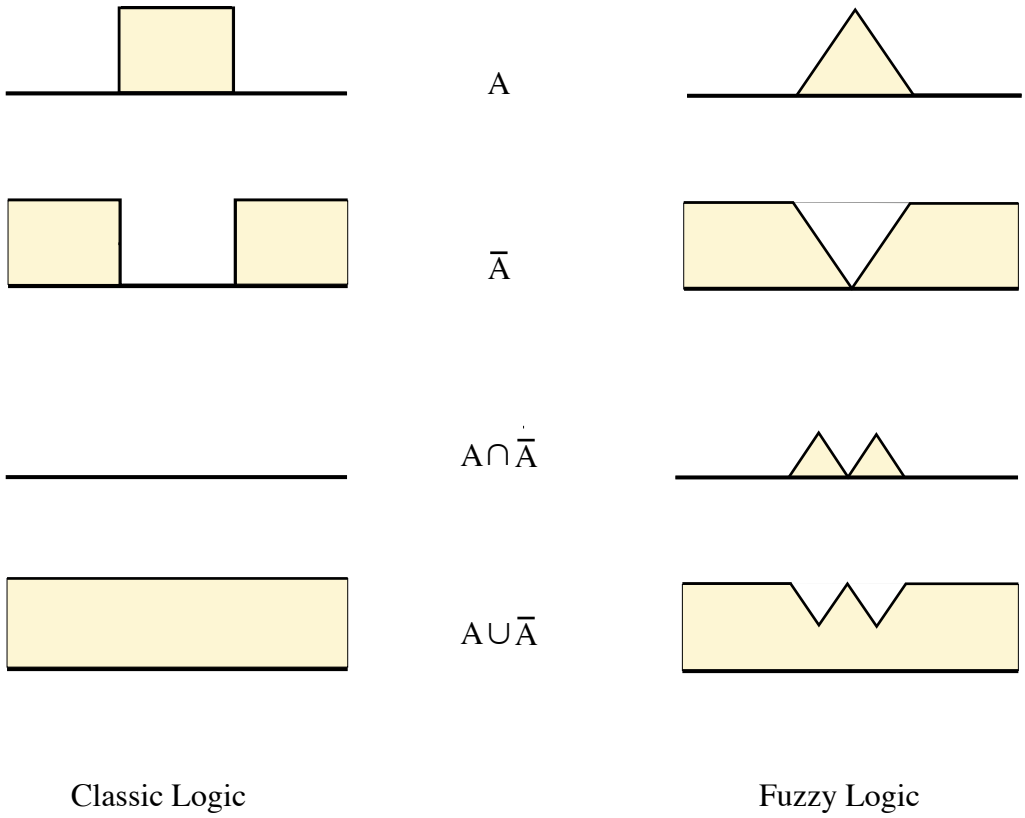

Figure 2-3. Comparisons of classic logic and fuzzy logic. For a given logic set A, complement, intersection and union operations based on classic logic and fuzzy logic are shown.

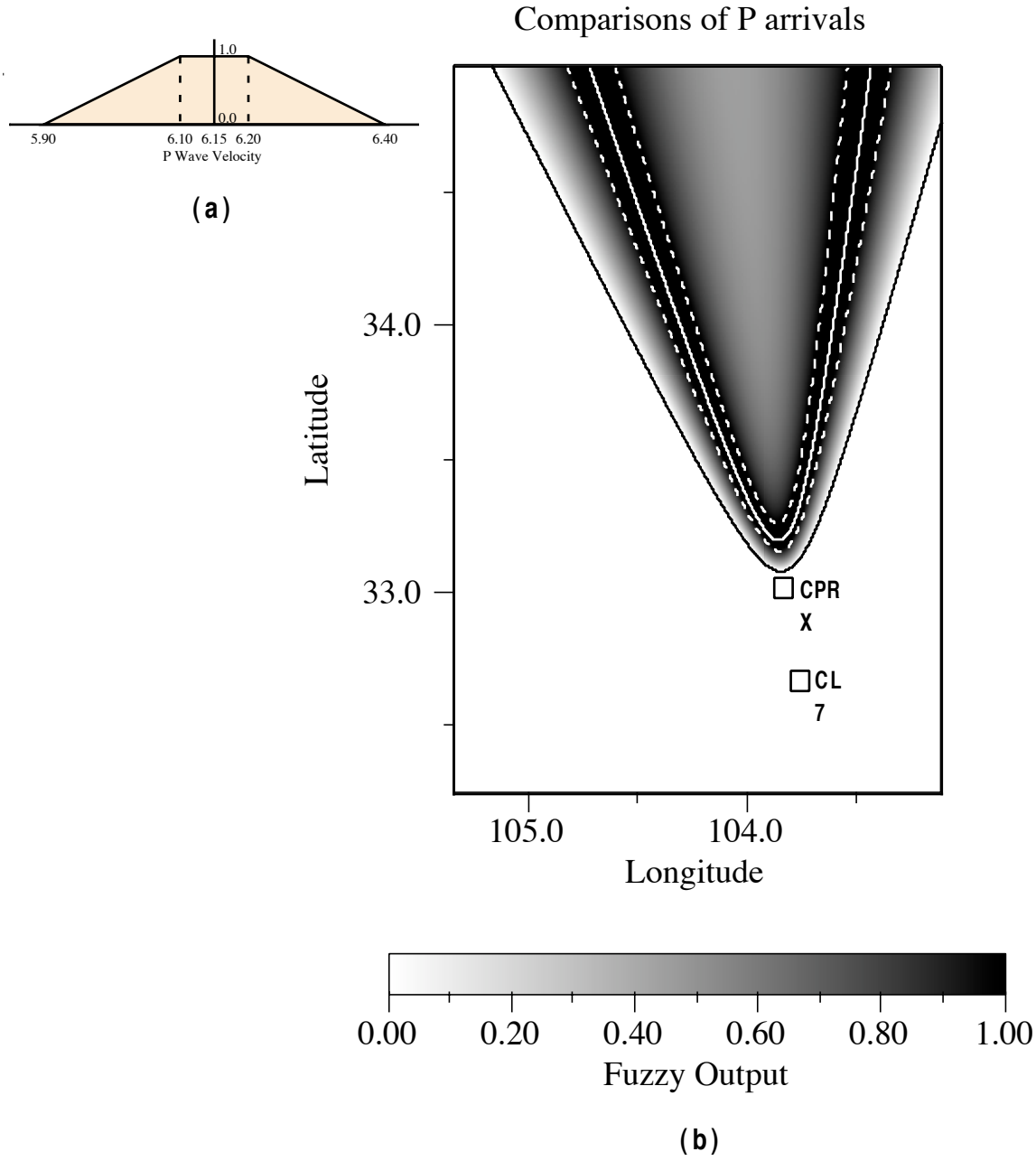

Figure 2-4. Results of P-P travel time interval between station CPRX and CL7. (a) P wave velocity model for mapping uncertainties in calculated wave velocities into logic space. (b) Derived travel distance curve. Theoretical travel distance curves for the velocity model are shown with solid and dashed white lines.

$$D_{12} = (V + \Delta V)(T_1 - T_2 + \Delta T) \tag{2-14}$$

and

$$\Delta V \cong \frac{D}{T_1 - T_2 + \Delta T} - V . \tag{2-15}$$

In Figure 2-4a, the region bounded by theoretical wave velocity V plus or minus one standard deviation yields a fuzzy output of 1. Surrounding this region is the area bounded by the highest and the lowest possible wave velocity. Note that in these two areas, the fuzzy logic outputs are less than one, which represents possible but less likely results.

Joint determination of earthquake location from equation (2-8) for individual time intervals in logic space is a straight forward logic operation. Fuzzy logic operations are identical to classic logic operations such as union, intersection, complement, and difference. In this study we use S-P, P-P, and S-S time intervals which can be divided into two groups, an S-P group and a P-P and S-S group. Evaluation of a trial location in logic space can therefore be expressed as

$$O = [(P - P) \cup (S - S)] \cap (S - P). \tag{2-16}$$

Earthquake Location Procedure for New Mexico

Problem Definition

In New Mexico earthquakes occur throughout the state, but recording is frequently by only one small aperture network (see Figure 2-6). Thus, many events are at large distances relative to the dimensions of the networks. SEISMOS, the currently used location program at New Mexico Tech (Hartse, 1991), uses the location of the closest seismic station as the initial estimate of the epicenter. The assumption is valid for events occurring within or near a seismic network. However, at event distance several times the network aperture, the assumption seldom applies, and the corresponding initial estimates of hypocenters provide little to no help in the location process.

Another problem with locating regional earthquakes comes from variability in crustal structure (Stewart and Pakiser, 1962; Toppozada, 1974; Sinno *et al*., 1986). Unlike local events, where we are able to solve for hypocenters using a detailed crustal model, the New Mexico area has large differences in crustal structure, for example Moho depths ranging from about 30 km to more than 50 km. Based on the available data, a crustal model applicable throughout the state is simply not possible. Sanford *et al*. (1991) circumvented the problem by ignoring Pn arrivals and by using only Pg and Sg arrivals with a half-space crustal model with P wave velocity of 6.15 km/s and a Poisson's ratio of 0.25. This procedure gives the best locations for earthquakes occurring within New Mexico and bordering areas.

Defining Fuzzy Sets

In this study, I fix focal depth for regional earthquakes and solve for the epicenter (x, y). I use a homogeneous half-space model with P wave velocity of 6.15 ± 0.05 (1 s.d.) km/s and Poisson's ratio of 0.25. Three fuzzy sets are defined:

1. P-P travel time interval (PP). Theoretical and observed P wave travel time intervals at two arbitrary stations for a trial epicenter are compared using equation (2-14). Deviation of P wave velocity with respect to the velocity model is then mapped into logic space as shown in Figure 2-5a. According to the model, deviations within 6.15 ± 0.05 km/s yield a fuzzy output of 1. Fuzzy outputs for larger deviations decrease linearly until the maximum possible velocity of 6.4 km/s or minimum possible velocity of 5.9 km/s are reached, which both have fuzzy outputs of 0.

2. S-S travel time interval (SS). The S-S time interval fuzzy set is similar to that for P-P time intervals. Figure 2-5b shows the fuzzy model for S wave velocity. The theoretical S wave velocity of 3.55 km/s is based on a P wave velocity of 6.15 km/s and a Poisson's ratio of 0.25. We assume maximum variations of Poisson's ratio ranging from 0.24 to 0.26, the maximum possible S wave velocity is 3.75 km/s (P wave velocity 6.4 km/s and

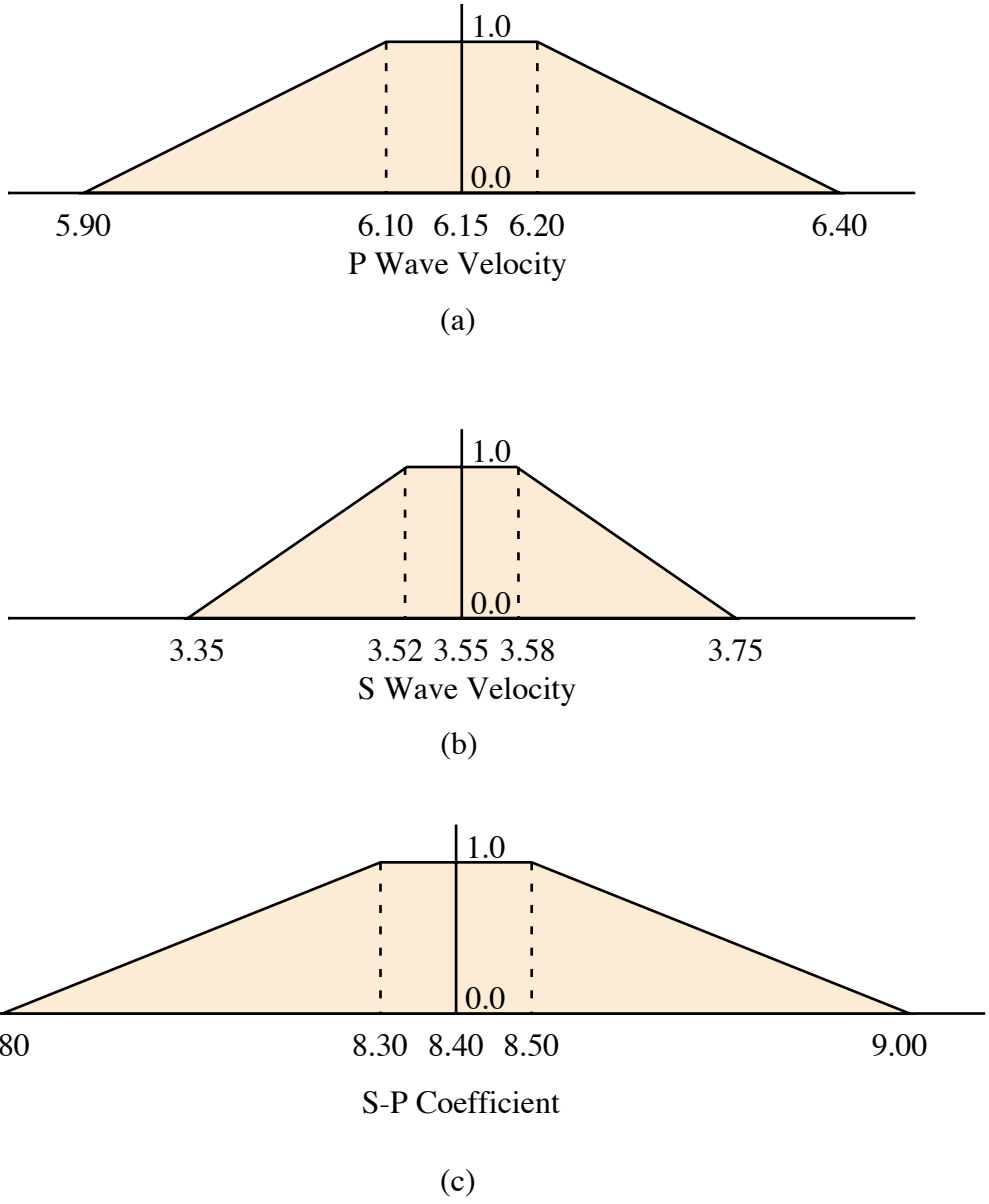

Figure 2-5. Velocity models for mapping uncertainties in calculated wave velocities into logic space. (a) P wave velocity. (b) S wave velocity. (c) S-P travel time coefficient.

Poisson's ratio 0.24) and minimum possible S wave velocity is 3.35 km/s (P wave velocity 5.9 km/s and Poisson's ratio 0.26). Deviations of S wave velocity 3.55 ± 0.03 km/s corresponding to a deviation between trial and observed time interval in equation (2-14) will yield a fuzzy output of 1.

3. S-P travel time interval (SP). S-P time intervals only apply to stations with both P and S readings. For a half-space model, S-P travel time interval can be expressed as

$$T_S - T_P = \frac{D}{V_S} - \frac{D}{V_P} \tag{2-17}$$

$$D = C(T_S - T_P), \tag{2-18}$$

where

$$C = \frac{V_P V_S}{V_P - V_S}. \tag{2-19}$$

Maximum and minimum factor C were obtained by mixing P and S velocity models. Finding distance is the objective of this set yet there is no direct way to calculate deviations of the velocity model with respect to travel time differences. To simplify the process, I assigned a fixed width of uncertainty as shown in Figure 2-5c. As usual, differences between theoretical and observed hypocentral distances for a trial hypocenter are examined and mapped into the logic space.

In summary, assume that a seismic network records n P phases, m S phases, and k P and S phases for an earthquake. The fuzzy output of a trial epicenter can be expressed as

$$O = [\sum_{t=1}^{(n-1)!} PP \cup \sum_{t=1}^{(m-1)!} SS] \cap \sum_{t=1}^{k} SP. \tag{2-20}$$

Example Earthquakes

Felt Earthquake

I chose one of the most recent felt earthquakes in New Mexico as an example to illustrate the procedure for locating a regional earthquake with a small aperture network.

This duration magnitude 3.0 earthquake occurred on 14 July 1998 at 05:38UT near Logan, New Mexico. Figure 2-6 shows the geographical locations of the earthquake and the seismic network in southeastern New Mexico that recorded it. The nearest station of the seismic network to the epicenter (CPRX) is ~260 km and the farthest (GDL2) is ~360 km. The aperture of the network with respect to the earthquake is ~15°. The epicenter is reasonably well constrained on the basis of felt reports and a final location incorporating readings from stations in central New Mexico.

Figure 2-7 shows the P-P and the S-S travel distance curves for stations CPRX and CL7. The two curves in the figure are theoretical relationships between epicentral distance D and azimuth θ based on comparisons of P and S travel time differences, respectively. A narrow band of fuzzy output 1 (shown in black) indicates areas in which observed P and S travel time differences matched theoretical travel time differences from the velocity model. Surrounding the black band are two gray bands in descending grayness, indicating decrease in fuzzy outputs or increasing mismatches between observed and theoretical travel time differences.

Ideally, the P-P and the S-S travel distance curves for two arbitrary stations should be identical in shape, given a perfect crustal model and phase readings. As a result of an imperfect crustal model and phase readings, these two curves rarely reproduce each other. In terms of azimuthal distributions of travel distance curves for any two seismic stations, the shape of the curve changes from a line perpendicular to the line connecting the two stations for identical arrival times to a hyperbolic curve bending toward the station with an earlier arrival time. As shown in Figure 2-7, the S-S hyperbola is wider than the P-P hyperbola, which suggests that the measured travel time interval for the P phase pair might be too large or for the S phase pair too small. Note that there is no correct answer at this stage and it requires more station readings to resolve the inconsistency.

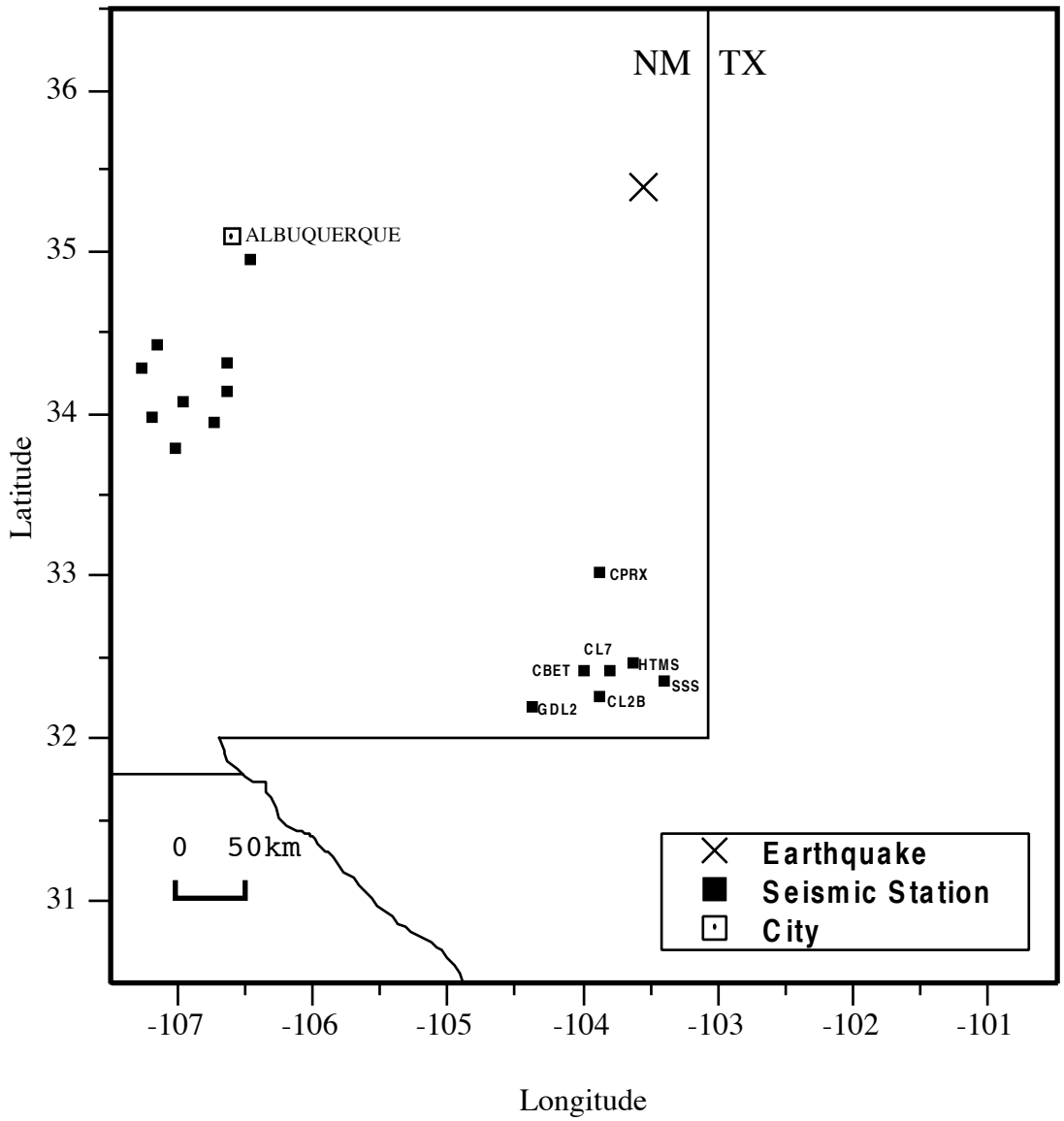

Figure 2-6. Geographical location of the Logan earthquake with respect to seismic networks in New Mexico. Data from the seven station network in SE New Mexico was used to evaluate the fuzzy logic location procedure.

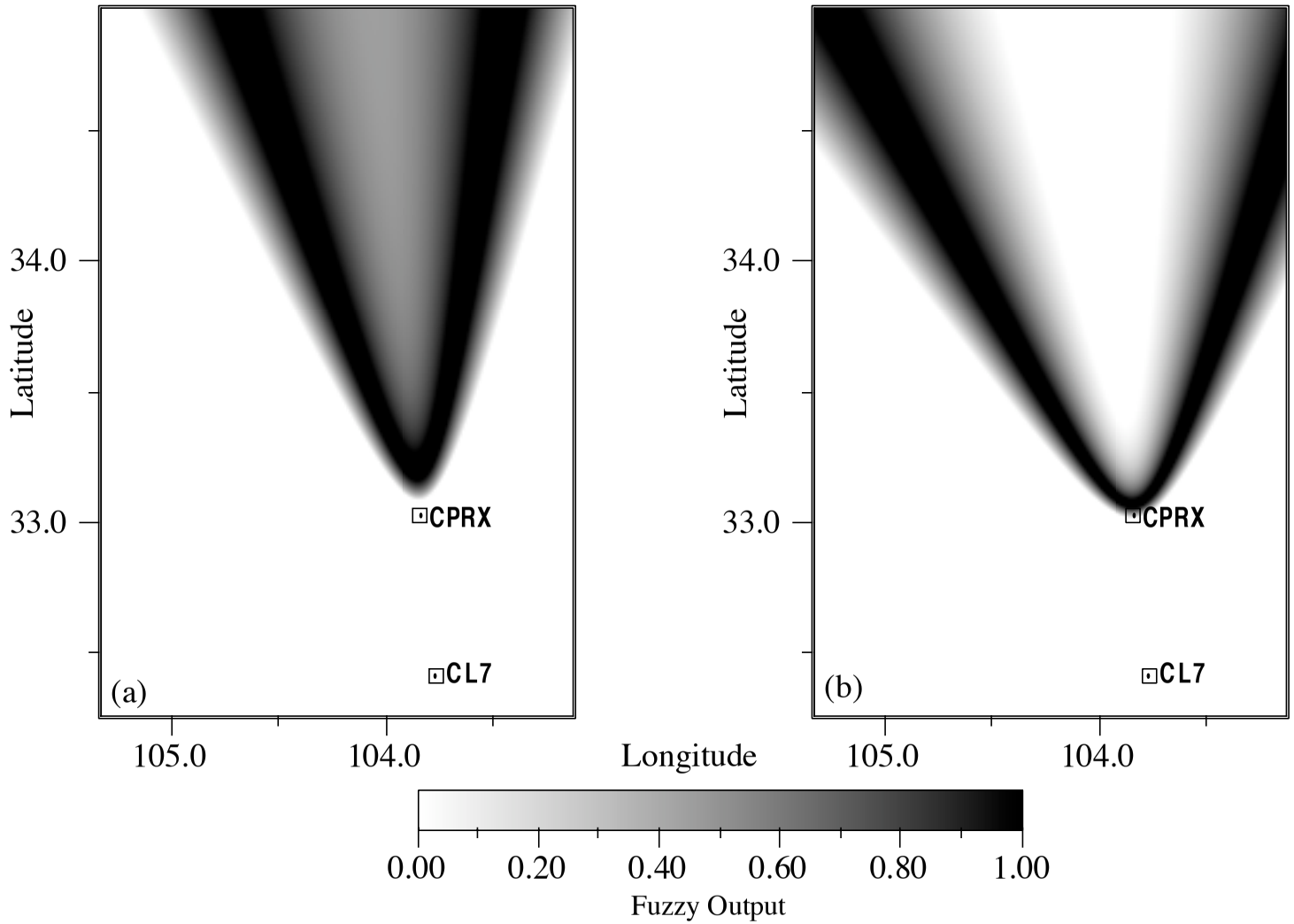

Figure 2-7. Results of (a) P-P and (b) S-S travel time intervals between station CPRX and CL7 after mapping uncertainties in calculated velocities into logic space. Differences in the hyperbolic-like curves are the result of reading errors.

Logic operations applied on these outputs depend on the purpose of applications. Figure 2-8 shows two of the most commonly used operations: Union and intersection. It is clear that the outputs of union operation retains more information but converges slower. On the other hand, an intersection operation results in faster convergence but tends to lose more information. A comparison of the intersection operation using classic and fuzzy logic procedures is shown in Figure 2-9.

Figure 2-10 shows results of P-P, S-S, and S-P travel distance curves, respectively. The study area was divided into a matrix of 100 by 100 cells of 10 km on each side, and the center of each cell was used as a trial epicenter. For each travel time interval, the fuzzy outputs of trial epicenters are the results of union operations for all combinations of travel time intervals. As expected, results of P-P (Figure 2-10a), and S-S (Figure 2-10b) travel distance curves reveal a prominent NNE trending azimuth. Circular travel distance curves of S-P time intervals (Figure 2-10c) constrain epicentral distance.

The matrix for deriving the final location of epicenter was reached by combining all three travel distance matrices based on equation (2-20). In Figure 2-11, unwanted or less likely trial epicenters were removed from the output matrix after logic operations. Therefore, the most likely location for the earthquake can then be easily resolved using a center of gravity method. For this example, the location derived by this method is almost identical to the location obtained from the traditional method with the addition of arrival times from three stations in another network.

In this example earthquake, I replaced some of the observed arrival times with erroneous arrival times to simulate typical errors caused by human operations or automated computer operations. Because uncertainties in the travel time differences in the G matrix are not redistributed throughout the matrix during the forward modeling process, the erroneous data are simply dismissed during the evaluation procedure. Figure 2-12 shows results of estimated epicenters for the Logan event after I included large and numerous

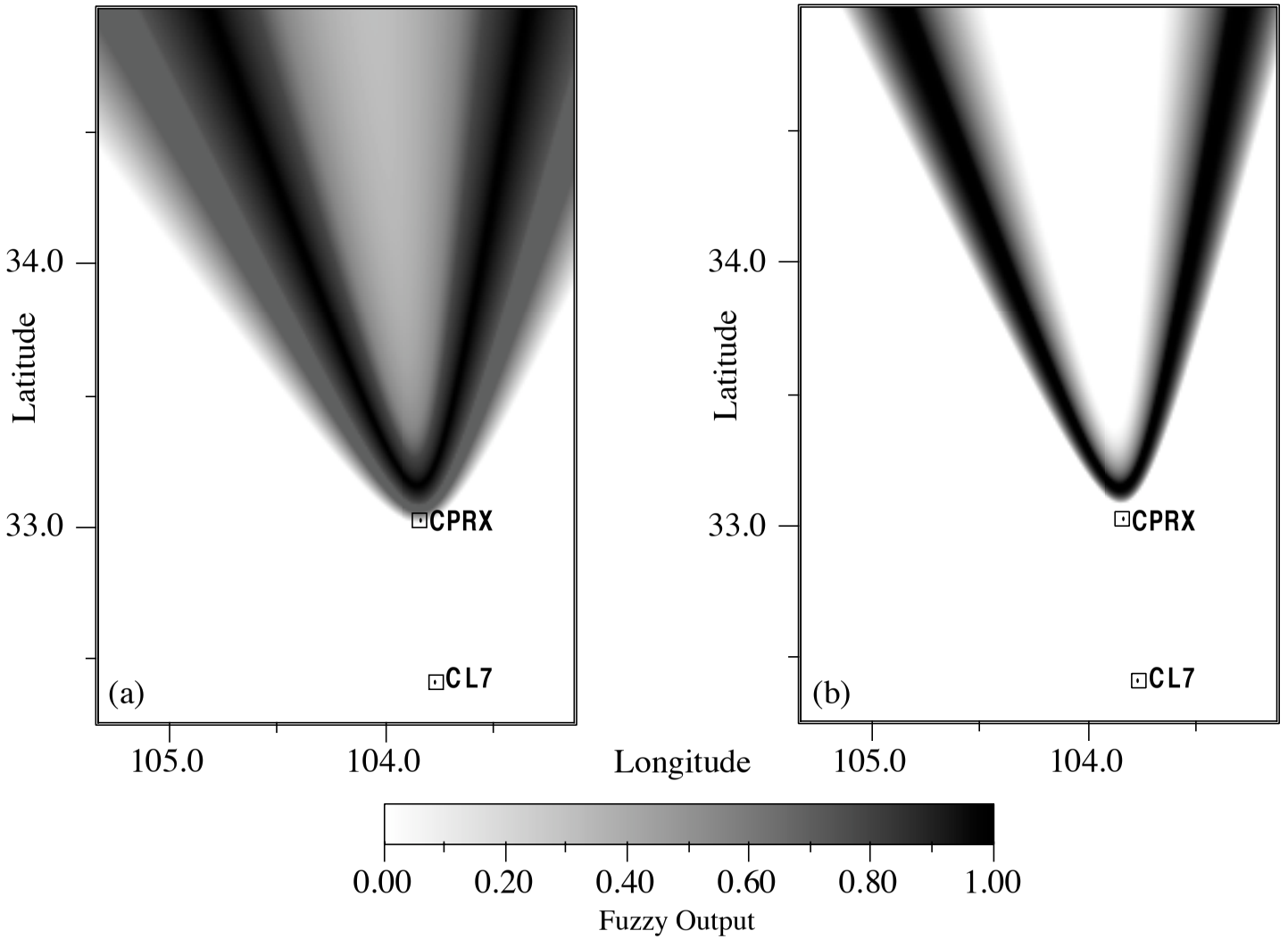

Figure 2-8. Results of fuzzy logic operation (a) Union and (b) Intersection for P-P and S-S travel time intervals between station CPRX and CL7.

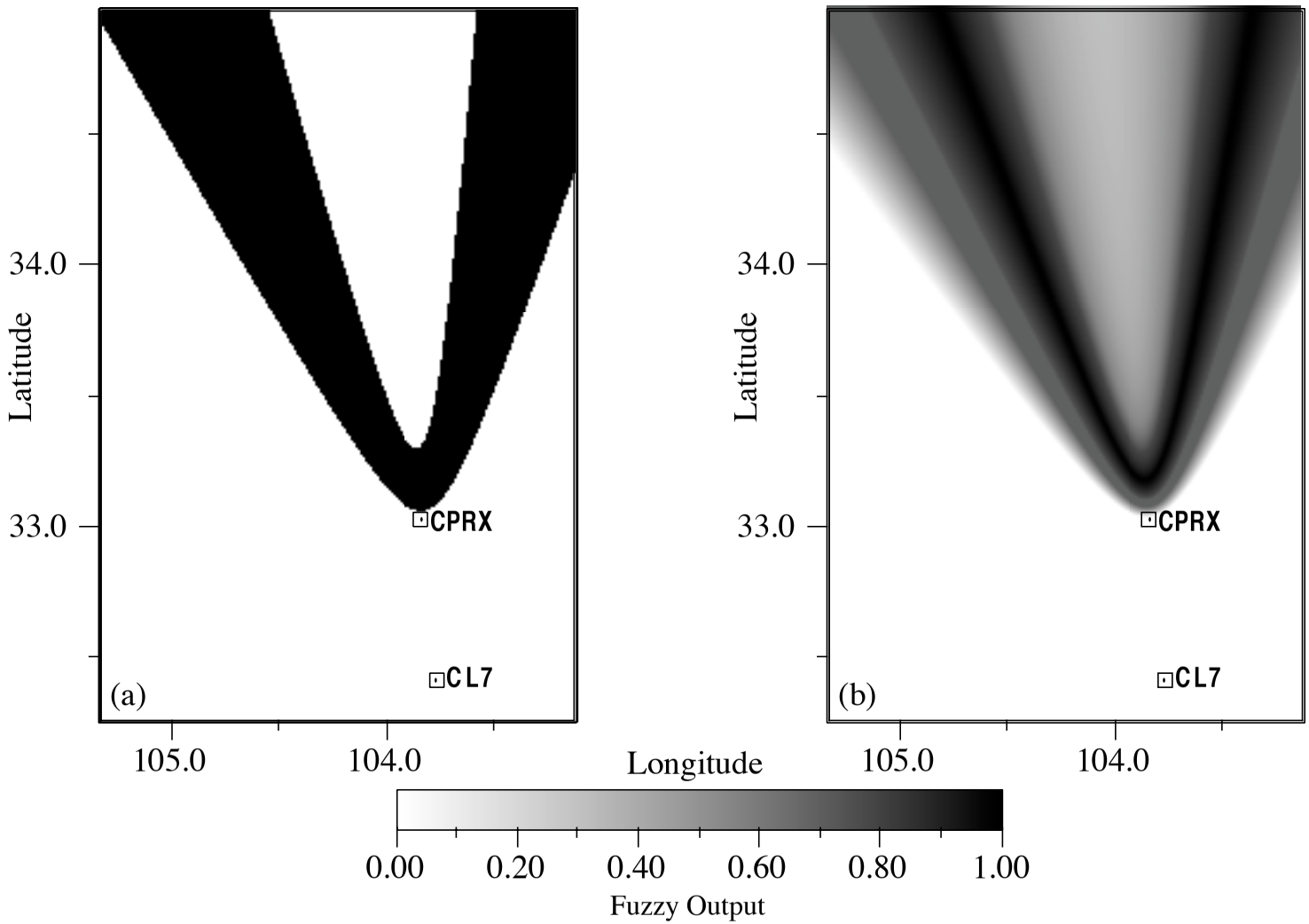

Figure 2-9. Results of (a) classic and (b) fuzzy logic Union operations for P-P and S-S travel time intervals between station CPRX and CL7.

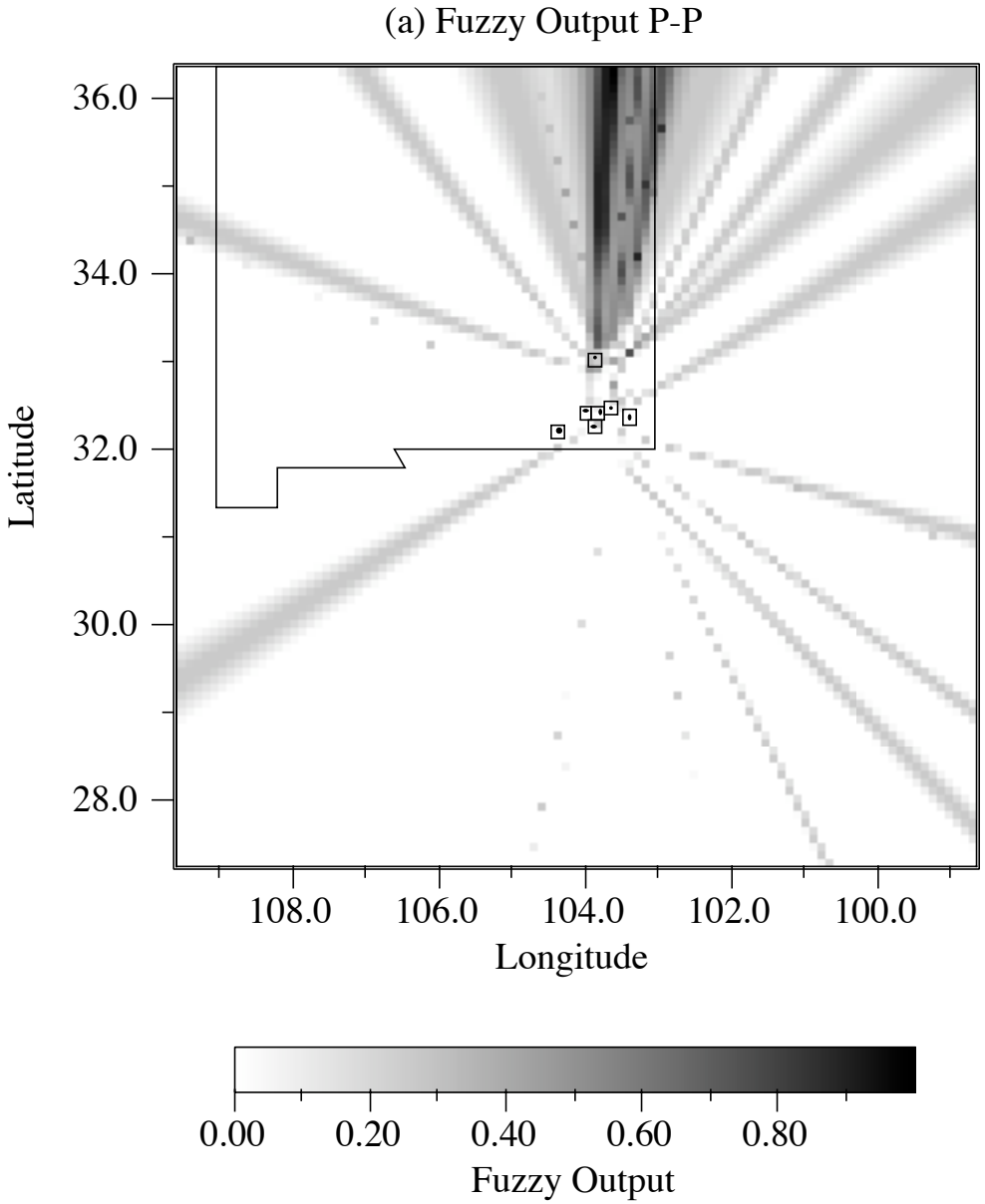

Figure 2-10a. Results of P-P travel time intervals for all recorded stations (6 stations). A total of 120 travel distance curves are plotted. The fuzzy logic operation union was applied to individual travel distance curves.

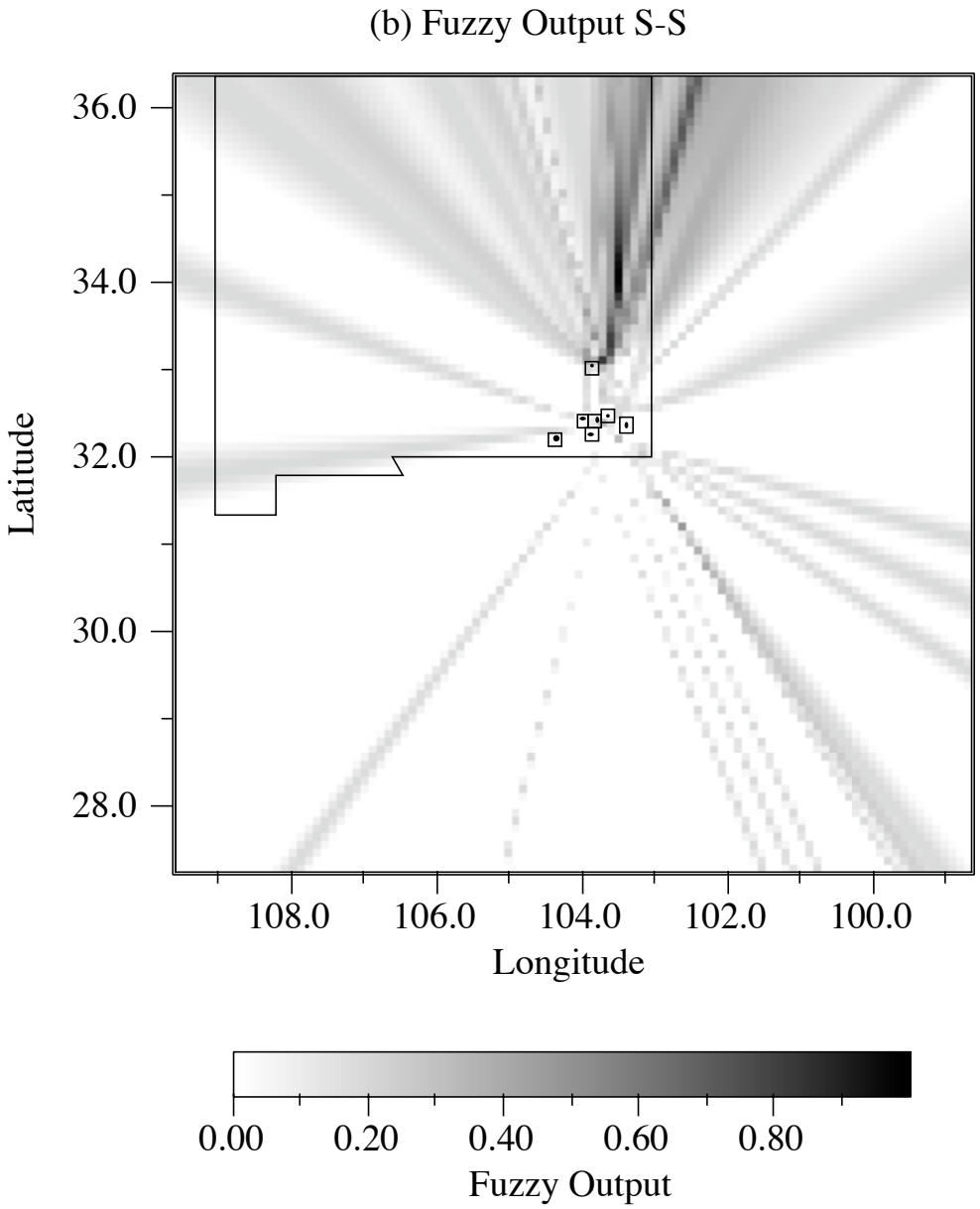

Figure 2-10b. Results of S-S travel time intervals for all recorded stations (7 stations). A total of 720 travel distance curves are plotted. The fuzzy logic operation union was applied to individual travel distance curves.

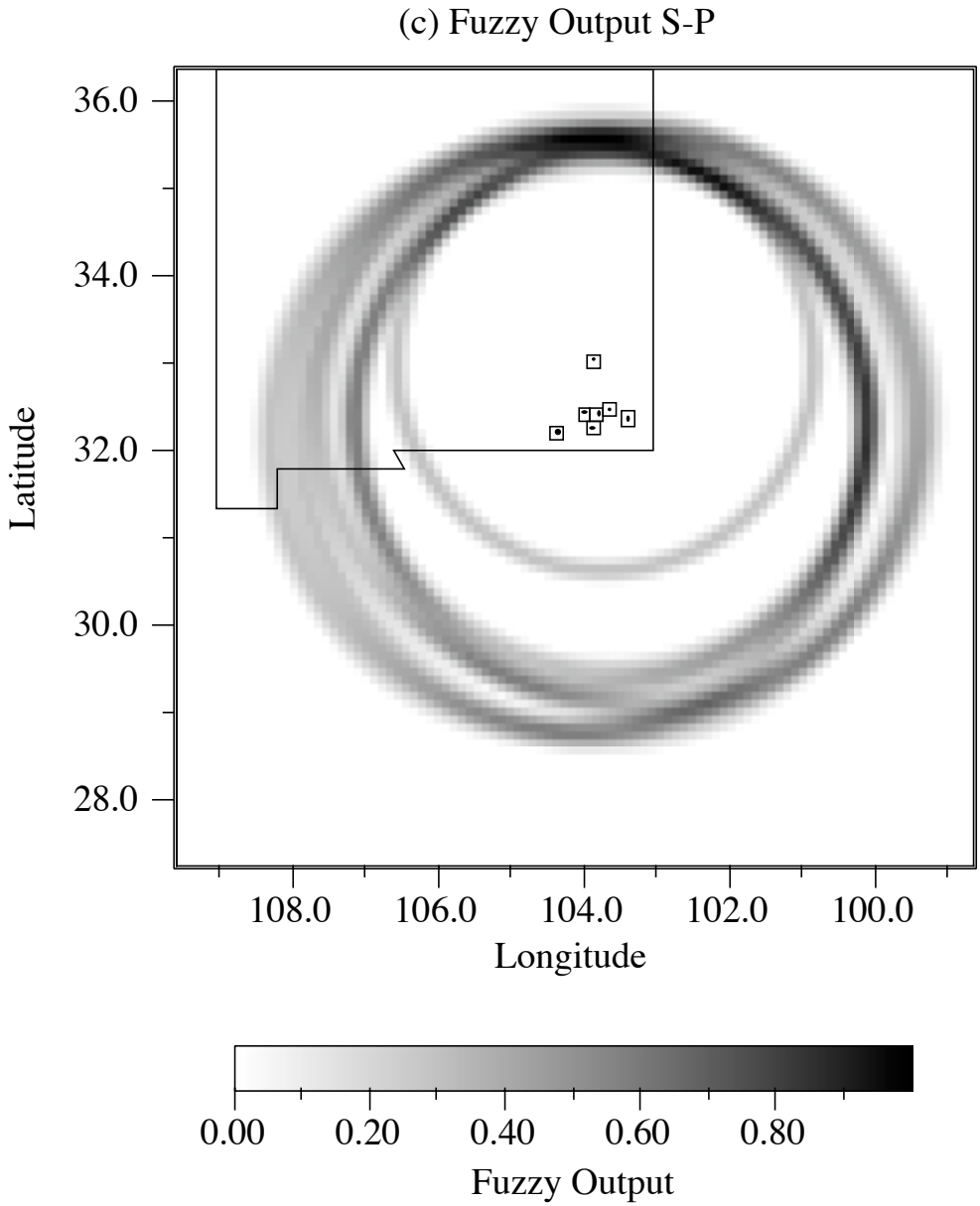

Figure 2-10c. Results of S-P travel time intervals for all recorded stations (6 stations). A total of 6 travel distance curves are plotted. The fuzzy logic operation union was applied to individual travel distance curves.

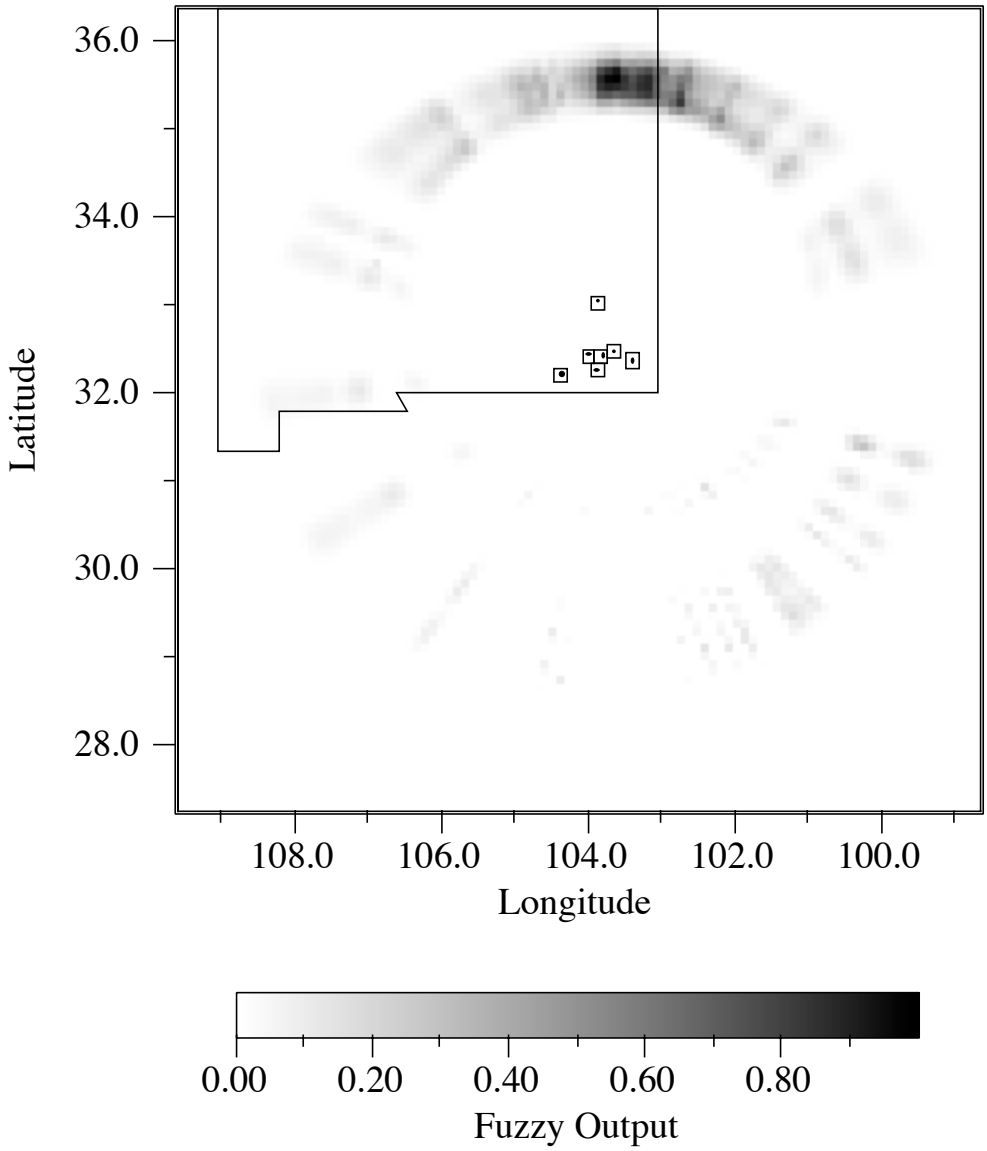

Figure 2-11. Resolution matrix for determining epicenter. This matrix was derived by combining the three individual matrices in Figure 10 using equation (19). The best location for the epicenter was obtained using a center of gravity method.

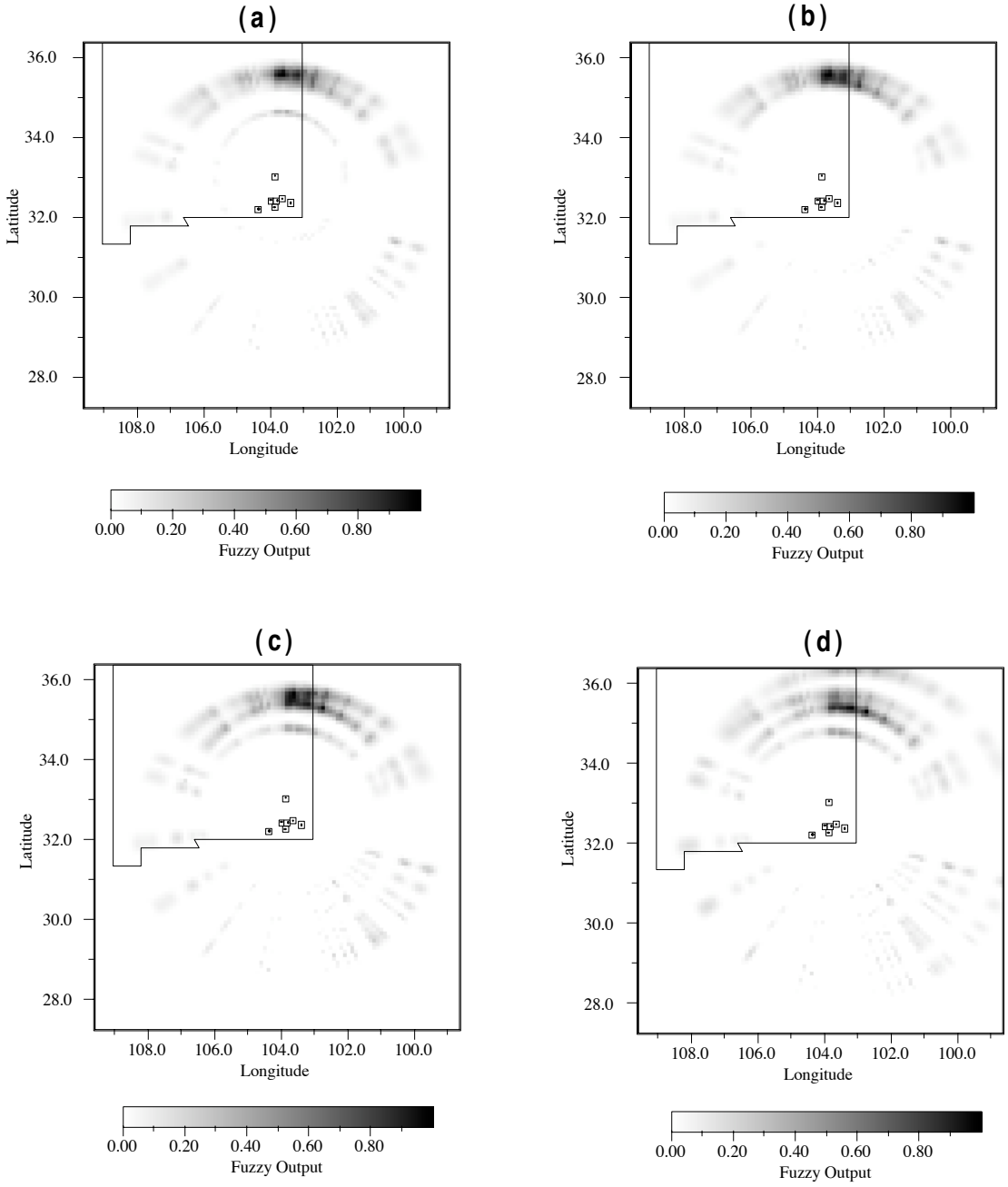

Figure 2-12. Resolution matrices with various levels of arrival time errors: (a) One P phase reading in error by 10 seconds; (b) One P and one S phase reading in error by 10 seconds; (c) Two P and one S phase readings in error by10 seconds; and (d) Two P and two S phase readings in error by 10 seconds.

erroneous data entries with respect to results from the actual observed data. In the test, from one to four actual P and/or S data entries among 13 available phase readings were offset by 10 seconds. Then the earthquake location was recalculated using both inverse and forward methods. A typical inverse method fails to solve the location of the epicenter as soon as a single faulty entry is included in the *G* matrix. In contrast, a faulty entry only appears as an isolated circle and/or non-correlated curves in the resolution matrix (Figure 2-12a). Even though faulty data do affect the final location for the earthquake, the effects of such faulty data have already been minimized during the process. It is clear that the forward process tolerated several erroneous arrival times in its *G* matrix and yielded approximately the same location as with the actual observed data.

Earthquake Swarm

The second example in this study is an ongoing earthquake swarm in southeastern New Mexico since 1997 with the strongest earthquake of magnitude 4.0. Figure 2-13a shows 43 locatable earthquakes of this swarm for the time period June 1, 1998 through December 31, 1998. Locations of earthquakes shown in the figure were derived from a fuzzy logic assisted SEISMOS program (Fuzzy/SEISMOS). Even though the epicentral distances of these earthquakes to the nearest seismic stations are less than 100 km, the quality of locations is not necessarily better due to the complexity of local crustal structure. Typical problems associated with this swarm are low signal to noise ratio, ambiguous phases, and a limited number of recording stations for the lower-magnitude earthquakes. Locations based solely on the SEISMOS program are shown in Figure 2-13b. In the later figure, earthquakes with a limited number of recording stations (five or less) may have erroneous epicenters. By plotting the discrepant events together (Figure 2-14) it is clear that these two clusters actually mirror each other.

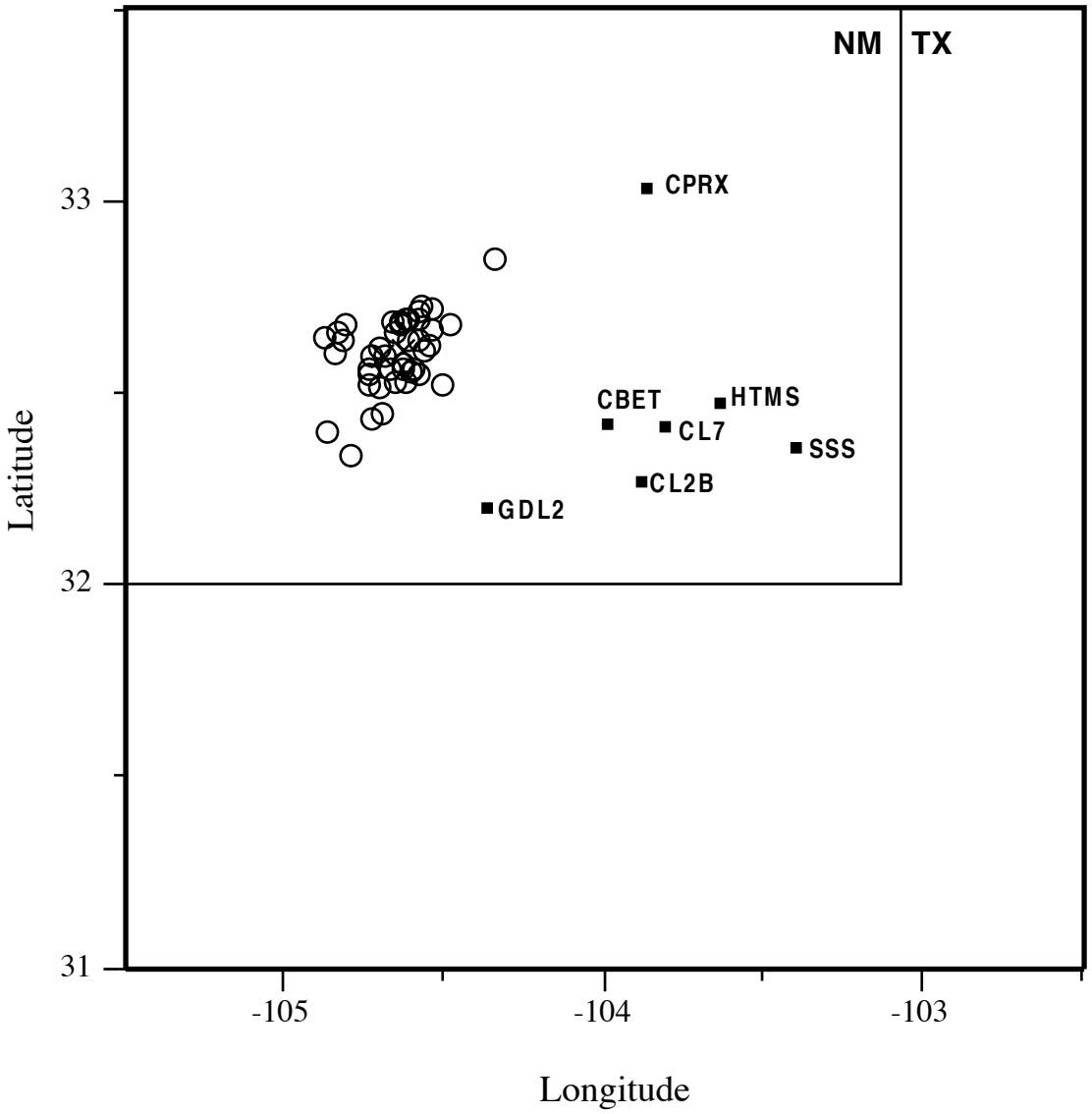

Figure 2-13a. Locations of epicenters derived from Fuzzy/SEISMOS program. A total number of 46 events are shown in the plot with number of recorded stations ranging from three to seven. Locations of all events resulted in a cluster of epicenters to the northwest of the seismic network.

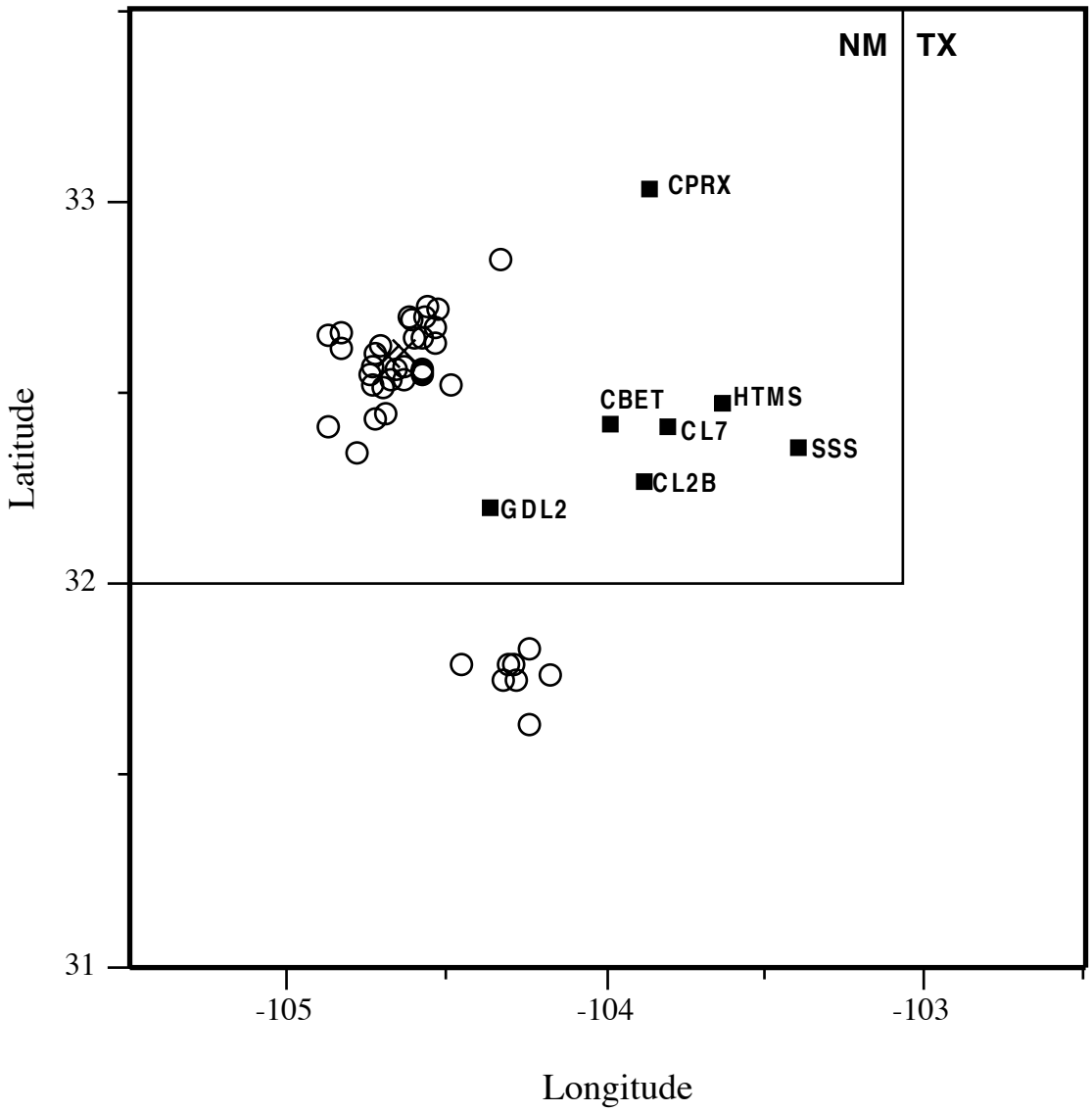

Figure 2-13b. Locations of epicenters derived from SEISMOS program. A total number of 46 events are shown in the plot with the number of recorded stations ranging from three to seven. Eight events yielded a different location to the southwest of the seismic network instead of northwest.

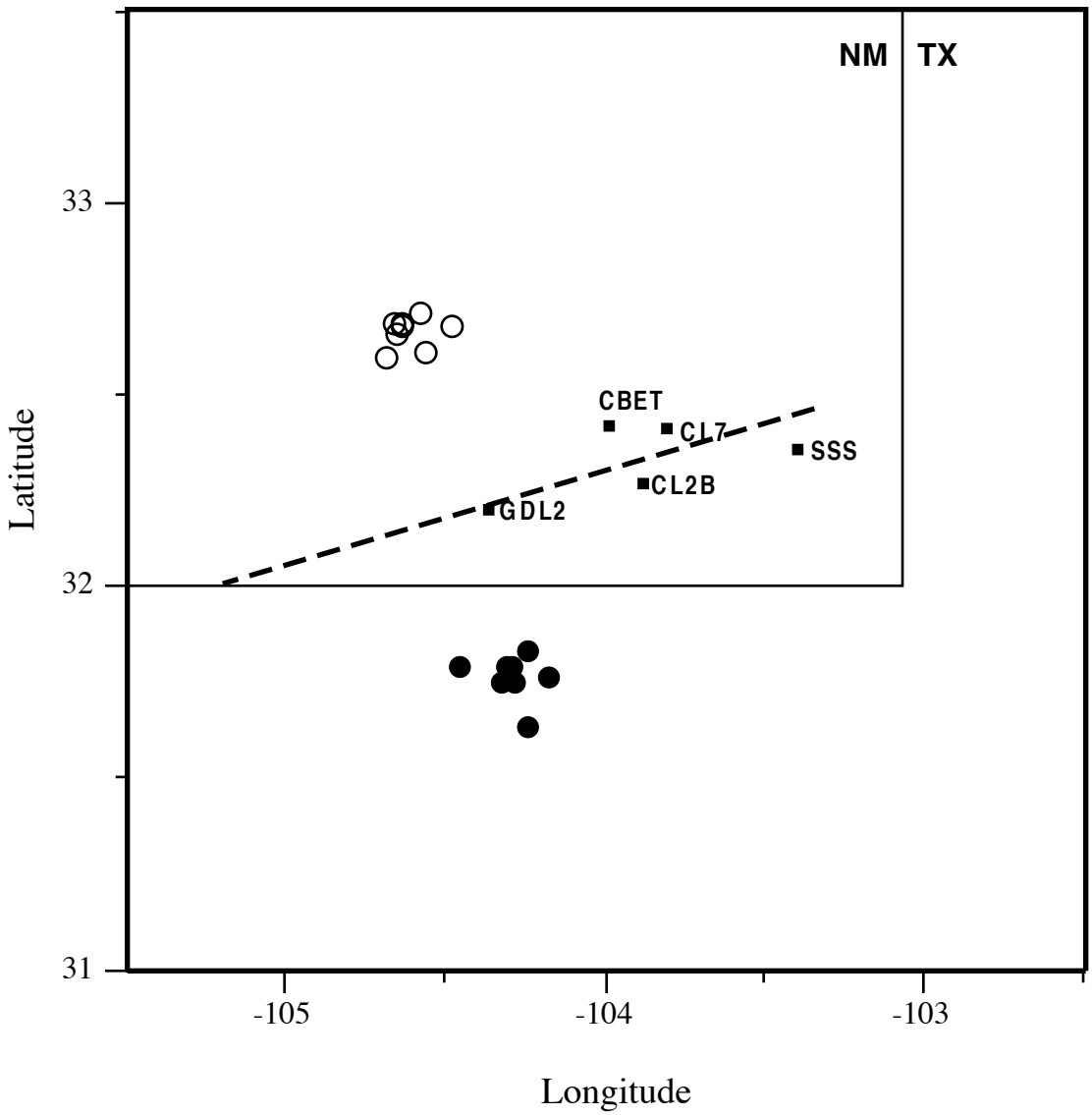

Figure 2-14. Events with discrepant locations of epicenters. The two clusters of epicenters are based on the same set of events except with outputs from two different location programs. The cluster with circular symbols are locations based on the Fuzzy/SEISMOS program and the cluster with black dots are based on the SEISMOS program. The dashed line indicates the center line dividing recorded seismic stations for the events in this example. Locations of epicenters determined for the rest of the swarm sequence (Figure 2-13) indicate that the circular cluster to the northwest is correct result.

Discussion

The most unique feature of the modified G matrix I used in this study is that it contains only arrival time differences between phases. In solving the data matrix, I divided the matrix into two matrices for deriving hypocentral distance and azimuthal angles with respect to seismic stations. Uncertainties in arrival time differences were mapped into the fuzzy logic space in terms of uncertainties in the velocity model. Locations of earthquakes were based on results of logic outputs in logic space by searching a gridded area.

The forward modeling method used in this study has advantages over inverse methods in handling uncertainties of arrival times and even manmade errors. As shown in equation (2-6), in the process of deriving a generalized inverse matrix G^{-g}, errors and uncertainties are redistributed throughout the matrix. A wrong entry of arrival time is likely to destroy the whole matrix. On the other hand, errors of arrival times are isolated in the forward method and have less effect on other data entries. In my example earthquake, I was able to introduce several P and/or S arrival time errors out of a 13 arrival time set without destroying the result. This technique can be incorporated into applications such as an automated triggering system which sometimes must contend with misidentified phases.

I have incorporated the fuzzy logic algorithm into the location program SEISMOS to increase stability in locating regional earthquakes. This technique was converted into a computer subroutine as an initial hypocenter estimator and incorporated into SEISMOS in early 1994 at New Mexico Tech (Lin and Sanford, 1994). The Fuzzy/SEISMOS combination has proved to be very effective in locating regional earthquakes.

3. Catalog of Instrumentally Recorded Earthquakes for New Mexico and Bordering Areas 1962-1998

In the period from 1962 through 1998, several organizations used instruments to locate and determine strengths of earthquakes in New Mexico and bordering areas; notably New Mexico Tech (NMT), Los Alamos National Laboratory (LANL), U.S. Geological Survey (USGS), the University of Texas at El Paso (UTEP) and the University of Texas at Austin (UTA). The periods of operation, number and sensitivity of instruments, and procedures for locating and assigning magnitudes were highly variable amongst these organizations during the 37-year period. For this reason, Sanford *et al.* (1997) undertook the project of collating data from all organizations into a comprehensive and consistent earthquake catalog for New Mexico and bordering areas. This catalog supercedes a listing of earthquakes submitted for the seismicity map published in conjunction with the Decade of North American Geology volume entitled Neotectonics of North America (Sanford *et al.*, 1991). It also supercedes listings appearing in New Mexico Geophysics Open-File Report 79 (Sanford *et al.*, 1995) and 83 (Sanford *et al.*, 1997).

Magnitudes

A major effort was made to have all magnitudes in the catalog based on or tied to a New Mexico duration magnitude scale (Newton *et al.*, 1976; Ake *et al.*, 1983). For determining magnitudes the relation

$$M_d = 2.79 \log \tau_d - 3.63, \qquad (3\text{-}1)$$

was used, where τ_d is the duration in seconds. This relation was first developed by Dan Cash at LANL (Newton *et al.*, 1976) for earthquakes in northern New Mexico. Later an essentially identical relation was derived at NMT (Ake *et al.*, 1983) for earthquakes in central and southern New Mexico. The duration magnitude scales for both organizations

are tied to the local magnitude scale which Hanks and Kanamori (1979) have demonstrated is equivalent to the moment magnitude.

Location Program

The location program selected for the catalog was SEISMOS (Hartse, 1991). Originally developed to obtain hypocenters for earthquakes within or near a local network, it was modified to also locate regional earthquakes. SEISMOS, like other inverse method location programs, e.g. HYPO71 (Lee and Lahr, 1975) and HYPOELLIPSE (Lahr, 1999), fails to obtain reasonable locations for regional events detected by small aperture networks. For the 37 years of New Mexico instrumental recording, this was a frequent occurrence. Lin (1994) and Lin and Sanford (1998) solved this problem by developing a fuzzy logic algorithm that obtains a highly reliable initial estimate of the epicenter for input into the SEISMOS program (see Chapter 2). Generation of the NMT catalog required relocation of nearly all of the earthquakes using SEISMOS modified to include the fuzzy logic algorithm.

Velocity Model

Sanford *et al.* (1991) have determined that the most accurate locations for regional earthquakes in New Mexico are obtained by using Pg and Sg arrivals only and a simple half-space crustal model with a velocity of 6.15 km/sec and a Poisson's ratio of 0.25. For earthquakes near Socorro, a more complex crustal structure is used in order to incorporate reflections into the location process (Hartse *et al.*, 1992).

Procedure for Refining Locations of Earthquakes

The strategy for compiling the master catalog was to remove redundant events, to establish consistent measurements of uncertainties in phase readings, and to derive earthquake locations based on the SEISMOS program and the half-space or the local crustal models. Artificial earthquakes (primarily explosions) were identified and removed during the process. In additional to the local and regional models, custom-derived velocity models were also used for specific earthquake swarms.

Initial Catalog. Earthquake listings from NMT, LANL, USGS, UTEP, and UTA were compiled and sorted chronologically into a single master catalog. At this stage, the NMT listing was the primary source for the new catalog and missing events were obtained from listings of the other organizations. For cases where an earthquake was located by more than one organization, the usual choice was to adopt the NMT location and magnitude. Magnitude differences for earthquakes co-located by NMT and the other institutes were used to establish correction factors to events in the catalog whose location and strength parameters were established by LANL, USGS, UTEP, or UTA. Appendix I shows listings of events used to establish correction factors for magnitudes derived by USGS, LANL, UTEP, and ASL. Table 3-1 summarizes the adjustments which range from –0.453 for UTEP to +0.104 for LANL.

Final Catalog. Preparation of the final catalog included the following procedures.

1. All earthquakes with readings on file at NMT were relocated using the program SEISMOS with application of fixed weighting factors; 0.075 for local events within 70 km of Socorro and 0.25 for regional events beyond that distance. During this process, the fuzzy logic subroutine embedded in SEISMOS was activated to resolve the locations of regional earthquakes with ambiguous phase readings and/or poor station configurations.
2. Explosions were identified and removed from the catalog.
3. Magnitudes of events contributed to the catalog by LANL, USGS, and UTEP were adjusted to comply with NMT duration magnitudes.

The final NMT catalog contains ~1916 earthquakes with magnitudes of 1.3 or greater that occurred within and bordering New Mexico; 79% from NMT, 13% from LANL, 7% from USGS, and 1% from UTEP. From this catalog I have identified 925 earthquakes with duration magnitude 2.0 or greater covering the region 31° N to 38° N and 101° W to 111° W (Appendix II). This restricted listing was used as the primary data for

Table 3-1. Applied Magnitude Adjustments for Events from Collaborated Institutes

Institute	Magnitude Adjustment	First Standard Deviation	Number of Events Compared
USGS	-0.185	0.395	182
LANL	0.104	0.332	28
UTEP	-0.453	0.409	7
ASL	0.397	0.275	7

the probabilistic seismic hazard analysis in Chapter 4.

Geographic Distribution of Earthquakes

A seismicity map based on the new catalog (Appendix II) is presented in Figure 3-1. The most striking feature of the seismicity in this figure is the tight cluster of earthquake activity in the Rio Grande valley near Socorro. This Socorro Seismic Anomaly (SSA) (Sanford *et al*., 1995) occupies only 0.7% of the total area but accounts for 27% of the earthquakes of magnitude 2.0 or greater in Figure 3-1. The SSA is believed to be the result of crustal extension over an inflating mid-crustal magma body. The magma body is ~150 m thick, ~19 km deep, and has a lateral extent of 3400 km^2 (Ake and Sanford, 1988; Hartse *et al*., 1992; Balch *et al*., 1997). Level-line data indicate that the surface above the magma body is undergoing uplift at a maximum rate of ~1.8 mm/year (Larsen *et al*., 1986) presumably because of injection of new magma into the thin extensive mid-crustal chamber.

In Figure 3-1 the pattern of seismicity outside the SSA is diffuse and well-defined seismic trends are not apparent. However, on the map of magnitude 3.0 or greater shocks (Figure 3-2), two interesting alignments of shocks do appear. Extending east-northeast from the SSA into the Great Plains of eastern New Mexico is a band of epicenters that straddles the trace of a prominent topographic lineation identified by Thelin and Pike (1991) on a digital shaded relief map they generated for the conterminous United States. The lineation, a possible fracture zone of Precambrian origin, extends 1400 km east-northeast from southwestern Arizona to the Texas Panhandle-Oklahoma border (Sanford and Lin, 1998). The ~85 km wide track of this feature is defined by a lineation of many features such as rivers, elongate depressions, faults, and probably the contemporaneous seismicity in Figure 3-1 and 3-2.

A large fraction of the earthquakes in northern New Mexico appear to be related to the Jemez lineament (Aldrich and Laughlin, 1984), a fracture zone that extends from

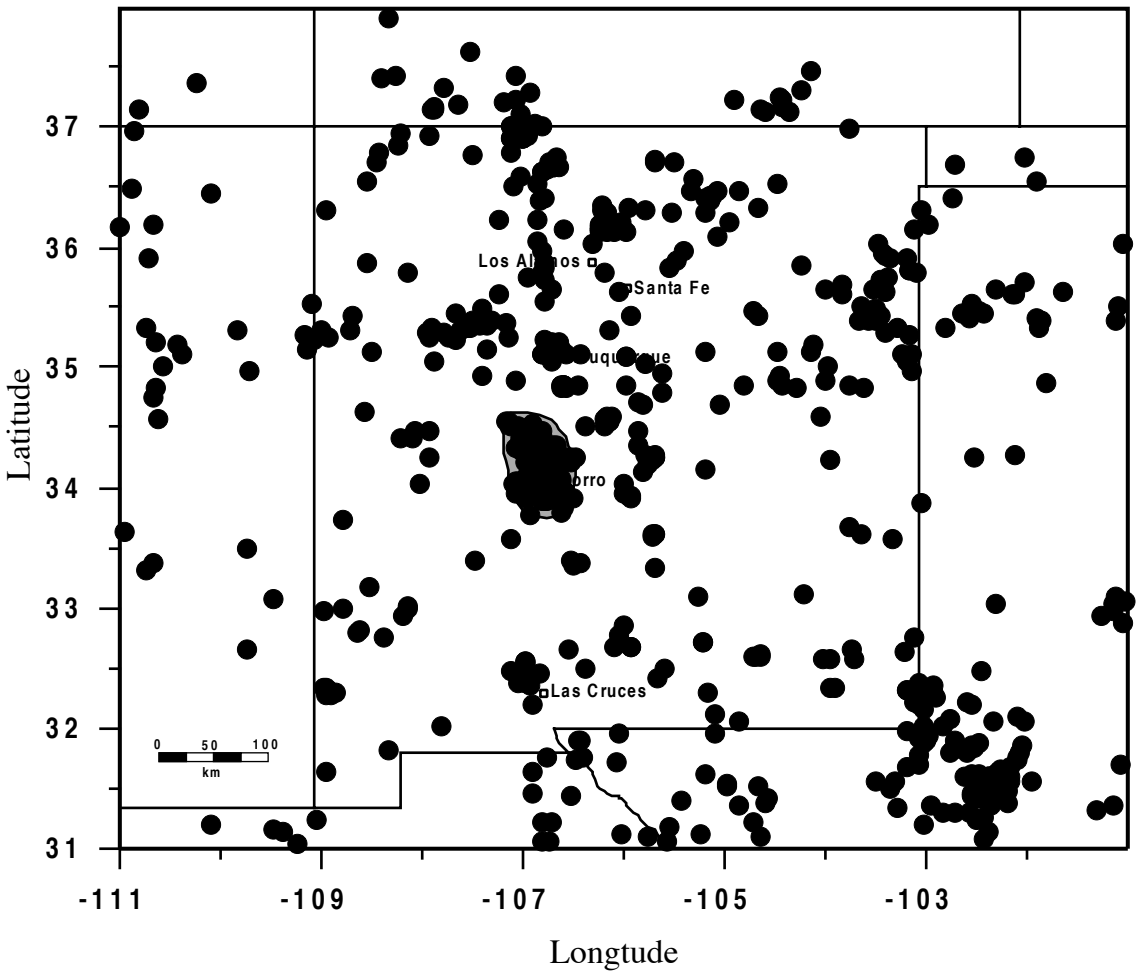

Figure 3-1. Seismicity of New Mexico and bordering areas; time period 1962-1998, moment magnitudes 2.0 or greater. A total number of 925 events are plotted on this map, 215 events inside the SSA (gray area).

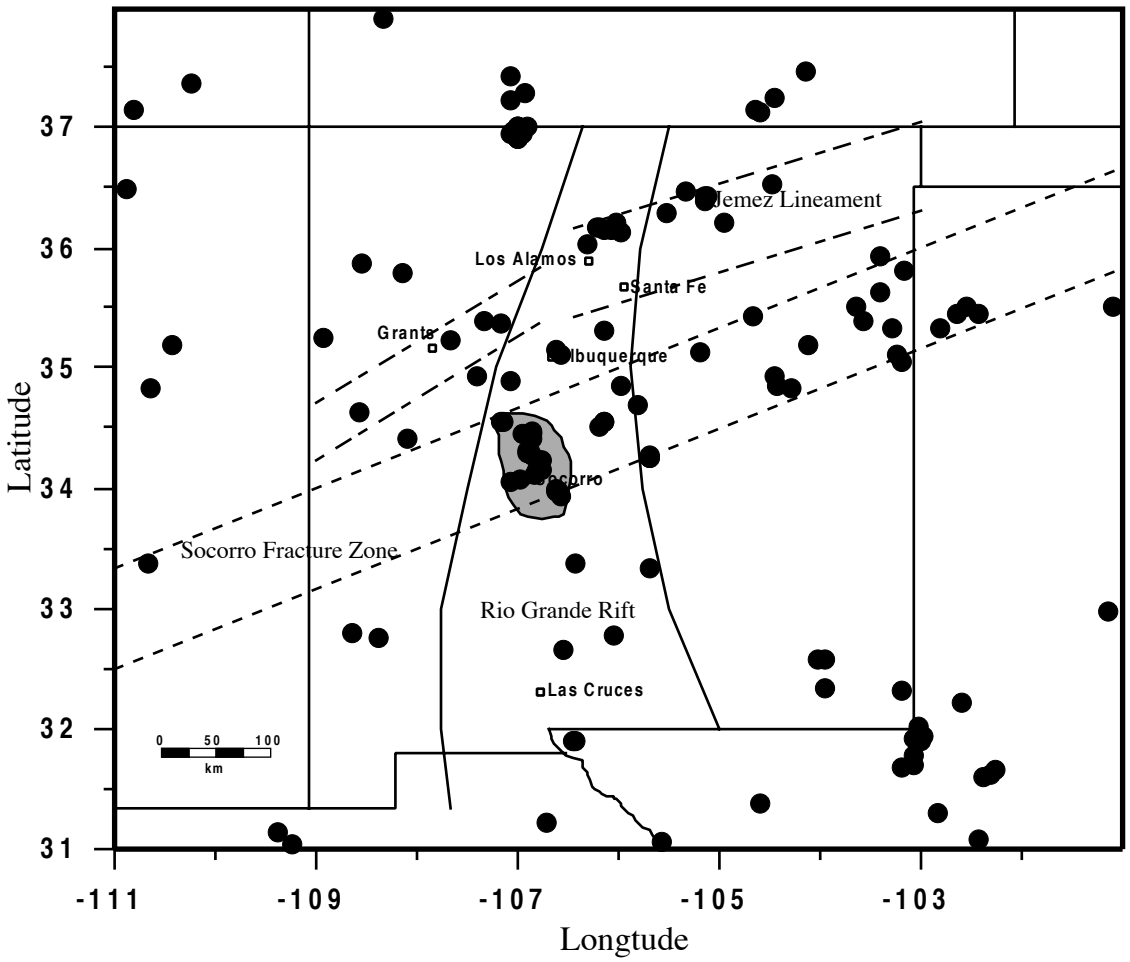

Figure 3-2. Seismicity of New Mexico and bordering areas; time period 1962-1998, moment magnitudes 3.0 or greater. A total number of 194 events are plotted on this map, 36 events inside the SSA (gray area). A total of 30 of the 158 events outside the SSA fall within the Socorro Fracture Zone. Also shown are the locations of the Rio Grande rift and the Jemez lineament.

southwest of Grants to Los Alamos and Espanola in the Rio Grande valley and then on along an east-northeast track to beyond the northeast corner of the state (Figure 3-2). The Jemez lineament is a 50 km to 80 km wide leaky fracture zone defined by many hundreds of magmatic eruptive centers, including the very large aseismic Jemez volcanic complex just west of Los Alamos (Sanford *et al.*, 1991).

It is unlikely that the SFZ and the Jemez lineament which occupy 20% of the total area would produce more than 40% of the seismicity outside the SSA. I have tested this possibility using a Monte Carlo technique. New Mexico and bordering areas were divided into small squares 10 km on a side. The earthquakes of magnitude 3.0 or greater located outside the SSA were randomly distributed over the region with no restrictions on the number of events in each block. This procedure was repeated nearly 1000 times without reproducing the distribution in Figure 3-2. Alignments of epicenter were generated but they were not as narrow nor did they contain as many earthquakes as appear along the SFZ and the Jemez lineament.

Perhaps the most unusual characteristic of earthquake activity from 1962-1998 is its failure to define the Rio Grande rift (RGR), a major continental rift extending north-south through the state from north of Taos to south of Las Cruces (Chapin, 1971 and 1979). The overwhelming majority of Quaternary faults in New Mexico (Machette *et al.*, 1998) are associated with the RGR and yet earthquakes are absent or nearly so over much of its extent; for example, from just south of Socorro to just north of Las Cruces.

Quality of Locations of Earthquakes

The program SEISMOS calculates a number of parameters that I have combined with other quantities to estimate the quality of the location: **R**, a measure of how well assumed errors in data match residuals; **1std epi**, epicenter error at one standard deviation; and **gap**, the maximum gap between recording stations in degrees. For the parameter **R**, a value greater than 1.0 indicates an underestimation of the assumed errors in the data and a

value less than 1.0 indicates an overestimation of assumed errors in the data. SEISMOS solutions with low **R** values generally overestimate the epicenter error and solutions with high **R** values underestimate the epicenter error.

Therefore, for assessing quality of location, I begin with a base value which is the product of **R** and **1std epi** and modify it according the factors **gap**, number of stations, and number of paired P and S arrivals. The procedure is outlined below:

1. **gap**-Maximum gap

   If **gap** <= 120 , multiply base by 1.0

   If 120 < **gap** <= 180 , multiply by 1.5

   If 180 < **gap** <= 240 , multiply by 2.0

   If 240 < **gap** <= 300 , multiply by 2.5

   If **gap** > 300 , multiply by 3.0

2. **N**-Number of stations recording earthquake

   If **N** >= 5, multiply by 1.0

   If **N** = 4, multiply by 1.5

   If **N** = 3, multiply by 2.0

3. **PS**-Number of paired P and S arrival times

   If **PS** >= 3, multiply by 1.0

   If **PS** = 2, multiply by 1.5

   If **PS** = 1, multiply by 2.0

   If **PS** = 0, multiply by 2.5

Modifications of the base epicenter error yielded values from less than 10 km to more than 40 km. I divided this error range into five categories as shown in the Table 3-2 and assigned the five qualitative designations of quality: Very Good, Good, Fair, Poor, and Very Poor. A map of epicenters with color symbols indicative of these five qualitative classifications is shown in Figure 3-3. A total of 585 events in the region with duration

Table 3-2. Classifications of Quality of Earthquake Locations

Modifications of Base Epicenter Error	**Number of Events**	**4. Assigned Quality**
err < 10 km	300	Very good
10 <= err < 20 km	117	Good
20 <= err < 30 km	73	Fair
30 <= err < 40 km	31	Poor
40 <= err	64	Very poor

magnitude of 2.0 or greater were evaluated.

The procedure I have followed to quantify quality of the locations is arbitrary in the choice of parameters used and the multiplication factors applied. However, it appears to yield values which are reasonable for the data set available. But these errors should not be interpreted as absolute because other factors, such as deviation of crustal structure from the assumed model, can produce locations which are not the true epicenters.

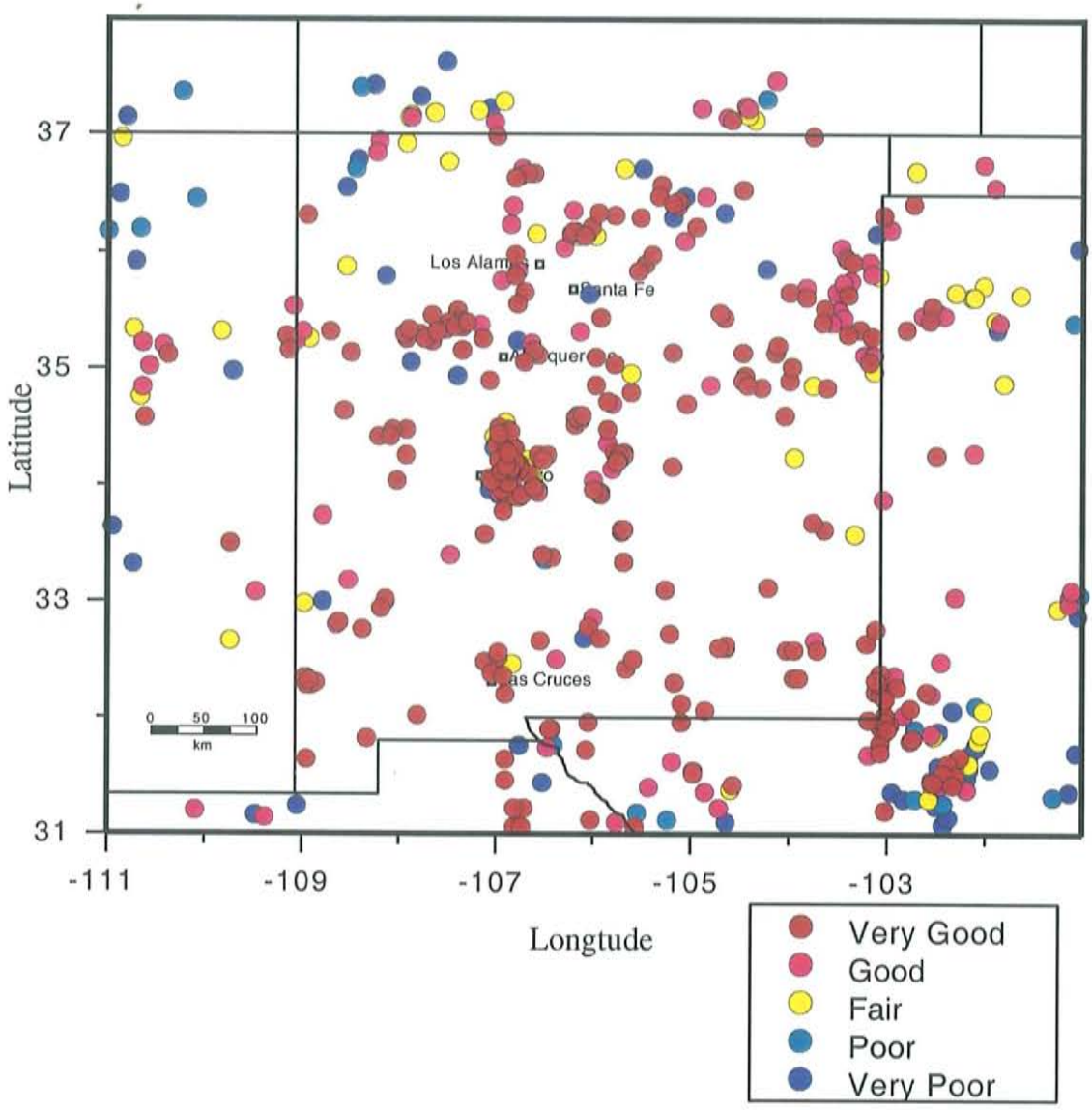

Figure 3-3. Quality of earthquake locations for the state of New Mexico and bordering areas; time period 1962 through 1998 and moment magnitudes of 2.0 or greater. For 585 mapped events, 300 are "Very good", 117 are "Good", 73 are "Fair", 31 are "Poor", and 64 are "Very poor".

4. Probabilistic Seismic Hazards for New Mexico Using Instrumental Data 1962 - 1998

The biggest challenge in estimating seismic hazards for New Mexico is to reconcile information collected on Holocene and Late Pleistocene fault scarps with modern earthquake data. Results of seismic hazard estimates based solely on fault scarp information or earthquake data are often contradictory (Machette, 1986; Lin *et al*., 1996; Lin *et al*., 1997). Therefore it is unwise to estimate short-term seismic hazards (tens of years) in New Mexico using data from active faults with latest movements approximately 6000 years or older, or to estimate long-term seismic hazards (hundreds of years) using 37 years of instrumental earthquake data from 1962-1998.

In this study I evaluated seismic hazards of New Mexico based on instrumental earthquake data from 1962 through 1998. The final products of this study are probabilistic seismic hazard maps showing peak horizontal ground accelerations at 10% and 2% probability of exceedance in a 50 year period. While the 10% probability map is best suitable for general purposes, the 2% probability map is designed for critical installations such as hospitals and schools.

This is the first chapter of a three chapter series on seismic hazards in New Mexico. A sensitivity study of the 50-year short-term estimates is discussed in the second chapter of the series (Chapter 5). Effects of active faults and pre-instrumental earthquakes (1869-1961) on short-term estimates and on long-term estimates will be discussed in the last chapter of the series (Chapter 6). In this chapter, I will describe the procedure for deriving probabilistic seismic hazard maps before introducing the final seismic hazard maps. In addition, I will present seismic risks associated with the highest seismic hazard area, the SSA, and a comparison between the NMT and the USGS hazard map.

Earthquake Data 1962-1998

The earthquake catalog for evaluating probabilistic seismic hazards is presented in Appendix II. The catalog is restricted to earthquakes of magnitude 2.0 or greater from 1962-1998 that occurred in New Mexico and bordering areas. The hazard analysis is restricted to earthquakes from the catalog that fall within the region shown in Figure 4-1. Earthquakes have occurred throughout this area and on the basis of the seismicity, boundaries between the major physiographic provinces are not defined. Among the recorded 681 events, 215 fall inside the boundary of the SSA. The ~5200 km^2 SSA occupies less than 1% of the total area of the region but accounts for about one third of its seismicity. Based on the distribution of seismicity in Figure 4-1, the region was divided into two source zones, the SSA and the rest of the state (RNM).

The complete catalog data for the 37 year period was the initial raw data for the seismic hazard analysis. Before I could utilize the earthquake catalog for hazard estimates, there were issues regarding the usability of the catalog that needed to be addressed.

Magnitudes. The magnitudes in the NMT catalog are directly or indirectly bound to the relation

$$M_D = 2.79 \log \tau_d - 3.63, \qquad (4\text{-}1)$$

where τ_d is the duration in seconds (Ake *et al*., 1983). This duration magnitude scale is based on New Mexico earthquakes and is tied to the local magnitude scale which is equivalent to the moment magnitude scale (Hanks and Kanamori, 1979). The latter is important because later in the chapter I use a moment magnitude-ground acceleration relationship to estimate ground accelerations for various sized earthquakes.

Completeness of data. The completeness of earthquake data was tested using the recurrence relation (Richter, 1958)

$$\log N = A - BM_l, \qquad (4\text{-}2)$$

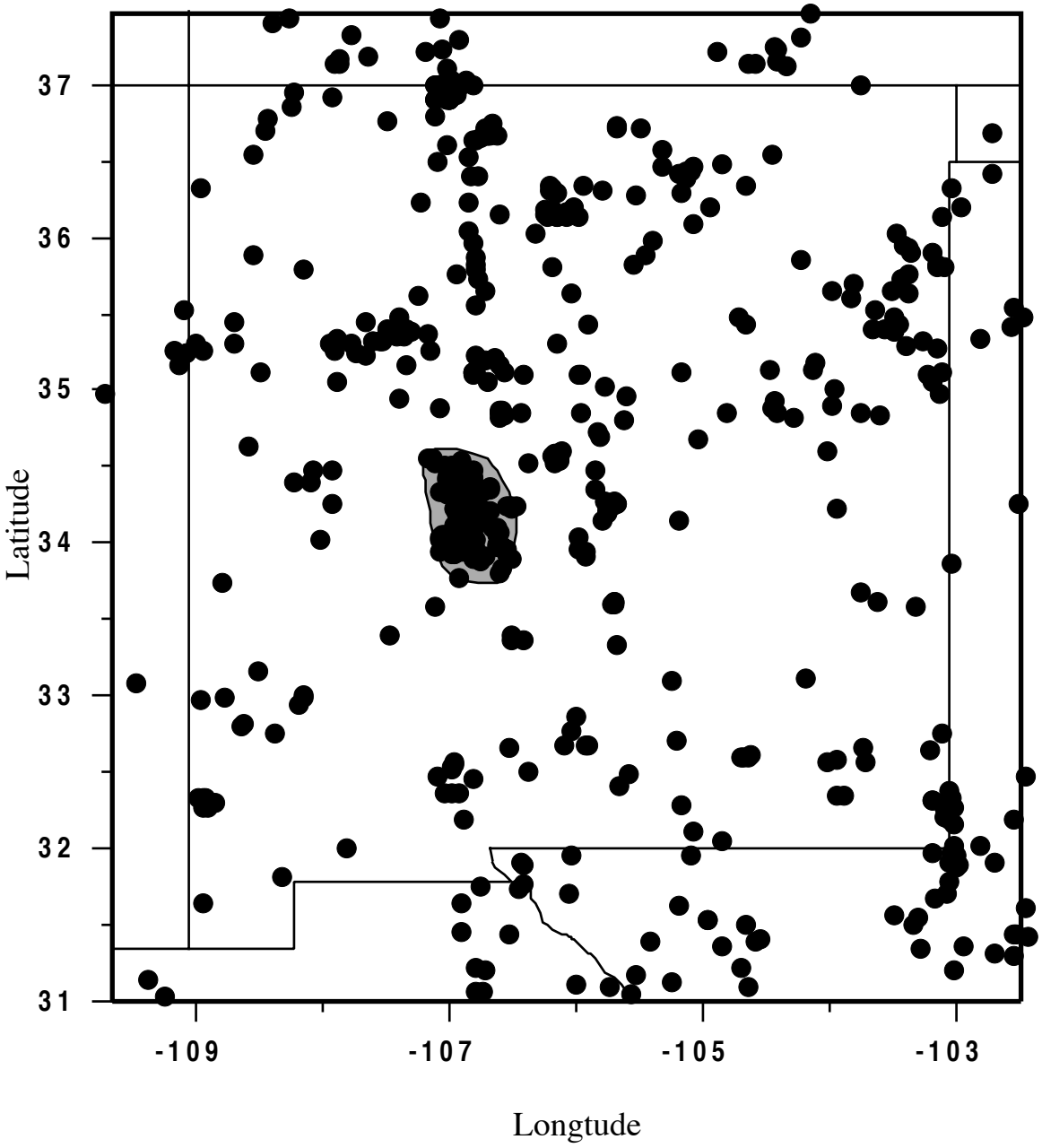

Figure 4-1. Seismicity of New Mexico from 1962 through 1998 with moment magnitudes greater than or equal to 2.0. The concentration of earthquake activity in the Socorro area accounts for 215 of the total 681 events in the region.

where N is the cumulative number of earthquakes. SSA and RNM data for the two time periods, 1962-1981 and 1982-1998, are shown in Figure 4-2 and 4-3 for two cut-off magnitudes, 1.3 and 2.0. The data were separated into these two time periods because of a marked improvement in instrumentation of the state beginning in 1982. The fall-off in cumulative number of events at magnitudes less than 2.0 for the time period 1962-1981 for both source zones indicates incompleteness of the earlier part of the data set below that magnitude. Therefore, in order to use the entire 37 years of data, it was necessary to restrict the analysis to the data set of magnitude 2.0 or greater.

Temporal variations in activity. The graphs of number of events versus time in Figure 4-4 clearly show that the level of activity has not been uniform for both the SSA and the RNM for the entire 37 year period. The seismicity for both source zones was temporally irregular at short and long intervals. For example, there were periods of up to two years without a magnitude 2.0 or greater shock within the SSA. The number of recorded events within the SSA for the period 1982-1998 was 147 which is significantly higher than the 68 shocks in the 20 year period 1962-1981. For the RNM, there were no very long term variations such as observed for the SSA, but intermediate-term variations with periods of ~5 years were recorded. The temporal variations illustrate the danger that exists in using short term histories of earthquake activity to estimate hazard.

Removal of dependent events. Aftershocks and swarm events were identified and removed using moving time-and-distance windows with parameters based on the spatial and temporal clustering of earthquakes from 1962-1998. For the SSA, earthquakes occurring within 7 days and 4 km of each other were removed from the data set leaving an event list of 125 earthquakes with magnitude 2.0 or greater. For the RNM, earthquakes occurring within 7 days and 25 km of each other were removed from the data set leaving an event list of 348 earthquakes with magnitude 2.0 or greater. Because the SSA had a tighter time-and-distance window than the RNM, more events were removed from the SSA (42%) than

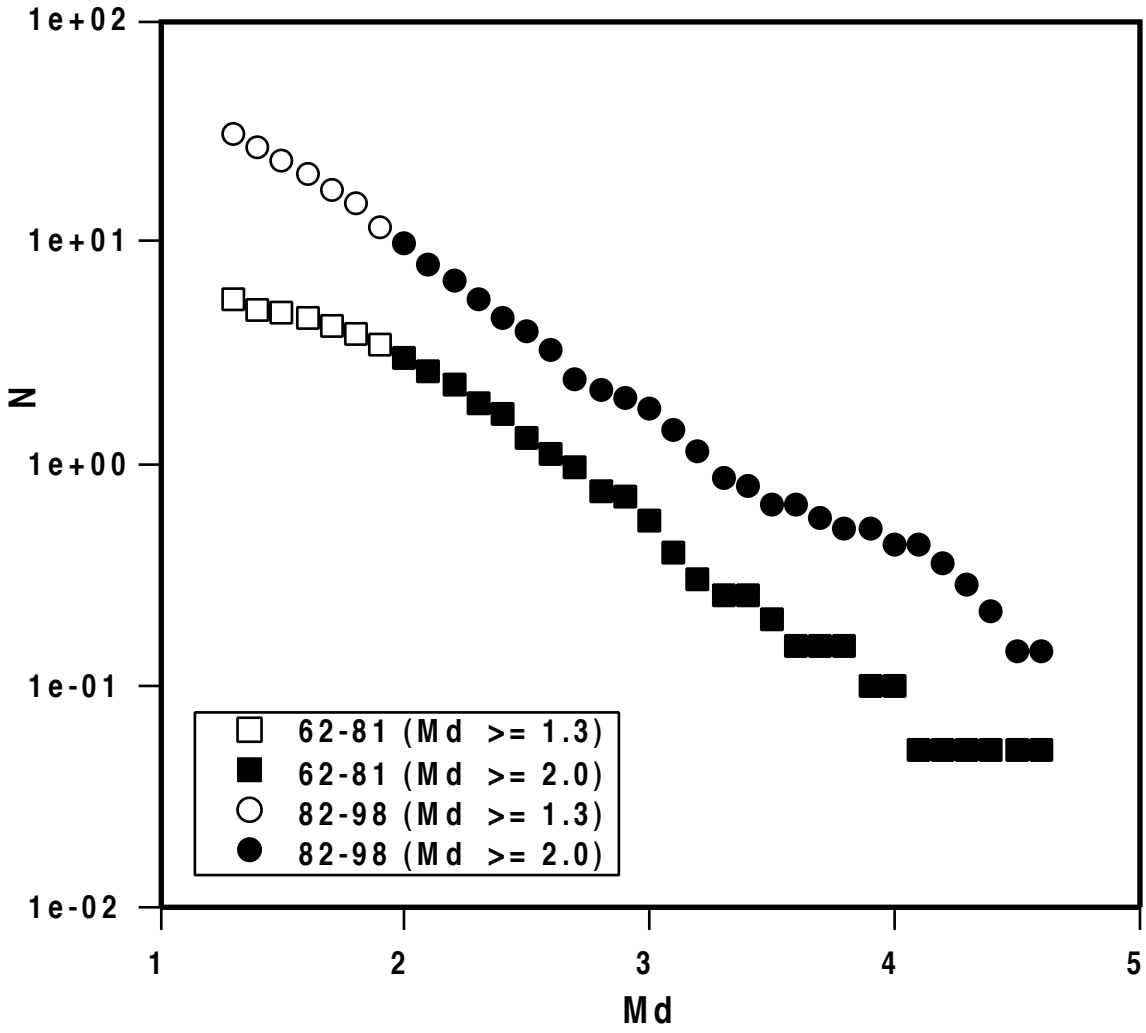

Figure 4-2. Annual recurrence relations for the SSA with different cut-off magnitudes and time periods. The fall-off in cumulative number of events at magnitudes less than 2.0 for the period 1962-1981 indicates incompleteness of the earlier part of the data set below that magnitude.

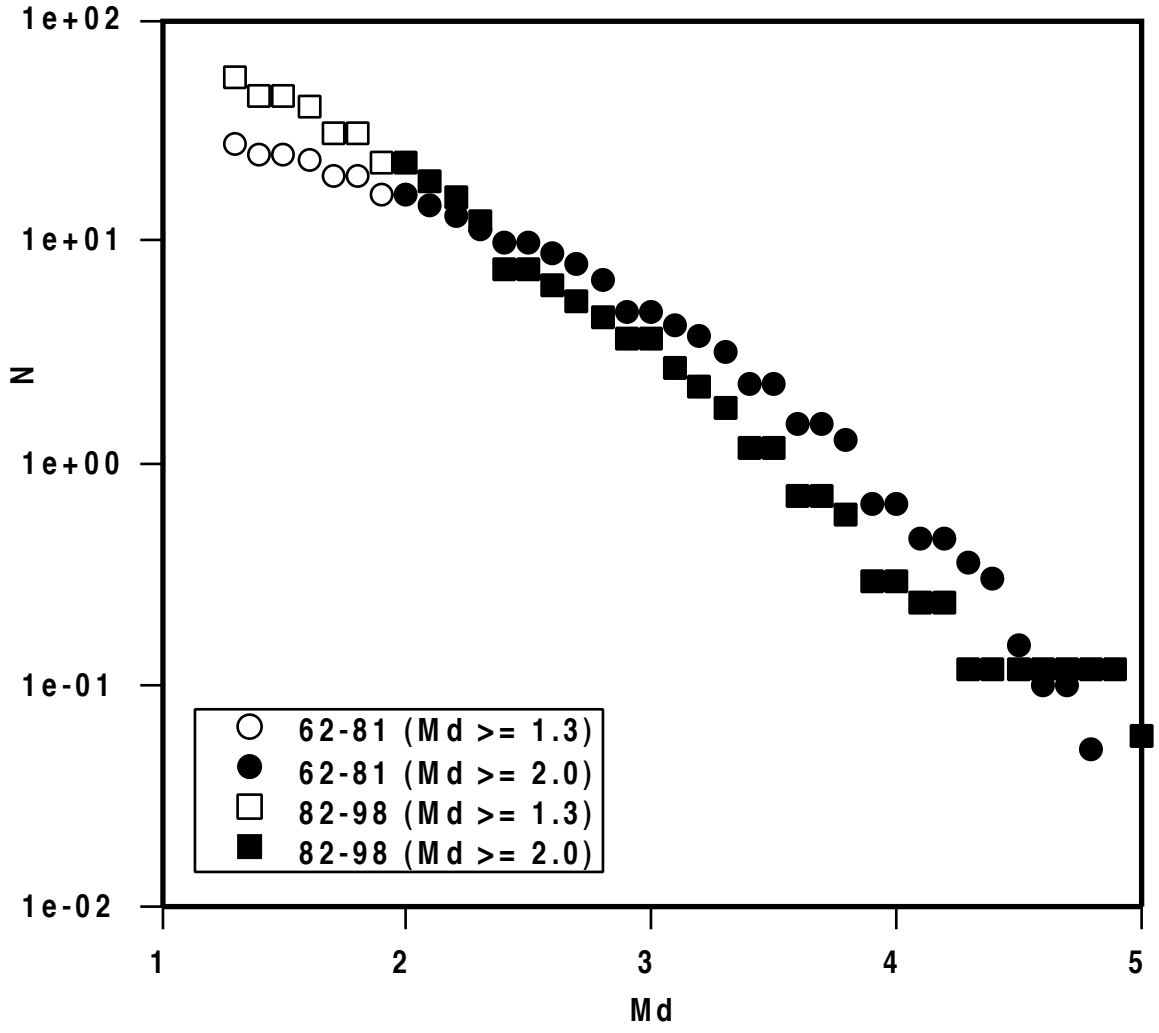

Figure 4-3. Annual recurrence relations for the RNM with different cut-off magnitudes and time periods. The fall-off in cumulative number of events at magnitudes less than 2.0 for the period 1962-1981 indicates incompleteness of the earlier part of the data set below that magnitude.

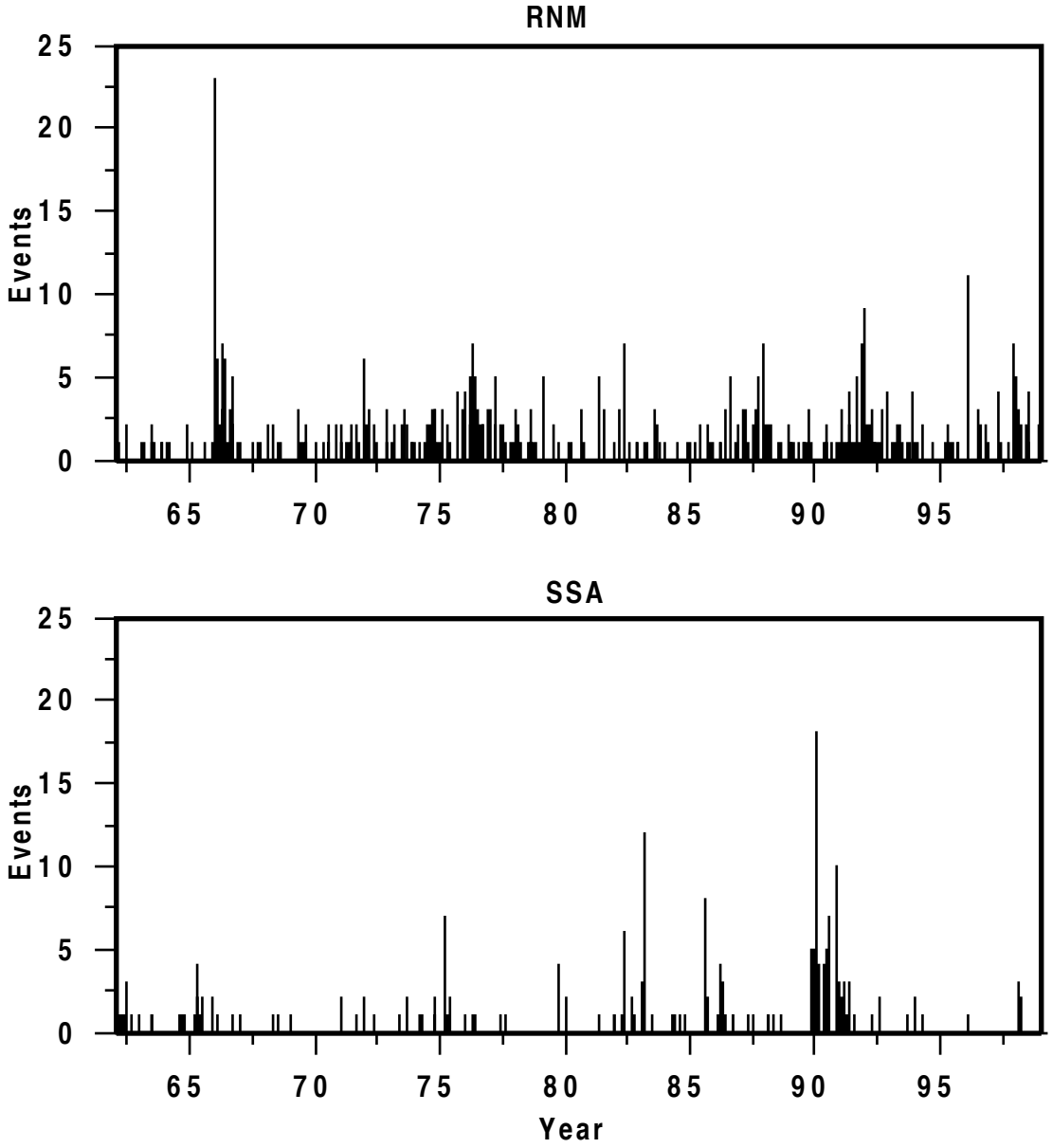

Figure 4-4. Temporal seismicity for the SSA and RNM with magnitude ≥ 2.0 for all recorded events. Individual peaks in the plots represent cumulated events per month. Original event list contains 466 events for the RNM (top) and 215 events for the SSA (bottom). Temporal variations in the number of recorded events for the two seismic source zones are mostly caused by earthquake swarms and aftershocks.

from the RNM (25%). Figure 4-5 and 4-6 illustrate how the removal of dependent events effects the spatial distribution and temporal variation of seismicity activity. Despite the fact that more than 30% of the events were removed from the original list, the distribution of seismicity almost remains unchanged. On the other hand, temporal variations in seismicity have been minimized as shown in Figure 4-6.

Figure 4-7a shows annual recurrence relations for the SSA and the RNM with a cut-off magnitude of 2.0 for the time period 1962-1998 with dependent events removed. Both seismic source zones show linear recurrence relations.

Recurrence Relation

A truncated exponential recurrence relationship (*Reiter*, 1990)

$$N(m) = N(m_o)\frac{e^{-\beta(m-m_o)} - e^{-\beta(m_u-m_o)}}{1 - e^{-\beta(m_u-m_o)}}, \qquad (4\text{-}3)$$

was used for the probabilistic seismic hazard assessment for both the SSA and the RNM. In equation (4-3), $N(m)$ is the number of earthquakes of magnitude m or larger, m_O and m_U are lower and upper bounds for the earthquakes, $N(m_O)$ is the number of earthquakes equal to the lower bound or greater and β is equivalent to the B value for the linear recurrence model based on natural rather than base 10 logarithms. The lower bound earthquake was set at magnitude 2.0, the cut-off for the 125 event data set for the SSA and the 348 event data set for the RNM. The upper bound was set at magnitude 6.5, the largest random earthquake likely to occur anywhere within the region in the next several hundred years.

For estimating slope B, I assumed a Poisson distribution and a magnitude bin size of 0.1. The uncertainty in the measurement of magnitudes was taken into account by using Bender's equation (Bender, 1983) for fitting β using magnitude grouped data,

$$f(k_1,k_2,....,k_n) = \frac{N!}{\prod_{i=1}^{n} k_i!}\left[\frac{1 - e^{-\beta\Delta m}}{1 - e^{-n\beta\Delta m}}\right]^N e^{-\beta\Delta m\sum_{i=1}^{n}(i-1)k_i} \qquad (4\text{-}4)$$

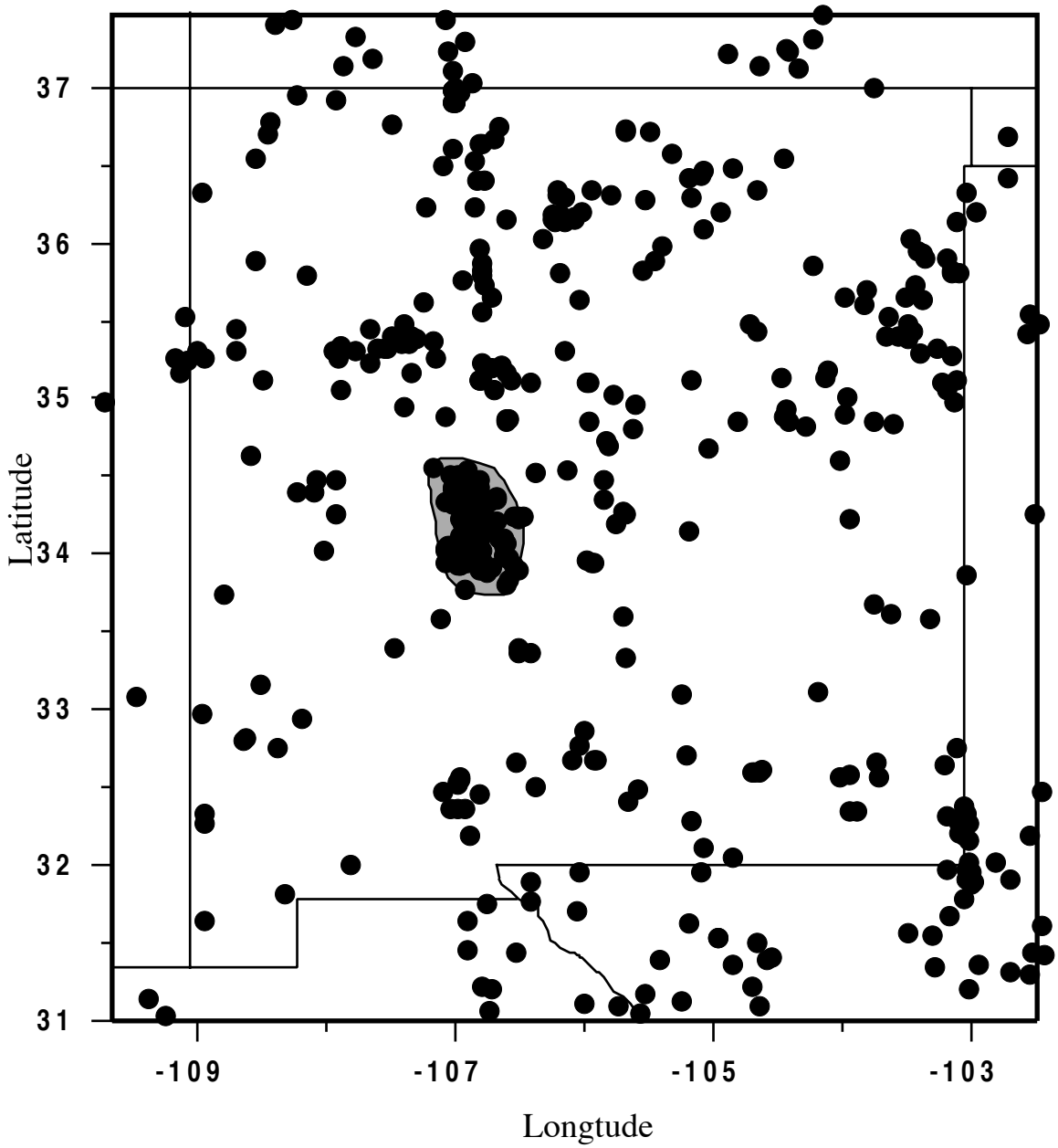

Figure 4-5. Seismicity of New Mexico from 1962 through 1998 with duration magnitudes greater than or equal to 2.0. Dependent events have been removed from the earthquake catalog. The final catalog contains 473 events (125 within the SSA).

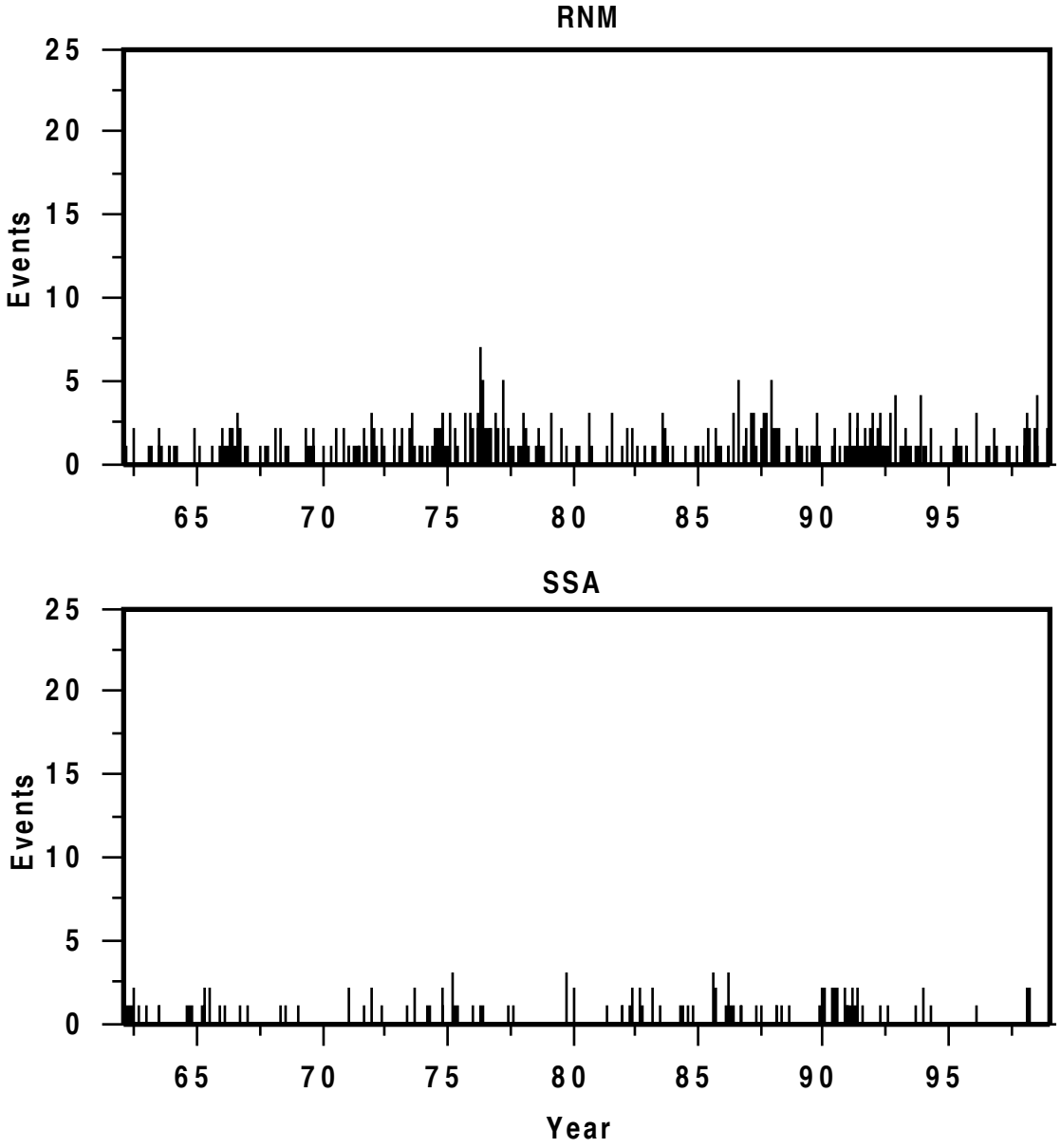

Figure 4-6. Temporal seismicity for the SSA and RNM with magnitude ≥ 2.0 after dependent events were removed. Individual peaks in the plots represent cumulated events per month. Original event list contains 348 events for the RNM (top) and 125 events for the SSA (bottom). Effects of temporal variations in the number of recorded events for the two seismic source zones have been minimized.

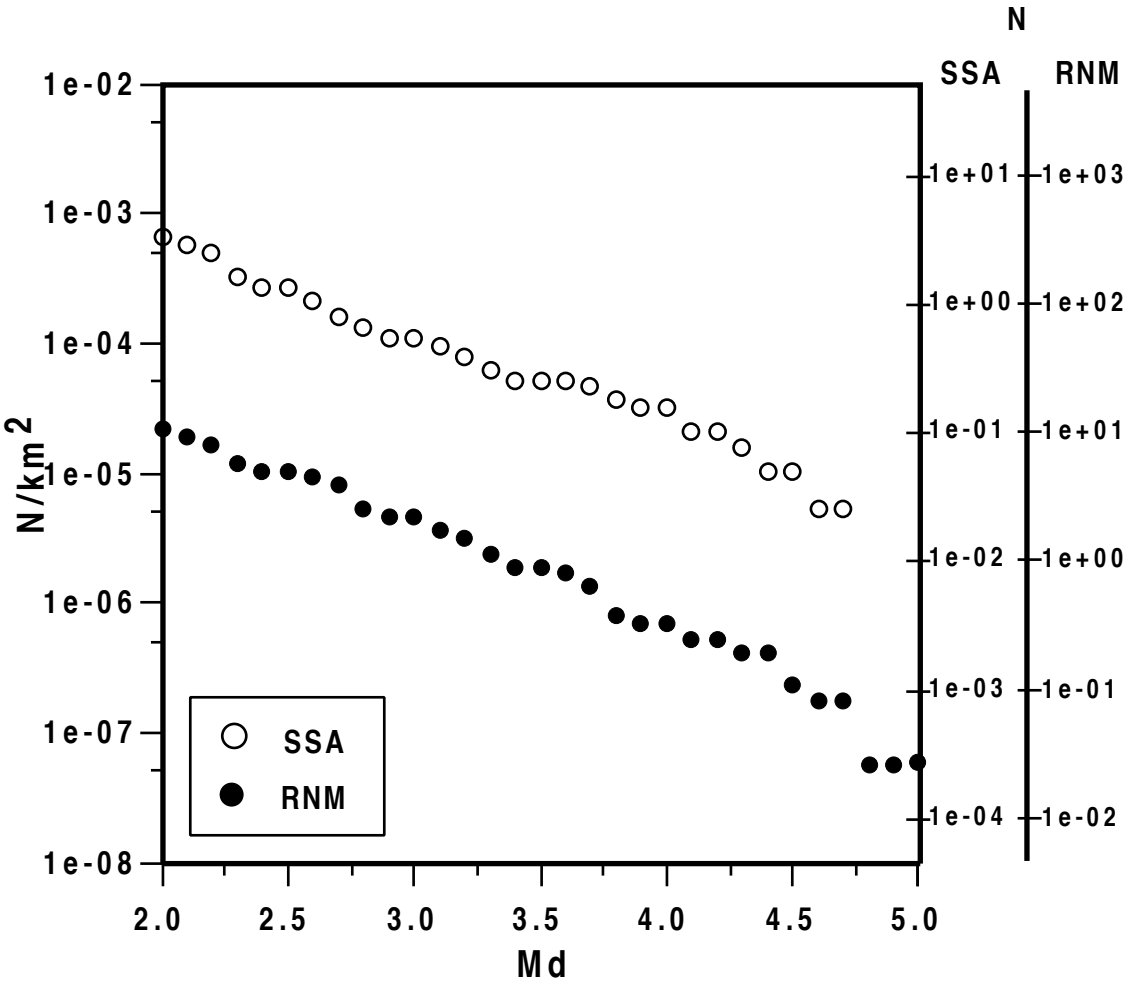

Figure 4-7a. Annual recurrence relations for the SSA and the RNM with a cut-off magnitude of 2.0 for the time period 1962-1998. Dependent events have been removed from the event list. The final catalog contains 473 events, 125 events are within the SSA. Earthquake data appear complete at magnitude 2.0 and above. Annual seismic density per square km for the SSA is about ~30 times higher than the RNM.

where k_i is equal to number of earthquakes in the *i*th magnitude bin interval. Equation (4-4) describes the probability of a particular combination of N magnitudes for a given population β. The maximum likelihood estimate of β is that value of β for which

$$\frac{\partial \log f(k_1, k_2, ..., k_n)}{\partial \beta} = 0 \qquad (4\text{-}5)$$

or the value for which

$$\frac{q}{1-q} - \frac{nq^n}{1-q^n} = \sum_{i=1}^{n} \frac{(i-1)k_i}{N} \qquad (4\text{-}6)$$

where $q = e^{-\beta \Delta m}$.

Figure 4-7b shows the maximum likelihood slope B for both the SSA and the RNM. It is clear that the two source zones have about the same slope B, the SSA is 0.8192 and the RNM 0.7023. However, the annual seismic density per square km for the SSA is about 30 times higher than the RNM. To simplify the computation process, I used a universal B of 0.7608 for the whole area, which is the mean B for the two source zones.

Probabilistic Ground Accelerations

For computing probabilistic ground accelerations for the region, I divided the area into small blocks of 20 x 20 km^2 and evaluated seismic hazards on the basis of blocks. The size of block was set so that it was large enough to accommodate maximum horizontal errors of epicenters for nearly all recorded earthquakes. Each block had its own recurrence relationship and during the hazard analysis interacts with the other blocks. Computational errors that arise when a gridded zone contains no events were avoided by assigning a level of background seismicity for the SSA and RNM equal to 25% of the average observed in each of these two source zones. Therefore, the cumulative number of events N in the recurrence model for each block is the combination of 75% of the events that occurred within the block and 25% background seismicity.

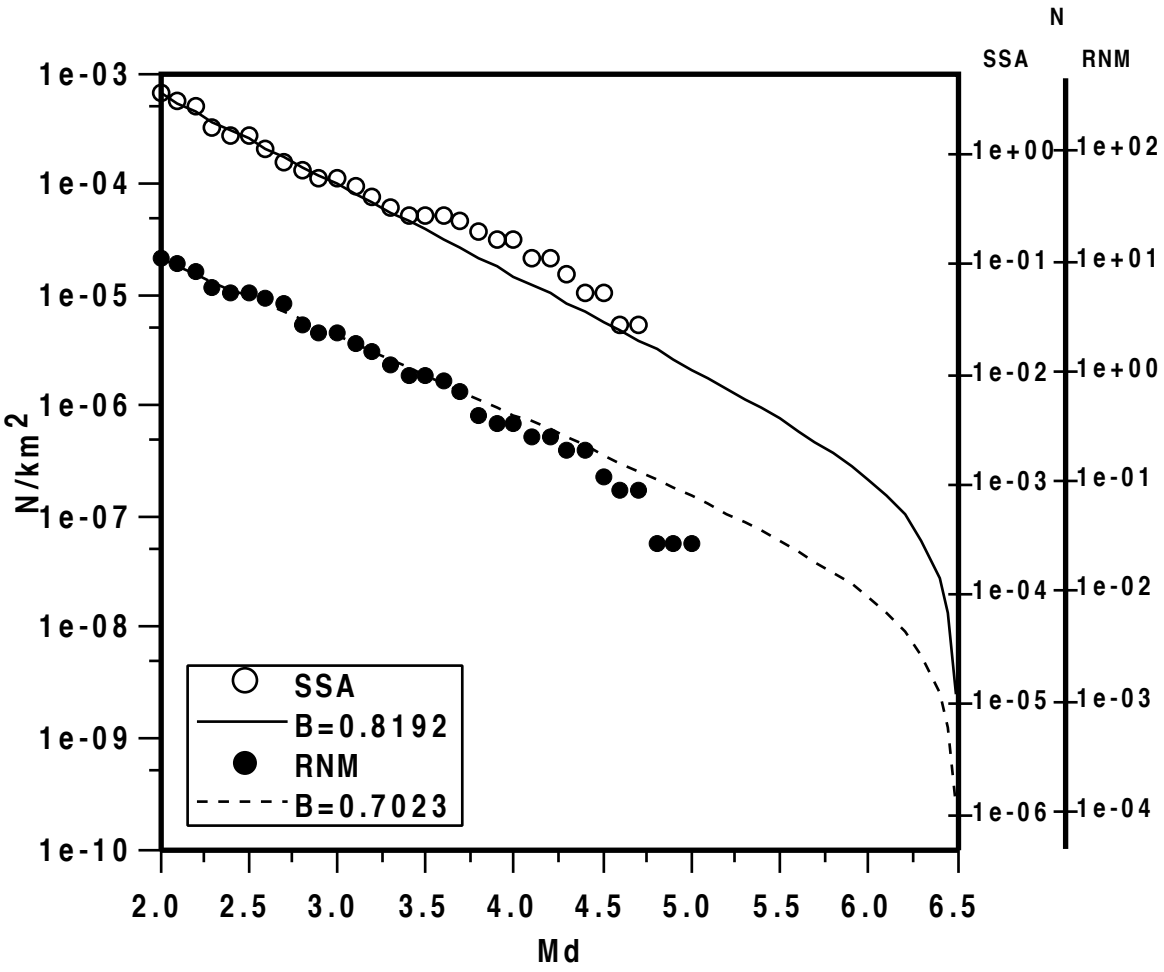

Figure 4-7b. Annual recurrence relations for SSA and RNM using the truncated exponential recurrence model. The maximum likehoods were derived assuming grouped magnitude data with equal observation periods from 1962 through 1998. Lower and upper bounds of magnitudes were set at 2.0 and 6.5, respectively.

Figure 8 shows the pseudo seismicity map based on micro-zoning of the study area. As shown in the figure, the distribution of seismicity is assumed uniform within each block and the level of darkness represents the annual $N(m_O)$ in equation (4-3).

Expected return intervals. Earthquakes with moment magnitudes of 4.0 or greater are considered capable of contributing to the seismic hazard. Therefore the interval between magnitude 4.0 and 6.5 was divided into magnitude bins with a size of 0.01 and the expected return intervals for each bin became

$$\tau = \frac{1}{N(m + \Delta m) - N(m)} \tag{4-7}$$

where Δm equals 0.01 in this study and the $N(m)$ values are annual rates of occurrence.

Probability of occurrence. Seismic hazard estimates were obtained by combining a temporal probability of occurrence with the spatial probability of occurrence. By assuming a Poisson distribution, each earthquake occurs independently of any other earthquake. Therefore, the temporal probability for each magnitude bin becomes

$$P_\tau = 1 - e^{-t/\tau} \tag{4-8}$$

where τ is the expected return interval and t the time periods of interest, which is 50 years in this study.

Ground acceleration footprints. Every earthquake will generate at the surface a roughly circular area within which the ground acceleration exceeds a value determined by the magnitude and depth of an earthquake. It is generally assumed that peak ground acceleration will occur during the arrival of the S phase, a body wave whose amplitude drops off inversely with the distance (R^{-1}) because of geometrical spreading and as e^{-gR} because of crustal absorption. An equation derived by Joyner and Fumal (1985) was selected to calculate peak horizontal ground acceleration

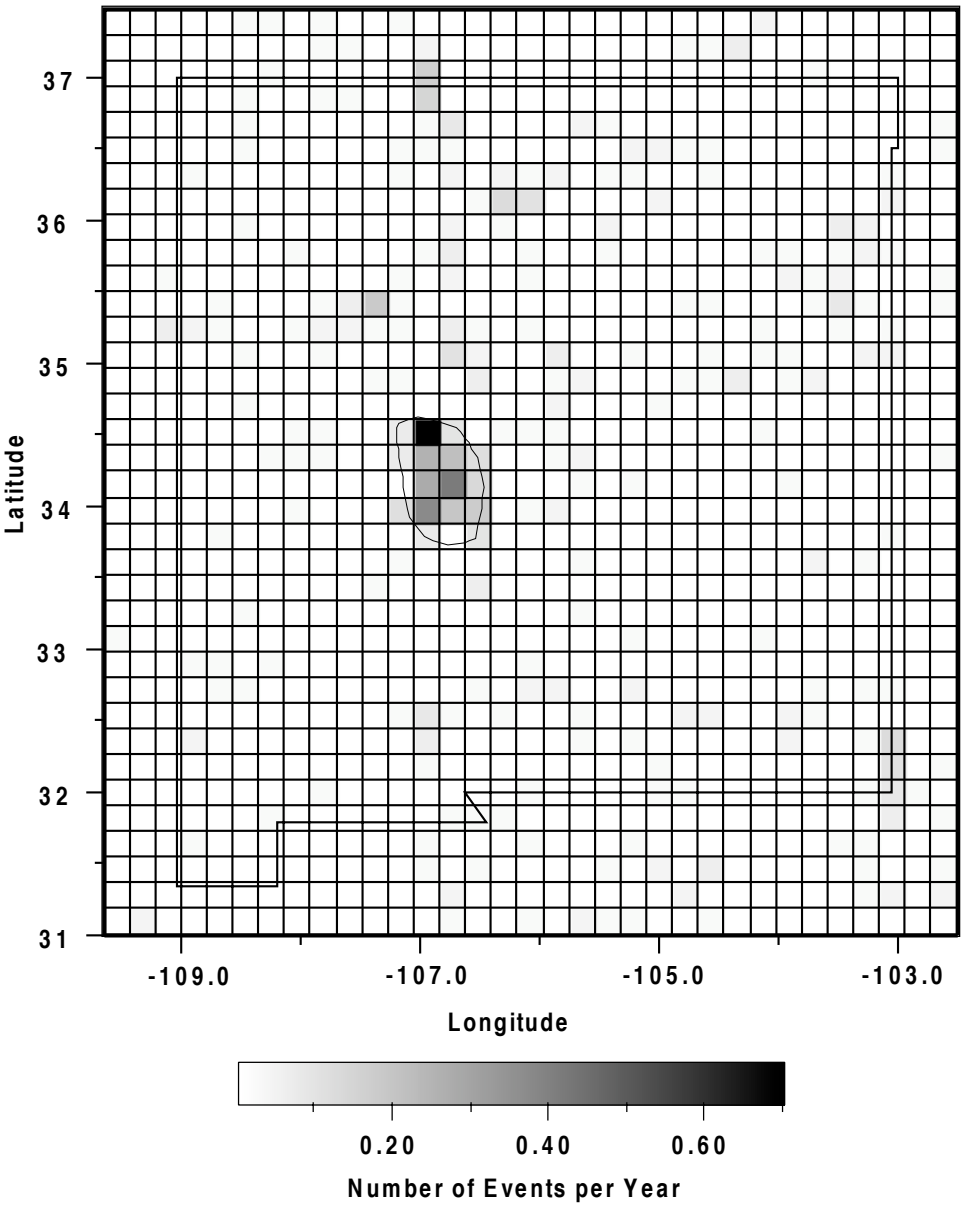

Figure 4-8. Micro-seismic source zones used in this study. 1188 micro-source zones with size of 20 x 20 km^2 were used in the study. The gray scale indicates expected recorded events of magnitude 2.0 and above per year. This model predicts 12.7 events of magnitude 2.0 and above annually for the entire region. Note that a swarm sequence is counted as one event.

$$\log a = 0.43 + 0.23(M_W - 6) - \log R - 0.0027R, \qquad (4\text{-}9)$$

M_W = moment magnitude,

$R = \sqrt{(R_o^2 + h^2)}$.

Equation (4-9) relates peak horizontal acceleration to the strength of the source (first and second terms), the inverse of hypocentral distance (third term), and crustal absorption (last term). I assumed that *h is* the vertical distance to the center of the rupture surface at 7 km and R_O in the horizontal distance from the recording site to the center of rupture surface.

Spatial probability of occurrence. probability of occurrence describes areas of influence for earthquakes of given magnitudes. The procedure for determining the areal probability that a prescribed acceleration will be equaled or exceeded at a specific point within or near a source zone can best be understood by considering a specific case. Figure 4-9 shows an example assuming that the SSA is the single source zone in the region and an earthquake of magnitude 6.0 occurs. This event will produce a footprint of 18 km radius with a perimeter acceleration of 0.13g. For purposes of calculating areal probabilities, it is important to note that the footprint also defines the region within which any earthquake of magnitude 6.0 can occur and produce accelerations ≥ 0.13g at the center of the region. Thus the probability that a magnitude 6.0 earthquake will produce an acceleration ≥ 0.13g at a point can be obtained from the ratio of the area of the footprint falling within the SSA to the total area of the SSA (Figure 4-9). If the footprint falls totally outside the SSA, the areal probability is 0, and if it falls totally within, the areal probability is the ratio of the footprint area (1033 km^2) to the total SSA area (5200 km^2) or 0.2. At the bottom of Figure 4-9 is a point just outside the boundary of the SSA, the areal probability for this point is 0.062.

Overall probability of occurrence. The overall probability that a prescribed level of acceleration will be equaled or exceeded in a 50 year period at a particular location was found from

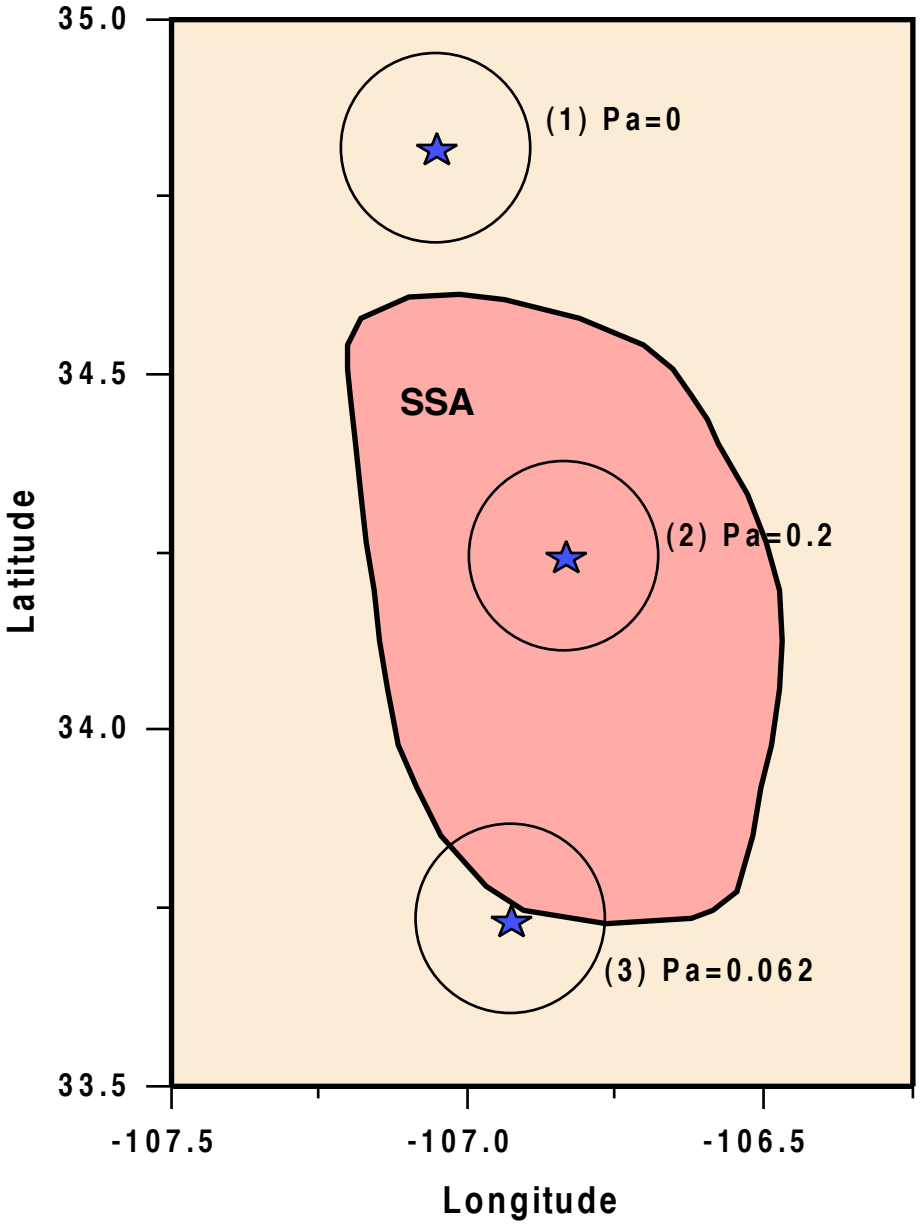

Figure 4-9. Areal probability (Pa) is defined as the ratio of the footprint area (1033 km^2) falling within the SSA to the total area of the SSA (5200 km^2). (1) The footprint falls outside the SSA, Pa=0/5200=0. (2) The footprint falls inside the SSA, Pa=1033/5200=0.2. (3) The footprint is 31% inside the SSA, Pa=(1033*0.31)/5200=0.062.

$$P_T = 1 - \prod_{i=1}^{n} P_i, \qquad (4\text{-}10)$$

where P_i is the product of the areal probability (P_a) and the Poisson probability ($1 - P_\tau$) (Equation 4-8) for the *i*th magnitude bin. In this study I evaluated seismic hazard using multiple source zones and allowed individual source zones to interact with each other. Therefore, the overall probability of occurrence in a 50 year period at a particular location becomes

$$P_T = 1 - \prod_{j=1}^{m} \prod_{i=1}^{n} P_{ij}, \qquad (4\text{-}11)$$

where *m* equals to the number of involved seismic source zones during the evaluation process.

For each block, probabilities of occurrence were calculated for ground accelerations ranging from 0.05g to 0.4g at 0.05g interval. Figure 4-10 illustrates a typical probability-ground acceleration curve derived for a specific grid. In this study, a total number of 1188 probability-ground acceleration curves were evaluated. Desired values of probability of ground acceleration can be interpolated directly from these curves.

Probabilistic Seismic Hazard Maps

Figure 4-11 and 4-12 show the seismic hazard maps in the format of peak horizontal ground accelerations at 10% and 2% probability of exceedance in 50 years. In general, seismic hazards for the area are considered from moderate to low. In the 10% probability map, the highest ground acceleration is 0.18g and the lowest is near 0g. Like for the distribution of seismicity, the physiographic provinces are not identifiable from the seismic hazard map. The area inside the SSA has the highest level of seismic hazard, 0.18g. Along the major population corridor of the state from Albuquerque to Santa Fe, the peak ground acceleration is ~0.08g, which generates Modified Mercalli Intensity (MMI) VI effects. In the 2% probability map, seismic hazard estimates increase substantially as was

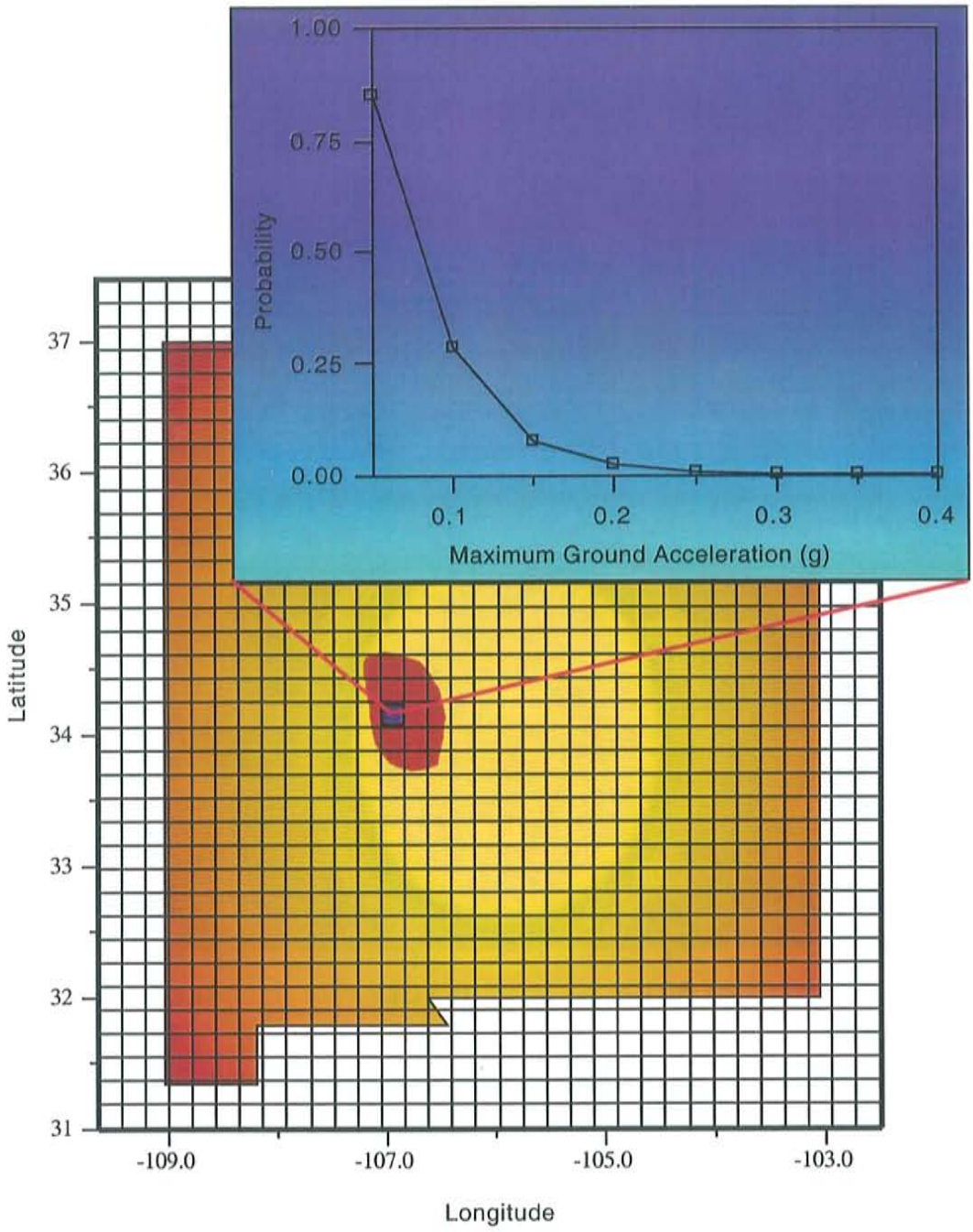

Figure 4-10. Schematic illustration of evaluation of probability-ground acceleration curves. A probability-ground acceleration curve was generated for each gridded area. Any desired value of probability of ground acceleration can be interpolated directly from the curve to represent the potential seismic hazard for the grid.

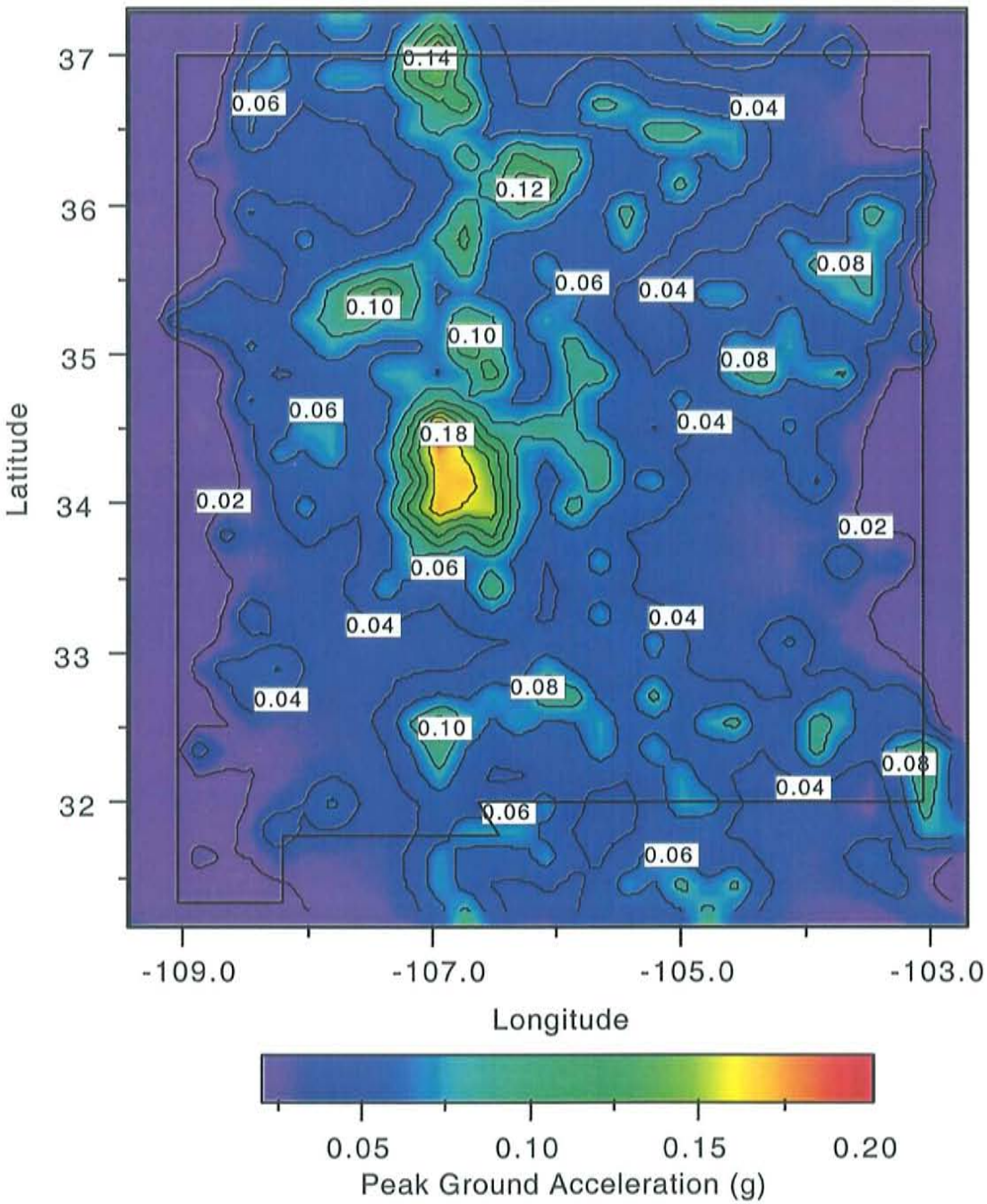

Figure 4-11. Probabilistic seismic hazard map for the state of New Mexico and bordering areas. The map is presented in the format of peak horizontal ground acceleration at 10% probability of exceedance in a 50 year period. The SSA has the highest level of seismic hazard: ~0.18g.

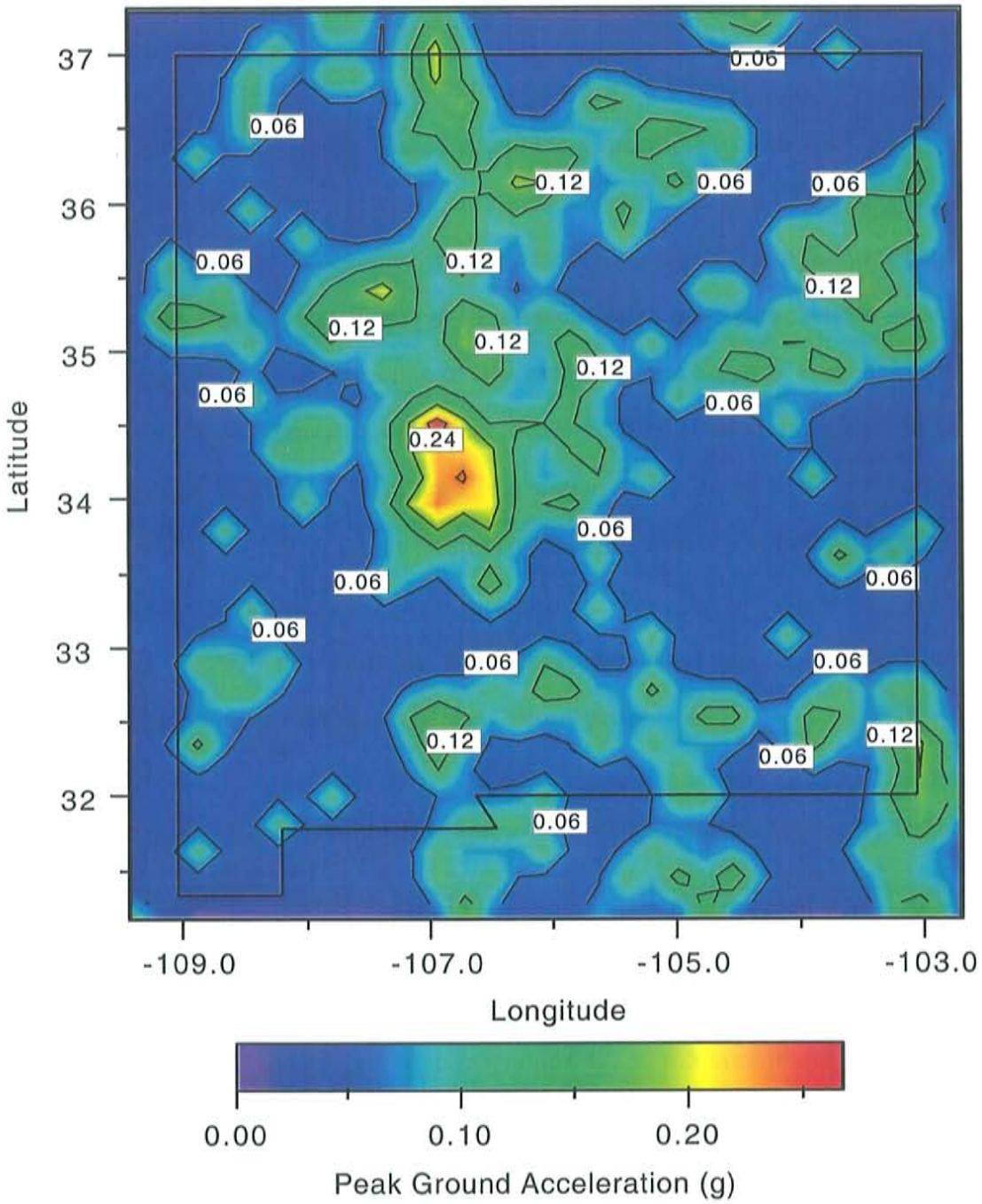

Figure 4-12. Probabilistic seismic hazard map for the state of New Mexico and bordering areas. The map is presented in the format of peak horizontal ground acceleration at 2% probability of exceedance in a 50 year period. The hazard map estimates over MMI VIII effects in the Socorro area and VI-VII effects in both Albuquerque and Los Alamos (see Appendix III).

expected. The highest level of seismic hazard inside the SSA increases from 0.18g to 0.26g, the latter producing MMI VIII effects.

I have selected six cities and two dam sites for detailed investigations. The selected cities consist of one town (Socorro) with the highest level of seismic hazard, three major population centers (Albuquerque, Santa Fe, and Las Cruces), two cities with nearby critical installations (Los Alamos and Carlsbad), and sites of the two largest dams (Elephant Butte and Navajo) in the state. Probability-ground acceleration curves for a 50 year period for these case studies are shown in Figure 4-13. As shown in the figure, seismic hazards for all study sites are considered moderate to low except for the Socorro area. The cities of Albuquerque and Los Alamos have the second highest level of seismic hazards but are considerably lower than the Socorro area. As shown in the figure, the estimated ground accelerations for the two cities are only comparable to the level of the Socorro area at lower probability of exceedance of ~2% in a 50 year period. This yields a much longer expected return interval of 2500 years for the cities of Albuquerque and Los Alamos than the expected return interval of 500 years for the Socorro area.

Seismic Risks

The SSA is the area with the highest level of seismic hazard in the state. The assessment for the area indicates that for a 50-year interval there is a 10% probability that horizontal accelerations will be 0.12g or greater within a NNW-oriented elliptical area extending from just north of San Antonio to Bernardo. Shown in Figure 4-14 is the distribution of earthquakes ranging from magnitude 4.0 to 6.5 contributing to the probable ground acceleration of 0.12g for the Socorro area at 10% probability of exceedance in a 50 year period. The dominant-magnitude earthquake in the figure is 4.9 and is equivalent to MMI VII effects. Listed below are some expected risks from MMI VII effects:

1. Significant damage to adobe structures and walls; some damage to ordinary masonry structures.

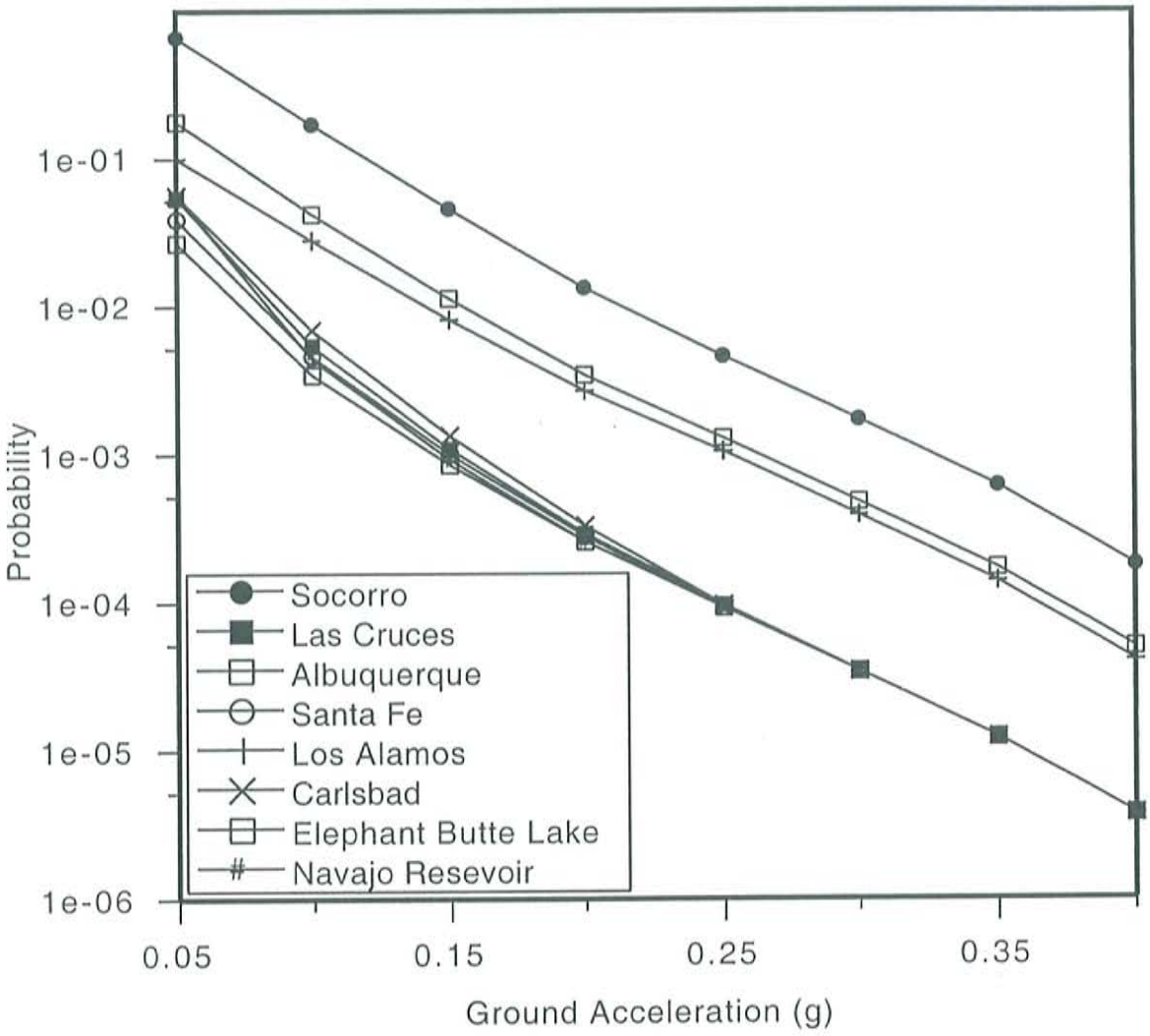

Figure 4-13. Probability-ground acceleration curves for six population centers and two dam sites for a period of 50 years. Two of the population centers are located near critical installations. The Socorro area has the highest seismic hazard among selected cities; Albuquerque and Los Alamos are second. The remaining population centers (Las Cruces, Santa Fe, and Carlsbad), and the two dam sites have nearly the same level of hazard.

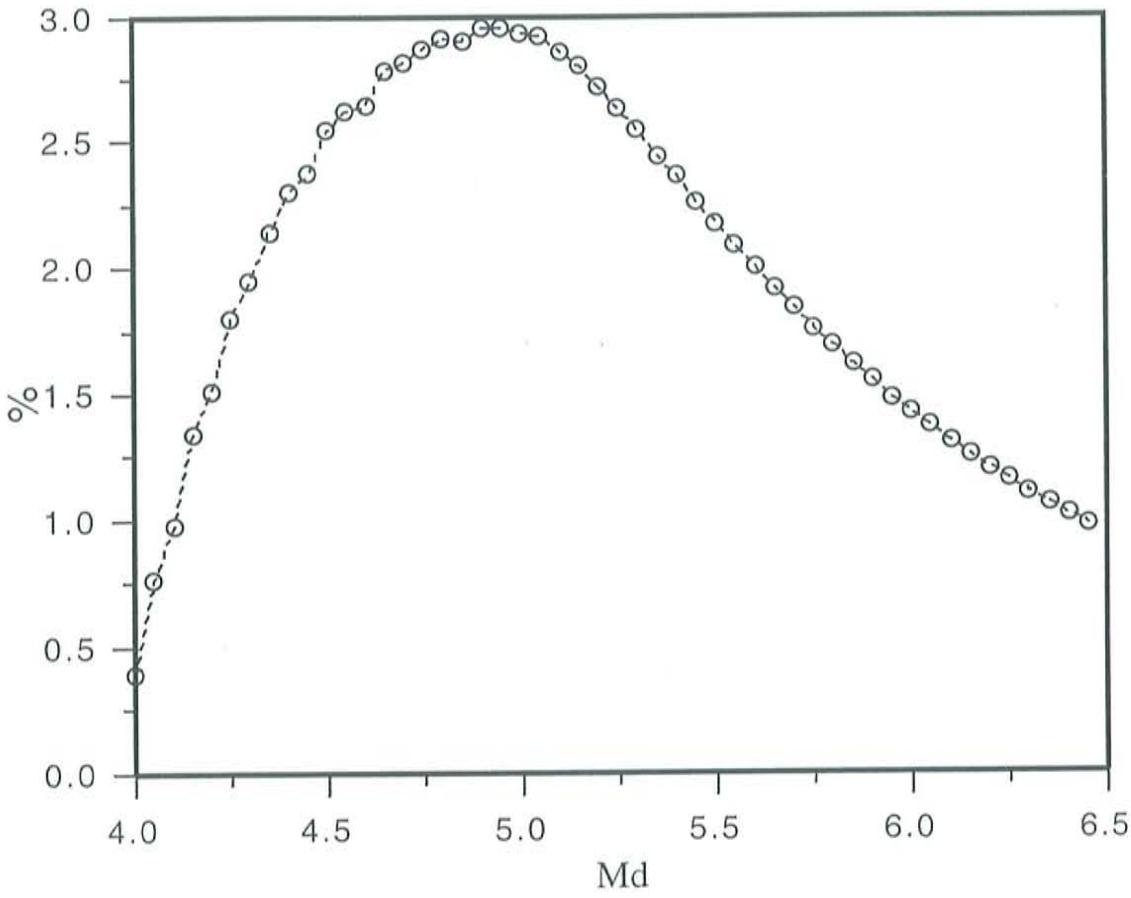

Figure 4-14. Distribution of earthquakes at various magnitudes contributing to the seismic hazard estimate for the Socorro area, which is 0.12g at 10% probability of exceedance in a 50 year period.

2. Fall of plaster, loose bricks, clay roof tiles, cornices, unbraced parapets, chimneys, etc.

3. Damage to concrete irrigation ditches.

In modern well-designed buildings, structural damage is unlikely from horizontal accelerations on the order of 0.12g. On the other hand, injuries and property loss from non-structural damage can be significant. Examples of non-structural damage at 0.12g that have the potential to produce serious injuries and/or loss of property are:

1. Rupture of gas lines.
2. Fall of suspended room heaters, coolers, fans, lighting fixtures, etc.
3. Breakage of containers of hazardous materials (chemical, medical, etc.).
4. Fall of book shelves, library stacks.
5. Broken windows, glassware.
6. Rupture of fire sprinklers and distribution lines.

Comparisons of Hazard Estimates

I compared the hazard estimates presented in this chapter with hazard estimates published by the USGS. For the Socorro area, the peak horizontal ground acceleration on the NMT seismic hazard map (50 years; 10% probability of exceedance) is 0.18g which is only slightly higher than the 1990 value on the equivalent USGS probabilistic hazard map (Algermissen *et al*., 1990). By contrast, the 1996 USGS probabilistic map estimates a horizontal acceleration for the Socorro area of 0.12g (Frankel *et al*. 1996), only 55% of the NMT estimate. Figure 4-15 shows the USGS hazard map covering the state of New Mexico. It is clear that the NMT hazard map is more complex and the estimated ground motions greater than the USGS map. However, these two maps generally agree on the areas with the highest seismic hazards.

Three important subjective parameters dictate differences in these maps, the cut-off magnitude, the level of smoothing, and the choices of seismic source zones.

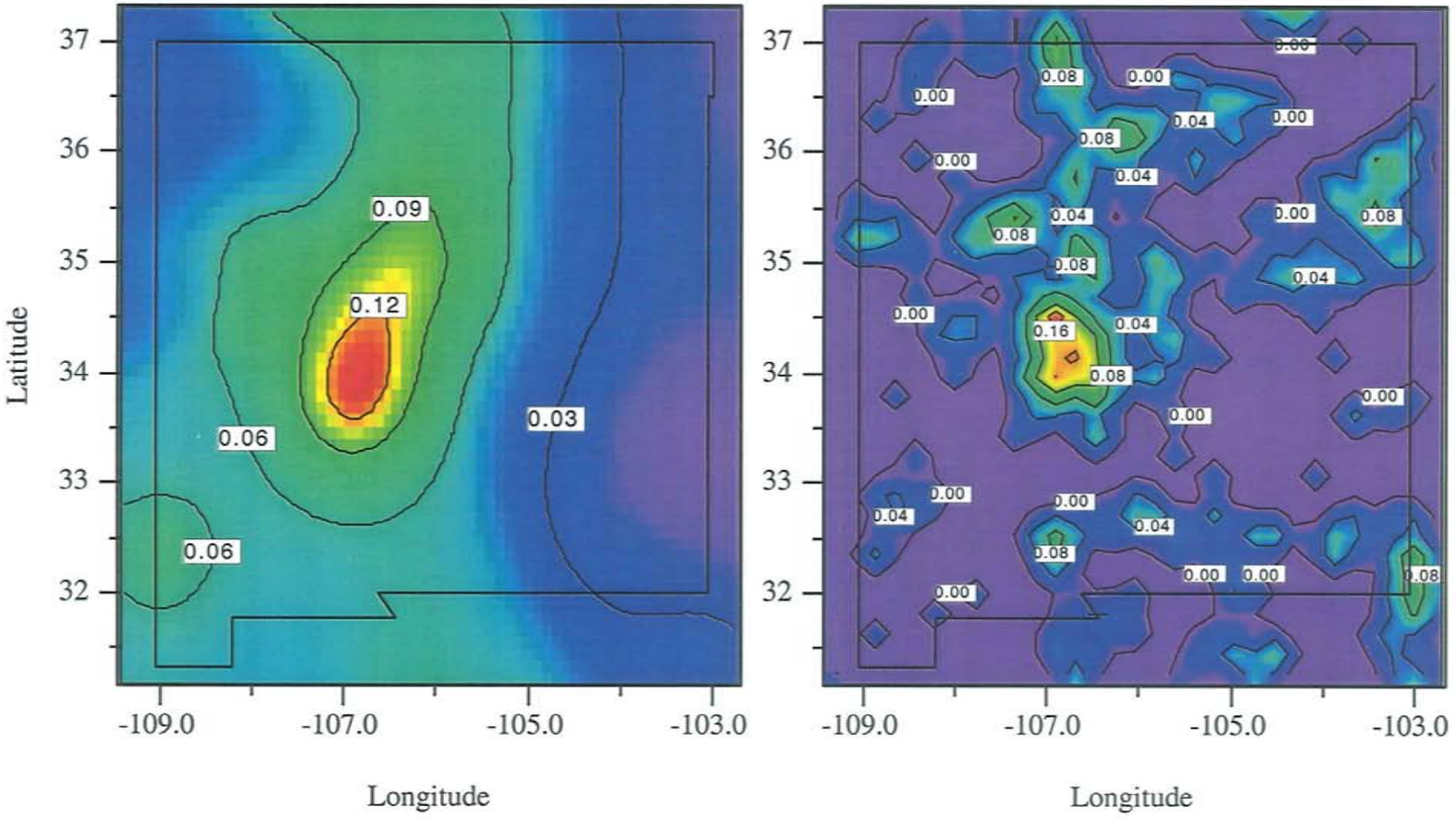

Figure 4-15. Probabilistic seismic hazard maps generated by NMT (right) and USGS (left) at 10% probability of exceedance in a 50 year period. The NMT is more complex than the USGS map and has higher estimated ground motions but both maps generally agree on the areas with highest seismic hazards.

1 he cut-off magnitude for the NMT hazard map is 2.0 and for the USGS it is 4.0. Figure 4-16 shows the recurrence relationship derived using earthquake data with a cut-off magnitude of 2.0. The total number of recorded events of magnitude 2.0 or greater in the region is 681 but only 20 events have magnitudes of 4.0 or greater. Thus, the New Mexico region with its moderate seismic activity and short 37-year record, a high cut-off magnitude may not leave enough data to reveal actual trends of seismicity.

2. The level of smoothing on the USGS map is substantially greater than on the NMT map. For the NMT map, the grid size was set at 20 x 20 km^2. Each block within the grid contains the actual event count for that block and was allowed to interact with other blocks during the process. In the USGS map, grid size was set at 0.1 degrees (approximately 10 x 11 km^2). Gaussian smoothing with a radius of 50 km was applied to the data set and no interactions among blocks was assumed during the process. This procedure produces lower upper bounds and higher lower bounds on the USGS seismic hazard map. The differences between these two maps are ~0.07g on the high end and ~0.02g on the low end. For the Socorro area, we suspect the recent USGS assessment of hazard is smaller because they have elected to distribute the seismicity of the SSA over a large area, perhaps a good fraction of the Rio Grande rift in New Mexico.

3. The third major factor that has affected the seismic hazard estimates is the choice of seismic source zones. For the NMT hazard map, I selected seismic source zones based on the distribution of seismicity. Therefore only two zones appeared justified for my analysis, the SSA and the RNM. Figure 4-17 shows the source zones selected by the USGS. New Mexico was divided into three source zones that generally follow boundaries of the Colorado Plateau, the Basin and Range including the Rio Grande rift, and the Great Plains. The selection of different seismic source zones is the main reason for the major contrasts in the two maps. Perhaps the difference is greatest for the eastern one-third of the state because of the north-south boundary between the Basin and Range and the Great

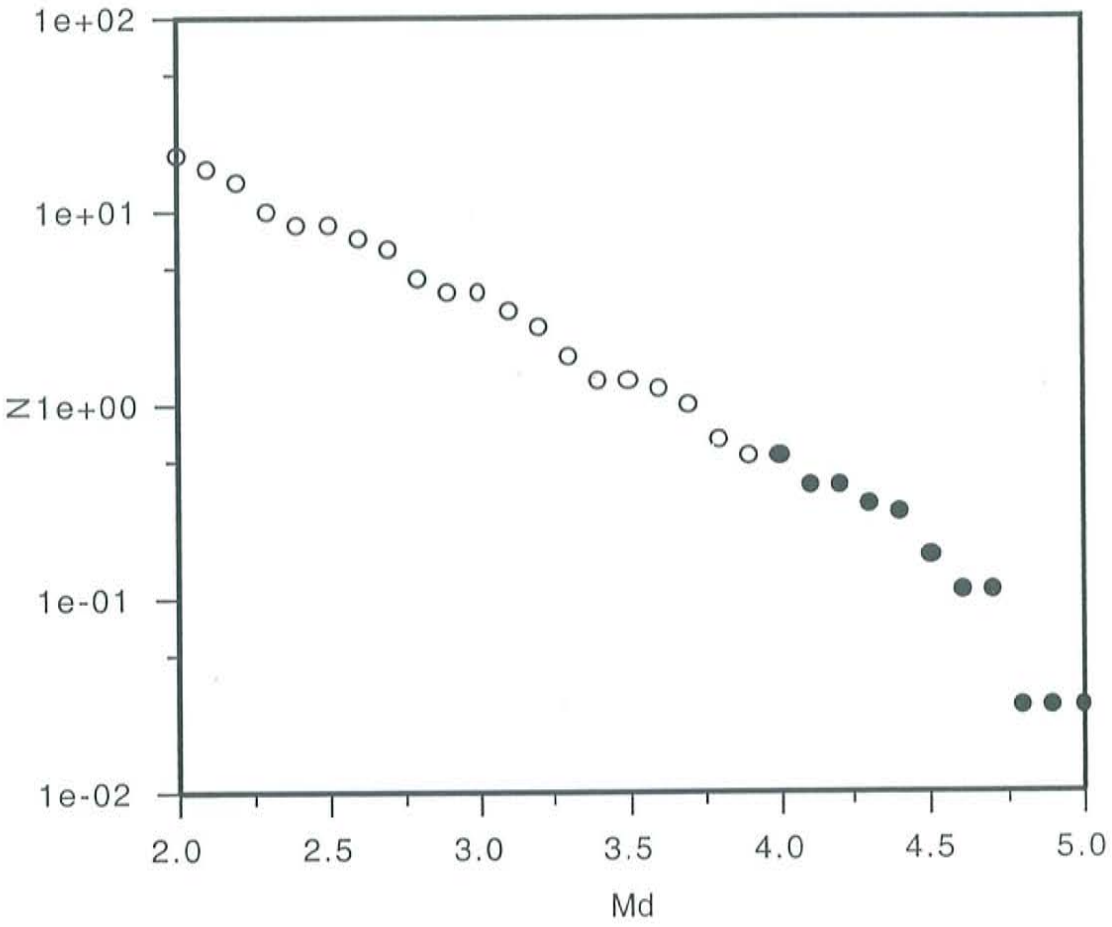

Figure 4-16. Annual recurrence relationships for earthquake data sets used by NMT and the USGS for estimating seismic hazards in New Mexico. A cut-off magnitude of 2.0 was used at NMT and the earthquake catalog contained 681 events. The USGS catalog used a cut-off magnitude of 4.0 which yielded only 20 events for the entire region.

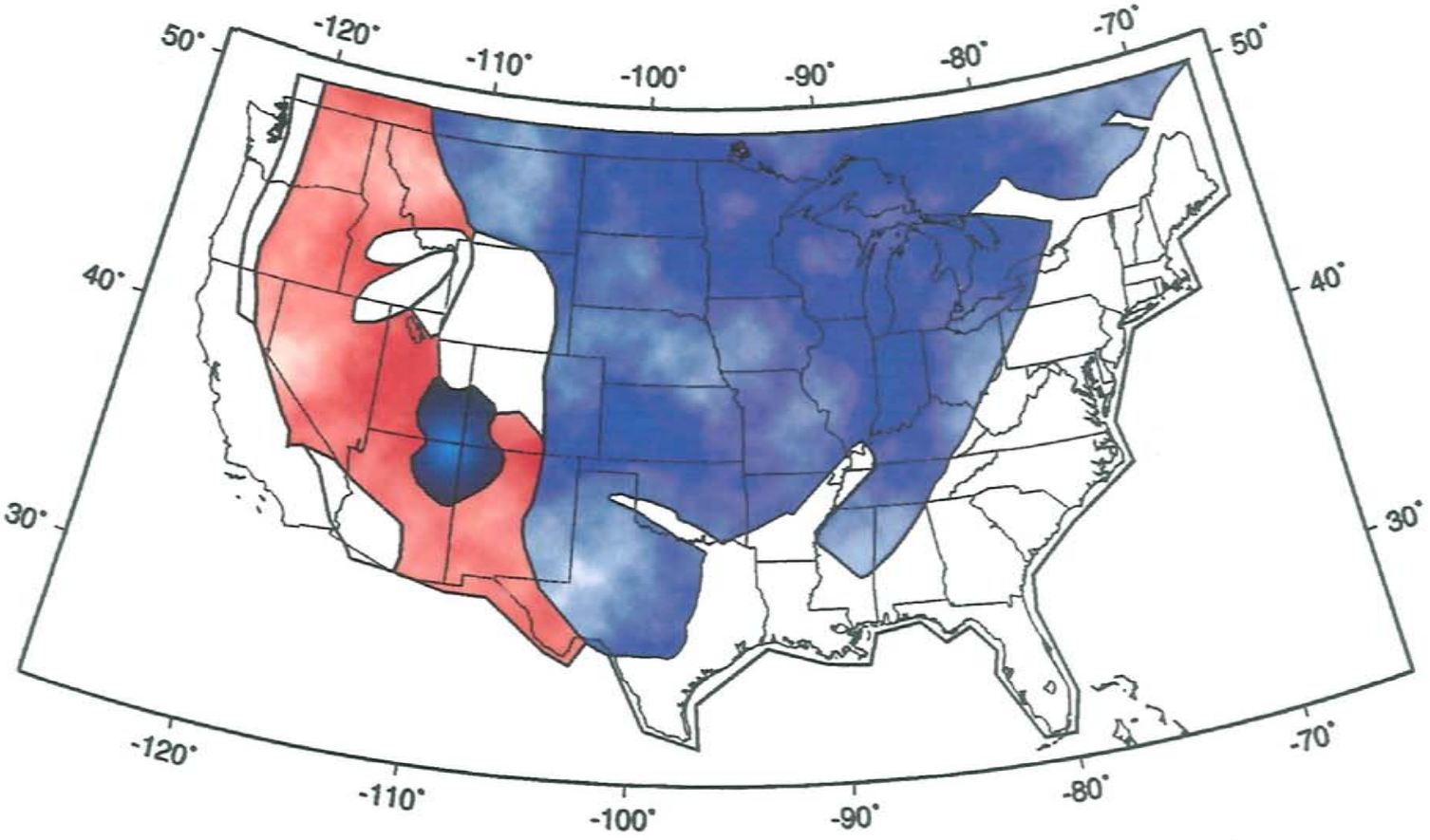

Figure 4-17. Background seismic source zones selected by the USGS. New Mexico was divided into three source zones: 1. Colorado Plateau zone in northwestern New Mexico; 2. Basin and Range zone including the Rio Grande rift; and 3. The Great Plains zone covering eastern New Mexico. In the NMT hazard map, only two source zones, the SSA, plus the rest of the state (RNM) were used.

Plains seismic source zones on the USGS map. On the USGS map there is a rapid eastward dropoff in seismic hazard along this boundary because the background seismicity for the Great Plains is much lower than for the Basin and Range. The NMT map does not show this uniform dropoff in seismic hazard because there is only one source zone for the entire area except for the small SSA. As a result, the NMT map has a seismic hazard that averages ~0.06g higher than the USGS map along the northeastern and southeastern border of New Mexico.

5. Sensitivity Study of Probabilistic Seismic Hazard Estimates for New Mexico

During the probabilistic seismic hazard evaluation for New Mexico using instrumental data 1962-1998, assumptions were required in deriving parameters for hazard estimates. Parameters such as the cut-off magnitude and the time-and-distance windows for removing dependent events affected the input earthquake data. Other selected parameters such as the choice of the maximum likelihood slope β and the maximum magnitude earthquake affected the outcome of hazard estimates. Though these parameters appeared reasonable in our analysis, it is important to study their stability and effects on the probabilistic hazard estimates.

It was demonstrated in Chapter 4 that moderate size earthquakes of magnitude 4.5-5.5 contributed the most in short-term probabilistic seismic hazard analysis in New Mexico. e the earthquake data set for deriving seismic hazard does not contain earthquakes of magnitude 5.0 or greater for the time period 1962-1998. In this chapter, I will focus on the factors that might effect the estimated recurrence rates for earthquakes of magnitude 4.5 or higher. These factors include: (1) Completeness of earthquake data 1962-1998; (2) Removal of dependent events; (3) Deviations of the maximum likelihood slope β; (4) Maximum magnitude earthquake; (5) Pre-instrumental earthquake data 1868-1961. Both pre-instrumental earthquake data and information from active faults were not included in the probabilistic hazard analysis due to lack of completeness for the entire study area. Instead they were used as independent factors to examine the stability of the hazard estimates. Recurrence rates of high magnitude earthquakes based on faults and their effects on probabilistic seismic hazard assessment will be discussed in the next chapter.

Completeness of Earthquake Data 1962-1998

It was demonstrated in Chapter 4 that the data were complete at the magnitude 2.0 or greater. Therefore, despite the differences in instrumentation for New Mexico for the period 1982-1998 and 1962-1981, recurrence relationships derived for these two periods should resemble each other, particularly for magnitudes less than 3.5. If the data were incomplete, one would expect to see a fall-off in cumulative number of events at low magnitudes. Shown in Figure 5-1 are recurrence relationships for both the SSA and the RNM for the time periods 1962-1981 and 1982-1998. All four recurrence relationship curves show much the same linear distribution of cumulative annual recurrence rates of earthquakes with respect to magnitude. No fall-offs in cumulative number of events at low magnitude range are observed.

At magnitude of 3.5 or above, all four curves show stepping effects in cumulative number of events because of long expected return intervals for high magnitude earthquakes in New Mexico. For example, the expected return intervals for a magnitude 4.0 event are 13 years for the SSA and 3 years for the RNM. Thus it is not surprising to see that the strongest recorded event for the SSA from 1962 through 1981, a 20 year period, was only 4.0. In fact, the frequently observed swarm type seismicity in the SSA, such as the Bernardo swarm sequence from 1989 to 1991 with 4 events of magnitudes 4.0 or greater, is responsible for a significant difference in recurrence relationships for the SSA for the two time periods. On the other hand, the expected return intervals for high magnitude events for the RNM are smaller than of the SSA, therefore more high magnitude events were observed during both time periods.

Removal of Dependent Events

The general consensus is that dependent events, for example aftershocks, need to be removed in order to satisfy a Poisson assumption. Figure 5-2 shows annual recurrence rates per square km for both the SSA and the RNM before and after dependent events were

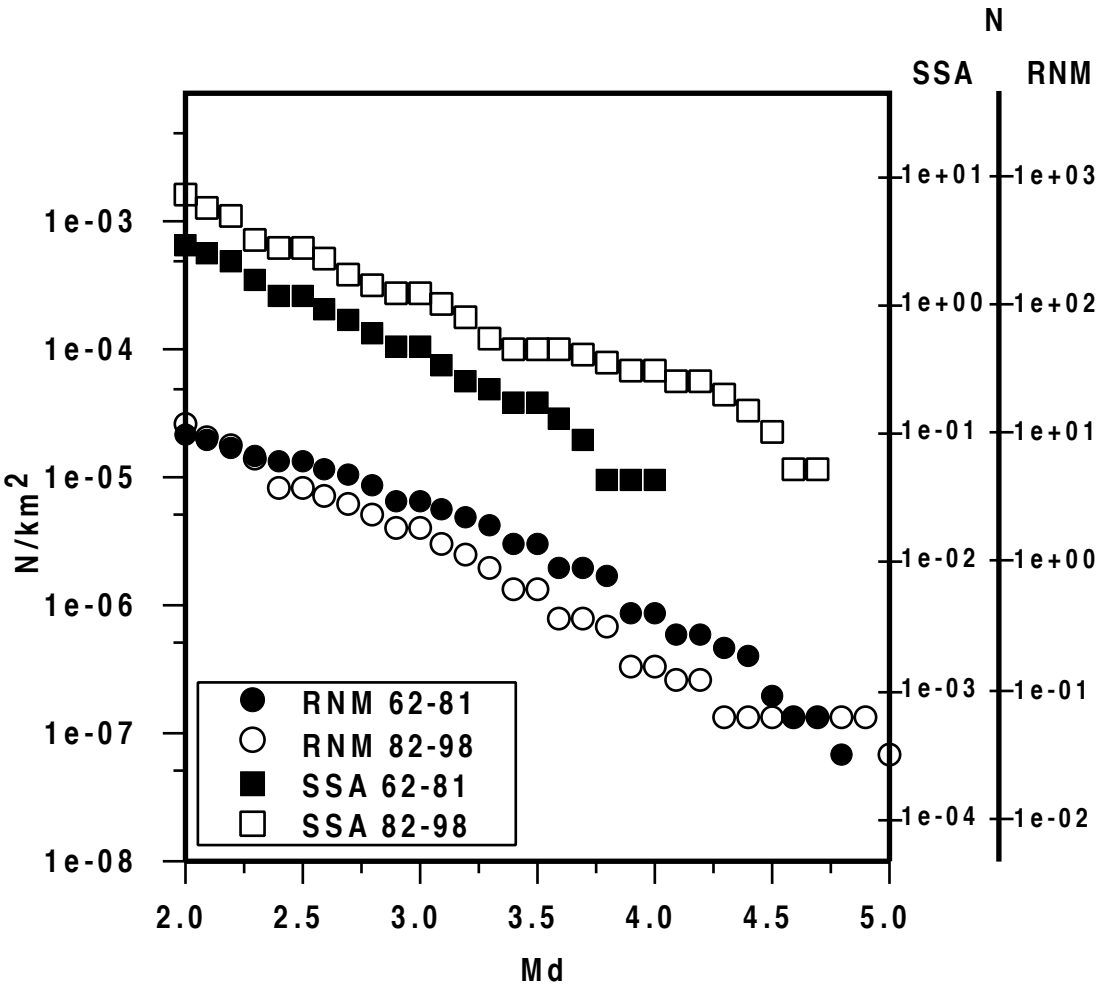

Figure 5-1. Annual recurrence relations for SSA and RNM for the time periods 1962-1981 and 1982-1998. Recurrence relations (slopes) indicate that no fall-off in cumulative number of earthquakes at low magnitude range for all four curves. At magnitudes of 3.5 or greater, the long expected return intervals of earthquakes produces differences in recurrence relations, especially for the SSA.

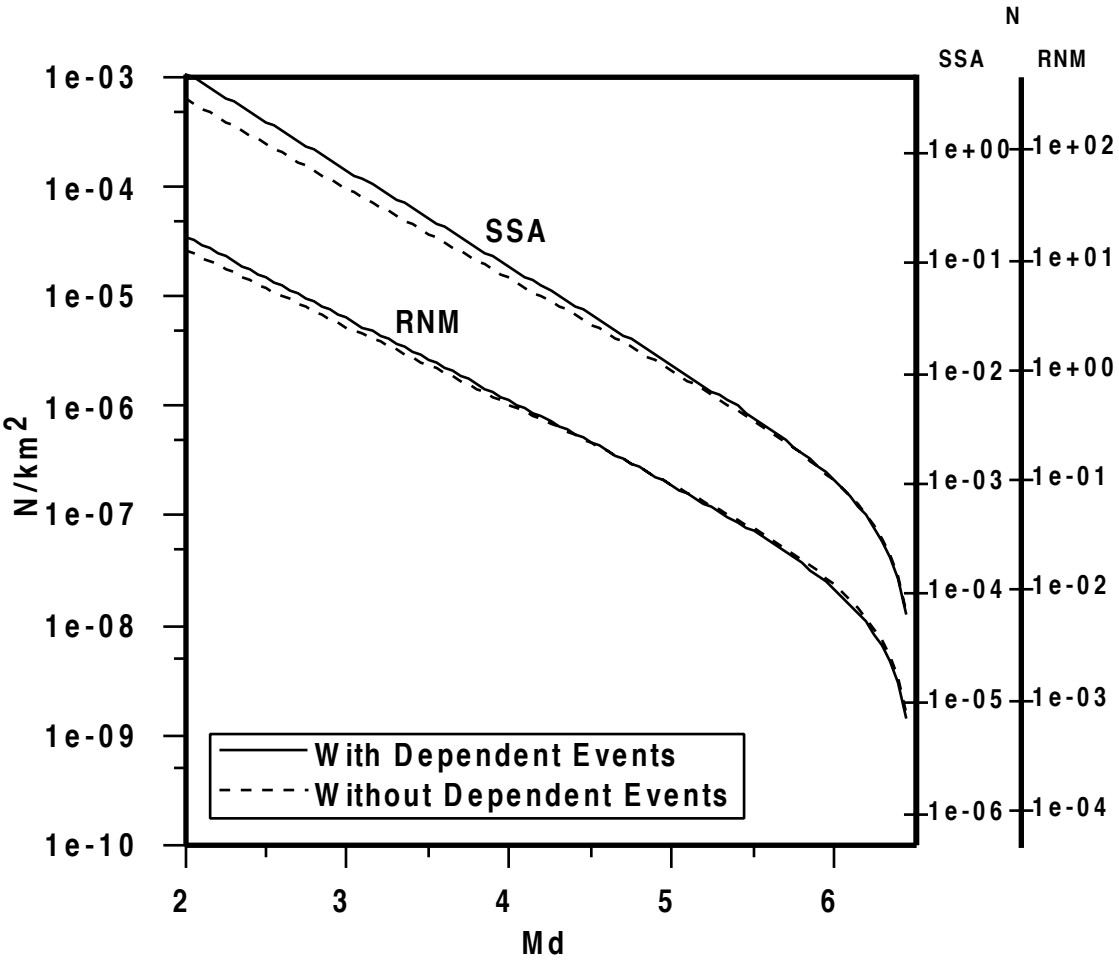

Figure 5-2. Annual recurrence relations for both the SSA and the RNM before and after dependent events were removed. For the SSA, 90 of the total 215 events (42%) were removed. The slope B changed from 0.882 to 0.819. For the RNM, 124 of the total 472 events (26%) were removed. The slope B changed from 0.746 to 0.702.

removed. For the SSA, 90 of the total 215 events (42%) were removed. The slope B changed from 0.882 to 0.819. For the RNM, 124 of the total 472 events (26%) were removed. The slope B changed from 0.746 to 0.702. The number of dependent events removed from the data set is a function of the space and time windows used. Although 4 km and 7 days for the SSA and 25 km and 7 days for the RNM appear reasonable, one cannot be certain whether too many or too few events have been removed with these parameters.

For both the SSA and the RNM, removed dependent events are mostly low magnitude earthquakes and the estimated maximum likelihood slope β becomes shallower, which produces small changes in the estimated recurrence rates for high magnitude earthquakes after dependent events are removed. During seismic hazard evaluation for New Mexico, only events with magnitude of 4.0 or greater were considered as dangerous and included in the hazard analysis. Therefore, for the RNM whose recurrence relationship shows almost no change above magnitude 4.0, removal of dependent events has very little effect on the seismic hazard estimates. For the SSA with more dependent events removed than the RNM, the hazard estimates are expected to be slightly lower.

Deviations of the Maximum Likelihood Slope β

The compiled earthquake data for the hazard estimates were measured in magnitude increments of 0.1. To avoid bias in estimating β using the sample mean magnitude, I adopted a distribution function (Bender, 1983) for the seismic hazard analysis. I divided the magnitude range between 2.0 and 6.5 into 45 intervals of width Δm of 0.1 for the observed 473 events (dependent events removed). The probability of a particular combination of 473 events for a given slope β value is obtained from equation (4-4) where $\beta = \log_e(10^B)$, N= total number of events, and k_i = number of earthquakes in the ith magnitude interval. The maximum likelihood slope β can be derived from the first

derivative of the distribution function as shown in equation (4-6). Figure 5-3 shows the distribution of β values (from equation (4-4)) for the recurrence relation based on instrumental data for the SSA and the RNM. The maximum likelihood slope β derived from the distribution function is 1.886 ± 0.20 (1 s.d.) for the SSA and 1.617 ± 0.15 (1 s.d.) for the RNM. Even though the SSA has a higher recurrence rate than the RNM, the likelihood slope of the SSA has a larger first standard deviation than the RNM. This is because that the number of earthquakes for the RNM (348) is much higher than the SSA (125), dependent events removed.

Examining the exponential truncated recurrence relationship (equation (4-3)), it is clear that changes in the maximum likelihood slope $\Delta\beta$ result in disproportional deviations in the estimated recurrence rates for earthquakes at different magnitudes as shown in following equation

$$N(m,\beta \pm \Delta\beta) = N(m_o)\frac{e^{-(\beta\pm\Delta\beta)(m-m_o)} - e^{-(\beta\pm\Delta\beta)(m_u-m_o)}}{1-e^{-(\beta\pm\Delta\beta)(m_u-m_o)}}. \qquad (5\text{-}1)$$

The selected slope β of 1.75 (B=0.76) for the probabilistic seismic hazard analysis for all of New Mexico was the average of slopes for the SSA and the RNM and is within the range of the first standard deviations for both source zones. To estimate uncertainties in recurrence relationships with respect to the selected likelihood slope β, I used the overlapped region of the first standard deviation for the two source zones, β values of 1.686 and 1.767, and compared them with the selected slope β of 1.75. Shown in Figure 5-4 are the ratios of the estimated recurrence rates using the average slope β and the two first standard deviation values. As shown in Figure 5-4, the maximum changes at Md = 6.5 are expected to be 7-22% depending on the selected slope β. Shown in Figure 5-5 are the estimated seismic hazards using the two selected slope β values, 1.686 and 1.767 compared with the estimates using the average β value. As shown in these figures, at 10%

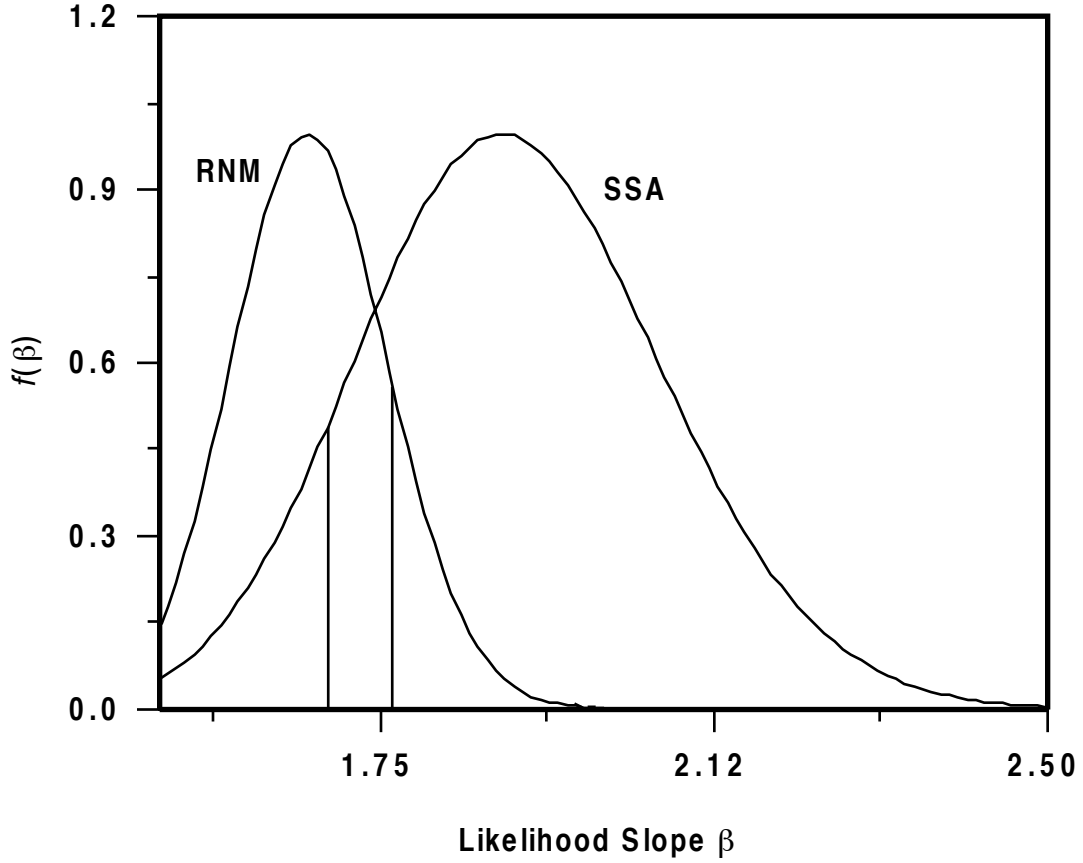

Figure 5-3. Distribution of β values from recurrence relations for both SSA and RNM based on instrumental data, dependent events removed. The maximum likelihood slope β is 1.886 (B=0.8192) for the SSA and 1.617 (B=0.7023) for the RNM.

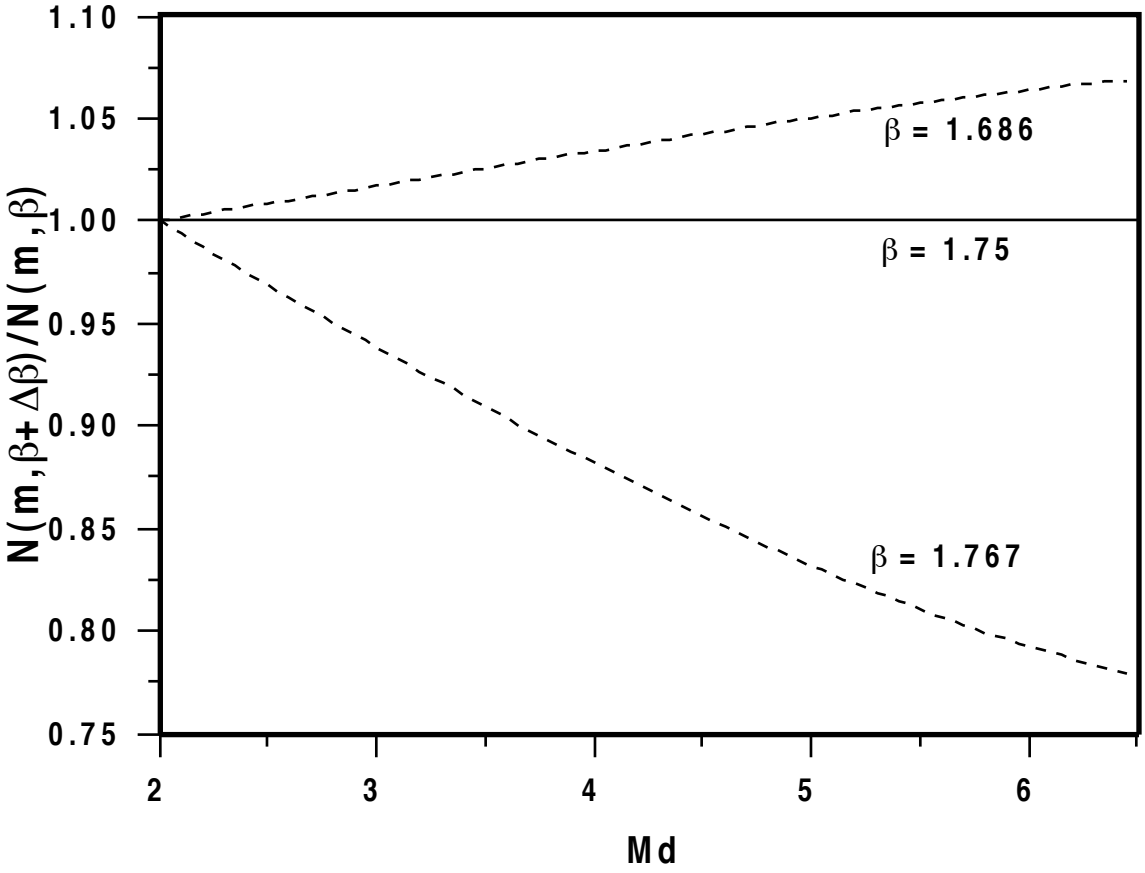

Figure 5-4. Ratios of the estimated recurrence rates using the average slope β and the two likelihood slope β values from estimates of one standard deviation for the two source zones (Figure 5-3). The differences in the estimated number of events at Md = 6.5 range 7-22% from the average slope β.

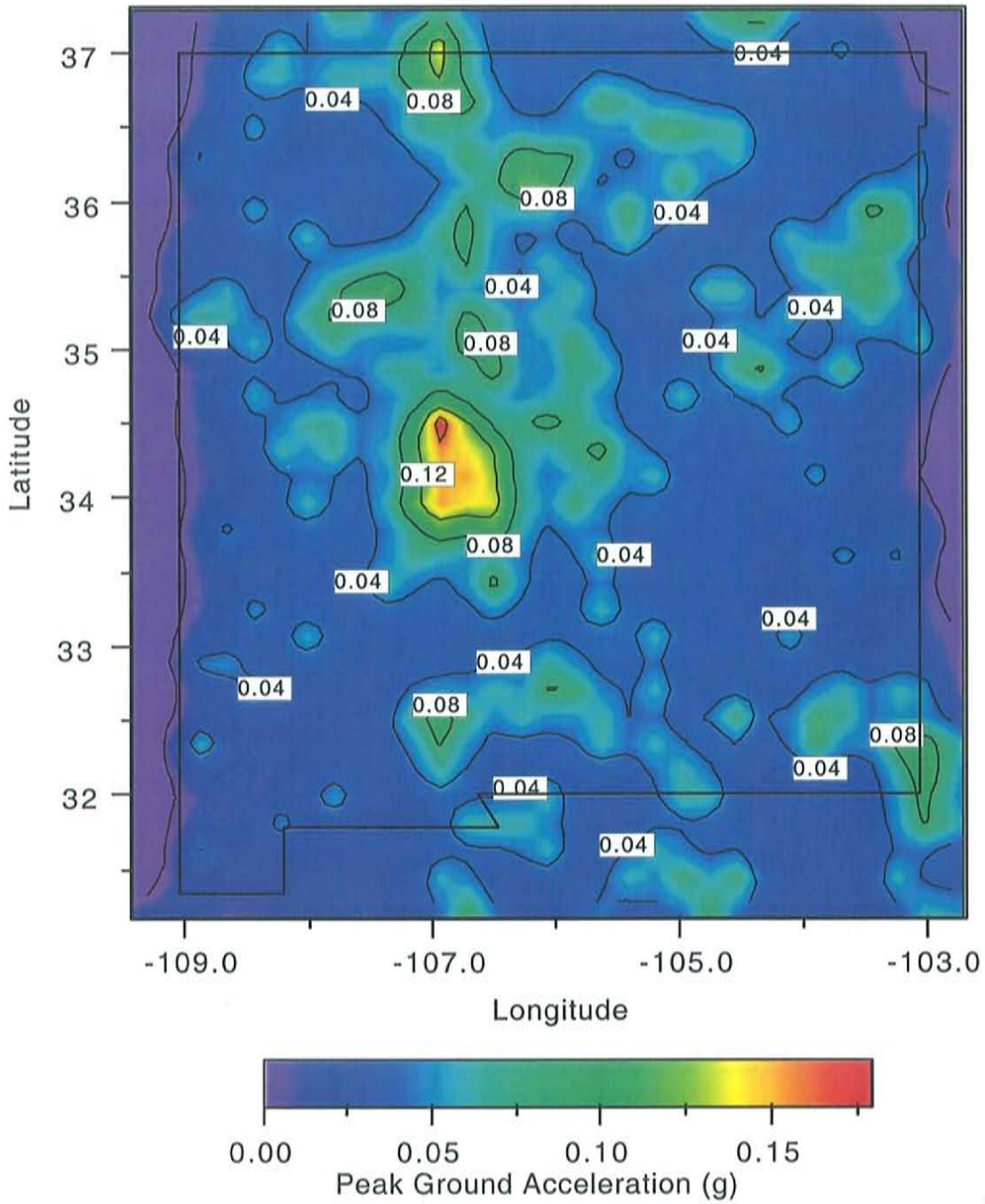

Figure 5-5a. Probabilistic seismic hazard map for the state of New Mexico and bordering areas. The map is presented in the format of peak horizontal ground acceleration at 10% probability of exceedance in a 50 year period. The SSA has the highest level of seismic hazard: ~0.18g. The slope β (1.75) is the average of the the maximum likelihood slopes for the two source zones.

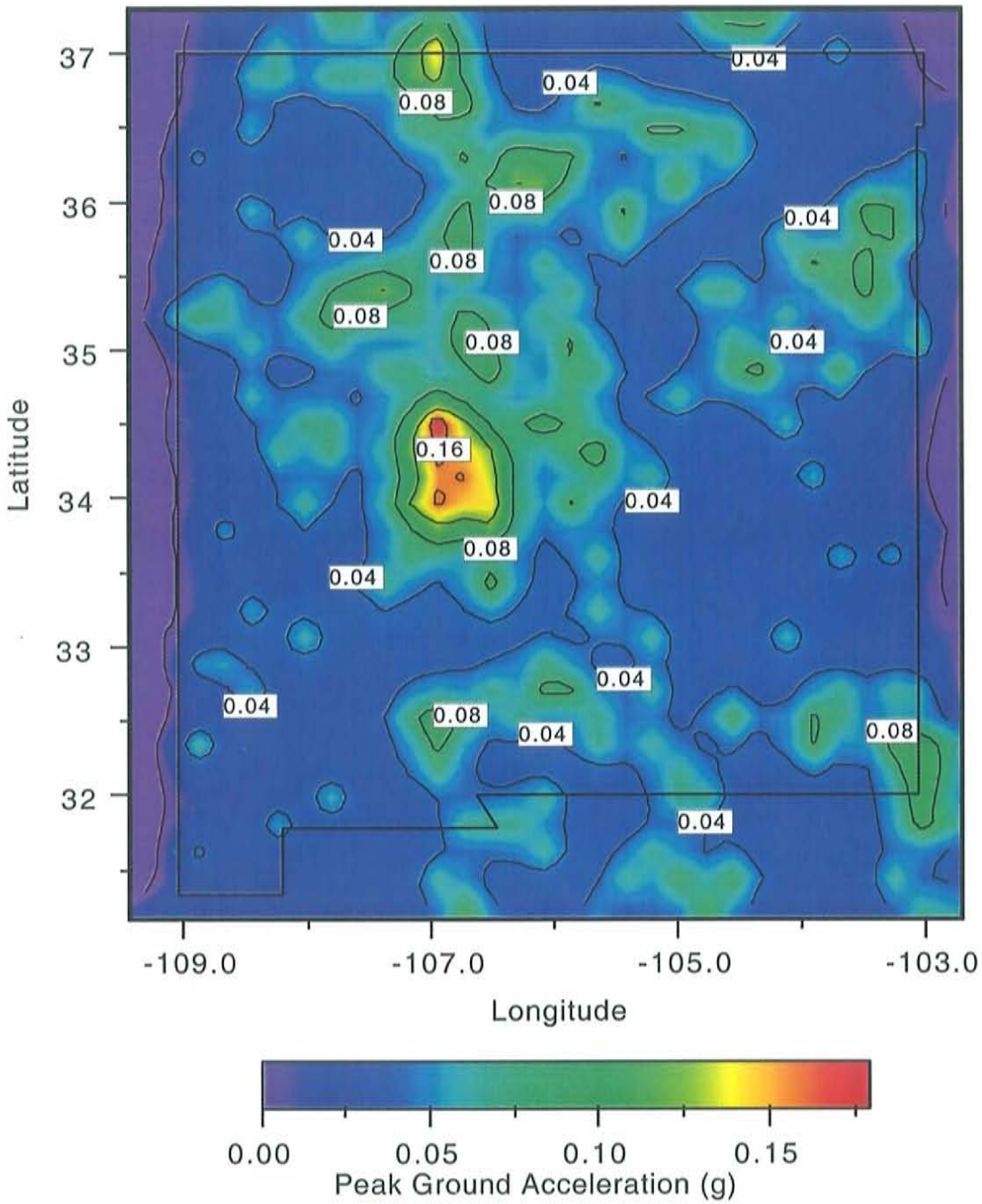

Figure 5-5b. Probabilistic seismic hazard map for the state of New Mexico and bordering areas. The map is presented in the format of peak horizontal ground acceleration at 10% probability of exceedance in a 50 year period. The SSA has the highest level of seismic hazard: ~0.19g. The slope β (1.686) is the maximum likelihood slope for the SSA minus one standard deviation.

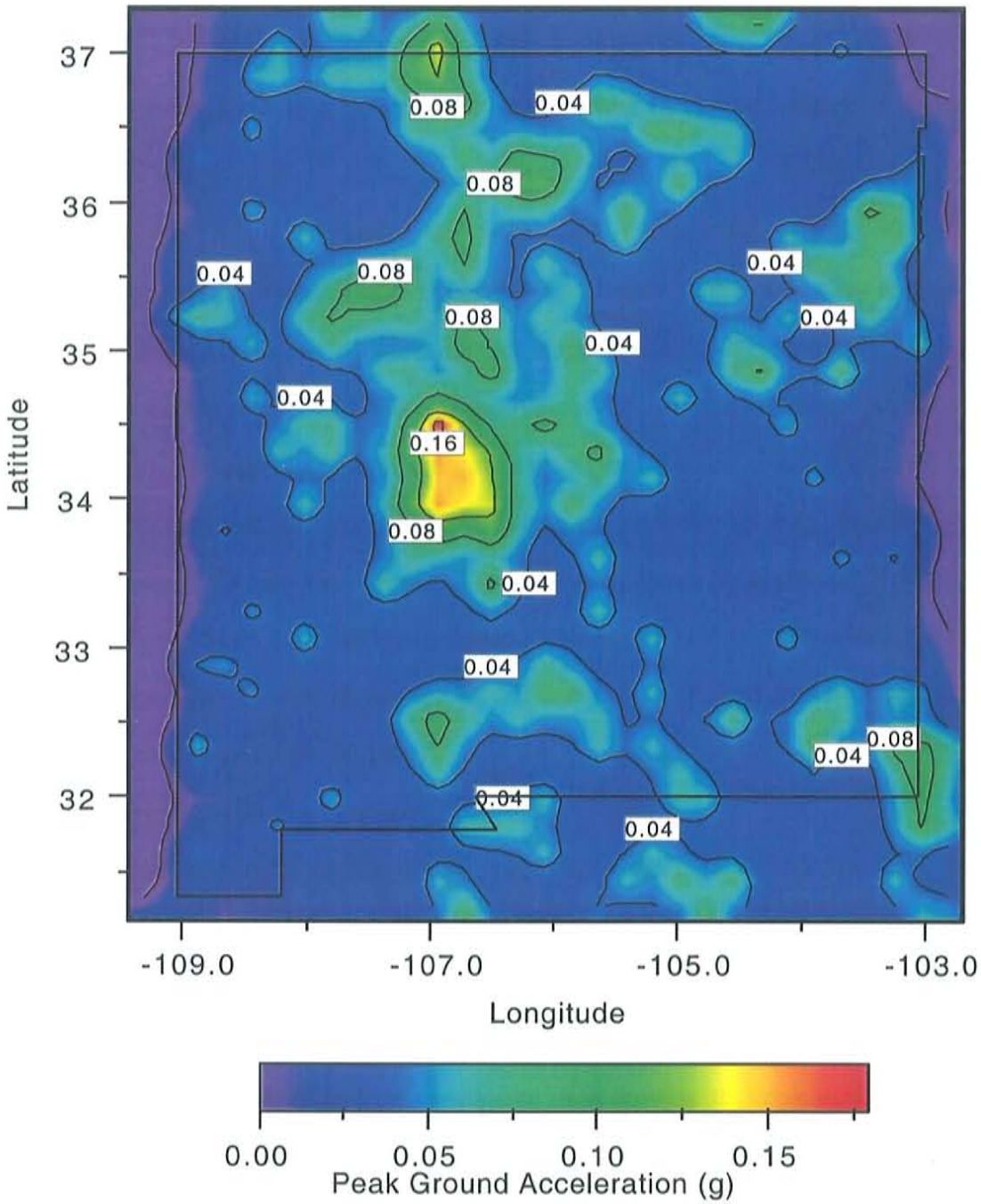

Figure 5-5c. Probabilistic seismic hazard map for the state of New Mexico and bordering areas. The map is presented in the format of peak horizontal ground acceleration at 10% probability of exceedance in a 50 year period. The SSA has the highest level of seismic hazard: ~0.18g. The slope β (1.767) is the maximum likelihood slope for the RNM plus one standard deviation.

probability of exceedance in a 50 year period the contours of ground accelerations show the same trends of seismic hazards but with variations of ~5% in ground acceleration.

Figure 5-6a shows the magnitude contribution curves for the Socorro area at 10% probability of exceedance in a 50 year period using the recurrence relationship slope β based on the average slope β and the two selected slope β values bounded by the first standard deviations. In the figure, the distribution curve shifts slightly to a higher magnitude range as the chosen slope β decreases. However, it is also clear that all three distribution curves are similar with a dominant magnitude of ~4.8±0.1 despite changes in the estimated annual recurrence rates for earthquakes at all magnitudes. As shown in Figure 5-6b, the steady increase in the cumulative percentile of hazard estimates versus magnitude indicates that all earthquakes in the range from 4.0 to 6.5 contribute to the hazard estimates. The slightly steeper slope occurring between magnitude 4.5 and 5.7 accounts for ~60% of the total hazard estimate. This suggests that earthquakes within this range are the dominant factor in seismic hazard analysis for a short return period such as 500 years (10% probability in 50 years).

Maximum Magnitude Earthquake

For the short-term seismic hazard estimates, it was assumed that an event of magnitude 6.5 on a blind fault was far more probable than a much stronger scarp producing earthquake of magnitude 6.75 or greater. Although the probabilities of occurrence for high magnitude earthquakes (> 6.5) can be easily incorporated into the recurrence relationship by raising the maximum magnitude earthquake, it is unwise to implement the strategy. This is because that the sampling period for instrumental earthquake data of 37 years is relatively short compared with the much longer expected return periods of at least hundreds to thousands of years for catastrophic earthquakes of magnitude 6.5 or higher in New Mexico. Simply increasing the maximum magnitude earthquake changes the sample mean. As was shown in equation (4-6) for deriving the maximum likelihood slope β, changes in

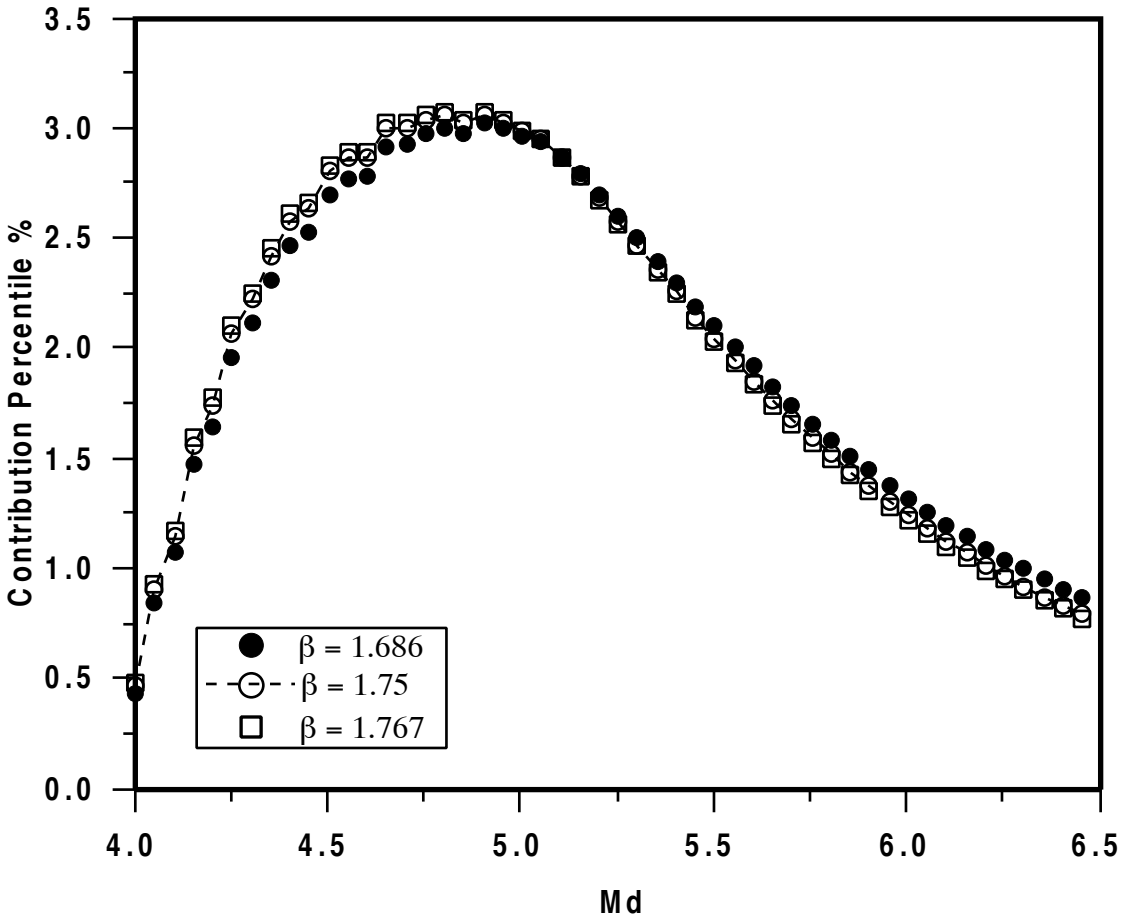

Figure 5-6a. Magnitude contribution curves for the Socorro area at 10% probability of exceedance in a 50 year period using the slope β values of 1.75, 1.686, and 1.767. All three curves have nearly the same distribution of contributions and dominant magnitude earthquake of ~4.8 +/- 0.1.

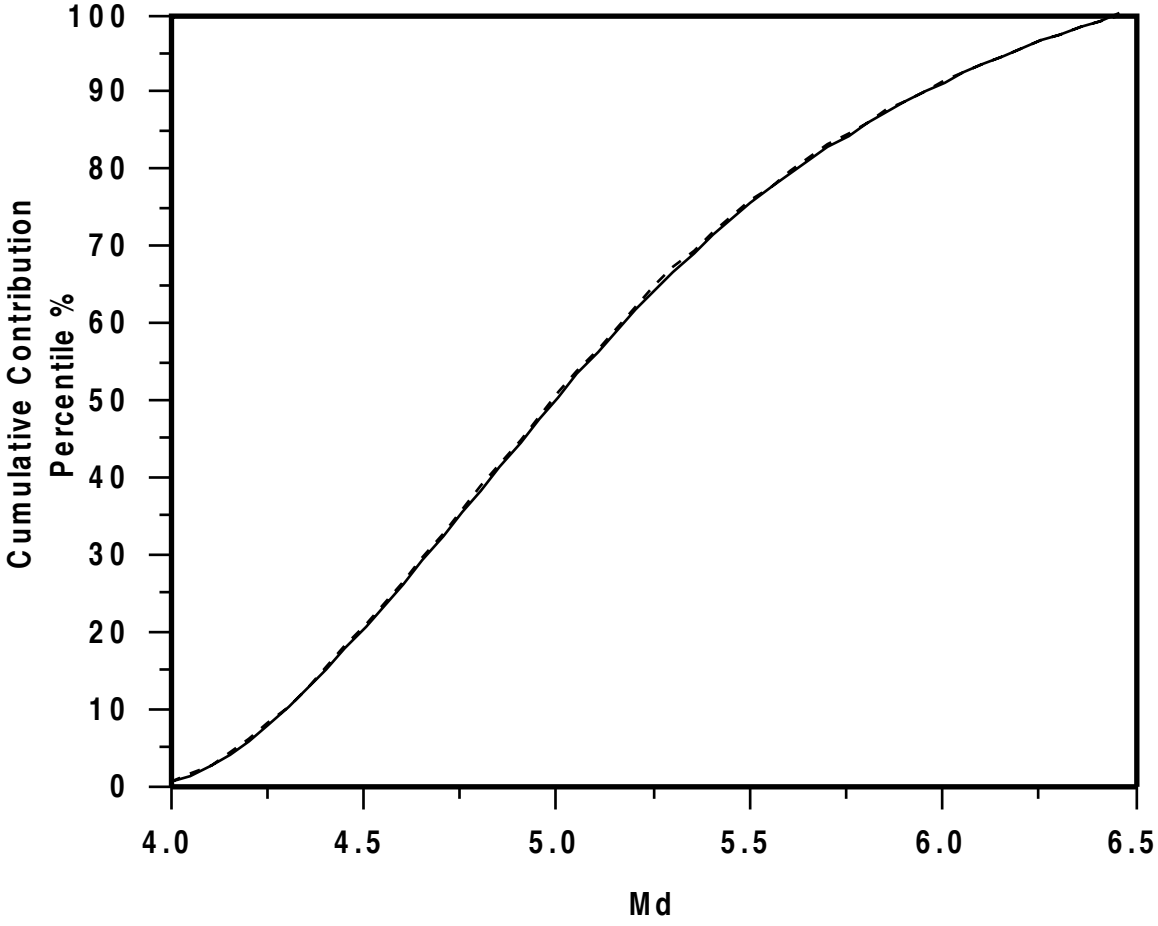

Figure 5-6b. Cumulative contribution curves for the Socorro area at 10% probability of exceedance in a 50 year period using the slope β values of 1.75, 1.686, and 1.767. The steady increase in the cumulative percentile of hazard estimates versus magnitude indicates that earthquakes at all magnitudes from 4.0 to 6.5 contribute to the hazard.

the maximum magnitude earthquake affects the number of magnitude bins n for a fixed number of observed earthquakes N and the derived slope β values. Figure 5-7 shows the maximum likelihood slope β values for different maximum magnitudes. The fitted slope β values have asymptotes of 1.89 for the SSA and 1.63 for the RNM as the maximum magnitude earthquake increases. Thus the effects of higher maximum magnitude earthquake on increasing seismic hazard estimates are likely to be partially offset by the increase in the maximum likelihood slope β. Figure 5-8 shows results of probabilistic hazard estimates for maximum magnitude earthquakes of 6.0, 7.0, and 8.0 using the corresponding fitted slope β values. The decrease in the highest level of seismic hazard obtained by reducing the maximum magnitude from 6.5 to 6.0 was only -0.02g and the increase in hazard by increasing the maximum magnitude to 8.0 was only +0.03g.

Pre-instrumental Earthquake Data 1868-1961

Sanford and Lin. (1998) have compiled a list of 30 strongest earthquakes in New Mexico of MMI VI or greater from 1868 through 1998. Equivalent magnitudes of these felt earthquakes were converted using the equation

$$M = \frac{2}{3} I_{\max} + 0.5 \qquad (5\text{-}2)$$

(Sanford, 1998). Even though this comprehensive list is likely complete as felt reports, it should not be presumed as complete regarding actual seismicity. A recent event on March 14, 1999 in southeastern New Mexico of magnitude 4.0 only received few felt reports even after the public were informed about the event. Considering the distance between the epicenter and the nearest residential area of only ~28 km, this suggests that it is possible for events occurring in the region from 1868-1961 to be unreported because of sparse distribution of population.

In an attempt to compare the seismic trends based on the short-term 37 year instrumental recording with the long-term 94 year pre-instrumental data, I selected the SSA

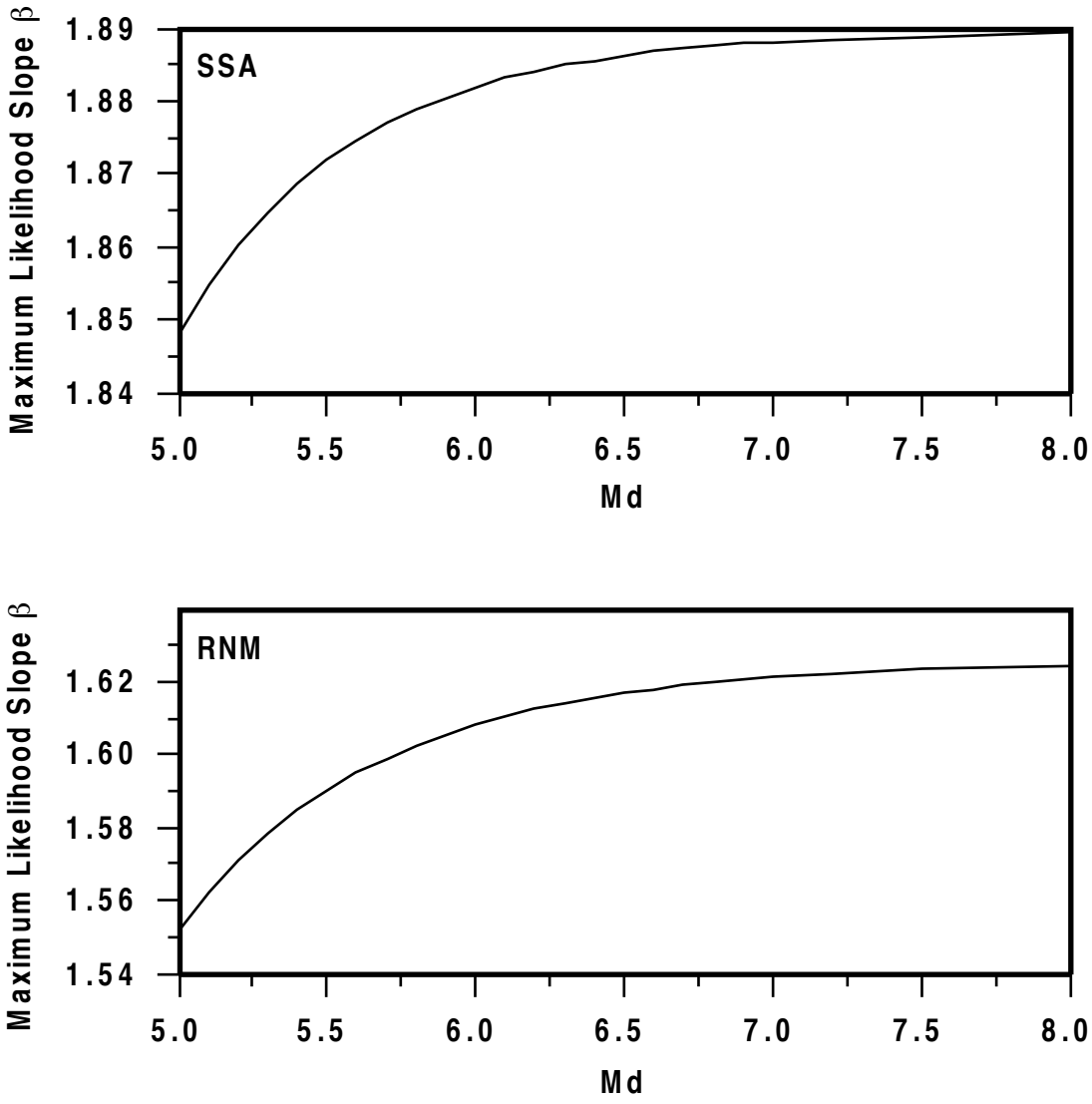

Figure 5-7. Maximum likelihood slope β for both SSA and RNM with respect to selected maximum magnitude. The asymptotes of the source zones are 1.62 for RNM and 1.89 for SSA.

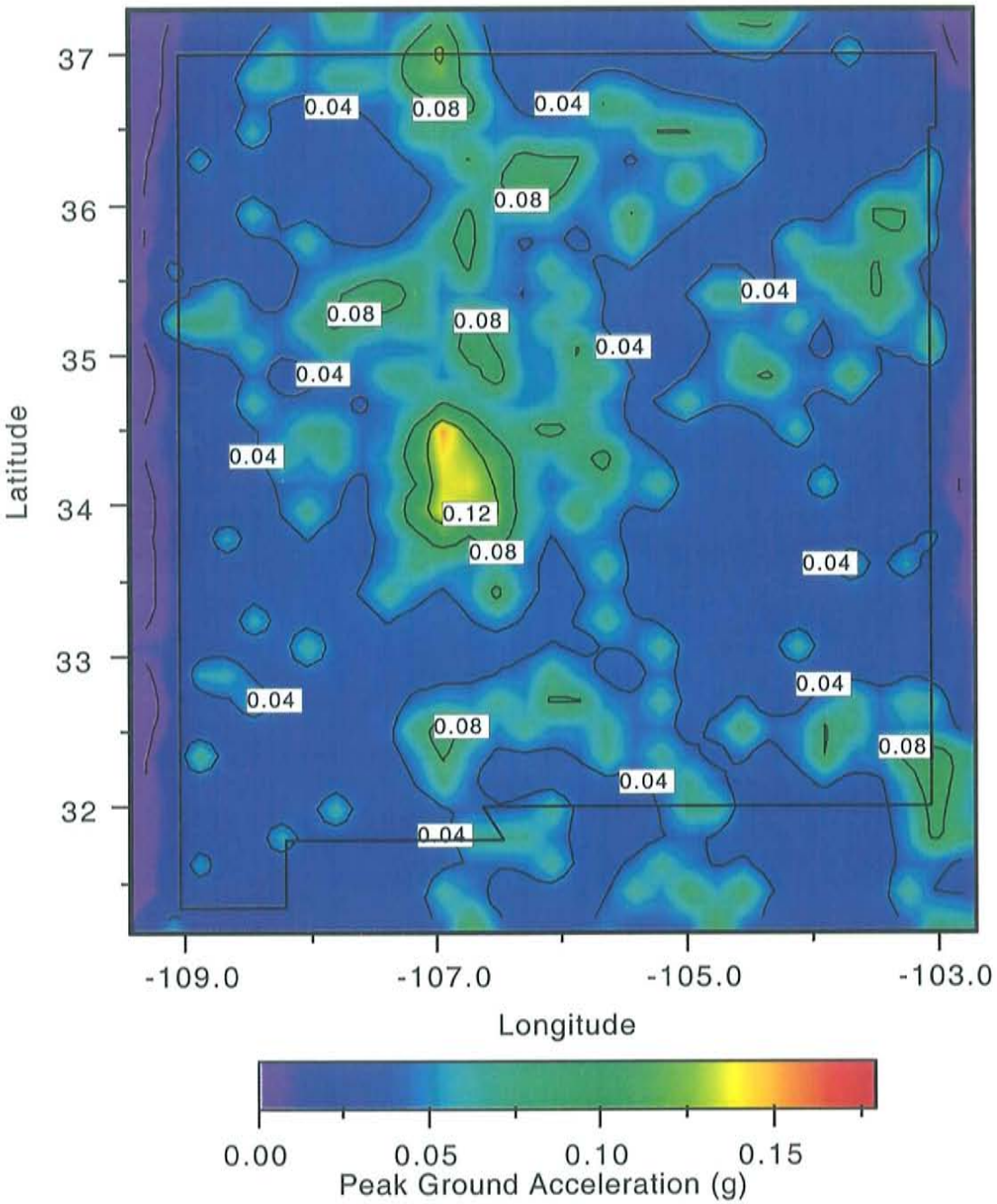

Figure 5-8a. Probabilistic seismic hazard map for the state of New Mexico and bordering areas. The map is presented in the format of peak horizontal ground accelerations at 10% probability of exceedance in a 50 year period. The SSA has the highest level of seismic hazardsof ~0.16g. The selected maximum magnitude earthquake is 6.0 and the β value is 1.745.

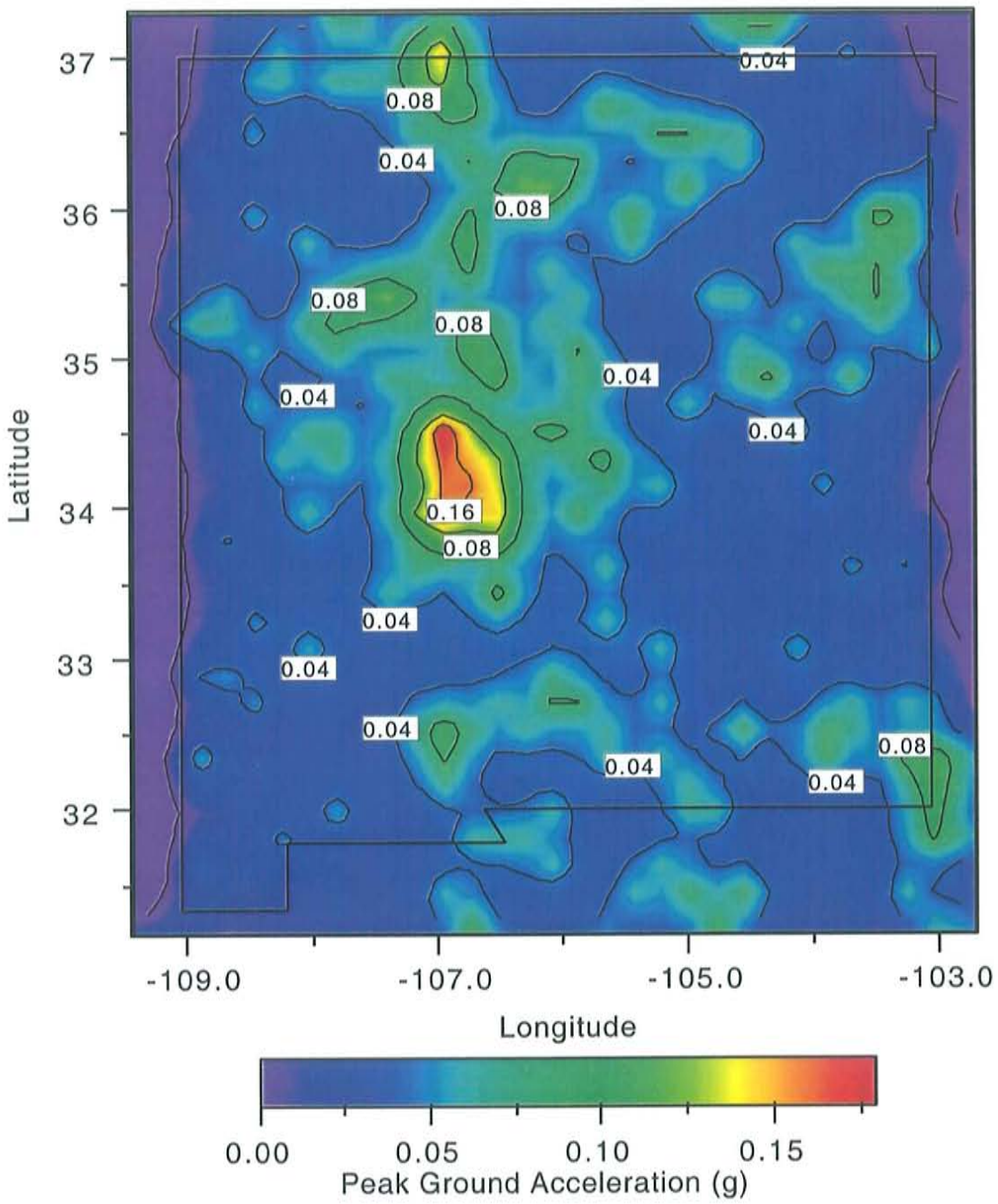

Figure 5-8b. Probabilistic seismic hazard map for the state of New Mexico and bordering areas. The map is presented in the format of peak horizontal ground accelerations at 10% probability of exceedance in a 50 year period. The SSA has the highest level of seismic hazardsof ~0.19g. The selected maximum magnitude earthquake is 7.0 and the β value is 1.754.

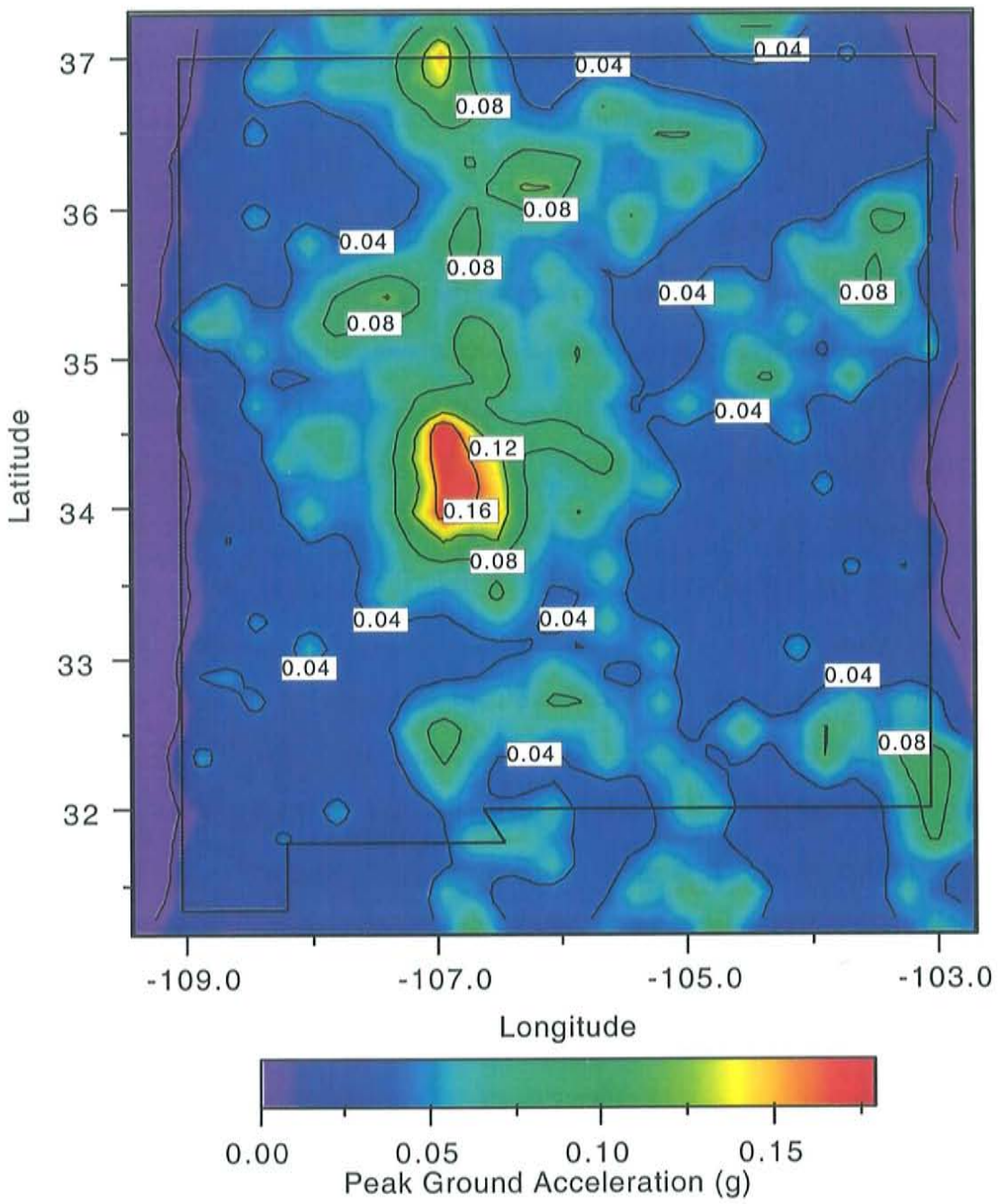

Figure 5-8c. Probabilistic seismic hazard map for the state of New Mexico and bordering areas. The map is presented in the format of peak horizontal ground accelerations at 10% probability of exceedance in a 50 year period. The SSA has the highest level of seismic hazardsof ~0.20g. The selected maximum magnitude earthquake is 8.0 and the β value is 1.757.

to be the test area because the seismic density for the SSA is relatively high compared with the RNM (~15 times) and the area was populated for the past 130 years. Table 5-1 lists the 28 pre-instrumental events of MMI V or greater for the SSA from 1868 through 1961. After conversion, the magnitudes of these 28 events range from 3.83 to 5.83.

It is difficult to identify and remove dependent events for pre-instrumental earthquakes because of ambiguous locations of epicenters and the high cut-off magnitude. While the space and time windows (4 km and 7 days) for removing dependent events for the SSA appear reasonable for instrumental data, the same parameter set may not be applicable to the pre-instrumental data. The uncertainty in epicenter for pre-instrumental data is larger and likely to be at least 10-20 km. In addition, the time window needs to be expanded to accommodate the higher cut-off magnitude of 3.8 for pre-instrumental data. By browsing through Table 5-1, it is clear that almost all removable events are magnitude 4.5 (MMI VI) or lower.

Figure 5-9 shows the annual recurrence relationships for both the instrumental and pre-instrumental earthquake data (with dependent events) for the SSA. In general, seismicity for the period 1868-1961 appears more active than the period 1962-1998. As shown in the figure, the ratio of annual recurrence rates at magnitude 5.8 for the pre-instrumental data to the instrumental data is 3.4. Such a large difference can not be accommodated by removing dependent events alone. In addition, the recurrence relationship for the pre-instrumental data with dependent events is shallower compared with the instrumental data without dependent events. This suggests that the pre-instrumental data might be incomplete in the low magnitude range 3.8-4.5 because the slope would have been even shallower if dependent events were removed.

Discussion

In this chapter I discuss factors that could have effected the probabilistic seismic hazard analysis for the state of New Mexico using only 37 year (1962-1998) of

Table 5-1. List of Pre-instrumental Earthquakes for the SSA for the Time Period 1868 through 1961with Modified Mercalli Intensity Scale V or Greater

	Date			Origin Time			Approximate location		Maximum intenity	
No.	Mon.	Day	Year	Hr.	Min.	Sec.	Lat. (N)	Long. (W)	(modified Mercalli)	Md
1.	Apr.	28 ,	1868				34.1	106.9	V	3.83
2.	Apr.		1869				34.1	106.9	VII	5.17
3.			1879				34.1	106.9	V	3.83
4.	Jul.	6 ,	1886				34.1	106.9	V	3.83
5.	Oct.	7 ,	1895				34.5	106.7	V	3.83
6.	Oct.	31 ,	1895	12			34.1	106.9	VI	4.50
7.			1897				34.1	106.9	VI	4.50
8.	Jan.	20 ,	1904	02	10		34.1	106.9	VI	4.50
9.	Jan.	20 ,	1904	09			34.1	106.9	V	3.83
10.	Jan.	30 ,	1904	12	30		34.1	106.9	V	3.83
11.	Mar.	9 ,	1904	07	30		34.1	106.9	V	3.83
12.	Sep.	6 ,	1904	11	30		34.1	106.9	V	3.83
13.	Jul.	2 ,	1906	10	15		34.1	106.9	VI	4.50
14.	Jul.	12 ,	1906	12	15		34.1	106.9	VII to VIII	5.50
15.	Jul.	16 ,	1906	19			34.1	106.9	VIII	5.83
16.	Nov.	15 ,	1906	12	15		34.1	106.9	VIII	5.83
17.	Dec.	19 ,	1906	12			34.1	106.9	VI	4.50
18.	Jul.	1 ,	1916	08	08		34.1	106.9	V	3.83
19.	Feb.	1 ,	1919	04	04		34.1	106.9	V	3.83
20.	Feb.	1 ,	1919	20	30		34.1	106.9	V	3.83
21.	Jan.	8 ,	1934	01	32		34.1	106.9	V	3.83
22.	Feb.	21 ,	1935	01	25		34.5	106.8	VI	4.50
23.	Feb.	21 ,	1935	03	05		34.5	106.8	V	3.83
24.	Aug.	4 ,	1941	07	40		34.1	106.9	V	3.83
25.	Jul.	22 ,	1960	15	49		34.3	106.9	V	3.83
26.	Jul.	23 ,	1960	14	16		34.4	106.9	VI	4.50
27.	Jul.	24 ,	1960	10	37		34.3	106.8	V	3.83
28.	Jul.	3 ,	1961	07	06		34.2	106.9	VI	4.50

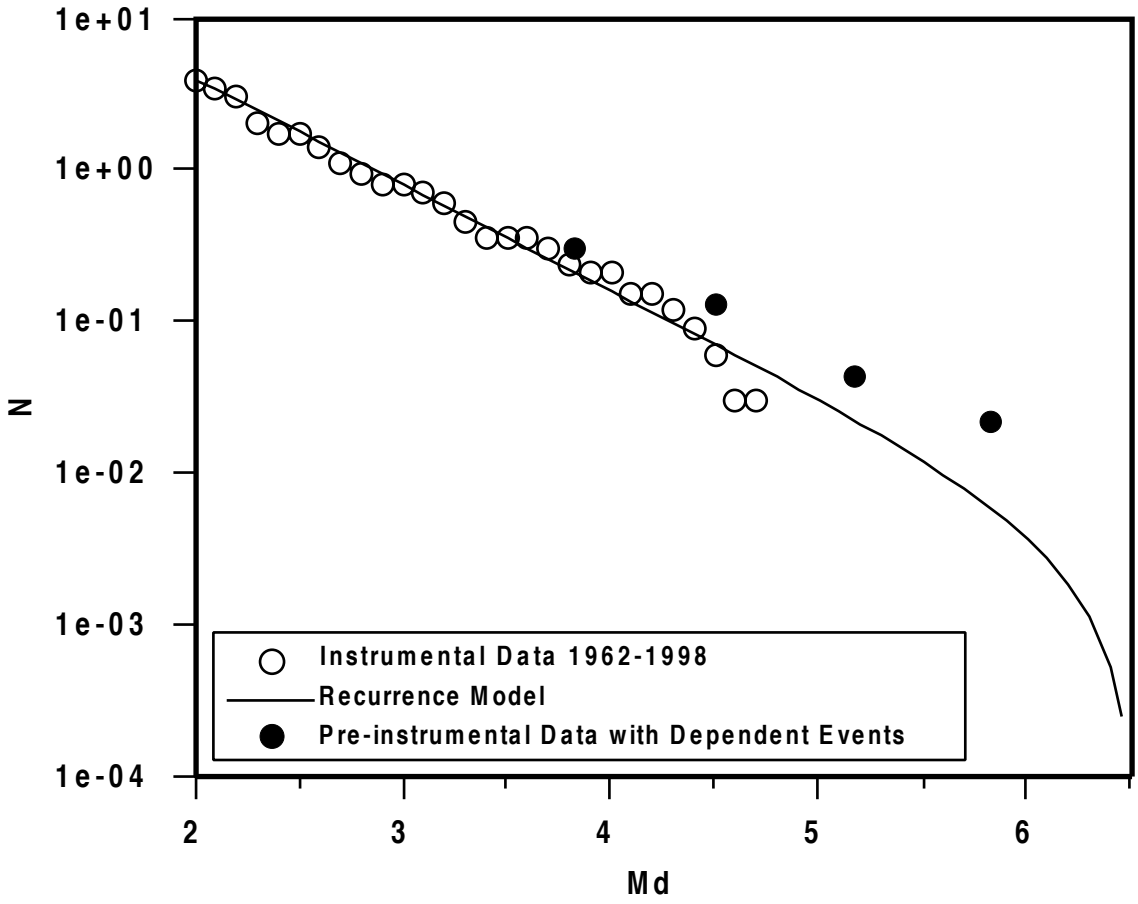

Figure 5-9. Annual recurrence relations for both the instrumental and pre-instrumental earthquake data for the SSA. Recrurrence relation based on the pre-instrumental data is higher than the instrumental data especially at high magnitude range of 5.0 and above.

instrumental earthquake data. Sensitivity analyses for the hazard estimates can be summarized as follows:

1. The instrumental earthquake data are likely to be complete at magnitude 2.0 or greater for the time period 1962 through 1998. Recurrence relationships for instrumental data without dependent events indicate no fall-off in cumulative number of earthquakes at low magnitude range. The strongest recorded earthquakes for the time period are only magnitude 4.7 for the SSA and 5.0 for the RNM. This can be attributed to the relatively short recording period compared with the long expected return periods for high magnitude earthquakes. For example, based on the recurrence models derived for both the SSA and the RNM, the strongest earthquake with a expected return interval equivalent to the period of recording (37 years) is magnitude 5.0 for the SSA and magnitude 5.3 for the RNM.

2. For the purpose of evaluating probabilistic seismic hazards for the state of New Mexico, the instrumental earthquake data are best suited for short-term estimates such as 10% probability of exceedance in a 50 year period because earthquakes of moderate magnitude 4.5-5.5 contribute the most to estimates of hazard. The same consideration applies when selecting the maximum magnitude earthquake for the recurrence model. For short-term hazard analysis, the selected maximum magnitude of 6.5 for New Mexico seems appropriate.

3. Recurrence relationships derived from pre-instrumental data from 1868 through 1961 for the SSA indicate higher level of activity than the instrumental data, which implies that the long term hazard for the SSA may be higher than estimates based on instrumental data alone. Assuming no drastic changes in seismic trends in the SSA for the past 130 year, the shallow slope of the recurrence relationship for the pre-instrumental data suggests that the earthquake data may be incomplete in the low magnitude range. However, the inconsistency in recurrence relationships between instrumental and pre-instrumental data for the SSA can not be resolved until a larger earthquake database is established.

6. Effects of Active Faults on Probabilistic Seismic Hazard Estimates

The level of historic seismicity (instrumental and pre-instrumental earthquake data) for New Mexico was moderate during the ~130 years of reliable records. For the purpose of seismic hazard evaluation, the paleoseismicity of faulting in the region provides a long-term perspective of recurrence rates for surface rupturing earthquakes.

In this chapter, I make a comparison between the recurrence rate of major earthquakes in the Rio Grande rift based on paleoseismic data with that obtained from an analysis of contemporary seismicity (1962-1998). In addition, I examine the effect of surface rupturing faults within the past 15 ka and random earthquakes on hidden faults on probabilistic seismic hazard analyses for the Socorro Seismic Anomaly (SSA).

Comparison of Recurrence Rates Based on Faults and Instrumental Data

Machette *et al.* (1998) have compiled a catalog of faults in New Mexico that have evidence of surface rupture during the Quaternary (<1.6 Ma). Their database includes 145 described Quaternary faults or fault zones of which 16 formed scarps within the past 15 ka. All of the latter group fall within or very near the boundaries of the Rio Grande rift which covers an area of ~110,000 km^2 in New Mexico. Machette *et al.* (1998) believe that the 16 faults may have produced 21 surface rupturing events which are assumed to be magnitude 7.0 or greater in this analysis. The 21 major earthquakes in 15,000 years over a 110,000 km^2 area yields a recurrence rate of 1.3×10^{-8} /yr/km^2.

The boundaries assumed for the RGR are: eastern side, a north-south line at 105˚20'; western side, a NNE trending line from 108˚ on the southern border to 107˚ on the northern border. Within this region, 184 earthquakes with magnitudes of 2.0 or greater

were located from 1962-1998. After dependent events were removed, the final catalog contained 119 earthquakes.

Figure 6-1 shows the estimated annual recurrence rates per square km for the SSA and the RGR (excluding the SSA) after dependent events were removed. Also shown is the annual recurrence rate of magnitude 7.0 or greater earthquakes based on the 21 surface rupturing events within the past 15 ka, a return interval of 750 years. The annual recurrence rate based on the faults in the Rio Grande rift is ~34% higher than the rate for the RGR based on instrumental data; yet it is significantly lower than the rate projected for the SSA. Considering the uncertainty in the completeness of the fault data and the short period of instrumental recordings, the earthquake and the fault data show reasonably good agreement in recurrence rates for magnitude 7.0 or greater earthquakes for the past 15 ka.

Effects of Active Faults on Estimates of Seismic Hazard- Socorro Seismic Anomaly

The history of paleoseismicity for active faults becomes important when evaluating seismic hazards with long expected return intervals. To demonstrate the effects of active faults on probabilistic seismic hazard estimates, I chose the SSA as the test area and assumed a uniform distribution of seismicity and a single source zone for deriving the background seismic hazard map. The procedure used for deriving probabilistic seismic hazard estimates is identical to the one used in Chapter 4. For modeling the recurrence relationship for the source zone, I used a truncated exponential recurrence model with maximum likelihood slope β of 1.89 (B=0.82). Shown in Figure 6-2 is a map of estimates of seismic hazard for the SSA in the format of peak horizontal ground accelerations at 10% probability of exceedance in a 50 year period. As expected the contours of horizontal ground acceleration in Figure 6-2 parallel the outline of the SSA and are most closely spaced along the boundary. The area within the SSA has a maximum ground acceleration of ~0.18g which produces Modified Mercalli intensity VII effects.

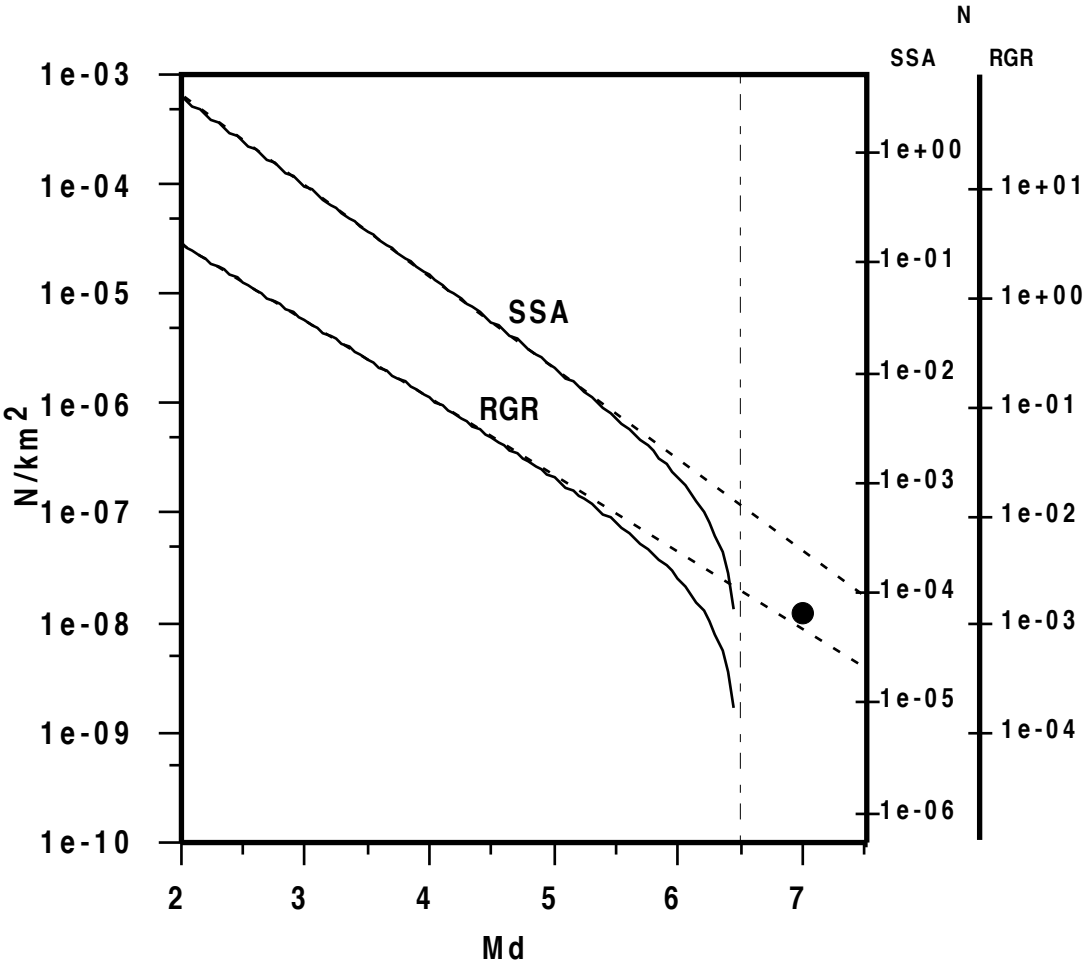

Figure 6-1. Annual recurrence relations for the SSA and the RGR after dependent events were removed. Also shown is the annual recurrence rate of magnitude 7.0 or greater earthquakes based on the 21 surface rupturing events within the past 15 ka, a return period of 750 years.

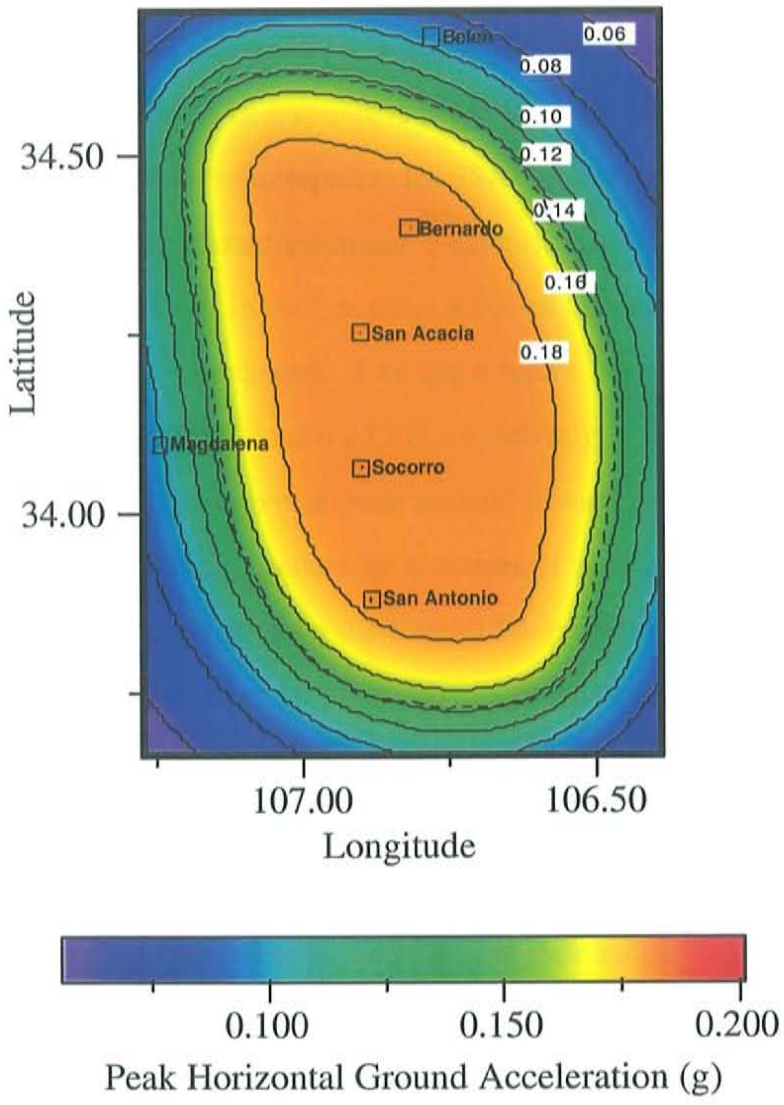

Figure 6-2. Peak horizontal ground accelerations at 10% probability of exceedance in a 50 year period. The seismic hazard map is based on the Joyner and Fumal (1985) attenuation relation with depth *h* equal to 7 km.

Identifiable Faults

Faults in the region with late Quaternary offsets were examined and three with the latest movements were selected: the La Jencia fault (LJF), the Socorro Canyon fault (SCF), and the Coyote Springs fault (CSF) (Machette *et al*. Among these selected faults, the LJF has the most recent movements with 5 to 6 episodes between 3 ka and 33 ka. The expected return interval for the fault system is roughly 6,000 years. Figure 6-3 shows the locations of these three faults with respect to the SSA. In order to evaluate effects of these three faults on the seismic hazard estimates, I assigned each fault a scenario earthquake with a specific return interval. In the first test, I assumed that all three faults are capable of generating magnitude 7.0 earthquakes. I assigned return intervals of 5,000 years to the LJF and 10,000 years to the SCF and the CSF, respectively.

I was able to determine probabilistic seismic hazards based solely on these three faults by following the same procedure as instrumental earthquakes. Figure 6-4 shows peak horizontal ground accelerations at 0.2% and 0.5% probabilities of exceedance in a 50 year period (expected return intervals of 25,000 and 10,000 years). Shown on the map are contours of ground acceleration of 0.3g or lower. Within the 0.3g contour, accelerations are higher but were not calculated because of uncertainty involved in the focal depth of earthquakes. The maps illustrate that at very long return intervals, active faults can dominate estimates of seismic hazard in the vicinity of their traces.

Figure 6-5 shows the seismic hazard maps before and after overlaying seismic hazard estimates for the faults on the map based on instrumental data. These two maps are presented in the format of peak horizontal ground accelerations at 10% probability of exceedance in a 50 year period. The area with the highest level of seismic hazard falls within the SSA and between the LJF and the SCF. For hazard estimates with the short expected return interval of 500 years, the increase in seismic hazard in the region is minor, from 0.18g to 0.20g.

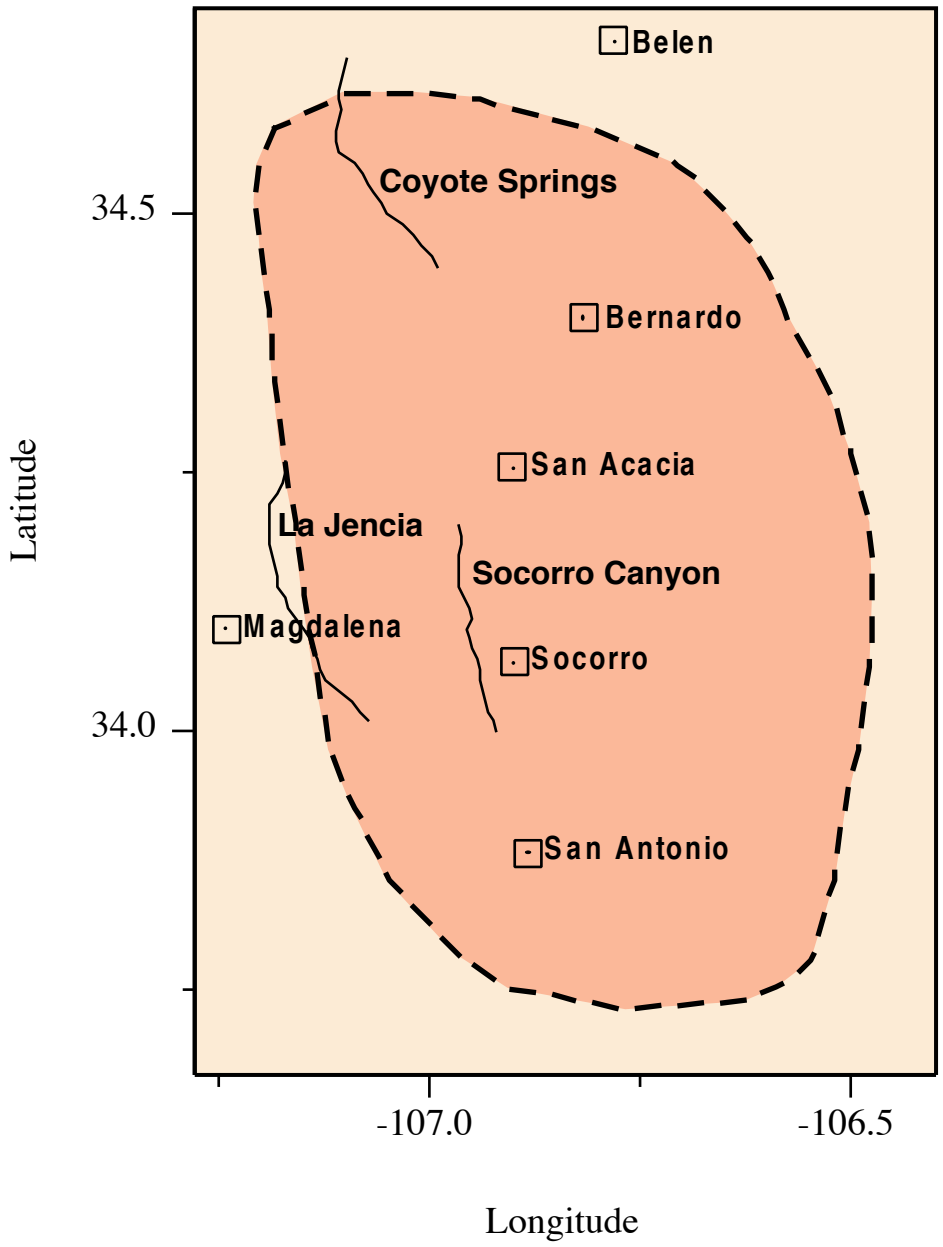

Figure 6-3. Locations of the La Jencia fault, the Socorro Canyon fault and the Coyote Springs fault. Among these faults, the La Jencia is the most active with five to six movements in 3-33 ka.

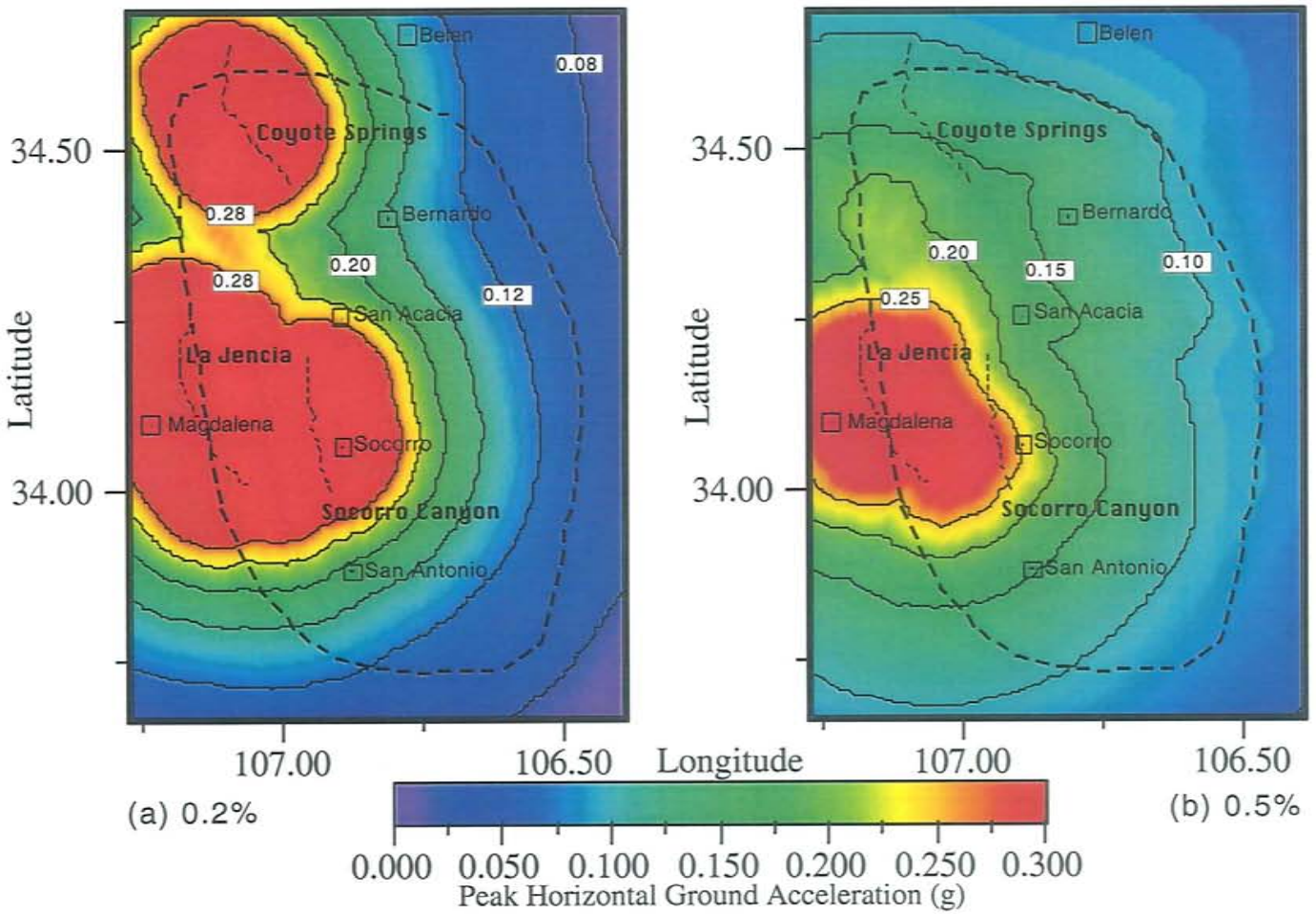

Figure 6-4. Horizontal peak ground accelerations at 0.2% and 0.5% probabilities of exceedance in a 50 year period based on the three active faults: the La Jencia fault, the Socorro Canyon fault and the Coyote Springs fault. All three faults were assigned scenario earthquakes of magnitude 7.0 with return intervals of 5,000 years for the LJF and 10,000 years for both the SCF and the CSF.

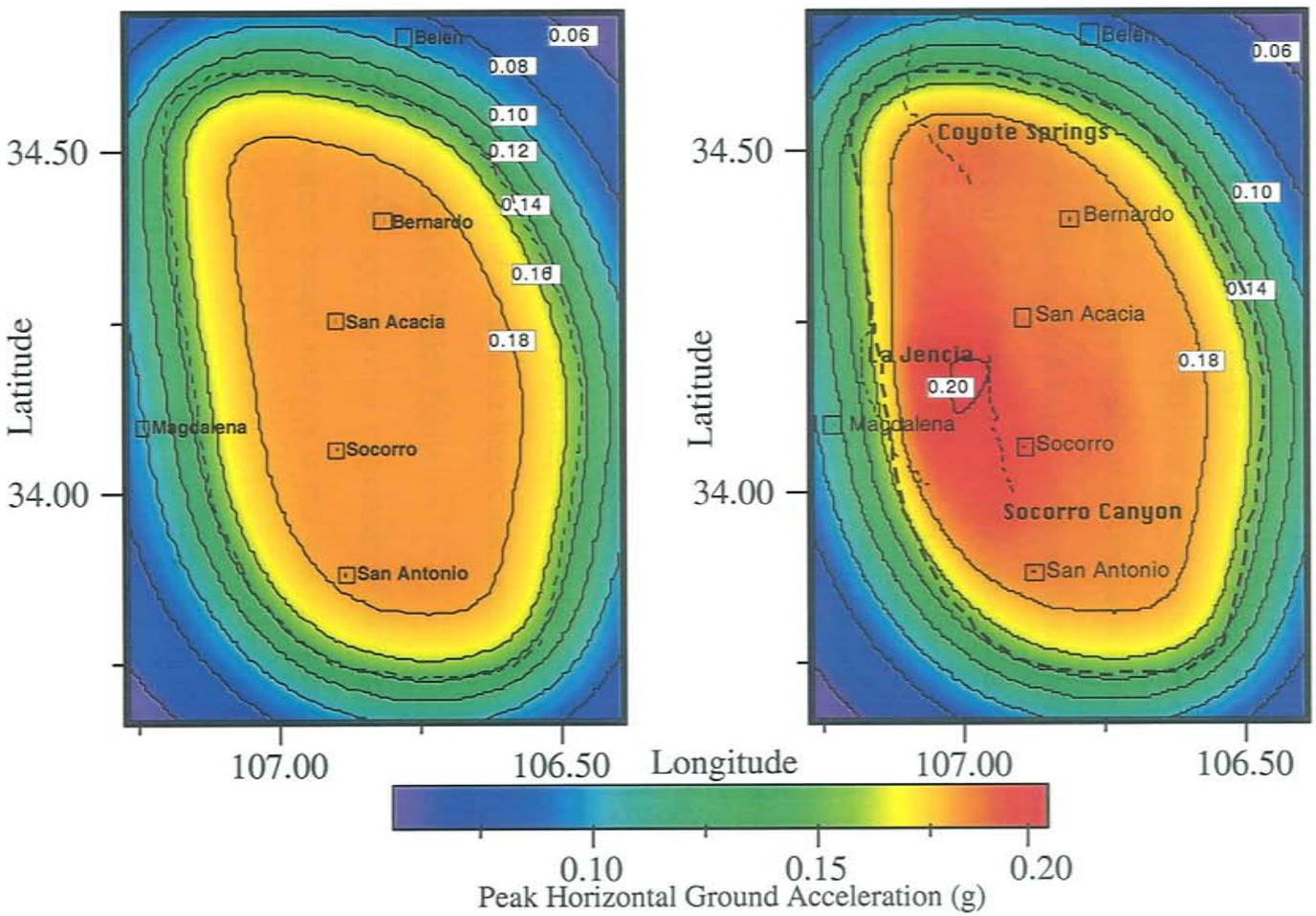

Figure 6-5. Peak horizontal ground accelerations at 10% probability of exceedance in a 50 year period based on (a) instrumental data; (b) both instrumental and fault data. All three faults were assigned with scenario earthquakes of magnitude 7.0 with return intervals of 5,000 years for the LJF and 10,000 years for both the SCF and the CSF.

I reexamined the effects of these three faults after reducing the expected return intervals by one half, i.e., the expected return interval for the LJF became 2,500 years and for the SCF and the CSF they became 5,000 years. Figure 6-6 shows the new probabilistic seismic hazard maps for peak ground accelerations at 0.2% and 0.5% probabilities of exceedance in a 50 year period. Both maps indicate that all three faults make significant contributions to estimated hazards at these large return intervals (25,000 and 10,000 years). On the other hand, combined hazard maps based on both instrumental earthquake data and active faults for a 50 year period and 10% probability of exceedance (500 year return interval) produce only a slightly higher level of hazard estimates (Figure 6-7). The highest level of seismic hazard increases from 0.18g to 0.21g and is located between the LJF and the SCF. Even though the return intervals for all three faults were reduced by one half, effects of the active faults on estimates of probabilistic seismic hazard are small. This is not a surprising result because 1) the projected return interval for a magnitude 7.0 event is ~3300 years within the SSA based on instrumental data and 2) it is demonstrated in Chapter 4 that high magnitude earthquakes (Md > 6) have little effect on 50 year 10% probability of exceedance hazard estimates.

Random Earthquakes on Hidden Faults

The selected upper bound magnitude of 6.5 for the recurrence model during probabilistic seismic hazard analysis is the size of earthquake that does not produce a noticeable fault scarp. In this section I simulate the effects of random earthquakes on hidden faults on estimates of probabilistic seismic hazard.

According the Wells and Coppersmith's empirical relation (1994) between moment magnitude (M) and surface rupture length (SSL)

$$M = 4.86 + 1.32\log(SRL), \qquad (6\text{-}1)$$

a magnitude 6.5 event is equivalent to a fault segment of 20 km in length. Assuming the total length of hidden faults is equivalent to the total length of mapped surface faults in the

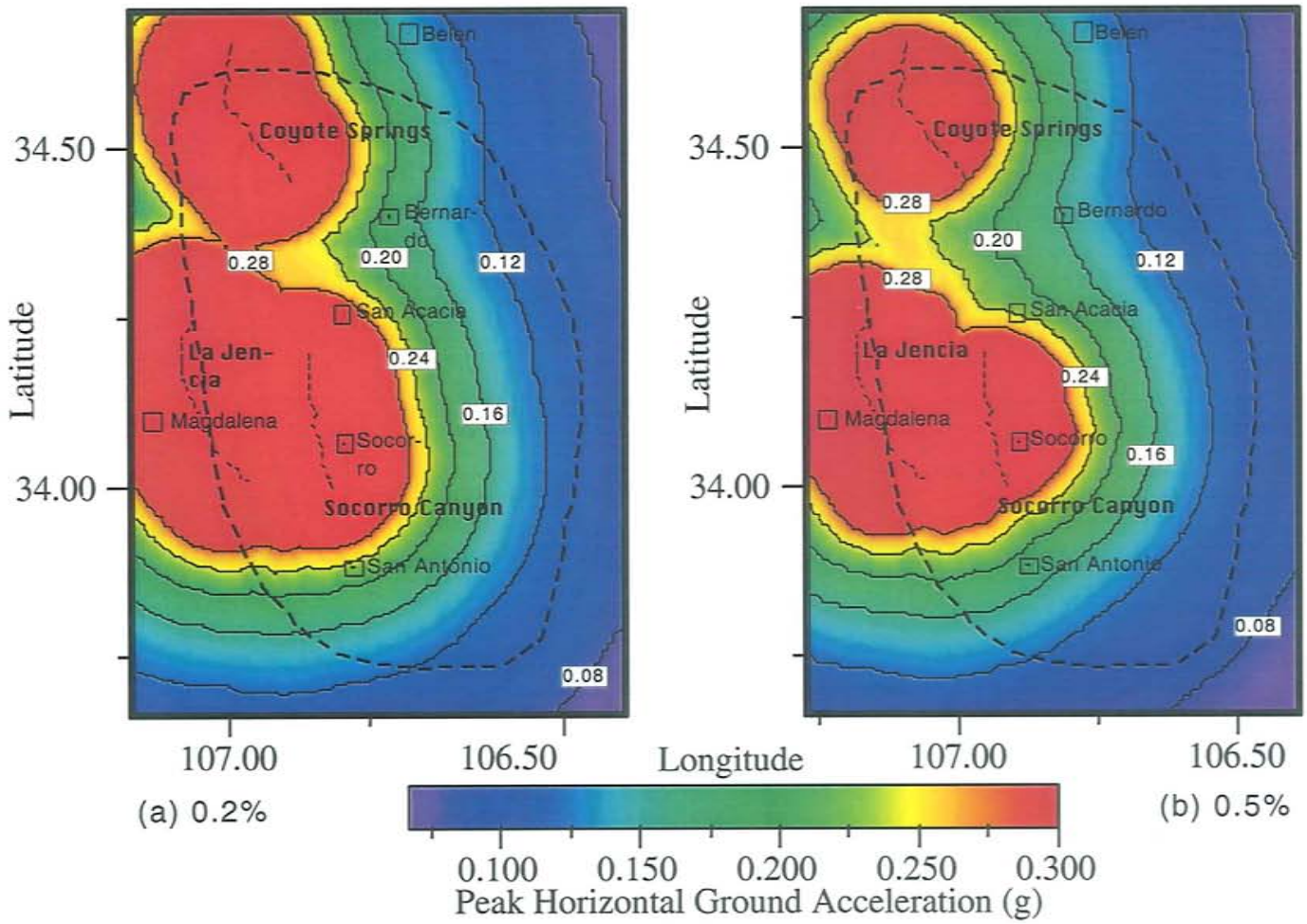

Figure 6-6. Peak horizontal ground accelerations at 0.2% and 0.5% probabilities of exceedance in a 50 year period based on the three active faults: the La Jencia fault, the Socorro Canyon fault and the Coyote Springs fault. All three faults were assigned with scenario earthquakes of magnitude 7.0 with return intervals of 2,500 years for the LJF and 5,000 years for both the SCF and the CSF.

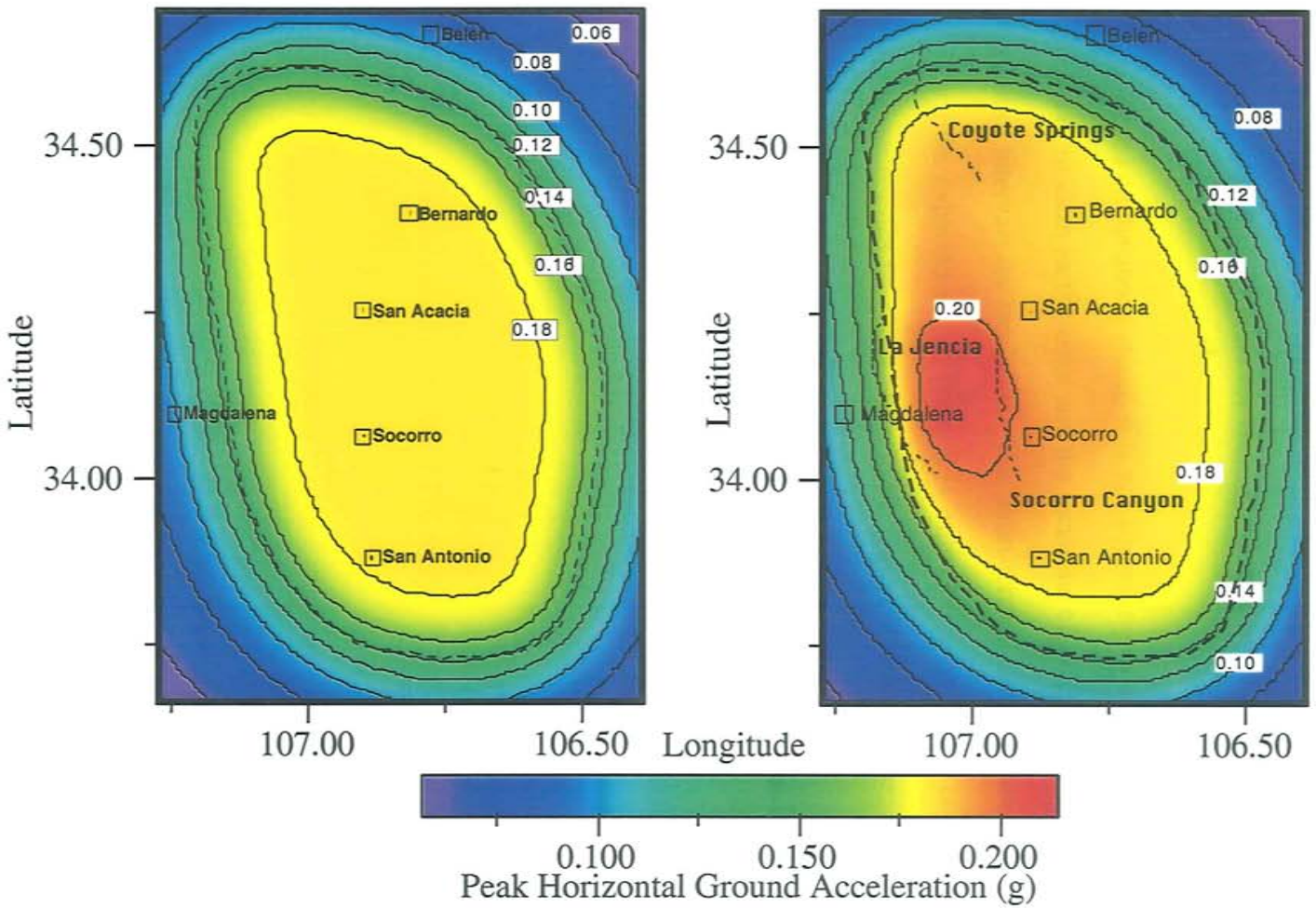

Figure 6-7. Peak horizontal ground accelerations at 10% probability of exceedance in a 50 year period based on (a) instrumental data; (b) both instrumental and fault data. All three faults were assigned with scenario earthquakes of magnitude 7.0 with return intervals of 2,500 years for the LJF and 5,000 years for both the SCF and the CSF.

SSA, the number of random earthquakes on hidden faults is ~30. By applying the projected return interval of 1432 years for magnitude 6.5 earthquakes using instrumental data (Figure 6-1) as the return interval for random earthquakes, this yields an average return interval of 43,000 years for each of the random earthquakes on hidden faults in the SSA.

Based on the above result, it is not surprising to see the inconsistency between the locations of modern earthquakes and the locations of mapped surface faults because of the long return intervals for the faults. For short-term hazard estimates (10% probability and 50 year), the expected return interval is only 500 years when compared with the much longer return periods for active faults in the region. Therefore, the inclusion of faults is not a crucial factor for hazard analysis with short return intervals.

7. Summary and Conclusions

For my study, I developed a procedure to compile a complete earthquake catalog for New Mexico and bordering areas and evaluated their seismic hazards. Completed products associated with the study include: 1) A fuzzy logic location algorithm for improving quality of location of regional earthquakes using a modified *G* matrix, 2) A complete earthquake catalog of magnitude 2.0 or greater earthquakes for New Mexico and bordering areas for the time period 1962-1998, and 3) Probabilistic seismic hazard maps at 10% and 2% probability of exceedance in a 50 year period for New Mexico and bordering areas. In addition, I have developed procedures for testing results of hazard estimates and for integrating faults into seismic hazard and sensitivity analyses.

Fuzzy Logic Algorithm

To improve the quality of locations of regional earthquakes in New Mexico, I have developed a fuzzy logic algorithm to incorporate with the existing location program SEISMOS used at New Mexico Tech. The major differences between the fuzzy logic approach and the generalized inversion method for most earthquake location programs are composition of the *G* matrix and the determination of epicenters for earthquakes.

A typical *G* matrix in inversion programs uses a travel time-distance equation describing the relation between the earthquake source and the seismic stations. The resulting *G* matrix usually contains 4 parameters, 3 spatial coordinates and the origin time. In my study, I reduce the 4 unknown parameters to 2 unknown parameters (azimuth and distance) for epicenter locations with a fixed focal depth parameter of 10 km. The origin time parameter is omitted during the earthquake location process and is calculated afterwards based on the derived epicenter. The modified *G* matrix without the origin time parameter contains only the S-P travel time intervals for individual stations and is expanded to accommodate both the P-P and the S-S travel time intervals for arbitrary station pairs.

Thus the modified *G* matrix usually contains more information than the regular *G* matrix for the same data set.

The modified *G* matrix is not suited for solving earthquake locations using inverse methods due to non-convergence properties for the P-P and the S-S travel time-distance relations. I circumvent this problem by mapping the *G* matrix into the fuzzy logic space and solve for earthquake locations using fuzzy logic operations. Three fuzzy sets are defined using a half-space model with a P wave velocity of 6.15 km/sec and a Poisson's ratio of 0.25. The three defined fuzzy sets are 1) P-P travel time intervals, 2) S-S travel time intervals, and 3) S-P travel time intervals. During the mapping process, the first two fuzzy sets are converted using union logic operations and the third fuzzy set is converted using intersect logic operations. After all phase pairs are mapped into the logic space, the most likely location of earthquake epicenter is determined using a simple center of gravity method.

Tests of the fuzzy logic algorithm show that this method is best used for locating regional earthquakes with ambiguous phase readings or with a small aperture array. This method can effectively avoid the local minima problem and provide a more reliable solution than the generalized inverse method. However, the advantage of this method is also its primary disadvantage. The grid size of the trial epicenters limits the accuracy of the location of earthquakes. I have programmed the algorithm as a computer subroutine and incorporated it into the SEISMOS program. Real world tests shows that such a combination provides reliable and accurate locations of earthquakes.

Earthquake Catalogs for New Mexico and Bordering Areas 1962-1998

The completion of the earthquake catalog for New Mexico and bordering areas 1962-1998 represents the outcome of the 37 years of seismological research at New Mexico Tech. This catalog covers the area longitude 101° W to 111° W and latitude 31° N to 38° N. For this study, I compile the earthquake catalog so that almost all events listed in

the catalog are based on the moment magnitude scale, the SEISMOS location program, and the half-space crustal model with a P wave velocity of 6.15 km/sec and a Poisson's ratio of 0.25. During the process, magnitude differences for earthquakes co-located by NMT and the other institutes were used to establish correction factors to events in the catalog whose location and strength parameters were established by LANL, USGS, UTEP, or UTA.

The final catalog contains 925 earthquakes of magnitude 2.0 or greater, 215 inside the Socorro Seismic Anomaly (SSA) (Appendix II), the most striking feature of the seismicity in the region. Quality assessment for the earthquake catalog shows that epicenters of most earthquakes (>70%) are considered as very good and good. Events with very poor rating of locations are mostly distributed near the boundaries of the survey area.

Probabilistic Seismic Hazard Map for New Mexico and Bordering Areas

I have evaluated probabilistic seismic hazards for New Mexico using instrumental earthquake data of magnitude 2.0 or greater for the time period 1962-1998. The probabilistic seismic hazard maps are presented in the format of 10% and 2% probability of exceedance in a 50 year period. I define two seismic source zones for the purpose of hazard analysis, the SSA and the rest of the state and bordering areas (RNM). Dependent events in the earthquake catalog were removed using a moving time and distance window of 7 days and 4 km for the SSA and 7 days and 25 km for the RNM. The final catalog contains 473 events of magnitude 2.0 or greater, 125 inside the SSA.

I use a truncated exponential recurrence model for the probabilistic seismic hazard assessment for both the SSA and the RNM with a upper and a lower bound magnitudes of 6.5 and 2.0, respectively. The maximum likelihood slope B is derived using the Bender's equation and the selected B value of 0.7608 for hazard analysis is the average of the SSA and the RNM. For computing probabilistic ground accelerations for the region, I divide the area into small blocks of 20 x 20 km^2 and evaluated seismic hazards on the basis of blocks.

The size of each block is selected to accommodate the uncertainty of earthquake epicenters. The number of earthquakes for each block is based on 75% of the seismicity within the block and 25% background seismicity. The use of a background seismicity is to avoid a computational error when there is no seismicity within a block.

I select the center point of each block as the representative point for the block. The probabilistic seismic hazard for the block is the combination of a temporal probability of occurrence and a spatial probability of occurrence. The temporal probability of occurrence is based on the Poisson distribution and the spatial probability of occurrence the Joyner and Fumal (1985) equation that correlates magnitude, hypocentral distance, and peak horizontal ground acceleration. By combining these two probabilities, I can evaluate the peak ground acceleration at a specific location with a given probability of exceedance. For my study, I evaluate probabilistic seismic hazards for New Mexico and bordering areas using 10% and 2% probability of exceedance in a 50 year period. The hazard map for 10% probability of exceedance in a 50 years is suitable for non-critical structures such as residential buildings or houses. For critical installations the hazard map of 2% probability of exceedance in a 50 year period should be used.

In general, the seismic hazards for the region are moderate to low. The seismic hazard map for 10% probability of exceedance in a 50 year period shows that the area inside the SSA has the highest level of seismic hazard, 0.18g. Along the major population corridor of the state from Albuquerque to Santa Fe, the peak ground acceleration is ~0.08g, which generates Modified Mercalli Intensity (MMI) VI effects. In terms of seismic risks for the region for an expected return interval of 500 years, structural damage to modern buildings is unlikely but non-structural damage within these buildings could produce serious injuries and/or loss of property.

Note that the probabilistic seismic hazard analysis is not a precision computation and that assumptions and justifiable judgements need to be made. For example, I have

compared the NMT hazard map with the USGS hazard map. Though these two maps generally agree on the areas with the highest seismic hazards, the NMT hazard map is more complex and the estimated ground motions greater than the USGS map. Three important subjective parameters dictate differences in these maps, the cut-off magnitude, the level of smoothing, and the choices of seismic source zones. While it appears that the NMT map reflects the seismic trends in the region, it is difficult to determine whether the map accurately represents the actual seismic hazards as is also the case with the USGS map.

I have conducted extensive sensitivity tests on the probabilistic seismic hazard maps to assess the uncertainties of the estimated hazards. From the magnitude contribution curves for the 50 year 10% probability of exceedance hazard map, it is clear that the range of dominant earthquakes for hazard estimates is between magnitude 4.5 and 5.5. Earthquakes of higher or lower magnitudes than this range do contribute to the hazard estimates but are less significant. I have examined how estimates of seismic hazard are effected by 1) the completeness of earthquake data 1962-1998, 2) the removal of dependent events, 3) the maximum likelihood recurrence slope β, and 4) the choice of the maximum magnitude earthquake. Results of these tests indicate that the most influential factor is the recurrence slope β. This factor determines the recurrence rates of earthquakes used for calculating hazards. However, because very few earthquakes of magnitude 4.0 or greater were observed during the 37 years of instrumental recording, the reliability of the slope β value can not be confirmed until more earthquake data are gathered

To compensate for the shortcoming of an earthquake catalog covering only 37 years, I have compared the recurrence rates of pre-instrumental data 1868-1961 (Md 4.5-5.8) in the SSA with the recurrence model based on instrumental earthquakes. In addition, the long-term average for active faults of 15 ka or younger age in the Rio Grande rift (RGR) is also compared with the average obtained from an extrapolation of the instrumental data. The recurrence relationship based on pre-instrumental earthquake data

shows a slightly higher but relatively good fit with the recurrence model from the 1962–1998 instrumental data.

For active faults in the RGR, I estimate their long-term average based on 16 faults with 21 movements for the past 15 ka (Machette *et al*., 1998); each movement equivalent to a magnitude 7.0 or greater earthquake. This yields an average return interval of 750 years. I rearrange the earthquake catalog to include only earthquakes within the boundaries of the RGR and extrapolate the recurrence model to magnitude 7.0 or greater; the estimated strengths of the 21 earthquakes. The result of this comparison shows a small difference in the recurrence rates of ~34%. Considering the uncertainties of the two data sets, the higher rate based on faults is probably not significant.

Finally, I did not include active faults in the region in the probabilistic hazard analysis because active faults as well as high magnitude earthquakes have very little effect on short-term hazard estimates (500 and 2500 year return periods) for the region. However, for hazard estimates with long return intervals, active faults should be included in the hazard analysis. I have demonstrated the effects of active faults on probabilistic seismic hazard estimates for the SSA in Chapter 6. At very low probabilities of exceedance (0.2% and 0.5%), the active faults are the dominant factor in hazard estimates in their immediate surroundings but their effects diminish fairly quickly as the distance increases.

References

Ake, J. P., A. R. Sanford, and S. J. Jarpe (1983). A magnitude scale for central New Mexico based on signal duration, *New Mexico Institute of Mining and Technology Geophysics Open-File Report 45*, Socorro, New Mexico, 26 pp.

Ake, J. P., and A. R. Sanford (1988). New evidence for existence and internal structure of a thin layer of magma at mid-crustal depths near Socorro, New Mexico, *Bull. Seism. Soc. Am.,* **78***,* 1335-1359.

Aldrich, M. J., Jr., and A. W. Laughlin (1984). A model for the tectonic development of the southeastern Colorado Plateau boundary, *J. Geophys. Res.* **89**, 10,207-10,218.

Algermissen, S.T., D.M. Perkins, P.C. Thenhaus, S.L. Hanson, and B.L. Bender (1990). Probabilistic earthquake acceleration and velocity maps for the United States and Puerto Rico, *U.S. Geol. Surv. Misc. Field Studies Map MF-2120.*

Balch, R. S., H. E. Hartse, A. R. Sanford, and K. W. Lin (1997). A new map of the geographic extent of the Socorro midcrustal magma body, *Bull. Seism. Soc. Am.,* **87***,* 174-182.

Bender, B. (1983). Maximum likelihood estimation of b values for magnitude grouped data, *Bull. Seism. Soc. Am.,* **73***,* 831-852.

Carpenter, P.J., and A.R. Sanford (1985). Apparent Q for upper crustal rocks of the central Rio Grande rift, *J. Geophys. Res.*, **90**, 8661-8674.

Chapin, C. E. (1971). The Rio Grande rift: Part 1, Modifications and additions. *New Mex. Geol. Soc., 22nd Annual Field Conference Guidebook*, 191-201.

Chapin, C. E. (1979). Evolution of the Rio Grande rift: A summary, in *Rio Grande Rift: Tectonics and Magmatism,* R. E. Riecker (editor), American Geophysical Union, Washington, D.C., 1-5.

Frankel, A., C. Mueller, T. Barnhard, D. Perkins, E.V. Leyendecker, N. Dickman, S. Hanson, and M. Hopper (1996). National Seismic-Hazard Maps: Documentation: June 1996, *U.S. Geol. Surv. Open-File Report 96-532*.

Hanks, T. C., and H. Kanamori (1979). A moment magnitude scale, *J. Geophys. Res.,* **84**, 2348-2350.

Hartse, H. E. (1991). Simultaneous hypocenter and velocity model estimation using direct and reflected phases from microearthquakes recorded within the central Rio Grande rift, *Ph.D. Dissertation*, New Mexico Institute of Mining and Technology, Socorro, New Mexico, 251 pp.

Hartse, H. E., A. R. Sanford, and J. S. Knapp (1992). Incorporating Socorro magma body reflections in to the earthquake location process, *Bull. Seism. Soc. Am.,* **82**, 2511-2532.

Jamshidi, M., N. Vadiee , and T.J. Ross, Editors (1993). *Fuzzy Logic and Control Software and Hardware Applications*, PTR Prentice-Hall Inc., New Jersey, 397 pp.

Joyner, W.B., and T.E. Fumal (1985). Predictive mapping of earthquake ground motion, in *Evaluating Earthquake Hazards in the Los Angeles Region - An Earth-Science Perspective*, edited by J.I. Ziony, *U.S. Geol. Surv. Professional Paper 1360*, 203-220.

Lahr, J.C. (1999). HYPOELLIPSE: a computer program for determining local earthuake hypocentral parameters, magnitude, and first motion pattern, *U.S. Geol. Surv. Open-File Report 99-23*.

Larsen, S., R. Reilinger, and L. Brown (1986). Evidence for ongoing crustal deformation related to magmatic activity near Socorro, New Mexico, *J. Geophys. Res.*, **91**, 6283-6292.

Lee, W. H. K. and J. C. Lahr (1975). HYPO71 (Revised): A computer program for determining hypocenter, magnitude, and first motion pattern of local earthquakes, *U.S. Geol. Surv. Open-File Rept. 75-311.*

Lienert, B.R. (1997). Assessment of earthquake location accuracy and confidence region estimates using known nuclear tests, *Bull. Seism. Soc. Am.,* **87**, 1150-1157.

Lin, K. W. (1994). Regional earthquake hypocenter location using a fuzzy logic algorithm enhanced SEISMOS program, *New Mexico Institute of Mining and Technology Geophysics Open-File Report 74*, Socorro, New Mexico, 82 pp.

Lin, K. W., A. R. Sanford, and I. C. Tsai (1997). Probabilistic seismic hazard estimates for New Mexico using instrumental data from 1962 through 1995, *New Mexico Institute of Mining and Technology Geophysics Open-File Report 84*, Socorro, New Mexico, 12 pp.

Lin, K. W., and A. R. Sanford (1998). Effects of active faults on probabilistic seismic hazard estimates for the Socorro area using instrumental data from 1962 through 1995, *New Mexico Institute of Mining and Technology Geophysics Open-File Report 88*, Socorro, New Mexico, 15 pp.

Lin, K. W., and A. R. Sanford (1998). Improving locations of regional earthquakes using a modified *G* matrix, *New Mexico Institute of Mining and Technology Geophysics Open-File Report 90*, Socorro, New Mexico, 26 pp.

Machette, M.N. (1986). History of Quaternary offset and paleoseismicity along the La Jencia fault, central Rio Grande rift, New Mexico, *Bull. Seism. Soc. Am.*, **76**, 259-272.

Machette, M. N., S. F. Personius, K. I. Kelson, K. M. Haller, and R. L. Dart (1998). Map and data for Quaternary faults and folds in New Mexico, *U.S. Geol. Surv., Open-File Report 98-521*, 443 pp.

Newton, C. A., D. J. Cash, K. H. Olsen, and E.F. Homuth (1976). LASL seismic programs in the vicinity of Los Alamos, New Mexico, *Los Alamos Scientific Laboratory Informal Report LA-6406-MS*, 42 pp.

Palvis, G. (1992). Apprasing relative earthquake location errors, *Bull. Seism. Soc. Am.,* **82**, 836-859.

Rinehart, E.J., and A.R. Sanford (1981). Upper crustal structure of the Rio Grande rift from inversion of microearthquake S-wave reflections, *Bull. Seismo. Soc. Am.,* **71**, 437-450.

Reiter, L. (1990). *Earthquake Hazard Analysis: Issues and Insights*, Columbia University Press, New York, 254 pp.

Richter, C. F. (1958). *Elementary Seismology*, W. H. Freeman, San Francisco, California, 768 pp.

Sanford, A. R., Olsen, K. H., and Jaksha L. H. (1981). Earthquakes in New Mexico, 1849-1977, *New Mexico Bureau of Mines and Mineral Resources Circular 171*, 20 pp.

Sanford, A. R., L. H. Jaksha, and D. J. Cash (1991). Seismicity of the Rio Grande rift in New Mexico, in *Neotectonics of North America*, D. B. Slemmons, E. R. Engdahl, M. D. Zoback, and D. D. Blackwell (Editors), Geological Society of America, 229-244.

Sanford, A.R. (1994). An Estimate of the Earthquake hazard in the Socorro area based on instrumental data: July, 1960 - December, 1993, *New Mexico Institute of Mining and Technology Geophysics Open-File Report* 72, Socorro, New Mexico, 3 pp.

Sanford, A.R., R.S. Balch, and K.W. Lin (1995). A seismic anomaly in the Rio Grande rift near Socorro, New Mexico, *New Mexico Institute of Mining and Technology Geophysics Open-File Report 78,* Socorro, New Mexico, 17 pp.

Sanford, A.R., K. W. Lin, I. C. Tsai, and L. H. Jaksha (1995). Preliminary listing and discussion of New Mexico earthquakes 1962-1994 with duration magnitudes of 3.0 or greater, *New Mexico Institute of Mining and Technology Geophysics Open-File Report 79*, Socorro, New Mexico, 13 pp.

Sanford, A.R., K.W. Lin, and I.C. Tsai, L.H. Jaksha (1995). Seismicity along a segment of a prominent ENE trending topographic lineament in New Mexico and West Texas, *New Mexico Institute of Mining and Technology Geophysics Open-File Report 81,* Socorro, New Mexico, 16 pp.

Sanford, A. R., K. W. Lin, and I. C. Tsai (1997). Preliminary seismicity map for New Mexico and bordering areas, *New Mexico Institute of Mining and Technology Geophysics Open-File Report 83*, Socorro, New Mexico, 2 pp.

Sanford, A. R. (1998). An empirical relation between magnitude and maximum intensity for New Mexico earthquakes, *New Mexico Institute of Mining and Technology Geophysics Open-File Report 86,* Socorro, New Mexico, 4 pp.

Sanford, A. R. and K. W. Lin (1998). Evidence for a 1400 km long Socorro Fracture Zone, *New Mexico Institute of Mining and Technology Geophysics Open-File Report 89*, Socorro, New Mexico, 18 pp.

Sinno, Y.A., P.H. Daggett, G.R. Keller, P. Morgan, and S.H. Harder (1986). Crustal structure of the southern Rio Grande rift determined from seismic refraction profiling, *J. Geophys. Res.,* **91**, 6143-6156.

Stewart, S.W. and Pakiser, L.C. (1962). Crustal structure in eastern New Mexico interpreted from the Gnome explosion, *Bull. Seism. Soc. Am.*, **52**, 1017-1030.

Thelin, G. P., and R. J. Pike (1991). *Landforms of the conterminous United States - a digital shaded-reflect portrayal*, Misc. Investigation Series Map I-2206, U.S. Geol. Survey, U.S. Dept. of Interior.

Toppozada, T.R. (1974). Seismic Investigation of Crustal Structure and Upper Mantle Velocity in the State of New Mexico and Vicinity, *Ph.D. Dissertation*, New Mexico Institute of Mining and Technology, Socorro, New Mexico, 152 pp.

Wells, D.L. and K.J. Coppersmith (1994). New empirical relationships among magnitude, rupture length, rupture width, and surface displacement, *Bull. Seism. Soc. Am.*, **84**, 974-1002.

Appendix I

Listings of Magnitude Differences Between New Mexico Tech and Contributing Institutes

For most events in the NMT catalogs, we were able to determine a duration magnitude (Newton et al., 1976; and Ake et al., 1983). For the remainder, we had to use magnitudes calculated by contributing institutions, adjusted by the average differences appearing in the tables of this appendix. Below are the institutions for which magnitude corrections were established.

USGS United States Geological Survey

LANL Los Alamos National Laboratory

UTEP University of Texas at El Paso

ASL Albuquerque Seismological Laboratory – USGS Facility

A correction was also established for CLN, an NMT station in SE New Mexico whose records were used to establish magnitudes for a large number of events from July 1974 through April 1979.

NMT-USGS Magnitude Comparisons

No.	yy	mm	dd	hh	mm	ss	lat	latm	long	longm	nmt	usgs	Difference
1.	62	01	03	23	01	51.21	34	50.90	103	45.09	2.9	2.6	**0.3**
2.	62	03	06	09	03	17.72	31	22.72	104	34.67	3.5	3.5	**0.0**
3.	63	02	22	07	02	06.72	32	21.78	106	58.22	2.4	2.5	**-0.1**
4.	63	06	06	08	06	32.80	36	32.38	104	27.41	4.0	3.8	**0.2**
5.	63	12	19	16	12	29.16	34	49.40	104	16.44	3.4	2.9	**0.5**
6.	64	02	11	09	02	30.32	34	13.73	103	56.14	2.1	2.5	**-0.4**
7.	64	10	20	00	10	04.09	30	44.98	106	51.91	3.5	3.3	**0.2**
8.	64	11	08	09	11	00.77	31	52.38	103	00.19	2.9	3.0	**-0.2**
9.	64	11	21	11	11	23.98	31	54.31	103	02.13	2.8	3.1	**-0.3**
10.	65	02	03	11	02	29.99	35	30.95	103	38.52	3.4	2.9	**0.5**
11.	65	02	03	19	02	32.54	31	55.40	102	57.47	3.3	3.3	**0.0**
12.	65	08	30	05	08	30.90	31	58.22	103	02.34	2.9	3.5	**-0.6**
13.	66	01	23	01	01	39.30	36	57.60	106	57.00	4.8	5.1	**-0.3**
14.	66	01	23	02	01	34.70	36	58.80	107	01.80	3.2	2.8	**0.4**
15.	66	01	23	02	01	14.10	36	57.00	107	03.00	2.7	2.7	**0.0**
16.	66	01	23	06	01	15.50	36	57.00	107	03.60	3.1	3.3	**-0.2**
17.	66	01	23	11	01	06.60	36	85.80	107	04.20	3.0	3.3	**-0.3**
18.	66	01	23	12	01	36.30	36	58.80	106	59.40	1.6	2.5	**-0.9**
19.	66	01	23	19	01	19.30	36	58.80	107	01.80	3.0	3.0	**0.0**
20.	66	01	23	20	01	17.80	36	59.40	107	04.80	2.1	2.3	**-0.2**
21.	66	01	23	23	01	09.30	36	58.80	107	00.60	3.9	3.8	**0.1**
22.	66	01	25	10	01	05.00	37	00.00	106	59.40	3.2	3.3	**-0.1**
23.	66	01	29	11	01	51.20	36	58.80	106	58.80	3.0	3.0	**0.0**
24.	66	02	17	00	02	14.00	36	58.80	107	01.20	2.7	2.5	**0.2**
25.	66	02	18	17	02	14.00	36	58.80	107	01.20	2.5	2.6	**-0.1**
26.	66	02	27	18	02	51.50	36	54.00	107	00.00	3.1	3.2	**-0.1**
27.	66	03	22	04	03	50.00	36	58.80	107	01.20	2.5	2.8	**-0.3**
28.	66	04	14	15	04	29.50	37	00.00	107	00.00	3.2	3.3	**-0.1**
29.	66	05	08	17	05	38.30	36	54.00	107	00.00	3.6	3.5	**0.1**
30.	66	05	08	17	05	36.80	37	00.00	107	00.00	3.5	3.2	**0.3**
31.	66	05	09	02	05	23.60	37	00.00	106	54.00	3.4	4.4	**-1.0**
32.	66	05	19	00	05	42.20	36	54.00	107	00.00	3.7	3.3	**0.4**
33.	66	06	01	17	06	12.90	36	54.00	107	00.00	3.1	3.0	**0.1**
34.	66	06	04	10	06	39.60	36	54.00	107	00.00	3.4	4.1	**-0.7**
35.	66	06	21	05	06	38.20	36	54.00	107	06.00	2.7	3.0	**-0.3**
36.	66	07	24	02	07	50.20	36	54.00	107	00.00	2.7	2.4	**0.3**
37.	66	08	12	09	08	53.90	36	36.00	107	01.20	2.6	2.8	**-0.2**
38.	66	08	14	15	08	48.15	32	00.47	103	00.61	3.9	3.4	**0.5**
39.	66	08	17	18	08	19.24	30	28.88	105	41.93	3.5	2.9	**0.6**
40.	66	08	19	04	08	45.00	30	18.00	105	36.00	4.3	4.1	**0.2**
41.	66	08	19	08	08	22.00	30	18.00	105	36.00	3.6	4.0	**-0.4**
42.	66	09	24	07	09	46.17	36	25.51	105	05.92	4.2	4.1	**0.1**

NMT-USGS Magnitude Comparisons

No.	yy	mm	dd	hh	mm	ss	lat	latm	long	longm	nmt	usgs	Difference
43.	66	09	24	08	09	07.68	36	28.19	105	19.33	3.2	3.4	**-0.2**
44.	66	09	25	10	09	40.34	36	23.29	105	07.73	4.1	4.0	**0.1**
45.	66	09	25	12	09	39.72	36	25.94	105	08.24	3.7	3.8	**-0.1**
46.	66	10	03	02	10	01.12	37	28.44	104	08.54	4.2	4.3	**-0.1**
47.	66	11	26	20	11	43.45	30	56.93	105	26.63	3.5	3.0	**0.5**
48.	66	11	28	02	11	57.00	30	24.00	105	24.00	3.8	3.8	**0.0**
49.	66	12	05	10	12	38.40	30	30.00	105	24.00	3.7	4.3	**-0.6**
50.	66	12	16	02	12	40.00	36	58.80	107	01.20	3.7	4.1	**-0.4**
51.	67	01	06	15	01	13.00	36	58.80	107	01.20	2.9	3.4	**-0.5**
52.	68	03	09	21	03	28.01	32	46.12	106	02.35	3.4	2.9	**0.5**
53.	68	05	02	02	05	45.13	33	05.75	105	14.36	2.6	2.6	**0.0**
54.	68	05	29	02	05	02.20	34	23.33	107	44.86	1.4	2.5	**-1.1**
55.	69	05	12	08	05	19.40	31	53.55	106	24.39	3.6	3.9	**-0.3**
56.	69	05	12	08	05	17.21	31	53.74	106	25.76	3.4	4.3	**-0.9**
57.	69	07	04	14	07	33.30	36	09.54	106	04.23	3.8	4.4	**-0.6**
58.	69	08	23	21	08	55.12	34	37.32	108	34.16	3.0	3.9	**-0.9**
59.	69	10	19	11	10	30.85	30	50.65	105	34.33	3.8	3.8	**0.0**
60.	69	12	25	12	12	10.07	33	21.72	110	38.70	3.9	4.4	**-0.5**
61.	70	01	12	11	01	15.04	35	56.20	103	23.10	3.9	3.5	**0.4**
62.	70	11	28	07	11	12.03	35	07.02	106	34.19	4.4	4.5	**-0.1**
63.	70	11	30	05	11	20.02	36	16.89	105	31.11	3.0	2.5	**0.5**
64.	71	01	04	07	01	06.77	35	09.39	106	36.03	4.4	4.7	**-0.3**
65.	71	02	18	11	02	14.24	36	18.37	105	46.83	2.9	3.7	**-0.8**
66.	71	04	28	11	04	52.37	36	09.10	106	04.68	2.7	4.0	**-1.3**
67.	71	06	04	03	06	14.96	36	08.75	106	12.94	2.7	3.8	**-1.1**
68.	71	07	30	01	07	51.12	31	46.72	103	03.30	3.6	3.7	**-0.2**
69.	71	07	31	14	07	48.99	31	41.90	103	03.95	3.3	3.6	**-0.3**
70.	71	09	24	01	09	53.88	31	39.86	103	10.64	3.0	3.2	**-0.2**
71.	71	12	06	05	12	12.70	36	08.45	106	08.41	3.3	4.2	**-0.9**
72.	72	03	28	01	03	33.52	36	12.01	106	00.81	3.5	2.7	**0.8**
73.	72	05	20	19	05	45.43	35	23.54	107	19.93	3.0	2.7	**0.3**
74.	72	07	26	04	07	45.42	32	34.07	104	00.75	3.1	2.9	**0.2**
75.	72	11	24	01	11	34.47	31	48.78	108	18.69	2.9	2.7	**0.2**
76.	72	12	09	05	12	00.87	31	45.34	106	24.26	2.6	3.0	**-0.4**
77.	72	12	10	14	12	51.45	31	44.15	106	27.16	2.3	3.0	**-0.7**
78.	72	12	18	04	12	36.23	35	21.98	107	09.74	3.0	2.7	**0.3**
79.	73	03	17	07	03	07.94	36	01.96	106	18.44	3.7	4.5	**-0.8**
80.	73	03	22	02	03	57.97	31	38.18	108	56.60	2.7	2.9	**-0.2**
81.	73	07	16	05	07	22.49	30	10.60	105	43.21	3.5	3.2	**0.3**
82.	73	09	23	03	09	54.66	37	08.42	104	38.04	3.4	4.2	**-0.8**
83.	73	11	14	07	11	10.86	36	59.09	106	59.20	2.6	2.6	**0.0**
84.	73	12	24	02	12	15.56	35	13.93	107	39.72	4.0	4.4	**-0.4**

NMT-USGS Magnitude Comparisons

No.	yy	mm	dd	hh	mm	ss	lat	latm	long	longm	nmt	usgs	Difference
85.	74	07	11	11	07	57.19	35	17.94	107	45.84	2.7	2.5	**0.2**
86.	74	08	26	07	08	21.52	34	28.00	105	51.13	2.6	2.7	**-0.1**
87.	74	08	30	22	08	35.65	34	52.84	107	04.23	3.1	2.9	**0.2**
88.	74	09	26	23	09	07.03	32	38.88	106	31.51	3.3	3.0	**0.3**
89.	74	09	29	13	09	43.78	32	47.57	108	37.64	3.6	3.7	**-0.1**
90.	74	10	02	02	10	21.31	31	52.46	100	51.74	2.5	2.6	**-0.1**
91.	74	10	11	11	10	25.67	32	48.35	108	37.11	2.5	2.6	**-0.1**
92.	74	10	15	12	10	38.71	35	15.13	107	08.21	2.7	2.5	**0.2**
93.	74	11	21	16	11	00.54	32	29.69	106	22.39	2.1	2.7	**-0.6**
94.	74	11	28	03	11	22.24	32	34.52	103	56.65	4.0	3.9	**0.1**
95.	74	12	28	23	12	08.12	34	57.59	105	36.48	2.2	2.6	**-0.4**
96.	75	02	02	20	02	22.47	35	03.19	103	11.26	3.0	2.9	**0.1**
97.	75	06	21	05	06	41.31	36	01.76	103	27.93	2.8	2.5	**0.3**
98.	75	08	01	07	08	39.55	30	29.25	104	35.84	3.6	4.8	**-1.2**
99.	75	09	29	11	09	43.49	35	58.15	106	47.87	2.8	3.2	**-0.4**
100.	75	12	03	10	12	23.07	32	44.61	108	21.82	3.8	3.9	**-0.1**
101.	76	01	05	06	01	29.23	35	52.69	108	32.06	4.7	5.0	**-0.3**
102.	76	01	25	04	01	27.61	31	56.50	103	00.34	3.8	3.9	**-0.1**
103.	76	04	03	20	04	50.89	31	14.56	103	06.07	1.9	2.5	**-0.6**
104.	76	09	19	10	09	44.59	30	28.35	104	34.46	3.0	2.7	**0.3**
105.	77	01	04	18	01	37.28	32	26.59	106	48.86	2.8	3.2	**-0.4**
106.	77	01	04	23	01	58.88	33	57.54	105	58.89	2.8	2.7	**0.1**
107.	77	06	07	23	06	18.64	32	47.27	100	44.39	3.8	4.0	**-0.2**
108.	77	06	08	00	06	28.74	32	49.86	100	49.54	2.9	2.9	**0.0**
109.	77	06	08	13	06	07.40	31	01.44	109	13.62	4.5	4.3	**0.2**
110.	77	06	08	13	06	29.42	32	52.03	101	02.60	2.6	2.6	**0.0**
111.	77	06	17	03	06	05.10	32	54.05	100	56.77	2.7	3.0	**-0.3**
112.	77	11	27	20	11	20.13	33	01.26	101	08.33	2.7	2.6	**0.1**
113.	77	11	28	01	11	54.60	32	58.51	101	08.37	3.4	3.5	**-0.1**
114.	81	05	04	10	05	31.87	32	19.37	108	58.29	2.4	3.0	**-0.6**
115.	81	05	07	01	05	20.13	32	15.86	108	56.08	2.8	3.2	**-0.4**
116.	81	12	04	08	12	26.06	34	24.11	108	12.60	2.8	2.8	**0.0**
117.	82	01	04	16	01	17.48	31	17.30	102	49.05	3.6	3.9	**-0.3**
118.	82	03	02	16	03	20.80	35	53.17	105	27.34	2.2	2.9	**-0.7**
119.	82	03	16	11	03	06.26	35	38.79	103	30.33	2.1	3.1	**-1.0**
120.	82	05	16	16	05	53.81	36	39.56	106	44.67	2.0	2.7	**-0.7**
121.	82	05	16	21	05	01.73	36	42.60	106	43.01	2.0	2.5	**-0.5**
122.	82	05	16	22	05	47.26	36	39.66	106	41.27	2.1	2.7	**-0.6**
123.	82	05	17	02	05	04.91	36	40.13	106	40.58	2.0	2.6	**-0.6**
124.	82	05	31	09	05	08.33	35	09.61	106	42.20	1.3	2.0	**-0.7**
125.	82	07	12	16	07	08.10	35	33.39	107	08.64	1.4	2.5	**-1.1**
126.	82	08	07	04	08	02.64	36	38.25	106	47.54	2.0	2.7	**-0.7**

NMT-USGS Magnitude Comparisons

No.	yy	mm	dd	hh	mm	ss	lat	latm	long	longm	nmt	usgs	Difference
127.	82	11	03	17	11	01.86	35	18.27	108	41.72	2.5	3.1	**-0.6**
128.	82	11	13	09	11	49.76	36	34.53	106	33.33	1.7	2.7	**-1.0**
129.	82	11	28	02	11	52.45	33	42.90	100	50.24	3.4	3.3	**0.1**
130.	83	03	03	18	03	18.63	29	57.81	104	20.87	2.8	3.4	**-0.6**
131.	83	04	03	04	04	28.58	35	26.56	102	38.07	3.0	3.4	**-0.5**
132.	83	04	30	07	04	20.47	33	21.91	106	24.97	3.5	3.5	**0.0**
133.	83	08	17	15	08	21.17	37	18.97	104	12.92	2.8	3.4	**-0.6**
134.	83	08	29	04	08	22.11	31	48.12	100	37.11	2.6	2.9	**-0.4**
135.	83	09	15	23	09	37.54	34	55.27	104	25.78	3.1	3.2	**-0.1**
136.	83	09	29	07	09	12.20	34	53.17	104	27.20	2.7	2.7	**0.0**
137.	84	05	21	13	05	11.87	35	36.78	102	07.46	2.6	3.1	**-0.5**
138.	84	09	11	14	09	30.63	31	36.34	100	45.38	3.0	3.2	**-0.2**
139.	84	09	19	06	09	28.85	31	46.50	100	39.42	3.0	3.2	**-0.2**
140.	84	12	04	20	12	30.77	32	38.19	103	12.75	2.1	2.9	**-0.8**
141.	85	04	14	21	04	02.93	35	15.56	108	55.52	3.4	3.4	**0.0**
142.	85	06	05	10	06	59.93	32	32.70	106	57.38	2.9	2.9	**0.0**
143.	85	09	06	05	09	45.70	32	31.79	106	58.51	2.6	2.6	**0.0**
144.	85	09	25	19	09	21.67	32	30.56	106	57.98	2.5	2.5	**0.0**
145.	85	11	12	06	11	13.96	28	07.71	104	05.34	3.8	4.3	**-0.5**
146.	85	12	15	07	12	52.63	35	26.23	104	39.86	3.0	3.6	**-0.6**
147.	86	01	30	22	01	41.38	31	59.21	100	54.05	3.3	3.3	**0.0**
148.	86	04	17	21	04	29.31	32	33.28	106	57.67	2.7	2.7	**0.0**
149.	86	05	14	15	05	03.41	37	21.67	110	13.79	3.0	3.2	**-0.2**
150.	86	07	17	21	07	56.72	35	20.37	110	43.92	2.4	2.6	**-0.2**
151.	86	08	27	18	08	58.02	35	07.23	105	10.15	3.1	3.2	**-0.1**
152.	86	11	05	13	11	53.65	36	33.07	101	53.10	2.0	2.4	**-0.4**
153.	86	12	11	01	12	54.63	35	23.45	101	05.73	2.3	2.5	**-0.2**
154.	87	09	09	09	09	18.86	37	24.04	108	23.64	2.1	2.5	**-0.4**
155.	88	01	15	07	01	33.33	37	13.75	107	02.90	3.1	3.1	**0.0**
156.	88	01	31	09	01	36.28	29	54.59	105	11.78	3.8	3.4	**0.4**
157.	89	01	29	05	01	15.55	35	10.98	104	06.20	3.4	3.4	**0.0**
158.	89	03	24	11	03	48.13	36	59.63	103	45.59	2.4	2.7	**-0.3**
159.	89	04	18	10	04	54.17	34	49.82	110	38.25	3.2	3.5	**-0.3**
160.	89	05	25	07	05	15.08	30	41.50	109	31.21	4.0	4.6	**-0.6**
161.	89	05	26	09	05	09.18	30	33.35	109	36.59	3.5	3.5	**0.0**
162.	89	07	17	20	07	27.15	35	11.64	110	25.32	3.0	3.0	**0.0**
163.	89	10	14	08	10	17.77	34	24.08	108	05.49	3.1	3.4	**-0.3**
164.	90	07	01	13	07	32.53	35	30.53	102	32.59	3.0	2.7	**0.3**
165.	90	07	22	21	07	04.95	34	50.96	105	57.64	3.7	3.7	**-0.1**
166.	90	10	31	15	10	59.43	30	53.94	109	12.15	3.8	3.8	**0.0**
167.	91	05	10	12	05	58.15	37	17.29	106	54.95	3.8	3.4	**0.4**
168.	91	09	04	20	09	16.92	33	00.19	108	08.35	2.3	2.3	**0.0**

NMT-USGS Magnitude Comparisons

No.	yy	mm	dd	hh	mm	ss	lat	latm	long	longm	nmt	usgs	Difference
169.	91	09	04	21	09	27.16	32	59.36	108	08.20	2.4	2.4	**0.0**
170.	91	09	06	01	09	47.36	32	55.72	108	10.52	2.8	2.8	**0.0**
171.	92	02	23	16	02	52.95	30	38.66	105	26.17	3.6	3.4	**0.2**
172.	92	05	02	10	05	34.59	37	13.24	104	53.05	2.4	3.1	**-0.7**
173.	92	08	26	03	08	51.16	32	12.56	102	35.52	3.2	3.0	**0.2**
174.	93	03	24	02	03	06.09	35	08.15	104	27.64	2.7	3.0	**-0.3**
175.	93	06	23	03	06	13.10	31	25.97	102	31.39	2.8	2.8	**0.0**
176.	93	07	16	20	07	16.03	29	52.59	107	06.71	3.5	3.8	**-0.3**
177.	93	09	29	02	09	24.19	35	48.96	103	09.35	3.0	3.3	**-0.3**
178.	93	10	05	04	10	24.67	30	08.96	109	01.04	3.5	4.0	**-0.5**
179.	93	11	30	03	11	36.28	35	48.53	103	09.40	3.3	3.3	**0.0**
180.	93	12	22	19	12	11.39	33	19.87	105	40.91	3.2	3.2	**0.0**
181.	95	03	19	18	03	44.76	34	50.87	104	24.85	3.0	3.3	**-0.3**
182.	95	07	04	03	07	05.62	36	12.12	104	56.64	3.6	3.8	**-0.2**
											Avg.		**-0.185**
											Std Dev.		**0.395**

NMT-LANL Magnitude Comparisons

No.	yy	mm	dd	hh	mm	ss	lat	latm	long	longm	nmt	usgs	Difference
1.	62	06	14	07	06	53.71	35	47.21	106	47.57	2.8	2.8	**0.0**
2.	63	11	25	12	11	33.04	36	34.48	105	18.53	2.2	2.4	**-0.2**
3.	65	12	29	00	12	24.32	35	01.64	105	46.67	2.7	3.1	**-0.4**
4.	66	08	12	09	08	53.90	36	36.00	107	01.20	2.6	2.4	**0.2**
5.	70	05	22	09	05	35.89	35	37.96	106	02.31	2.3	1.5	**0.8**
6.	70	07	31	11	07	30.84	35	18.58	106	08.39	3.2	2.7	**0.5**
7.	70	08	07	11	08	07.00	35	25.53	105	54.36	2.5	2.0	**0.5**
8.	70	11	28	07	11	12.03	35	07.02	106	34.19	4.4	3.8	**0.6**
9.	70	11	30	05	11	20.02	36	16.89	105	31.11	3.0	3.2	**-0.2**
10.	71	01	04	07	01	06.77	35	09.39	106	36.03	4.4	3.8	**0.6**
11.	71	02	18	11	02	14.24	36	18.37	105	46.83	2.9	2.8	**0.1**
12.	71	04	28	11	04	52.37	36	09.10	106	04.68	2.7	2.7	**0.0**
13.	71	06	04	03	06	14.96	36	08.75	106	12.94	2.7	3.0	**-0.3**
14.	71	06	24	22	06	37.31	36	45.90	105	50.41	1.7	2.3	**-0.6**
15.	71	12	06	05	12	12.70	36	08.45	106	08.41	3.3	3.2	**0.1**
16.	71	12	06	05	12	49.37	36	10.24	106	11.28	3.1	2.8	**0.3**
17.	71	12	06	06	12	09.01	36	09.84	106	11.59	3.2	3.1	**0.1**
18.	71	12	11	02	12	23.98	36	09.14	106	35.40	2.8	2.5	**0.3**
19.	72	03	28	01	03	33.52	36	12.01	106	00.81	3.5	3.4	**0.1**
20.	72	03	28	02	03	16.85	36	08.40	106	04.47	2.9	2.7	**0.2**
21.	72	03	31	20	03	19.78	36	07.80	105	58.46	3.2	3.2	**-0.1**
22.	72	12	18	04	12	36.23	35	21.98	107	09.74	3.0	2.7	**0.3**
23.	74	05	04	08	05	59.80	34	53.00	106	16.00	1.3	1.3	**0.0**
24.	74	06	22	09	06	42.62	35	02.85	106	41.77	2.6	2.4	**0.2**
25.	74	10	15	12	10	38.71	35	15.13	107	08.21	2.7	2.6	**0.1**
26.	74	10	18	04	10	57.20	35	12.72	106	38.00	2.4	2.3	**0.1**
27.	75	09	29	11	09	43.49	35	58.15	106	47.87	2.8	3.0	**-0.3**
28.	76	07	06	04	07	49.53	35	29.82	104	50.70	1.3	1.5	**-0.2**
											Avg.		**0.104**
											Std Dev.		**0.332**

NMT-UTEP Magnitude Comparisons

No.	yy	mm	dd	hh	mm	ss	lat	latm	long	longm	nmt	usgs	Difference
1.	75	12	12	14	12	34.71	31	36.40	102	18.41	3.0	3.4	**-0.4**
2.	76	1	22	7	1	56.90	31	56.99	103	1.54	2.0	2.8	**-0.9**
3.	76	1	25	4	1	27.61	31	56.50	103	0.34	3.8	3.9	**-0.1**
4.	76	6	15	8	6	20.14	31	35.75	102	21.99	2.8	2.7	**0.1**
5.	76	8	10	9	8	8.79	31	45.95	102	1.77	1.6	2.4	**-0.8**
6.	76	8	10	10	8	12.21	31	47.69	102	3.65	2.0	2.9	**-0.9**
7.	77	3	20	7	3	8.97	32	12.43	103	6.09	2.0	2.2	**-0.2**
											Avg.		**-0.453**
											Std Dev.		**0.409**

NMT-ASL* Magnitude Comparisons

No.	yy	mm	dd	hh	mm	ss	lat	latm	long	longm	nmt	usgs	Difference
1.	76	04	01	14	04	27.63	33	51.59	105	58.30	1.6	1.3	**0.3**
2.	76	04	01	14	04	58.54	33	56.30	105	55.54	2.7	2.2	**0.5**
3.	76	04	01	14	04	16.71	33	54.73	105	55.50	2.1	1.3	**0.8**
4.	76	04	18	03	04	18.89	33	54.79	105	57.78	1.8	1.4	**0.4**
5.	76	12	23	08	12	59.85	34	43.04	105	50.02	2.7	2.1	**0.6**
6.	77	01	04	23	01	58.88	33	57.54	105	58.89	2.8	2.9	**-0.1**
7.	77	01	05	12	01	03.58	34	01.95	105	58.98	2.5	2.2	**0.3**
											Avg.		**0.397**
											Std Dev.		**0.275**

* ASL - Albuquerque Seismological Laboratory is a USGS facility that produced catalogs of earthquakes in the central Rio Grande valley of New Mexico from 1976 - 1992

NMT-CLN Magnitude Comparisons

No.	yy	mm	dd	hh	mm	ss	lat	latm	long	longm	nmt	usgs	Difference
1.	74	07	31	17	07	48.52	33	06.63	104	11.63	2.1	1.9	**0.2**
2.	74	08	17	07	08	17.44	30	10.65	105	43.16	2.1	3.1	**-1.0**
3.	74	08	26	07	08	21.52	34	28.00	105	51.13	2.6	2.4	**0.2**
4.	74	09	26	23	09	07.03	32	38.88	106	31.51	3.3	2.3	**1.0**
5.	74	10	02	02	10	21.31	31	52.46	100	51.74	2.5	2.5	**0.0**
6.	74	10	27	16	10	55.68	30	37.95	104	49.79	2.0	2.6	**-0.6**
7.	74	11	01	15	11	11.74	31	44.57	106	44.70	2.2	2.6	**-0.4**
8.	74	11	12	02	11	34.89	32	08.32	102	40.09	1.9	1.4	**0.5**
9.	74	11	21	16	11	00.54	32	29.69	106	22.39	2.1	2.3	**-0.2**
10.	74	11	21	18	11	06.44	32	04.37	102	44.98	2.2	2.2	**0.0**
11.	74	11	22	08	11	03.05	32	56.38	101	15.59	2.2	2.0	**0.2**
12.	74	11	22	14	11	12.82	33	46.87	105	12.46	1.7	2.0	**-0.3**
13.	74	11	28	03	11	22.24	32	34.52	103	56.65	4.0	3.9	**0.1**
14.	75	08	01	07	08	39.55	30	29.25	104	35.84	3.6	3.9	**-0.3**
15.	75	08	03	03	08	50.31	30	42.85	104	27.19	1.9	2.1	**-0.2**
16.	75	10	10	11	10	55.33	33	21.37	105	01.15	1.8	2.1	**-0.3**
17.	76	01	15	20	01	58.35	30	58.93	102	19.40	2.1	2.0	**0.0**
18.	76	01	21	23	01	18.54	30	57.10	102	17.59	2.0	1.9	**0.1**
19.	76	01	22	07	01	56.90	31	56.99	103	01.54	2.0	2.5	**-0.6**
20.	76	01	25	04	01	27.61	31	56.50	103	00.34	3.8	3.1	**0.7**
21.	76	01	28	07	01	48.04	31	59.46	100	53.35	1.9	2.5	**-0.7**
22.	76	02	14	05	02	22.73	31	38.03	102	28.02	1.6	1.7	**-0.1**
23.	76	03	05	02	03	13.07	31	39.42	102	14.92	3.2	2.4	**0.8**
24.	76	03	09	06	03	46.27	29	38.93	104	13.03	3.9	4.0	**-0.1**
25.	76	03	12	12	03	56.06	29	45.57	104	42.09	3.0	3.5	**-0.5**
26.	76	03	20	12	03	21.00	31	16.41	104	56.26	1.7	1.9	**-0.2**
27.	76	04	01	14	04	27.63	33	51.59	105	58.30	1.6	2.5	**-0.9**
28.	76	04	01	14	04	58.54	33	56.30	105	55.54	2.7	2.6	**0.1**
29.	76	04	01	14	04	16.71	33	54.73	105	55.50	2.1	1.4	**0.7**
30.	76	04	03	20	04	50.89	31	14.56	103	06.07	1.9	2.9	**-1.0**
31.	76	05	03	06	05	59.07	32	24.50	105	39.69	2.6	2.4	**0.2**
32.	76	05	21	13	05	30.21	32	29.28	105	35.39	2.2	2.3	**-0.1**
33.	76	06	15	08	06	20.14	31	35.75	102	21.99	2.8	2.3	**0.5**
34.	76	07	28	12	07	51.08	33	01.38	102	17.25	2.0	2.0	**0.0**
35.	76	08	10	09	08	08.79	31	45.95	102	01.77	1.6	1.7	**-0.1**
36.	76	08	10	10	08	12.21	31	47.69	102	03.65	2.0	1.9	**0.1**
37.	76	08	29	19	08	25.08	30	05.95	105	10.57	2.1	2.4	**-0.3**
38.	76	08	30	13	08	27.80	32	40.52	106	05.28	2.5	2.3	**0.2**
39.	76	09	19	10	09	44.59	30	28.35	104	34.46	3.0	3.2	**-0.2**
40.	77	03	20	07	03	08.97	32	12.43	103	06.09	2.0	2.1	**-0.1**
41.	77	06	07	23	06	18.64	32	47.27	100	44.39	3.8	3.5	**0.3**
42.	77	06	08	00	06	28.74	32	49.86	100	49.54	2.9	2.8	**0.1**

NMT-CLN Magnitude Comparisons

No.	yy	mm	dd	hh	mm	ss	lat	latm	long	longm	nmt	usgs	Difference
43.	77	06	08	13	06	10.58	32	55.34	100	48.98	3.6	3.4	**0.2**
44.	77	06	08	13	06	29.42	32	52.03	101	02.60	2.6	2.9	**-0.3**
45.	77	11	14	07	11	26.82	31	31.47	104	57.60	2.7	2.2	**0.5**
46.	77	11	27	20	11	20.13	33	01.26	101	08.33	2.7	2.8	**-0.1**
											Avg.		**-0.028**
											Std Dev.		**0.442**

Appendix II

Earthquake Catalogs for New Mexico and Bordering Areas: 1962 through 1998; Moment Magnitude ≥ 2.0

Two catalogs are presented, one for the Socorro Seismic Anomaly (SSA), and the other for the remainder of the state (RNM) and bordering areas. For each event, the catalogs indicate (1) organizations which have calculated magnitudes and the magnitude selected, and (2) the organization whose location is used. The symbols used for the latter are:

nmt	New Mexico Tech
lanl	Los Alamos National Laboratory
utep	University of Texas at El Paso
uta	University of Texas at Austin
asl	Albuquerque Seismological Laboratory – USGS Facility
usgs	United States Geological Survey

Also in the magnitude columns is the symbol cln. This is the designation for a NMT station in SE New Mexico whose records were used to establish magnitudes for a large number of events from July 1974 through April 1979.

SSA 1962-1998

No.	Date			Time			Latitude		Longitude		Magnitude								Location by:					
	yr.	mo.	dy.	hr.	mn.	sec.	deg.	min.	deg.	min.	nmt	lanl	utep	uta	asl	usgs	cln	Selected	nmt	lanl	utep	uta	asl	usgs
1.	62	03	22	04	23	53.91	34	14.73	106	32.97	2.6							2.6	√					
2.	62	04	09	23	42	58.73	34	14.40	106	27.43	2.3							2.3	√					
3.	62	05	02	23	21	19.58	34	10.13	106	44.46	2.0							2.0	√					
4.	62	06	05	19	30	43.96	34	21.05	106	58.70	2.5							2.5	√					
5.	62	06	12	19	10	21.56	34	20.21	106	59.97	2.2							2.2	√					
6.	62	06	27	04	49	16.89	33	59.69	106	52.86	2.2							2.2	√					
7.	62	09	01	16	15	05.70	34	14.07	106	31.25	2.3							2.3	√					
8.	62	12	15	20	20	34.21	33	56.21	106	55.42	2.2							2.2	√					
9.	63	06	02	05	07	34.85	34	13.17	106	30.13	2.5							2.5	√					
10.	63	07	03	19	08	00.57	33	56.43	106	56.07	2.5							2.5	√					
11.	64	08	24	12	22	50.67	33	58.63	106	54.86	2.0							2.0	√					
12.	64	09	15	03	56	53.41	34	02.25	106	53.90	2.1							2.1	√					
13.	64	10	20	22	15	14.78	34	02.55	106	36.63	2.1							2.1	√					
14.	65	03	09	19	04	48.97	33	55.75	106	57.36	2.5							2.5	√					
15.	65	04	10	07	01	54.63	33	55.87	106	58.10	2.1							2.1	√					
16.	65	04	17	06	08	55.59	33	56.15	106	54.42	2.0							2.0	√					
17.	65	05	27	07	30	45.09	33	53.89	106	45.44	2.1							2.1	√					
18.	65	05	27	18	50	54.70	33	53.40	106	45.84	2.3							2.3	√					
19.	65	05	27	18	58	40.42	33	52.83	106	45.34	2.4							2.4						
20.	65	05	29	13	01	08.00	33	53.70	106	45.33	2.0							2.0						√
21.	65	06	04	01	58	57.55	33	53.30	106	45.32	2.0							2.0						√
22.	65	07	18	20	37	47.64	34	14.41	106	30.18	2.1							2.1						√
23.	65	07	28	03	52	06.75	33	53.76	106	48.49	2.9							2.9						√
24.	65	12	22	03	33	29.60	34	01.31	106	46.83	2.1							2.1						√
25.	65	12	22	04	04	51.90	34	01.20	106	46.80	2.0							2.0						√
26.	66	02	07	09	10	16.04	34	25.52	106	54.52	2.6							2.6						√
27.	66	10	06	10	19	08.20	34	02.39	107	04.37	2.5							2.5						√

SSA 1962-1998

No.	Date			Time			Latitude		Longitude		Magnitude								Location by:					
	yr.	mo.	dy.	hr.	mn.	sec.	deg.	min.	deg.	min.	nmt	lanl	utep	uta	asl	usgs	cln	Selected	nmt	lanl	utep	uta	asl	usgs
28.	67	01	16	18	14	37.20	34	26.20	106	51.35	2.4							2.4						√
29.	68	05	15	10	13	09.40	34	16.20	106	50.40	3.2							3.2						√
30.	68	07	25	04	54	34.30	33	59.40	106	51.00	2.3							2.3						√
31.	69	01	30	05	17	38.40	34	13.20	106	45.00	4.0							4.0						√
32.	71	01	06	10	56	31.50	34	09.00	106	47.40	3.4							3.4						√
33.	71	01	27	07	56	28.30	34	03.60	106	36.00	2.7							2.7						√
34.	71	09	13	20	46	37.50	34	05.09	106	48.58	2.1							2.1						√
35.	71	12	12	18	31	56.90	34	08.90	106	49.40	2.2							2.2						√
36.	71	12	23	14	21	37.00	34	25.20	107	01.20	2.9							2.9						√
37.	72	05	16	22	13	44.80	34	12.00	106	52.80	2.2							2.2						√
38.	73	06	30	04	59	26.42	34	25.64	106	48.57	2.2							2.2						√
39.	73	09	10	20	29	22.70	34	25.20	106	51.00	3.1	2.9						3.1						√
40.	73	09	22	23	38	35.80	34	27.60	106	57.00	3.6	3.6						3.6						√
41.	74	03	13	16	15	28.78	34	25.97	106	53.51	2.4	2.0						2.4						√
42.	74	04	12	18	14	40.00	34	30.00	106	55.20	2.5	1.8						2.5						√
43.	74	10	15	10	05	02.40	33	50.00	106	35.00	2.0	2.3						2.0						√
44.	74	10	15	10	07	57.90	33	54.00	106	30.00	2.4	2.4						2.4						√
45.	74	11	01	10	45	49.60	33	48.00	106	36.00	2.2	2.2						2.2						√
46.	75	03	04	07	16	52.70	34	30.00	106	54.00	2.1	1.8						2.1						√
47.	75	03	05	03	48	05.30	34	33.00	107	07.20	3.0	2.7						3.0						√
48.	75	03	06	07	56	55.90	34	33.00	107	08.40	3.0	2.5						3.0						√
49.	75	03	07	03	16	13.70	34	33.00	107	08.40	3.5	3.2						3.5						√
50.	75	03	07	07	11	50.90	34	30.78	107	06.60	2.2	1.8						2.2						√
51.	75	03	07	17	36	08.70	34	33.00	107	09.60	3.8	3.4						3.8						√
52.	75	03	07	18	33	33.90	34	30.66	107	02.04	2.3	2.0						2.3						√
53.	75	04	16	13	52	04.76	34	20.05	107	04.04	2.0							2.0						√
54.	75	06	27	01	39	24.70	34	11.40	106	55.80	2.8	2.2						2.8						√

SSA 1962-1998

No.	Date			Time			Latitude		Longitude		Magnitude								Location by:					
	yr.	mo.	dy.	hr.	mn.	sec.	deg.	min.	deg.	min.	nmt	lanl	utep	uta	asl	usgs	cln	Selected	nmt	lanl	utep	uta	asl	usgs
55.	75	06	28	07	20	23.20	34	12.00	106	54.00	2.7	2.4						2.7						√
56.	76	01	14	07	01	31.50	34	06.00	106	48.00	2.4	1.8						2.4						
57.	76	05	09	03	54	09.36	34	13.80	106	53.40	2.4	2.2						2.4	√					
58.	76	06	09	17	37	46.22	34	30.00	106	58.00	2.6	2.2						2.6	√					
59.	77	06	02	06	48	00.00	34	01.20	107	03.60	2.2							2.2	√					
60.	77	08	19	09	22	03.40	34	03.18	107	02.10	2.7	2.6						2.7						
61.	79	10	20	21	05	36.90	33	54.28	106	42.97	2.9	2.2						2.9	√					
62.	79	10	21	11	28	00.00	34	05.64	106	38.88	2.4	1.7						2.4	√					
63.	79	10	22	05	10	15.40	34	05.64	106	38.88	2.2	1.5						2.2	√					
64.	79	10	25	22	12	10.00	34	03.00	107	03.00	3.0	2.5						3.0	√					
65.	80	02	15	11	52	35.17	34	31.99	106	54.15	2.6	2.3						2.6	√					
66.	80	02	28	16	39	45.33	34	24.63	107	00.82	2.4	2.8						2.4	√					
67.	81	05	09	12	35	52.95	34	04.31	106	58.12	3.1							3.1	√					
68.	81	12	01	22	34	35.95	34	22.80	106	52.20	2.1	2.0						2.1	√					
69.	82	01	06	08	30	29.49	34	10.20	106	46.26	2.6							2.6	√					
70.	82	04	11	15	03	31.67	34	08.37	106	45.07	2.0							2.0	√					
71.	82	05	17	11	35	48.47	34	05.01	106	53.33	2.3							2.3	√					
72.	82	05	18	06	00	08.21	34	05.41	106	54.45	2.4							2.4	√					
73.	82	05	18	06	08	38.03	34	04.46	106	52.27	2.5							2.5	√					
74.	82	05	22	02	28	56.92	34	06.63	106	54.32	2.6							2.6	√					
75.	82	05	24	06	32	51.54	34	05.26	106	54.10	2.9							2.9	√					
76.	82	05	29	05	50	58.51	34	04.41	106	51.68	2.2							2.2	√					
77.	82	09	18	03	41	14.62	34	18.11	106	48.86	2.2							2.2	√					
78.	82	09	20	03	55	16.87	33	56.60	107	03.67	2.8							2.8	√					
79.	82	10	07	12	41	25.83	34	18.49	106	48.47	2.3							2.3	√					
80.	83	02	25	02	57	54.73	34	18.17	106	52.64	2.6							2.6	√					
81.	83	02	26	11	15	41.53	34	18.01	106	52.78	3.0							3.0	√					

SSA 1962-1998

No.	Date			Time			Latitude		Longitude		Magnitude								Location by:					
	yr.	mo.	dy.	hr.	mn.	sec.	deg.	min.	deg.	min.	nmt	lanl	utep	uta	asl	usgs	cln	Selected	nmt	lanl	utep	uta	asl	usgs
82.	83	02	28	23	12	42.15	34	18.16	106	52.77	2.3							2.3	√					
83.	83	03	02	23	22	19.69	34	17.91	106	52.94	4.2							4.2	√					
84.	83	03	02	23	50	36.33	34	18.53	106	52.16	2.7							2.7	√					
85.	83	03	03	02	06	28.03	34	18.34	106	52.61	2.1							2.1	√					
86.	83	03	03	17	40	11.74	34	18.26	106	52.30	2.0							2.0	√					
87.	83	03	04	00	00	22.30	34	18.21	106	52.85	2.0							2.0	√					
88.	83	03	04	05	26	10.81	34	17.95	106	52.76	2.0							2.0	√					
89.	83	03	08	06	19	00.39	34	17.82	106	52.11	2.2							2.2		√				
90.	83	03	09	09	05	59.98	34	18.46	106	51.89	2.3							2.3		√				
91.	83	03	15	09	27	02.98	34	16.93	106	52.54	2.6							2.6		√				
92.	83	03	17	22	35	52.61	34	18.10	106	53.22	3.0							3.0		√				
93.	83	03	23	01	00	32.46	34	17.31	106	52.45	2.0							2.0		√				
94.	83	03	31	16	10	08.94	34	18.27	106	52.75	2.2							2.2	√					
95.	83	07	28	13	58	47.54	33	53.20	106	47.24	2.2							2.2	√					
96.	84	05	08	07	38	55.64	34	12.19	106	40.91	2.0							2.0	√					
97.	84	06	26	03	45	59.33	34	10.03	106	50.76	2.0							2.0		√				
98.	84	08	26	02	19	55.04	34	18.74	106	49.18	2.5							2.5	√					
99.	84	11	05	08	45	00.37	34	18.56	106	48.96	2.1							2.1		√				
100.	85	08	16	14	56	53.10	34	07.17	106	49.66	4.1							4.1		√				
101.	85	08	17	05	14	46.57	34	07.37	106	49.59	2.0							2.0		√				
102.	85	08	18	15	48	15.64	34	07.37	106	49.60	2.0							2.0		√				
103.	85	08	19	19	35	33.94	34	07.36	106	49.52	2.2							2.2	√					
104.	85	08	29	01	19	35.17	34	19.73	106	43.83	2.3							2.3		√				
105.	85	08	31	02	47	43.35	34	07.50	106	49.53	2.2							2.2	√					
106.	85	08	31	20	37	43.62	34	07.37	106	49.72	2.0							2.0	√					
107.	85	08	31	22	47	43.35	34	07.60	106	49.52	2.2							2.2	√					
108.	85	09	18	19	38	00.42	34	11.27	106	47.95	2.2							2.2	√					

SSA 1962-1998

No.	Date			Time			Latitude		Longitude		Magnitude								Location by:					
	yr.	mo.	dy.	hr.	mn.	sec.	deg.	min.	deg.	min.	nmt	lanl	utep	uta	asl	usgs	cln	Selected	nmt	lanl	utep	uta	asl	usgs
109.	85	09	21	08	04	00.41	34	07.63	106	49.61	2.1							2.1		√				
110.	86	02	24	15	47	48.06	34	19.32	106	58.08	2.6							2.6	√					
111.	86	04	04	17	33	20.85	34	08.36	106	49.67	2.1							2.1		√				
112.	86	04	28	12	59	49.73	34	01.71	106	49.78	2.3							2.3	√					
113.	86	04	29	08	30	31.27	34	01.73	106	49.25	2.1							2.1	√					
114.	86	04	29	12	09	03.98	34	06.94	106	50.37	2.1							2.1	√					
115.	86	05	16	13	20	23.75	34	28.14	106	48.15	2.5							2.5		√				
116.	86	05	17	07	16	22.46	34	28.26	106	48.24	2.1							2.1		√				
117.	86	05	17	07	41	42.21	34	27.98	106	48.15	2.1							2.1		√				
118.	86	06	12	11	52	41.91	34	20.44	106	42.54	2.0							2.0			√			
119.	86	09	24	22	41	15.67	34	07.63	106	49.66	2.1							2.1	√					
120.	86	10	05	15	55	35.27	34	08.84	106	44.85	3.0							3.0	√					
121.	87	05	01	04	12	27.69	33	57.47	106	46.92	2.3							2.3		√				
122.	87	07	25	01	06	34.91	34	17.18	106	52.87	2.0							2.0	√					
123.	88	02	29	23	23	07.01	33	55.04	106	57.21	2.2							2.2	√					
124.	88	03	20	20	47	40.62	34	20.68	106	39.98	2.7							2.7			√			
125.	88	05	19	04	26	29.53	34	05.80	106	37.32	2.5							2.5	√					
126.	88	09	08	12	01	57.32	34	21.57	106	40.33	2.0							2.0			√			
127.	89	11	29	06	54	38.84	34	27.50	106	52.71	4.7							4.7		√				
128.	89	11	29	07	10	37.77	34	26.96	106	52.86	2.0							2.0	√					
129.	89	11	29	12	22	04.71	34	27.28	106	51.98	2.2							2.2	√					
130.	89	11	29	23	56	48.91	34	27.46	106	52.01	2.7							2.7	√					
131.	89	11	30	01	42	59.23	34	27.10	106	52.82	2.4							2.4		√				
132.	89	12	21	13	49	44.33	33	46.49	106	55.21	2.3							2.3	√					
133.	89	12	22	15	13	39.69	34	27.78	106	52.33	2.0							2.0	√					
134.	89	12	24	15	15	21.54	34	28.25	106	52.71	2.5							2.5	√					
135.	90	01	03	14	58	39.82	34	26.88	106	51.92	2.4							2.4			√			

SSA 1962-1998

No.	Date			Time			Latitude		Longitude		Magnitude								Location by:					
	yr.	mo.	dy.	hr.	mn.	sec.	deg.	min.	deg.	min.	nmt	lanl	utep	uta	asl	usgs	cln	Selected	nmt	lanl	utep	uta	asl	usgs
136.	90	01	29	13	16	10.96	34	27.45	106	52.27	4.6							4.6	√					
137.	90	01	29	15	36	17.93	34	27.61	106	52.54	2.9							2.9	√					
138.	90	01	29	22	58	29.78	34	27.43	106	52.44	2.1							2.1	√					
139.	90	01	31	01	08	19.67	34	27.53	106	51.58	4.4							4.4	√					
140.	90	02	04	02	12	06.23	34	27.26	106	52.02	2.3							2.3	√					
141.	90	02	04	15	55	19.86	34	27.61	106	52.23	2.6							2.6	√					
142.	90	02	06	09	33	17.64	34	26.75	106	52.17	2.1							2.1	√					
143.	90	02	18	01	06	16.41	33	58.40	106	34.68	2.0							2.0	√					
144.	90	02	21	12	02	19.30	33	57.98	106	34.82	3.4							3.4	√					
145.	90	02	21	12	03	56.25	33	59.03	106	36.19	3.4							3.4		√				
146.	90	02	21	13	28	50.76	33	58.84	106	36.17	2.4							2.4	√					
147.	90	02	21	14	39	29.79	33	57.98	106	34.92	2.1							2.1	√					
148.	90	02	21	17	26	16.17	33	58.44	106	35.49	2.0							2.0			√			
149.	90	02	21	17	35	06.12	33	57.96	106	34.63	2.9							2.9			√			
150.	90	02	21	17	36	33.35	33	57.48	106	33.06	2.6							2.6		√				
151.	90	02	21	22	37	01.01	33	58.14	106	34.84	2.5							2.5	√					
152.	90	02	22	15	32	43.89	33	57.91	106	34.59	2.6							2.6	√					
153.	90	02	23	04	05	57.77	33	57.47	106	33.89	2.4							2.4	√					
154.	90	02	26	10	10	20.09	33	58.29	106	35.22	2.1							2.1	√					
155.	90	02	27	13	23	21.45	33	55.84	106	32.95	3.9							3.9	√					
156.	90	02	27	13	44	26.48	33	58.41	106	37.21	2.2							2.2			√			
157.	90	02	27	13	50	41.42	33	58.46	106	35.81	3.2							3.2	√					
158.	90	03	02	18	20	18.86	33	57.91	106	34.57	3.2							3.2		√				
159.	90	03	02	18	23	20.00	33	58.29	106	35.41	3.2							3.2		√				
160.	90	03	05	04	22	35.12	33	58.47	106	34.84	2.0							2.0	√					
161.	90	03	05	07	28	30.49	33	58.41	106	35.16	2.0							2.0	√					
162.	90	05	05	16	26	22.99	34	26.81	106	53.04	3.7							3.7	√					

No.	Date			Time			Latitude		Longitude		Magnitude								Location by:					
	yr.	mo.	dy.	hr.	mn.	sec.	deg.	min.	deg.	min.	nmt	lanl	utep	uta	asl	usgs	cln	Selected	nmt	lanl	utep	uta	asl	usgs
163.	90	05	05	22	23	54.90	34	26.63	106	52.92	2.5							2.5			√			
164.	90	05	06	12	20	35.91	34	26.48	106	52.62	2.7							2.7		√				
165.	90	05	14	22	50	20.63	34	26.91	106	52.17	2.2							2.2	√					
166.	90	06	07	22	42	55.72	34	26.77	106	52.65	2.1							2.1	√					
167.	90	07	21	19	28	23.25	34	26.76	106	52.12	3.0							3.0	√					
168.	90	07	21	20	30	31.54	34	26.93	106	51.88	3.1							3.1	√					
169.	90	07	21	23	48	05.17	34	26.54	106	51.78	3.2							3.2	√					
170.	90	07	22	00	10	10.23	34	27.63	106	52.31	2.0							2.0	√					
171.	90	07	31	07	32	40.48	34	26.69	106	52.23	3.3							3.3	√					
172.	90	08	14	14	45	32.52	34	26.87	106	51.69	2.0							2.0		√				
173.	90	08	18	13	08	12.81	33	58.08	106	35.79	2.5							2.5		√				
174.	90	08	18	17	27	31.78	33	58.14	106	35.66	2.0							2.0		√				
175.	90	08	18	17	48	02.99	33	58.09	106	35.84	2.2							2.2		√				
176.	90	08	18	19	57	18.46	33	58.30	106	35.33	2.0							2.0		√				
177.	90	08	25	03	59	05.55	33	58.42	106	36.30	2.0							2.0		√				
178.	90	08	25	04	35	42.20	33	58.39	106	34.36	2.4							2.4		√				
179.	90	11	08	10	46	53.99	34	26.50	106	51.88	4.3							4.3	√					
180.	90	11	08	11	03	46.79	34	26.56	106	52.18	3.1							3.1		√				
181.	90	11	08	12	28	48.48	34	26.91	106	51.98	2.3							2.3	√					
182.	90	11	08	15	13	09.64	34	26.56	106	51.62	2.0							2.0		√				
183.	90	11	10	12	18	17.10	34	26.50	106	51.56	3.1							3.1	√					
184.	90	11	12	03	30	47.21	34	26.78	106	52.37	2.1							2.1	√					
185.	90	11	12	13	23	45.27	34	26.63	106	51.94	2.0							2.0	√					
186.	90	11	12	22	47	24.86	34	26.69	106	51.89	2.8							2.8	√					
187.	90	11	15	07	25	24.64	34	26.93	106	52.06	3.6							3.6	√					
188.	90	11	22	10	20	31.24	34	26.89	106	52.08	2.4							2.4		√				
189.	90	12	05	03	36	44.51	34	26.45	106	52.19	2.6							2.6		√				

SSA 1962-1998

No.	Date			Time			Latitude		Longitude		Magnitude								Location by:					
	yr.	mo.	dy.	hr.	mn.	sec.	deg.	min.	deg.	min.	nmt	lanl	utep	uta	asl	usgs	cln	Selected	nmt	lanl	utep	uta	asl	usgs
190.	90	12	05	05	15	04.20	34	26.47	106	52.28	2.1							2.1		√				
191.	90	12	10	07	08	16.65	34	26.88	106	52.02	2.1							2.1		√				
192.	91	01	03	12	49	19.01	34	26.94	106	51.11	2.6							2.6		√				
193.	91	02	12	08	27	48.18	33	59.65	106	36.79	2.6							2.6		√				
194.	91	02	26	21	21	33.37	34	27.67	106	51.81	2.4							2.4		√				
195.	91	03	05	20	17	11.14	34	28.30	106	51.00	3.0							3.0		√				
196.	91	03	06	14	36	59.18	34	26.75	106	52.01	2.0							2.0		√				
197.	91	03	30	19	24	25.01	34	01.25	107	02.38	2.4							2.4		√				
198.	91	04	02	01	48	03.23	34	27.34	106	52.33	2.2							2.2		√				
199.	91	06	05	18	44	14.84	34	27.24	106	50.87	3.1							3.1		√				
200.	91	06	22	22	35	34.50	34	27.08	106	51.34	2.0							2.0	√					
201.	91	06	22	22	53	34.31	34	27.67	106	51.23	2.1							2.1		√				
202.	91	08	20	17	02	27.30	34	01.41	107	01.68	2.3							2.3		√				
203.	92	04	13	08	50	35.86	34	26.74	106	52.03	2.2							2.2		√				
204.	92	08	24	01	25	35.21	34	00.46	106	51.62	2.6							2.6	√					
205.	92	08	24	02	56	43.24	33	58.94	106	51.98	2.3							2.3	√					
206.	93	09	05	18	15	38.81	34	27.01	106	51.28	2.0							2.0	√					
207.	94	01	01	02	51	31.52	34	25.34	106	58.45	2.5							2.5	√					
208.	94	01	12	16	54	43.94	34	18.88	107	01.22	2.3							2.3	√					
209.	94	04	29	14	54	18.67	34	01.29	107	02.37	2.2							2.2	√					
210.	96	02	28	03	18	21.24	34	12.87	106	57.24	2.1							2.1	√					
211.	98	03	11	09	51	03.71	34	06.97	106	50.44	2.3							2.3	√					
212.	98	03	11	15	50	49.43	34	07.45	106	51.17	2.2							2.2	√					
213.	98	03	25	06	25	57.22	34	06.94	106	56.98	2.3							2.3	√					
214.	98	04	07	00	21	35.88	34	08.94	106	53.05	2.0							2.0	√					
215.	98	04	22	02	42	37.59	34	15.78	106	51.66	2.0							2.0	√					

RNM and Bordering Areas 1962-1998

No.	Date			Time			Latitude		Longitude		Magnitude								Location by:					
	yr.	mo.	dy.	hr.	mn.	sec.	deg.	min.	deg.	min.	nmt	lanl	utep	uta	asl	usgs	cln	Selected	nmt	lanl	utep	uta	asl	usgs
1.	62	01	03	23	29	51.21	34	50.90	103	45.09	2.9					2.6		2.9	√					
2.	62	03	06	09	59	17.72	31	22.72	104	34.67	3.5					3.5		3.5	√					
3.	62	06	14	07	27	53.71	35	47.21	106	47.57	2.8	2.8						2.8	√					
4.	62	06	25	02	35	28.59	34	01.54	108	00.78	2.2							2.2	√					
5.	63	02	22	07	02	06.72	32	21.78	106	58.22	2.4					2.5		2.4	√					
6.	63	03	06	14	49	35.17	33	23.54	107	27.51	2.2							2.2	√					
7.	63	06	06	08	05	32.80	36	32.38	104	27.41	4.0					3.8		4.0	√					
8.	63	06	23	07	52	37.40	36	24.83	102	43.00	2.8							2.8	√					
9.	63	07	23	05	13	48.17	32	58.06	108	57.31	2.9							2.9	√					
10.	63	08	19	00	08	24.13	32	27.93	107	05.74	2.4							2.4	√					
11.	63	10	21	11	17	30.03	33	19.17	110	43.22	2.5							2.5	√					
12.	63	11	25	12	52	33.04	36	34.48	105	18.53	2.2	2.4						2.2	√					
13.	63	12	19	16	47	29.16	34	49.40	104	16.44	3.4					2.9		3.4	√					
14.	64	02	11	09	24	30.32	34	13.73	103	56.14	2.1					2.5		2.1	√					
15.	64	03	03	01	26	25.55	34	50.36	103	36.02	2.9							2.9	√					
16.	64	10	20	00	53	04.09	30	44.98	106	51.91	3.5					3.3		3.5	√					
17.	64	11	08	09	25	00.77	31	52.38	103	00.19	2.9					3.0		2.9	√					
18.	64	11	21	11	21	23.98	31	54.31	103	02.13	2.8					3.1		2.8	√					
19.	65	02	03	11	32	29.99	35	30.95	103	38.52	3.4					2.9		3.4	√					
20.	65	02	03	19	59	32.54	31	55.40	102	57.47	3.3					3.3		3.3	√					
21.	65	04	13	09	35	46.00	30	18.00	105	06.00	3.4							3.4	√					
22.	65	08	30	05	17	30.90	31	58.22	103	02.34	2.9					3.5		2.9	√					
23.	65	12	29	00	50	24.32	35	01.64	105	46.67	2.7	3.1						2.7	√					
24.	66	01	23	01	56	39.30	36	57.60	106	57.00	4.8					5.1		4.8	√					
25.	66	01	23	02	08	34.70	36	58.80	107	01.80	3.2					2.8		3.2						√
26.	66	01	23	02	13	14.10	36	57.00	107	03.00	2.7					2.7		2.7						√
27.	66	01	23	06	14	15.50	36	57.00	107	03.60	3.1					3.3		3.1						√

RNM and Bordering Areas 1962-1998

No.	Date			Time			Latitude		Longitude		Magnitude								Location by:					
	yr.	mo.	dy.	hr.	mn.	sec.	deg.	min.	deg.	min.	nmt	lanl	utep	uta	asl	usgs	cln	Selected	nmt	lanl	utep	uta	asl	usgs
28.	66	01	23	08	58	20.00	36	58.80	107	01.20	3.4							3.4						√
29.	66	01	23	10	53	09.80	36	58.20	107	03.60	2.1							2.1						√
30.	66	01	23	11	01	06.60	36	85.80	107	04.20	3.0					3.3		3.0						√
31.	66	01	23	19	43	19.30	36	58.80	107	01.80	3.0					3.0		3.0						√
32.	66	01	23	20	42	17.80	36	59.40	107	04.80	2.1					2.3		2.1						√
33.	66	01	23	23	48	09.30	36	58.80	107	00.60	3.9					3.8		3.9						√
34.	66	01	24	22	06	49.30	36	57.60	106	58.80	2.7							2.7						√
35.	66	01	25	10	38	05.00	37	00.00	106	59.40	3.2					3.3		3.2						√
36.	66	01	25	15	06	37.00	36	58.80	107	01.20						2.5		2.3						√
37.	66	01	25	15	32	47.30	36	58.80	106	56.40	2.2							2.2						√
38.	66	01	25	19	53	06.30	36	59.40	106	58.80	2.0							2.0						√
39.	66	01	27	03	59	00.80	37	01.80	106	58.20	2.1							2.1						√
40.	66	01	27	07	48	29.50	36	58.20	106	58.20						2.5		2.3						√
41.	66	01	27	09	28	58.90	37	01.20	107	01.90	2.3							2.3						√
42.	66	01	28	14	53	01.70	36	58.80	106	56.40	2.0							2.0						√
43.	66	01	29	11	21	51.20	36	58.80	106	58.80	3.0					3.0		3.0						√
44.	66	01	29	18	38	48.30	36	58.80	106	59.40	2.5							2.5						√
45.	66	01	29	19	25	06.00	36	57.60	106	58.20	2.5							2.5						√
46.	66	01	31	15	43	52.70	36	56.40	106	55.80						2.3		2.1						√
47.	66	02	06	12	03	52.40	36	54.00	107	06.00	2.0							2.0						√
48.	66	02	06	12	06	18.00	36	58.80	107	01.20	2.2							2.2						√
49.	66	02	11	12	08	44.30	36	57.60	106	59.40	2.0							2.0						√
50.	66	02	17	00	27	14.00	36	58.80	107	01.20	2.7					2.5		2.7						√
51.	66	02	18	17	56	14.00	36	58.80	107	01.20	2.5					2.6		2.5						√
52.	66	02	27	18	07	51.50	36	54.00	107	00.00	3.1					3.2		3.1						√
53.	66	03	22	04	39	50.00	36	58.80	107	01.20	2.5					2.8		2.5						√
54.	66	03	24	08	24	04.50	37	00.00	107	06.00	2.4							2.4						√

RNM and Bordering Areas 1962-1998

No.	Date			Time			Latitude		Longitude		Magnitude								Location by:					
	yr.	mo.	dy.	hr.	mn.	sec.	deg.	min.	deg.	min.	nmt	lanl	utep	uta	asl	usgs	cln	Selected	nmt	lanl	utep	uta	asl	usgs
55.	66	04	14	15	07	29.50	37	00.00	107	00.00	3.2					3.3		3.2						√
56.	66	04	21	14	14	18.20	35	19.51	103	15.94	3.4							3.4	√					
57.	66	04	28	11	07	28.90	37	00.00	107	06.00	2.2							2.2						√
58.	66	05	04	05	40	37.50	36	48.00	107	06.00	2.7							2.7						√
59.	66	05	08	17	23	38.30	36	54.00	107	00.00	3.6					3.5		3.6						√
60.	66	05	08	17	50	36.80	37	00.00	107	00.00	3.5					3.2		3.5						√
61.	66	05	09	01	26	45.00	37	00.00	106	48.00	2.7							2.7						√
62.	66	05	09	02	08	53.60	36	54.00	107	00.00	2.8							2.8						√
63.	66	05	09	02	57	23.60	37	00.00	106	54.00	3.4					4.4		3.4						√
64.	66	05	19	00	26	42.20	36	54.00	107	00.00	3.7					3.3		3.7						√
65.	66	06	01	17	17	12.90	36	54.00	107	00.00	3.1					3.0		3.1						√
66.	66	06	02	21	59	11.60	36	54.00	107	00.00						3.3		3.1						√
67.	66	06	04	10	29	39.60	36	54.00	107	00.00	3.4					4.1		3.4						√
68.	66	06	08	23	33	14.90	36	54.00	107	06.00	2.4							2.4						√
69.	66	06	21	05	24	38.20	36	54.00	107	06.00	2.7					3.0		2.7						√
70.	66	06	26	18	41	40.50	36	54.00	107	01.20	2.8							2.8						√
71.	66	07	24	02	48	50.20	36	54.00	107	00.00	2.7					2.4		2.7						√
72.	66	08	02	13	54	38.20	36	54.00	107	01.20	2.0							2.0						√
73.	66	08	12	09	18	53.90	36	36.00	107	01.20	2.6	2.4				2.8		2.6						√
74.	66	08	14	15	25	48.15	32	00.47	103	00.61	3.9					3.4		3.9	√					
75.	66	08	17	18	47	19.24	30	28.88	105	41.93	3.5					2.9		3.5	√					
76.	66	08	19	04	15	45.00	30	18.00	105	36.00	4.3					4.1		4.3						√
77.	66	08	19	08	38	22.00	30	18.00	105	36.00	3.6					4.0		3.6						√
78.	66	09	17	09	25	26.07	32	38.69	109	43.77	2.5							2.5	√					
79.	66	09	17	21	30	14.72	34	53.32	103	58.81	2.7							2.7	√					
80.	66	09	24	07	33	46.17	36	25.51	105	05.92	4.2					4.1		4.2	√					
81.	66	09	24	08	27	07.68	36	28.19	105	19.33	3.2					3.4		3.2	√					

RNM and Bordering Areas 1962-1998

No.	Date			Time			Latitude		Longitude		Magnitude								Location by:					
	yr.	mo.	dy.	hr.	mn.	sec.	deg.	min.	deg.	min.	nmt	lanl	utep	uta	asl	usgs	cln	Selected	nmt	lanl	utep	uta	asl	usgs
82.	66	09	25	10	10	40.34	36	23.29	105	07.73	4.1					4.0		4.1	√					
83.	66	09	25	12	22	39.72	36	25.94	105	08.24	3.7					3.8		3.7	√					
84.	66	10	03	02	26	01.12	37	28.44	104	08.54	4.2					4.3		4.2	√					
85.	66	10	06	06	29	52.17	35	08.01	104	07.31	2.9							2.9	√					
86.	66	11	26	20	05	43.45	30	56.93	105	26.63	3.5					3.0		3.5	√					
87.	66	11	28	02	20	57.00	30	24.00	105	24.00	3.8					3.8		3.8						√
88.	66	12	05	10	10	38.40	30	30.00	105	24.00	3.7					4.3		3.7						√
89.	66	12	16	02	00	40.00	36	58.80	107	01.20	3.7					4.1		3.7						√
90.	67	01	06	15	41	13.00	36	58.80	107	01.20	2.9					3.4		2.9						√
91.	67	07	29	05	49	40.31	33	09.63	108	30.39	2.5							2.5	√					
92.	67	09	29	03	52	48.51	32	11.16	106	52.88	2.4							2.4	√					
93.	67	11	25	19	01	39.12	36	43.05	105	29.36	2.7							2.7	√					
94.	68	03	09	21	54	28.01	32	46.12	106	02.35	3.4					2.9		3.4	√					
95.	68	03	23	11	53	38.01	32	40.05	105	54.52	2.6							2.6	√					
96.	68	05	02	02	56	45.13	33	05.75	105	14.36	2.6					2.6		2.6	√					
97.	68	05	19	11	02	56.98	34	28.22	107	55.37	2.8							2.8	√					
98.	68	07	27	12	08	15.96	36	18.97	103	02.03	2.9							2.9	√					
99.	68	08	22	02	22	26.21	34	20.60	105	50.54	2.2							2.2	√					
100.	69	05	12	08	26	19.40	31	53.55	106	24.39	3.6					3.9		3.6	√					
101.	69	05	12	08	49	17.21	31	53.74	106	25.76	3.4					4.3		3.4	√					
102.	69	05	28	05	06	21.71	35	28.99	107	23.11	2.2							2.2	√					
103.	69	06	08	11	36	01.92	34	09.07	105	11.27	2.6							2.6	√					
104.	69	07	04	14	43	33.30	36	09.54	106	04.23	3.8					4.4		3.8	√					
105.	69	08	23	21	41	55.12	34	37.32	108	34.16	3.0					3.9		3.0	√					
106.	69	09	13	23	05	34.04	36	42.76	105	40.43	2.9							2.9	√					
107.	69	09	15	10	47	46.22	35	15.72	109	09.40	2.4							2.4	√					
108.	69	10	19	11	51	30.85	30	50.65	105	34.33	3.8					3.8		3.8	√					

RNM and Bordering Areas 1962-1998

No.	Date			Time			Latitude		Longitude		Magnitude								Location by:					
	yr.	mo.	dy.	hr.	mn.	sec.	deg.	min.	deg.	min.	nmt	lanl	utep	uta	asl	usgs	cln	Selected	nmt	lanl	utep	uta	asl	usgs
109.	69	12	25	12	49	10.07	33	21.72	110	38.70	3.9					4.4		3.9						√
110.	70	01	12	11	21	15.04	35	56.20	103	23.10	3.9					3.5		3.9	√					
111.	70	02	03	05	59	35.61	37	55.08	108	18.66						4.0		3.8						√
112.	70	05	22	09	43	35.89	35	37.96	106	02.31	2.3	1.5						2.3	√					
113.	70	07	03	11	41	26.02	35	13.97	106	46.93	2.1							2.1	√					
114.	70	07	31	11	57	30.84	35	18.58	106	08.39	3.2	2.7						3.2	√					
115.	70	08	03	19	24	19.04	34	33.91	110	37.09	2.7							2.7	√					
116.	70	08	07	11	59	07.00	35	25.53	105	54.36	2.5	2.0						2.5	√					
117.	70	11	28	07	40	12.03	35	07.02	106	34.19	4.4	3.8				4.5		4.4	√					
118.	70	11	30	05	35	20.02	36	16.89	105	31.11	3.0	3.2				2.5		3.0	√					
119.	71	01	04	07	39	06.77	35	09.39	106	36.03	4.4	3.8				4.7		4.4	√					
120.	71	01	04	13	15	29.15	35	09.39	106	36.03	2.5							2.5	√					
121.	71	02	18	11	28	14.24	36	18.37	105	46.83	2.9	2.8				3.7		2.9	√					
122.	71	04	28	11	36	52.37	36	09.10	106	04.68	2.7	2.7				4.0		2.7	√					
123.	71	05	22	22	31	19.36	35	26.56	107	38.74	2.2							2.2	√					
124.	71	06	04	03	55	14.96	36	08.75	106	12.94	2.7	3.0				3.8		2.7	√					
125.	71	07	30	01	45	51.12	31	46.72	103	03.30	3.6					3.7		3.6	√					
126.	71	07	31	14	53	48.99	31	41.90	103	03.95	3.3					3.6		3.3	√					
127.	71	09	23	21	14	18.61	37	07.40	104	20.67	2.5							2.5	√					
128.	71	09	24	01	01	53.88	31	39.86	103	10.64	3.0					3.2		3.0	√					
129.	71	10	15	14	17	27.38	36	56.97	108	12.68	2.0							2.0	√					
130.	71	12	06	05	18	12.70	36	08.45	106	08.41	3.3	3.2				4.2		3.3	√					
131.	71	12	06	05	22	49.37	36	10.24	106	11.28	3.1	2.8						3.1	√					
132.	71	12	06	05	38	07.70	36	08.12	106	08.71		2.5						2.6	√					
133.	71	12	06	06	14	09.01	36	09.84	106	11.59	3.2	3.1						3.2	√					
134.	71	12	11	02	28	23.98	36	09.14	106	35.40	2.8	2.5						2.8	√					
135.	71	12	27	11	08	51.44	35	45.06	106	56.65	2.2							2.2	√					

RNM and Bordering Areas 1962-1998

No.	Date			Time			Latitude		Longitude		Magnitude								Location by:					
	yr.	mo.	dy.	hr.	mn.	sec.	deg.	min.	deg.	min.	nmt	lanl	utep	uta	asl	usgs	cln	Selected	nmt	lanl	utep	uta	asl	usgs
136.	72	02	20	23	22	54.76	36	28.11	105	03.76	2.1							2.1	√					
137.	72	02	27	15	50	03.92	32	51.12	105	59.73	2.6							2.6	√					
138.	72	03	28	01	53	33.52	36	12.01	106	00.81	3.5	3.4				2.7		3.5	√					
139.	72	03	28	02	03	16.85	36	08.40	106	04.47	2.9	2.7						2.9	√					
140.	72	03	31	20	14	19.78	36	07.80	105	58.46	3.2	3.2						3.2	√					
141.	72	05	06	07	35	05.04	35	24.83	107	21.89	2.0							2.0	√					
142.	72	05	20	19	15	45.43	35	23.54	107	19.93	3.0					2.7		3.0	√					
143.	72	07	26	04	35	45.42	32	34.07	104	00.75	3.1					2.9		3.1	√					
144.	72	11	24	01	13	34.47	31	48.78	108	18.69	2.9					2.7		2.9	√					
145.	72	12	09	05	58	00.87	31	45.34	106	24.26	2.6					3.0		2.6	√					
146.	72	12	10	14	37	51.45	31	44.15	106	27.16	2.3					3.0		2.3	√					
147.	72	12	18	04	07	36.23	35	21.98	107	09.74	3.0	2.7				2.7		3.0	√					
148.	73	02	26	10	51	30.32	35	51.08	104	13.78	2.2							2.2	√					
149.	73	03	17	06	32	56.25	31	35.56	102	21.55	2.5							2.5	√					
150.	73	03	17	07	43	07.94	36	01.96	106	18.44	3.7					4.5		3.7	√					
151.	73	03	22	02	45	57.97	31	38.18	108	56.60	2.7					2.9		2.7	√					
152.	73	07	04	07	54	06.51	31	05.23	105	44.33	2.5							2.5	√					
153.	73	07	16	05	27	22.49	30	10.60	105	43.21	3.5					3.2		3.5	√					
154.	73	07	27	02	46	45.50	36	32.92	108	31.90	2.5							2.5	√					
155.	73	08	02	09	20	36.63	31	02.42	105	33.74	3.6							3.6	√					
156.	73	08	03	22	48	58.34	37	19.47	107	46.15	2.2							2.2	√					
157.	73	08	04	06	15	53.54	35	06.35	103	13.20	3.0							3.0	√					
158.	73	09	19	13	28	19.54	37	08.07	104	34.60		3.0						3.1	√					
159.	73	09	23	03	08	54.66	37	08.42	104	38.04	3.4					4.2		3.4	√					
160.	73	11	14	07	56	10.86	36	59.09	106	59.20	2.6					2.6		2.6	√					
161.	73	12	24	02	20	15.56	35	13.93	107	39.72	4.0					4.4		4.0	√					
162.	74	01	17	23	04	20.10	36	11.28	106	11.58		2.1						2.2		√				

RNM and Bordering Areas 1962-1998

No.	Date			Time			Latitude		Longitude		Magnitude								Location by:					
	yr.	mo.	dy.	hr.	mn.	sec.	deg.	min.	deg.	min.	nmt	lanl	utep	uta	asl	usgs	cln	Selected	nmt	lanl	utep	uta	asl	usgs
163.	74	03	23	10	44	15.00	36	30.00	107	04.98		2.4						2.5		√				
164.	74	06	22	09	53	42.62	35	02.85	106	41.77	2.6	2.4						2.6	√					
165.	74	07	11	11	26	57.19	35	17.94	107	45.84	2.7					2.5		2.7	√					
166.	74	07	31	17	34	48.52	33	06.63	104	11.63	2.1						1.9	2.1	√					
167.	74	08	17	07	35	17.44	30	10.65	105	43.16	2.1						3.1	2.1	√					
168.	74	08	26	07	33	21.52	34	28.00	105	51.13	2.6					2.7	2.4	2.6	√					
169.	74	08	30	22	57	35.65	34	52.84	107	04.23	3.1					2.9		3.1	√					
170.	74	09	26	23	44	07.03	32	38.88	106	31.51	3.3					3.0	2.3	3.3	√					
171.	74	09	29	13	13	43.78	32	47.57	108	37.64	3.6					3.7		3.6	√					
172.	74	09	29	14	26	58.77	32	58.83	108	45.86	2.5							2.5	√					
173.	74	10	02	02	40	21.31	31	52.46	100	51.74	2.5					2.6	2.5	2.5	√					
174.	74	10	11	11	07	25.67	32	48.35	108	37.11	2.5					2.6		2.5	√					
175.	74	10	15	12	47	38.71	35	15.13	107	08.21	2.7	2.6				2.5		2.7	√					
176.	74	10	18	04	30	57.20	35	12.72	106	38.00	2.4	2.3						2.4	√					
177.	74	10	27	16	18	55.68	30	37.95	104	49.79	2.0						2.6	2.0	√					
178.	74	11	01	15	06	11.74	31	44.57	106	44.70	2.2						2.6	2.2	√					
179.	74	11	21	16	22	00.54	32	29.69	106	22.39	2.1					2.7	2.3	2.1	√					
180.	74	11	21	18	59	06.44	32	04.37	102	44.98	2.2						2.2	2.2	√					
181.	74	11	22	08	53	03.05	32	56.38	101	15.59	2.2						2.0	2.2	√					
182.	74	11	28	03	35	22.24	32	34.52	103	56.65	4.0					3.9	3.9	4.0	√					
183.	74	12	28	23	24	08.12	34	57.59	105	36.48	2.2					2.6		2.2	√					
184.	75	01	16	04	34	37.55	31	12.11	106	42.44	3.3							3.3	√					
185.	75	01	30	16	00	37.01	30	56.93	103	04.71	2.1							2.1	√					
186.	75	02	02	01	59	45.57	31	38.29	106	53.91	2.0							2.0	√					
187.	75	02	02	20	39	22.47	35	03.19	103	11.26	3.0					2.9		3.0	√					
188.	75	02	09	09	12	35.70	36	10.98	106	13.98		2.0						2.1		√				
189.	75	05	16	07	26	24.47	36	20.33	104	39.01	2.6							2.6	√					

RNM and Bordering Areas 1962-1998

No.	Date			Time			Latitude		Longitude		Magnitude								Location by:					
	yr.	mo.	dy.	hr.	mn.	sec.	deg.	min.	deg.	min.	nmt	lanl	utep	uta	asl	usgs	cln	Selected	nmt	lanl	utep	uta	asl	usgs
190.	75	05	21	04	46	59.00	36	44.76	106	39.72		2.0						2.1		√				
191.	75	06	21	05	41	41.31	36	01.76	103	27.93	2.8					2.5		2.8	√					
192.	75	07	25	08	11	40.09	29	49.31	102	37.38						2.8	3.1	2.6	√					
193.	75	08	01	07	27	39.55	30	29.25	104	35.84	3.6					4.8	3.9	3.6	√					
194.	75	09	06	03	46	49.99	36	11.22	106	10.50		2.3						2.4		√				
195.	75	09	10	01	01	48.20	36	43.98	105	40.02		2.0						2.1		√				
196.	75	09	29	11	09	43.49	35	58.15	106	47.87	2.8	3.0				3.2		2.8	√					
197.	75	09	29	13	17	18.99	36	02.76	106	51.00		2.0						2.1		√				
198.	75	12	03	10	12	23.07	32	44.61	108	21.82	3.8					3.9		3.8	√					
199.	75	12	03	13	41	32.10	35	47.88	106	10.56		2.5						2.6		√				
200.	75	12	12	14	24	34.71	31	36.40	102	18.41	3.0		3.4					3.0	√					
201.	76	01	05	06	23	29.23	35	52.69	108	32.06	4.7					5.0		4.7	√					
202.	76	01	10	01	49	58.77	31	47.15	102	45.31			3.1				2.1	2.1	√					
203.	76	01	15	20	43	58.35	30	58.93	102	19.40	2.1						2.0	2.1	√					
204.	76	01	19	04	03	30.72	31	54.37	103	03.47			3.5			3.5	2.4	3.3	√					
205.	76	01	21	23	11	18.54	30	57.10	102	17.59	2.0						1.9	2.0	√					
206.	76	01	22	07	21	56.90	31	56.99	103	01.54	2.0		2.8				2.5	2.0	√					
207.	76	01	25	04	48	27.61	31	56.50	103	00.34	3.8		3.9			3.9	3.1	3.8	√					
208.	76	03	05	02	58	13.07	31	39.42	102	14.92	3.2						2.4	3.2	√					
209.	76	03	09	06	49	46.27	29	38.93	104	13.03	3.9						4.0	3.9	√					
210.	76	03	12	12	39	56.06	29	45.57	104	42.09	3.0						3.5	3.0	√					
211.	76	03	27	22	25	21.53	32	13.35	103	04.07			1.5				2.0	2.0	√					
212.	76	03	30	09	27	03.46	36	40.88	102	42.68						2.7		2.5	√					
213.	76	04	01	14	46	58.54	33	56.30	105	55.54	2.7				2.2		2.6	2.7	√					
214.	76	04	01	14	51	16.71	33	54.73	105	55.50	2.1				1.3		1.4	2.1	√					
215.	76	04	06	18	09	00.64	33	56.33	105	56.52						2.7	2.9	2.5	√					
216.	76	04	11	07	44	01.96	36	17.58	106	09.12		1.9						2.0		√				

RNM and Bordering Areas 1962-1998

No.	Date			Time			Latitude		Longitude		Magnitude								Location by:					
	yr.	mo.	dy.	hr.	mn.	sec.	deg.	min.	deg.	min.	nmt	lanl	utep	uta	asl	usgs	cln	Selected	nmt	lanl	utep	uta	asl	usgs
217.	76	04	16	18	09	00.64	33	56.33	105	56.52	2.7							2.7	√					
218.	76	04	21	08	40	05.39	32	14.74	102	53.42			2.5			2.5	2.2	2.3	√					
219.	76	05	01	11	13	39.54	32	22.00	103	03.59			3.0			3.0	2.4	2.8	√					
220.	76	05	02	00	32	35.71	36	24.12	106	45.72		2.7						2.8		√				
221.	76	05	03	06	52	59.07	32	24.50	105	39.69	2.6						2.4	2.6	√					
222.	76	05	06	17	18	23.61	31	57.96	103	11.08			2.6				2.0	2.0	√					
223.	76	05	11	23	04	39.90	32	17.47	102	55.15							2.0	2.0	√					
224.	76	05	20	19	43	20.16	35	31.67	109	05.56	2.8							2.8	√					
225.	76	05	21	13	17	30.21	32	29.28	105	35.39	2.2						2.3	2.2	√					
226.	76	05	24	23	40	29.70	34	51.13	104	48.18							2.2	2.2	√					
227.	76	06	15	08	50	20.14	31	35.75	102	21.99	2.8		2.7				2.3	2.8	√					
228.	76	06	16	22	29	03.07	33	29.45	109	43.47	2.8							2.8	√					
229.	76	06	24	15	27	31.01	35	38.36	103	23.13						3.5		3.3	√					
230.	76	06	26	12	55	39.04	36	10.08	106	12.42		2.0						2.1		√				
231.	76	06	30	00	25	04.64	35	09.41	107	20.52	2.7							2.7	√					
232.	76	07	05	12	39	19.42	36	09.42	106	14.16		2.3						2.4		√				
233.	76	07	06	12	48	44.66	36	09.66	106	13.62		2.0						2.1		√				
234.	76	07	28	12	21	51.08	33	01.38	102	17.25	2.0						2.0	2.0	√					
235.	76	08	05	22	23	29.65	30	51.91	101	43.61							2.1	2.1	√					
236.	76	08	06	21	12	38.60	31	46.80	102	35.40			2.6					2.1			√			
237.	76	08	10	10	15	12.21	31	47.69	102	03.65	2.0		2.9				1.9	2.0	√					
238.	76	08	15	19	12	04.05	30	07.31	105	16.32							2.5	2.5	√					
239.	76	08	25	01	27	40.50	31	32.81	101	56.30			2.8				2.3	2.3	√					
240.	76	08	29	19	49	25.08	30	05.95	105	10.57	2.1						2.4	2.1	√					
241.	76	08	30	13	07	27.80	32	40.52	106	05.28	2.5						2.3	2.5	√					
242.	76	08	31	12	45	13.52	31	27.70	102	10.88							2.2	2.2	√					
243.	76	09	03	21	00	24.70	31	33.00	103	28.80			2.5					2.0			√			

RNM and Bordering Areas 1962-1998

No.	Date			Time			Latitude		Longitude		Magnitude								Location by:					
	yr.	mo.	dy.	hr.	mn.	sec.	deg.	min.	deg.	min.	nmt	lanl	utep	uta	asl	usgs	cln	Selected	nmt	lanl	utep	uta	asl	usgs
244.	76	09	17	02	47	45.70	32	14.10	103	03.36			3.0			3.0	2.6	2.8	√					
245.	76	09	17	03	56	29.67	31	26.52	102	31.48			3.4			3.1	2.3	2.9	√					
246.	76	09	19	10	40	44.59	30	28.35	104	34.46	3.0					2.7	3.2	3.0	√					
247.	76	10	22	05	06	11.18	31	32.85	102	09.38			2.9				2.2	2.2	√					
248.	76	10	25	00	27	04.14	31	50.43	102	31.51			3.0				2.3	2.3	√					
249.	76	10	26	10	44	44.10	31	19.80	103	16.80			2.8					2.4			√			
250.	76	12	12	23	00	13.68	31	34.09	102	27.82			3.2					2.8	√					
251.	76	12	19	21	26	13.72	31	52.29	102	27.29			2.6					2.2	√					
252.	76	12	19	23	56	47.06	32	16.04	103	05.07			2.9			2.9		2.7	√					
253.	76	12	23	08	36	59.85	34	43.04	105	50.02	2.7				2.1			2.7	√					
254.	76	12	31	07	53	58.37	36	40.44	106	41.10		2.1						2.2		√				
255.	77	01	04	18	31	37.28	32	26.59	106	48.86	2.8					3.2		2.8	√					
256.	77	01	04	23	41	58.88	33	57.54	105	58.89	2.8				2.9	2.7		2.8	√					
257.	77	01	05	12	19	03.58	34	01.95	105	58.98	2.5				2.2			2.5	√					
258.	77	01	29	09	40	44.14	30	35.01	104	35.39							2.2	2.2	√					
259.	77	02	04	07	48	15.37	30	35.18	104	42.02							2.0	2.0	√					
260.	77	03	05	03	00	56.38	35	46.95	108	08.29						4.6		4.4	√					
261.	77	03	14	10	10	25.31	33	02.42	101	00.65							2.7	2.7	√					
262.	77	03	20	07	54	08.97	32	12.43	103	06.09	2.0		2.2				2.1	2.0	√					
263.	77	04	03	19	26	49.25	36	08.40	106	13.20		2.3						2.4		√				
264.	77	04	07	05	45	40.44	32	11.26	103	03.23			2.9			2.9	2.0	2.7	√					
265.	77	04	07	22	32	24.19	31	21.24	102	56.37			1.8				2.0	2.0	√					
266.	77	04	12	23	18	26.75	31	16.96	102	33.10			2.2				2.3	2.3	√					
267.	77	04	26	09	03	06.95	31	53.23	102	59.19			3.1			3.3	2.2	3.1	√					
268.	77	04	28	12	55	40.37	31	49.51	102	31.06			2.2				2.5	2.5	√					
269.	77	06	07	23	01	18.64	32	47.27	100	44.39	3.8					4.0	3.5	3.8	√					
270.	77	06	08	00	51	28.74	32	49.86	100	49.54	2.9					2.9	2.8	2.9	√					

RNM and Bordering Areas 1962-1998

No.	Date			Time			Latitude		Longitude		Magnitude								Location by:					
	yr.	mo.	dy.	hr.	mn.	sec.	deg.	min.	deg.	min.	nmt	lanl	utep	uta	asl	usgs	cln	Selected	nmt	lanl	utep	uta	asl	usgs
271.	77	06	08	13	09	07.40	31	01.44	109	13.62	4.5					4.3		4.5						√
272.	77	06	08	13	29	10.58	32	55.34	100	48.98	3.6						3.4	3.6	√					
273.	77	06	08	13	39	29.42	32	52.03	101	02.60	2.6					2.6	2.9	2.6	√					
274.	77	06	17	03	37	05.10	32	54.05	100	56.77	2.7					3.0		2.7	√					
275.	77	06	28	23	59	46.00	31	32.40	103	18.00			2.8					2.3			√			
276.	77	07	01	01	06	19.20	31	30.00	103	20.40			2.5					2.0			√			
277.	77	07	02	01	24	41.17	36	13.86	107	13.14		1.9						2.0		√				
278.	77	07	22	04	01	10.31	31	48.12	102	43.14			3.4			3.0	1.5	2.8	√					
279.	77	08	21	03	01	12.40	30	32.52	104	54.72				3.3		2.6	2.9	2.4	√					
280.	77	08	22	15	10	56.20	35	37.02	107	13.98		2.0			0.9			2.1		√				
281.	77	10	13	21	36	12.51	32	54.84	100	48.63	2.2							2.2	√					
282.	77	11	14	07	26	26.82	31	31.47	104	57.60	2.7						2.2	2.7	√					
283.	77	11	27	20	48	20.13	33	01.26	101	08.33	2.7					2.6	2.8	2.7	√					
284.	77	11	28	01	40	54.60	32	58.51	101	08.37	3.4					3.5		3.4	√					
285.	77	12	31	13	19	04.50	31	36.00	102	27.60			2.6					2.1			√			
286.	78	01	02	10	10	47.10	31	36.00	102	31.80			2.6					2.2			√			
287.	78	01	12	14	55	04.52	31	29.44	102	18.11							2.2	2.2	√					
288.	78	01	19	03	42	36.53	32	33.67	103	42.67							2.1	2.1	√					
289.	78	01	21	01	17	02.40	31	30.06	104	39.15				3.2				2.3				√		
290.	78	02	05	14	19	54.23	31	24.42	104	33.07							2.1	2.1	√					
291.	78	02	18	14	22	34.85	31	12.78	104	41.63						2.5		2.3	√					
292.	78	03	02	10	04	51.31	31	35.07	102	22.75			3.6			3.5		3.3	√					
293.	78	03	02	11	55	57.10	31	35.40	102	36.60			2.6					2.1			√			
294.	78	04	07	00	57	40.27	31	57.23	106	01.45			3.6				2.1	2.1	√					
295.	78	06	29	20	58	50.19	31	04.69	102	25.23						3.4		3.2	√					
296.	78	07	18	12	07	32.20	30	21.54	104	21.63							2.4	2.4	√					
297.	78	07	21	05	02	35.43	34	41.07	105	02.43					2.5	2.8	2.9	2.6	√					

RNM and Bordering Areas 1962-1998

No.	Date			Time			Latitude		Longitude		Magnitude								Location by:					
	yr.	mo.	dy.	hr.	mn.	sec.	deg.	min.	deg.	min.	nmt	lanl	utep	uta	asl	usgs	cln	Selected	nmt	lanl	utep	uta	asl	usgs
298.	78	08	14	13	29	39.26	31	34.78	102	10.87	2.2							2.2	√					
299.	78	09	25	01	44	31.13	35	44.10	106	45.84		1.9			1.5			2.0		√				
300.	78	09	28	22	01	47.86	35	06.24	106	48.36		2.1			1.1			2.2		√				
301.	78	09	29	09	38	39.20	35	06.60	106	48.24		2.2			1.5			2.3		√				
302.	78	09	29	20	07	42.28	31	31.11	102	25.44			2.7				2.1	2.1	√					
303.	78	09	30	23	31	38.19	31	21.80	102	10.40			2.2				2.2	2.2	√					
304.	78	10	06	15	23	46.79	31	33.01	102	21.30							2.0	2.0	√					
305.	78	11	28	05	25	39.56	35	12.06	106	42.54		1.9			1.7			2.0		√				
306.	79	03	05	13	00	05.62	36	18.72	106	12.00		2.7				2.5		2.8		√				
307.	79	03	07	22	11	35.46	36	19.14	106	11.58		1.9						2.0		√				
308.	79	03	10	13	53	24.47	35	06.90	106	48.00		2.2			1.6			2.3		√				
309.	79	03	30	09	28	02.22	35	07.14	106	48.06		2.0						2.1		√				
310.	79	03	30	10	41	55.17	35	06.72	106	47.76		2.6			2.5			2.7		√				
311.	79	04	28	01	01	38.16	30	28.26	104	43.25							2.1	2.1	√					
312.	79	07	08	15	55	04.30	35	06.72	106	48.54		2.0						2.1		√				
313.	79	07	17	07	26	14.05	32	39.11	103	43.94	2.0							2.0	√					
314.	79	08	03	05	29	36.78	32	52.47	100	48.84						2.6		2.4	√					
315.	79	10	11	22	32	25.30	37	01.74	106	52.26		2.0						2.1		√				
316.	80	03	22	00	48	12.35	34	41.62	105	48.14						3.4		3.2	√					
317.	80	04	24	19	12	33.48	35	52.44	106	46.98		1.9						2.0		√				
318.	80	06	09	22	37	09.90	35	30.78	101	04.92						3.4		3.2						√
319.	80	09	11	17	34	33.66	36	28.74	104	50.22						3.1		2.9	√					
320.	80	09	11	18	09	07.65	35	23.40	107	21.62					1.8			2.2	√					
321.	80	09	12	21	37	37.23	36	17.06	105	10.45						2.8		2.6	√					
322.	80	10	11	20	31	41.00	36	31.80	106	51.00		2.2			2.2			2.3		√				
323.	81	05	03	22	54	09.48	32	16.18	108	54.11	2.0							2.0	√					
324.	81	05	04	10	55	31.87	32	19.37	108	58.29	2.4					3.0		2.4	√					

RNM and Bordering Areas 1962-1998

No.	Date			Time			Latitude		Longitude		Magnitude								Location by:					
	yr.	mo.	dy.	hr.	mn.	sec.	deg.	min.	deg.	min.	nmt	lanl	utep	uta	asl	usgs	cln	Selected	nmt	lanl	utep	uta	asl	usgs
325.	81	05	07	01	38	20.13	32	15.86	108	56.08	2.8					3.2		2.8	√					
326.	81	05	10	08	28	13.04	32	17.83	108	50.81	2.1							2.1	√					
327.	81	05	11	23	28	13.13	32	19.13	108	55.21	2.3							2.3	√					
328.	81	08	05	03	19	57.51	36	19.16	108	57.04	2.0							2.0	√					
329.	81	08	13	23	39	53.08	31	53.78	102	42.14	2.2							2.2	√					
330.	81	08	14	02	06	57.36	35	15.31	107	54.39	2.1							2.1	√					
331.	81	12	04	08	51	26.06	34	24.11	108	12.60	2.8					2.8		2.8	√					
332.	82	01	04	16	56	17.48	31	17.30	102	49.05	3.6					3.9		3.6	√					
333.	82	03	02	16	05	20.80	35	53.17	105	27.34	2.2					2.9		2.2	√					
334.	82	03	16	11	03	06.26	35	38.79	103	30.33	2.1					3.1		2.1	√					
335.	82	03	16	12	24	50.00	35	45.52	103	22.42	2.0							2.0	√					
336.	82	05	01	20	39	32.72	32	19.82	103	02.63	2.1							2.1	√					
337.	82	05	16	16	16	53.81	36	39.56	106	44.67	2.0					2.7		2.0	√					
338.	82	05	16	21	24	01.73	36	42.60	106	43.01	2.0					2.5		2.0	√					
339.	82	05	16	22	02	47.26	36	39.66	106	41.27	2.1					2.7		2.1	√					
340.	82	05	17	00	08	07.14	36	38.25	106	47.79	2.4							2.4	√					
341.	82	05	17	00	52	59.88	36	40.47	106	37.16	2.0							2.0	√					
342.	82	05	17	02	46	04.91	36	40.13	106	40.58	2.0					2.6		2.0	√					
343.	82	08	07	04	48	02.64	36	38.25	106	47.54	2.0					2.7		2.0	√					
344.	82	10	17	20	33	50.55	30	54.10	102	42.32	2.0							2.0	√					
345.	82	11	03	17	54	01.86	35	18.27	108	41.72	2.5					3.1		2.5	√					
346.	82	11	25	18	49	37.36	32	53.40	100	46.98	2.3							2.3	√					
347.	82	11	28	02	36	52.45	33	42.90	100	50.24	3.4					3.3		3.4	√					
348.	82	12	30	05	07	56.29	37	26.05	108	15.45	2.1							2.1	√					
349.	83	01	29	11	44	52.09	31	45.00	102	04.79	2.2							2.2	√					
350.	83	03	03	18	14	18.63	29	57.81	104	20.87	2.8					3.4		2.8	√					
351.	83	03	25	23	18	31.91	35	47.99	103	05.49	2.0							2.0	√					

RNM and Bordering Areas 1962-1998

No.	Date			Time			Latitude		Longitude		Magnitude								Location by:					
	yr.	mo.	dy.	hr.	mn.	sec.	deg.	min.	deg.	min.	nmt	lanl	utep	uta	asl	usgs	cln	Selected	nmt	lanl	utep	uta	asl	usgs
352.	83	04	03	04	55	28.58	35	26.56	102	38.07	3.0					3.4		3.0	√					
353.	83	04	30	07	34	20.47	33	21.91	106	24.97	3.5					3.5		3.5	√					
354.	83	08	14	18	08	13.41	38	14.30	107	14.81	2.7							2.7	√					
355.	83	08	17	15	03	21.17	37	18.97	104	12.92	2.8					3.4		2.8	√					
356.	83	08	21	00	53	53.07	35	14.36	109	03.80	2.2							2.2	√					
357.	83	08	23	15	05	07.36	31	10.33	105	31.46	2.1							2.1	√					
358.	83	08	29	04	23	22.11	31	48.12	100	37.11	2.6					2.9		2.6	√					
359.	83	09	01	07	56	02.65	31	11.97	110	04.65	2.1							2.1	√					
360.	83	09	15	23	25	37.54	34	55.27	104	25.78	3.1					3.2		3.1	√					
361.	83	09	29	07	44	12.20	34	53.17	104	27.20	2.7					2.7		2.7	√					
362.	83	10	28	12	41	47.66	35	23.63	107	29.21	2.2							2.2	√					
363.	83	12	03	23	46	52.04	30	58.28	103	19.22	2.1							2.1	√					
364.	84	01	03	09	59	59.22	30	45.46	103	02.65	2.0							2.0	√					
365.	84	01	30	19	58	57.45	34	28.52	108	04.10	2.0							2.0	√					
366.	84	02	14	01	35	41.58	34	48.53	100	35.98	2.0							2.0	√					
367.	84	03	12	14	58	54.82	29	16.48	105	27.55	2.2							2.2	√					
368.	84	05	21	13	31	11.87	35	36.78	102	07.46	2.6					3.1		2.6	√					
369.	84	06	27	03	12	04.12	31	13.24	102	28.60	2.0							2.0	√					
370.	84	07	21	05	55	01.20	33	34.42	107	06.15	2.3							2.3	√					
371.	84	08	26	22	22	08.06	30	22.83	104	16.23	2.1							2.1	√					
372.	84	09	11	14	47	30.63	31	36.34	100	45.38	3.0					3.2		3.0	√					
373.	84	09	19	02	50	28.18	27	24.06	107	36.57	3.1							3.1	√					
374.	84	09	19	06	15	28.85	31	46.50	100	39.42	3.0					3.2		3.0	√					
375.	84	10	11	18	59	31.59	31	56.98	100	33.44	2.4							2.4	√					
376.	84	11	11	02	19	09.04	36	26.81	110	05.59	2.3							2.3	√					
377.	84	12	04	12	16	38.91	30	05.91	101	55.70	2.3							2.3	√					
378.	84	12	04	20	36	30.77	32	38.19	103	12.75	2.1					2.9		2.1	√					

RNM and Bordering Areas 1962-1998

No.	Date			Time			Latitude		Longitude		Magnitude								Location by:					
	yr.	mo.	dy.	hr.	mn.	sec.	deg.	min.	deg.	min.	nmt	lanl	utep	uta	asl	usgs	cln	Selected	nmt	lanl	utep	uta	asl	usgs
379.	85	01	06	14	30	07.93	35	57.05	103	24.63	2.2							2.2	√					
380.	85	01	29	05	37	59.67	35	27.74	111	40.68	2.2							2.2	√					
381.	85	01	30	13	47	24.36	35	01.48	111	44.68	2.2							2.2	√					
382.	85	02	02	02	43	45.21	36	11.11	110	39.16	2.1							2.1	√					
383.	85	04	14	21	48	02.93	35	15.56	108	55.52	3.4					3.4		3.4	√					
384.	85	06	05	10	36	59.93	32	32.70	106	57.38	2.9					2.9		2.9	√					
385.	85	06	26	16	49	29.21	35	32.30	102	32.59	2.7							2.7	√					
386.	85	09	06	05	22	45.70	32	31.79	106	58.51	2.6					2.6		2.6	√					
387.	85	09	18	14	49	38.22	30	54.16	103	24.96	2.0							2.0	√					
388.	85	09	25	19	23	21.67	32	30.56	106	57.98	2.5					2.5		2.5	√					
389.	85	11	12	06	50	13.96	28	07.71	104	05.34	3.8					4.3		3.8	√					
390.	85	11	17	08	31	17.08	35	21.85	107	21.85	2.0							2.0	√					
391.	85	12	15	07	14	52.63	35	26.23	104	39.86	3.0					3.6		3.0	√					
392.	86	01	30	22	26	41.38	31	59.21	100	54.05	3.3					3.3		3.3	√					
393.	86	02	14	17	34	22.09	31	31.62	100	45.52	2.6							2.6	√					
394.	86	03	11	05	57	06.81	32	06.68	105	04.64	2.0							2.0	√					
395.	86	04	03	07	31	48.61	29	06.69	104	07.49	2.3							2.3	√					
396.	86	04	17	21	04	29.31	32	33.28	106	57.67	2.7					2.7		2.7	√					
397.	86	05	14	15	03	03.41	37	21.67	110	13.79	3.0					3.2		3.0	√					
398.	86	05	23	05	10	04.48	35	00.45	110	33.21	2.0							2.0	√					
399.	86	06	04	05	43	14.75	35	58.48	105	23.38	2.2							2.2	√					
400.	86	06	12	03	52	16.33	33	04.70	109	27.87	2.2							2.2	√					
401.	86	06	27	09	47	14.47	32	03.45	102	00.45	2.2							2.2	√					
402.	86	07	17	21	13	56.72	35	20.37	110	43.92	2.4					2.6		2.4	√					
403.	86	08	06	13	39	11.73	33	51.77	103	01.97	2.4							2.4	√					
404.	86	08	12	04	19	37.78	35	54.20	103	11.02	2.2							2.2	√					
405.	86	08	12	05	57	01.37	35	42.73	102	00.79	2.3							2.3	√					

RNM and Bordering Areas 1962-1998

No.	Date			Time			Latitude		Longitude		Magnitude								Location by:					
	yr.	mo.	dy.	hr.	mn.	sec.	deg.	min.	deg.	min.	nmt	lanl	utep	uta	asl	usgs	cln	Selected	nmt	lanl	utep	uta	asl	usgs
406.	86	08	13	12	13	52.01	38	35.62	108	12.85	2.5							2.5	√					
407.	86	08	25	03	22	49.72	35	19.41	107	31.04	2.0							2.0	√					
408.	86	08	27	18	06	58.02	35	07.23	105	10.15	3.1					3.2		3.1	√					
409.	86	11	03	21	33	22.23	31	05.39	104	38.24	2.0							2.0	√					
410.	86	11	05	13	34	53.65	36	33.07	101	53.10	2.0					2.4		2.0	√					
411.	86	11	17	00	26	35.72	33	04.97	100	44.06	2.0							2.0	√					
412.	86	11	24	18	48	01.50	31	40.50	102	09.57	2.0							2.0	√					
413.	86	12	06	05	33	55.92	31	35.67	102	09.54	2.4							2.4	√					
414.	86	12	06	06	57	10.06	31	28.28	102	13.72	2.1							2.1	√					
415.	86	12	06	20	44	15.97	31	43.38	102	05.15	2.2							2.2	√					
416.	86	12	11	01	22	54.63	35	23.45	101	05.73	2.3					2.5		2.3	√					
417.	86	12	17	17	57	00.93	35	21.19	107	21.09	2.2							2.2	√					
418.	86	12	23	03	20	36.52	31	08.74	109	27.76	2.3							2.3	√					
419.	86	12	25	07	52	34.02	35	05.55	105	58.12	2.5							2.5	√					
420.	87	01	15	11	28	34.10	34	06.46	100	09.20	2.2							2.2	√					
421.	87	01	26	06	11	48.38	29	19.69	104	50.59	2.6							2.6	√					
422.	87	02	09	04	14	02.17	30	41.43	103	26.81	2.3							2.3	√					
423.	87	02	17	08	30	53.03	30	36.17	104	31.20	2.1							2.1	√					
424.	87	03	19	12	20	48.74	35	18.30	109	49.09	2.2							2.2	√					
425.	87	03	26	07	40	08.06	30	57.44	103	16.67	2.6							2.6	√					
426.	87	03	27	04	36	49.64	34	47.67	105	36.58	2.4							2.4	√					
427.	87	03	31	02	04	16.80	31	31.17	104	57.16	2.8							2.8	√					
428.	87	04	16	10	55	18.42	38	24.14	106	13.51	2.4							2.4	√					
429.	87	04	16	11	36	59.19	35	09.57	109	07.61	2.4							2.4	√					
430.	87	04	17	01	28	55.84	35	28.19	102	28.20	2.4							2.4	√					
431.	87	04	29	13	36	31.39	32	40.36	105	55.30	2.3							2.3	√					
432.	87	05	04	21	58	55.68	34	56.17	107	23.84	3.1							3.1	√					

RNM and Bordering Areas 1962-1998

No.	Date			Time			Latitude		Longitude		Magnitude								Location by:					
	yr.	mo.	dy.	hr.	mn.	sec.	deg.	min.	deg.	min.	nmt	lanl	utep	uta	asl	usgs	cln	Selected	nmt	lanl	utep	uta	asl	usgs
433.	87	07	04	13	57	53.53	33	43.73	108	46.73	2.1							2.1	√					
434.	87	07	05	17	13	02.38	30	50.91	104	46.03	2.0							2.0	√					
435.	87	07	21	01	26	29.60	35	02.75	107	52.76	2.3							2.3	√					
436.	87	09	09	09	44	18.86	37	24.04	108	23.64	2.1					2.5		2.1	√					
437.	87	09	10	14	16	23.35	32	19.43	108	56.25	2.0							2.0	√					
438.	87	09	11	17	34	36.78	33	36.30	103	37.19	2.0							2.0	√					
439.	87	10	02	07	15	12.84	37	08.73	107	51.76	2.4							2.4	√					
440.	87	10	02	10	02	50.45	37	09.87	107	51.47	2.3							2.3	√					
441.	87	10	02	20	50	19.76	37	08.71	107	53.89	2.4							2.4	√					
442.	87	10	10	23	31	56.08	35	17.84	107	56.03	2.2							2.2	√					
443.	87	10	23	20	19	56.07	35	20.15	107	53.15	2.2							2.2	√					
444.	87	12	03	21	59	55.43	36	47.09	108	25.11	2.3							2.3	√					
445.	87	12	09	22	04	16.69	36	51.22	108	14.24	2.0							2.0	√					
446.	87	12	16	09	30	42.38	37	06.49	107	00.31	2.1							2.1	√					
447.	87	12	18	09	32	02.27	37	10.82	107	37.66	2.3							2.3	√					
448.	87	12	18	13	51	02.07	37	12.71	107	10.91	2.0							2.0	√					
449.	87	12	20	04	01	34.64	32	17.62	103	04.45	2.2							2.2	√					
450.	87	12	21	04	48	47.74	35	21.09	107	24.33	2.2							2.2	√					
451.	87	12	28	05	21	26.85	31	27.93	102	14.94	2.1							2.1	√					
452.	88	01	15	07	33	33.33	37	13.75	107	02.90	3.1					3.1		3.1	√					
453.	88	01	26	20	38	39.79	31	14.62	102	25.16	2.3							2.3	√					
454.	88	01	31	09	24	36.28	29	54.59	105	11.78	3.8					3.4		3.8	√					
455.	88	01	31	18	36	45.04	29	49.25	105	07.97	2.3							2.3	√					
456.	88	01	31	21	06	01.72	29	54.24	105	06.18	2.3							2.3	√					
457.	88	02	14	07	39	52.66	36	10.29	110	59.88	2.7							2.7	√					
458.	88	02	22	18	57	10.33	35	07.26	108	29.09	2.1							2.1	√					
459.	88	03	09	20	11	39.87	35	49.54	106	46.63	2.0							2.0	√					

RNM and Bordering Areas 1962-1998

No.	Date			Time			Latitude		Longitude		Magnitude								Location by:					
	yr.	mo.	dy.	hr.	mn.	sec.	deg.	min.	deg.	min.	nmt	lanl	utep	uta	asl	usgs	cln	Selected	nmt	lanl	utep	uta	asl	usgs
460.	88	03	21	20	02	17.42	35	39.28	103	58.65	2.1							2.1	√					
461.	88	04	05	05	01	47.28	31	26.27	102	19.70	2.1							2.1	√					
462.	88	04	05	20	38	25.24	36	42.16	108	27.07	2.2							2.2	√					
463.	88	04	07	02	50	33.13	31	06.57	106	00.10	2.2							2.2	√					
464.	88	04	11	06	46	01.83	28	54.77	103	06.85	2.2							2.2	√					
465.	88	07	04	01	53	53.58	33	44.45	100	44.45	2.0							2.0	√					
466.	88	07	20	13	06	06.98	29	46.45	102	25.63	2.2							2.2	√					
467.	88	07	20	15	19	21.71	29	36.15	102	09.32	2.5							2.5	√					
468.	88	08	03	03	58	24.22	36	20.50	106	12.34	2.3							2.3	√					
469.	88	09	19	06	05	05.33	32	27.63	102	26.98	2.0							2.0	√					
470.	88	11	30	14	01	25.06	30	19.26	109	51.32	2.1							2.1	√					
471.	88	12	25	07	52	33.98	35	05.56	105	57.76	2.5							2.5	√					
472.	88	12	31	14	33	02.44	31	07.66	109	22.09	3.0							3.0	√					
473.	89	01	29	05	07	15.55	35	10.98	104	06.20	3.4					3.4		3.4	√					
474.	89	02	21	18	22	42.02	35	17.56	103	23.56	2.3							2.3	√					
475.	89	03	24	11	26	48.13	36	59.63	103	45.59	2.4					2.7		2.4	√					
476.	89	04	18	10	45	54.17	34	49.82	110	38.25	3.2					3.5		3.2	√					
477.	89	05	01	12	05	44.14	35	54.38	103	21.16	2.1							2.1	√					
478.	89	05	08	03	12	12.48	34	44.52	110	38.91	2.2							2.2	√					
479.	89	05	18	02	35	45.21	35	06.95	110	22.65	2.0							2.0	√					
480.	89	05	25	07	43	15.08	30	41.50	109	31.21	4.0					4.6		4.0	√					
481.	89	05	26	09	08	09.18	30	33.35	109	36.59	3.5					3.5		3.5	√					
482.	89	05	26	11	51	50.58	30	32.46	110	21.81	2.6							2.6	√					
483.	89	06	02	08	48	11.99	30	52.87	106	42.58	2.6							2.6	√					
484.	89	06	05	16	53	34.23	32	05.81	102	05.64	2.1							2.1	√					
485.	89	06	09	17	03	23.71	31	13.70	109	01.57	2.7							2.7	√					
486.	89	06	28	22	57	57.78	30	55.76	105	04.94	2.3							2.3	√					

RNM and Bordering Areas 1962-1998

No.	Date			Time			Latitude		Longitude		Magnitude								Location by:					
	yr.	mo.	dy.	hr.	mn.	sec.	deg.	min.	deg.	min.	nmt	lanl	utep	uta	asl	usgs	cln	Selected	nmt	lanl	utep	uta	asl	usgs
487.	89	07	07	15	49	28.28	35	28.22	104	42.48	2.3							2.3	√					
488.	89	07	17	20	10	27.15	35	11.64	110	25.32	3.0					3.0		3.0	√					
489.	89	07	23	10	39	54.94	37	53.44	112	20.45	3.0							3.0	√					
490.	89	07	25	23	42	00.52	30	54.02	101	45.70	2.1							2.1	√					
491.	89	08	08	12	59	21.63	31	17.93	102	42.01	2.3							2.3	√					
492.	89	09	05	00	29	48.73	34	15.26	102	30.02	2.5							2.5	√					
493.	89	09	06	01	10	52.74	35	55.09	110	42.28	2.8							2.8	√					
494.	89	09	06	12	37	00.81	35	12.42	110	37.24	2.9							2.9	√					
495.	89	09	06	18	27	04.30	36	58.38	110	50.85	2.6							2.6	√					
496.	89	09	15	12	31	07.79	36	06.90	111	37.08	2.0							2.0	√					
497.	89	10	14	00	06	42.17	34	30.98	106	22.58	2.2							2.2	√					
498.	89	10	14	08	05	17.77	34	24.08	108	05.49	3.1					3.4		3.1	√					
499.	89	10	27	10	32	39.52	36	25.03	105	10.99	2.0							2.0	√					
500.	89	11	02	02	24	41.45	33	01.42	100	56.38	2.0							2.0	√					
501.	89	11	16	23	41	52.59	35	06.53	103	07.29	2.6							2.6	√					
502.	89	11	19	03	21	20.73	37	38.04	107	30.14	2.2							2.2	√					
503.	89	12	28	02	14	47.78	31	41.73	101	03.33	2.1							2.1	√					
504.	90	03	09	06	14	45.75	35	36.11	102	07.14	2.3							2.3	√					
505.	90	03	30	19	40	37.50	32	57.71	100	32.01	2.3							2.3	√					
506.	90	03	30	19	53	21.12	32	59.22	100	33.50	2.2							2.2	√					
507.	90	05	10	08	01	43.25	31	08.16	102	22.15	2.2							2.2	√					
508.	90	05	16	11	07	48.30	31	51.30	102	02.46	2.4							2.4	√					
509.	90	05	22	03	02	21.98	30	14.19	102	05.59	2.2							2.2	√					
510.	90	06	18	01	54	37.34	34	58.61	109	42.53	2.0							2.0	√					
511.	90	06	22	12	09	07.06	32	34.78	100	45.34	2.2							2.2	√					
512.	90	07	01	13	06	32.53	35	30.53	102	32.59	3.0					2.7		3.0	√					
513.	90	07	02	21	45	31.55	32	21.76	107	02.45	2.6							2.6	√					

RNM and Bordering Areas 1962-1998

No.	Date			Time			Latitude		Longitude		Magnitude								Location by:					
	yr.	mo.	dy.	hr.	mn.	sec.	deg.	min.	deg.	min.	nmt	lanl	utep	uta	asl	usgs	cln	Selected	nmt	lanl	utep	uta	asl	usgs
514.	90	07	13	22	20	21.41	34	51.75	101	48.49	2.7							2.7	√					
515.	90	07	22	21	27	04.95	34	50.96	105	57.64	3.7					3.7		3.7	√					
516.	90	08	03	15	31	40.32	32	12.30	100	41.55	3.4							3.4	√					
517.	90	09	10	10	35	02.08	30	45.47	105	32.60	2.4							2.4	√					
518.	90	09	29	01	43	37.92	31	31.64	100	10.95	2.0							2.0	√					
519.	90	09	30	13	34	47.00	35	36.05	103	49.97	2.1							2.1	√					
520.	90	10	31	15	10	59.43	30	53.94	109	12.15	3.8					3.8		3.8	√					
521.	90	11	19	07	36	04.07	36	13.60	106	50.15	2.4							2.4	√					
522.	90	12	20	09	12	35.34	35	16.43	103	08.67	2.5							2.5	√					
523.	91	02	01	23	35	04.00	35	23.74	103	39.49	2.4							2.4	√					
524.	91	02	03	02	45	05.12	33	34.61	100	22.08	2.2							2.2	√					
525.	91	02	03	23	55	58.07	35	00.10	103	57.77	2.1							2.1	√					
526.	91	02	09	10	41	55.53	34	15.55	107	55.11	2.0							2.0	√					
527.	91	03	10	20	19	15.30	30	28.01	103	58.35	2.1							2.1	√					
528.	91	03	10	21	49	24.26	33	34.66	103	19.71	2.0							2.0	√					
529.	91	03	31	04	00	05.06	30	28.05	106	29.16	2.0							2.0	√					
530.	91	04	08	11	25	57.98	34	58.80	103	07.89	2.1							2.1	√					
531.	91	05	10	12	15	58.15	37	17.29	106	54.95	3.8					3.4		3.8	√					
532.	91	05	16	02	10	15.90	33	40.22	103	44.98	2.0							2.0	√					
533.	91	05	29	06	50	07.53	35	14.93	107	43.33	2.1							2.1	√					
534.	91	05	30	15	21	11.22	35	19.13	107	36.31	2.2							2.2	√					
535.	91	06	04	01	02	38.42	32	03.03	102	18.83	2.0							2.0	√					
536.	91	06	19	04	32	42.74	35	38.63	106	42.69	2.0							2.0	√					
537.	91	07	16	21	24	18.10	33	05.60	101	07.10	2.1							2.1	√					
538.	91	07	17	11	21	18.54	36	46.07	107	29.56	2.1							2.1	√					
539.	91	08	01	05	04	11.75	34	35.44	104	01.43	2.7							2.7	√					
540.	91	08	17	12	27	16.92	32	05.22	100	59.39	2.0							2.0	√					

RNM and Bordering Areas 1962-1998

No.	Date			Time			Latitude		Longitude		Magnitude								Location by:					
	yr.	mo.	dy.	hr.	mn.	sec.	deg.	min.	deg.	min.	nmt	lanl	utep	uta	asl	usgs	cln	Selected	nmt	lanl	utep	uta	asl	usgs
541.	91	09	04	20	42	16.92	33	00.19	108	08.35	2.3					2.3		2.3	√					
542.	91	09	04	21	07	27.16	32	59.36	108	08.20	2.4					2.4		2.4	√					
543.	91	09	06	01	43	47.36	32	55.72	108	10.52	2.8					2.8		2.8	√					
544.	91	09	11	05	43	14.04	31	03.25	106	47.49	2.2							2.2	√					
545.	91	09	11	06	03	48.40	31	03.16	106	43.73	2.3							2.3	√					
546.	91	09	22	02	17	38.41	31	19.11	101	17.71	2.1							2.1	√					
547.	91	09	30	15	11	07.44	31	50.91	100	43.77	2.2							2.2	√					
548.	91	10	05	16	41	22.78	31	23.07	105	24.67	2.2							2.2	√					
549.	91	12	09	12	12	59.09	34	51.00	106	34.75	2.3							2.3	√					
550.	91	12	09	12	15	16.95	34	51.19	106	35.64	2.0							2.0	√					
551.	91	12	09	12	47	16.92	34	51.55	106	35.93	2.9							2.9	√					
552.	91	12	09	12	50	20.97	34	49.21	106	35.87	2.6							2.6	√					
553.	91	12	09	21	07	50.30	34	50.93	106	35.27	2.4							2.4	√					
554.	91	12	10	03	32	43.65	34	50.37	106	33.58	2.3							2.3	√					
555.	91	12	12	14	27	42.25	35	06.12	106	25.04	2.3							2.3	√					
556.	92	01	02	11	45	35.30	32	18.15	103	11.18	5.0							5.0	√					
557.	92	01	02	15	40	07.40	32	18.15	103	11.18	2.4							2.4	√					
558.	92	01	07	23	54	16.00	32	18.15	103	11.18	2.4							2.4	√					
559.	92	01	09	01	15	32.13	34	50.68	106	34.60	2.0							2.0	√					
560.	92	01	09	18	24	43.00	32	18.15	103	11.18	2.8							2.8	√					
561.	92	01	11	07	55	01.60	32	18.15	103	11.18	2.0							2.0	√					
562.	92	01	12	09	48	24.21	33	51.68	100	27.59	2.1							2.1	√					
563.	92	01	13	14	07	27.04	34	51.50	106	34.72	2.3							2.3	√					
564.	92	01	16	08	44	15.68	34	51.29	106	25.90	2.2							2.2	√					
565.	92	01	19	07	43	18.28	35	23.13	103	29.63	2.4							2.4	√					
566.	92	02	10	05	03	38.45	34	51.37	106	35.63	2.1							2.1	√					
567.	92	02	10	11	48	06.58	34	51.17	106	36.17	2.5							2.5	√					

RNM and Bordering Areas 1962-1998

No.	Date			Time			Latitude		Longitude		Magnitude								Location by:					
	yr.	mo.	dy.	hr.	mn.	sec.	deg.	min.	deg.	min.	nmt	lanl	utep	uta	asl	usgs	cln	Selected	nmt	lanl	utep	uta	asl	usgs
568.	92	02	23	16	17	52.95	30	38.66	105	26.17	3.6					3.4		3.6	√					
569.	92	02	24	21	18	08.87	30	35.76	105	28.30	2.1							2.1	√					
570.	92	03	01	07	11	50.60	30	33.16	105	28.18	2.2							2.2	√					
571.	92	03	01	07	50	12.30	30	33.16	105	28.18	2.2							2.2	√					
572.	92	03	01	09	12	57.55	30	33.16	105	28.18	2.6							2.6	√					
573.	92	03	01	23	58	11.97	35	18.22	108	59.70	2.3							2.3	√					
574.	92	03	10	23	03	01.07	30	29.07	109	03.63	3.7							3.7	√					
575.	92	03	13	11	19	57.38	36	12.57	111	36.46	3.2							3.2	√					
576.	92	03	13	11	28	47.02	36	12.57	111	36.46	2.8							2.8	√					
577.	92	03	15	15	04	49.44	33	37.74	110	56.09	2.2							2.2	√					
578.	92	03	24	08	29	01.40	35	49.44	105	32.14	2.0							2.0	√					
579.	92	04	03	23	37	34.59	32	15.80	103	01.51	2.1							2.1	√					
580.	92	04	07	03	05	52.17	31	33.54	102	17.44	2.3							2.3	√					
581.	92	04	08	05	34	00.06	36	11.54	102	57.41	2.0							2.0	√					
582.	92	05	02	10	19	34.59	37	13.24	104	53.05	2.4					3.1		2.4	√					
583.	92	05	06	01	41	04.21	36	11.31	111	43.27	2.2							2.2	√					
584.	92	06	14	12	44	58.07	32	18.06	103	05.83	2.3							2.3	√					
585.	92	06	29	11	32	55.62	31	25.05	102	28.26	2.0							2.0	√					
586.	92	07	30	03	13	34.67	33	21.42	106	29.72	2.8							2.8	√					
587.	92	08	11	08	01	04.11	35	26.34	108	41.08	2.1							2.1	√					
588.	92	08	17	23	11	59.08	35	19.99	101	52.30	2.1							2.1	√					
589.	92	08	19	01	04	14.49	33	06.51	100	55.10	2.2							2.2	√					
590.	92	08	26	03	24	51.16	32	12.56	102	35.52	3.2					3.0		3.2	√					
591.	92	09	15	03	31	19.36	32	09.40	103	01.12	2.2							2.2	√					
592.	92	09	29	04	22	56.86	33	23.71	106	30.68	2.3							2.3	√					
593.	92	09	29	15	55	51.62	31	26.30	106	31.05	2.2							2.2	√					
594.	92	12	02	00	06	36.62	31	25.49	102	21.25	2.4							2.4	√					

RNM and Bordering Areas 1962-1998

No.	Date			Time			Latitude		Longitude		Magnitude								Location by:					
	yr.	mo.	dy.	hr.	mn.	sec.	deg.	min.	deg.	min.	nmt	lanl	utep	uta	asl	usgs	cln	Selected	nmt	lanl	utep	uta	asl	usgs
595.	92	12	17	14	00	41.41	35	19.50	107	32.50	2.0							2.0	√					
596.	92	12	17	14	22	39.88	35	28.99	103	29.09	2.3							2.3	√					
597.	92	12	27	04	57	51.18	36	23.83	106	49.05	2.3							2.3	√					
598.	93	02	11	20	13	41.55	31	07.18	105	13.97	2.0							2.0	√					
599.	93	03	24	02	32	06.09	35	08.15	104	27.64	2.7					3.0		2.7	√					
600.	93	04	25	09	29	57.10	37	08.98	110	47.50	4.2							4.2	√					
601.	93	04	29	08	21	16.22	36	29.86	110	52.50	4.9							4.9	√					
602.	93	05	05	20	24	43.49	32	17.10	105	09.44	2.1							2.1	√					
603.	93	05	16	18	28	20.67	30	26.55	105	03.75	2.2							2.2	√					
604.	93	05	17	10	58	08.58	31	25.14	102	19.73	2.3							2.3	√					
605.	93	05	28	13	30	33.39	32	44.75	103	07.11	2.5							2.5	√					
606.	93	05	31	09	42	10.25	30	53.14	106	25.26	2.0							2.0	√					
607.	93	06	23	02	50	05.31	31	25.57	102	32.29	2.5							2.5	√					
608.	93	06	23	03	23	13.10	31	25.97	102	31.39	2.8					2.8		2.8	√					
609.	93	06	23	03	24	09.01	31	25.97	102	31.39	2.1							2.1	√					
610.	93	06	24	09	41	43.57	31	28.72	102	26.88	2.1							2.1	√					
611.	93	07	03	08	13	18.76	31	29.88	102	20.26	2.2							2.2	√					
612.	93	07	15	03	55	11.38	29	45.60	104	19.44	3.1							3.1	√					
613.	93	07	15	23	39	12.50	29	47.96	104	34.32	2.1							2.1	√					
614.	93	07	16	20	43	16.03	29	52.59	107	06.71	3.5					3.8		3.5	√					
615.	93	07	18	07	36	22.21	29	48.63	107	09.31	2.5							2.5	√					
616.	93	07	19	03	10	56.21	29	58.08	107	04.82	2.7							2.7	√					
617.	93	07	20	07	05	19.29	29	57.78	107	00.90	2.2							2.2	√					
618.	93	08	15	07	29	12.75	29	20.12	109	52.67	2.7							2.7	√					
619.	93	08	29	10	34	41.75	32	21.05	102	54.37	2.5							2.5	√					
620.	93	09	05	18	48	50.46	32	16.80	100	57.33	2.0							2.0	√					
621.	93	09	29	02	01	24.19	35	48.96	103	09.35	3.0					3.3		3.0	√					

RNM and Bordering Areas 1962-1998

No.	Date			Time			Latitude		Longitude		Magnitude								Location by:					
	yr.	mo.	dy.	hr.	mn.	sec.	deg.	min.	deg.	min.	nmt	lanl	utep	uta	asl	usgs	cln	Selected	nmt	lanl	utep	uta	asl	usgs
622.	93	10	05	04	24	24.67	30	08.96	109	01.04	3.5					4.0		3.5	√					
623.	93	10	31	05	03	48.88	29	08.45	110	00.58	3.4							3.4	√					
624.	93	11	17	14	39	12.64	35	23.09	101	50.95	2.3							2.3	√					
625.	93	11	18	03	19	13.09	35	24.05	101	53.09	2.5							2.5	√					
626.	93	11	24	01	19	05.99	35	38.20	101	37.47	2.2							2.2	√					
627.	93	11	25	17	38	49.08	34	16.16	102	05.96	2.6							2.6	√					
628.	93	11	30	03	07	36.28	35	48.53	103	09.40	3.3					3.3		3.3	√					
629.	93	12	01	20	42	50.31	35	41.89	103	48.76	2.0							2.0	√					
630.	93	12	05	00	58	24.06	27	59.26	102	03.64	4.2							4.2	√					
631.	93	12	05	03	35	14.14	27	53.85	102	03.49	3.5							3.5	√					
632.	93	12	10	09	17	04.43	36	08.41	103	07.09	2.2							2.2	√					
633.	93	12	22	19	25	11.39	33	19.87	105	40.91	3.2					3.2		3.2	√					
634.	93	12	31	09	18	58.98	32	00.08	107	48.16	2.3							2.3	√					
635.	94	01	06	18	27	59.79	31	57.28	105	05.56	2.4							2.4	√					
636.	94	02	07	15	04	35.88	32	20.99	106	54.82	2.0							2.0	√					
637.	94	02	13	20	28	03.77	29	48.99	105	10.09	2.6							2.6	√					
638.	94	03	15	20	00	55.78	30	06.72	103	33.61	2.0							2.0	√					
639.	94	05	12	23	20	00.73	31	26.44	106	53.77	2.0							2.0	√					
640.	94	05	20	01	29	38.53	36	19.87	105	56.72	2.2							2.2	√					
641.	94	09	24	14	59	42.07	30	15.24	106	01.14	2.4							2.4	√					
642.	94	09	24	20	56	17.38	31	25.65	102	21.52	2.0							2.0	√					
643.	94	10	30	21	46	44.69	35	43.50	103	26.09	2.2							2.2	√					
644.	94	11	24	12	09	53.12	32	23.22	100	47.75	2.7							2.7	√					
645.	94	12	06	11	19	53.79	35	39.31	102	17.73	2.0							2.0	√					
646.	95	03	19	18	36	44.76	34	50.87	104	24.85	3.0					3.3		3.0	√					
647.	95	05	11	13	17	47.40	32	42.35	105	12.01	2.4							2.4	√					
648.	95	05	27	20	18	00.19	31	20.49	102	20.54	2.3							2.3	√					

RNM and Bordering Areas 1962-1998

No.	Date			Time			Latitude		Longitude		Magnitude								Location by:					
	yr.	mo.	dy.	hr.	mn.	sec.	deg.	min.	deg.	min.	nmt	lanl	utep	uta	asl	usgs	cln	Selected	nmt	lanl	utep	uta	asl	usgs
649.	95	05	30	04	14	00.00	32	42.48	105	12.32	2.1							2.1	√					
650.	95	06	28	03	39	01.69	35	24.49	102	33.92	2.5							2.5	√					
651.	95	07	04	03	59	05.62	36	12.12	104	56.64	3.6					3.8		3.6	√					
652.	95	09	10	20	02	47.50	36	55.42	107	54.95	2.0							2.0	√					
653.	95	10	19	00	45	49.52	32	02.99	104	50.33	2.0							2.0	√					
654.	95	10	20	07	15	25.93	36	02.10	101	02.57	2.0							2.0	√					
655.	95	10	25	15	40	26.55	30	21.06	103	25.00	2.2							2.2	√					
656.	95	11	30	05	32	24.99	30	52.56	107	04.40	2.0							2.0	√					
657.	96	03	03	02	47	56.42	31	21.19	104	50.97	2.1							2.1	√					
658.	96	03	15	12	03	24.96	33	35.95	105	42.30	2.6							2.6	√					
659.	96	03	15	12	03	44.17	33	36.78	105	41.34	2.5							2.5	√					
660.	96	03	15	13	17	57.00	33	36.08	105	41.87	2.7							2.7	√					
661.	96	03	15	13	54	50.55	33	36.73	105	41.32	2.1							2.1	√					
662.	96	03	24	20	16	12.76	34	15.30	105	41.00	3.1							3.1	√					
663.	96	03	24	20	19	23.11	34	16.22	105	41.32	3.3							3.3	√					
664.	96	03	24	13	03	57.13	34	16.30	105	45.91	2.0							2.0	√					
665.	96	03	24	20	45	08.07	34	15.21	105	41.42	2.3							2.3	√					
666.	96	03	25	06	43	49.67	35	20.08	102	48.27	3.2							3.2	√					
667.	96	03	29	07	18	33.04	34	14.35	105	42.75	2.4							2.4	√					
668.	96	07	22	10	06	14.44	34	15.52	105	40.83	3.4							3.4	√					
669.	96	07	22	10	07	33.19	34	14.26	105	44.10	2.2							2.2	√					
670.	96	07	22	10	13	36.75	34	14.68	105	42.94	2.3							2.3	√					
671.	96	11	18	15	55	36.15	31	12.98	106	47.47	2.2							2.2	√					
672.	96	12	28	18	32	37.53	31	11.77	103	00.85	2.2							2.2	√					
673.	96	08	01	05	55	59.70	37	09.69	104	24.93	2.5							2.5	√					
674.	96	08	01	05	44	27.67	37	14.75	104	26.04	3.3							3.3	√					
675.	96	11	01	03	09	33.14	37	13.57	104	24.45	2.9							2.9	√					

RNM and Bordering Areas 1962-1998

No.	Date			Time			Latitude		Longitude		Magnitude								Location by:					
	yr.	mo.	dy.	hr.	mn.	sec.	deg.	min.	deg.	min.	nmt	lanl	utep	uta	asl	usgs	cln	Selected	nmt	lanl	utep	uta	asl	usgs
676.	97	05	19	21	40	06.70	34	14.58	105	44.58	2.3							2.3	√					
677.	97	05	19	21	40	33.44	34	08.37	105	47.25	2.3							2.3	√					
678.	97	05	19	21	50	22.87	34	12.00	105	45.36	2.0							2.0	√					
679.	97	05	20	09	41	05.82	34	11.28	105	44.53	2.7							2.7	√					
680.	97	06	02	06	44	16.03	31	24.68	102	26.03	2.3							2.3	√					
681.	97	10	19	11	12	09.74	32	20.08	103	56.16	3.2							3.2	√					
682.	97	11	14	11	25	38.02	36	45.58	102	00.69	2.5							2.5	√					
683.	97	12	31	13	28	30.97	34	33.34	106	08.15	3.0							3.0	√					
684.	97	12	31	13	32	07.92	34	33.32	106	07.98	3.0							3.0	√					
685.	97	12	31	13	34	59.61	34	33.59	106	08.16	3.0							3.0	√					
686.	97	12	31	16	40	11.33	34	34.31	106	09.02	2.6							2.6	√					
687.	97	12	31	17	49	16.28	34	33.73	106	10.59	2.1							2.1	√					
688.	97	12	31	23	16	24.95	34	31.02	106	10.09	3.2							3.2	√					
689.	97	12	31	23	17	37.62	34	34.73	106	08.85	2.4							2.4	√					
690.	98	01	04	08	05	31.91	34	32.57	106	07.48	3.8							3.8	√					
691.	98	01	04	08	08	53.91	34	35.00	106	09.74	2.3							2.3	√					
692.	98	01	04	12	17	14.00	34	34.34	106	09.25	2.3							2.3	√					
693.	98	01	04	13	53	15.94	34	35.80	106	05.96	2.1							2.1	√					
694.	98	01	14	08	55	19.05	31	42.26	106	02.91	2.2							2.2	√					
695.	98	02	17	18	43	12.43	35	22.95	107	18.13	2.3							2.3	√					
696.	98	02	27	01	47	06.98	31	20.62	101	08.15	2.1							2.1	√					
697.	98	03	19	13	53	49.87	35	33.54	106	46.75	2.5							2.5	√					
698.	98	03	20	01	42	12.93	32	35.83	104	40.38	2.0							2.0	√					
699.	98	03	24	00	55	20.73	31	37.07	105	11.33	2.0							2.0	√					
700.	98	04	20	01	35	36.75	35	26.15	103	26.98	2.1							2.1	√					
701.	98	04	27	15	22	47.61	35	27.24	102	25.43	3.0							3.0	√					
702.	98	06	16	05	52	19.68	32	35.10	104	37.76	2.0							2.0	√					

RNM and Bordering Areas 1962-1998

No.	Date			Time			Latitude		Longitude		Magnitude								Location by:						
	yr.	mo.	dy.	hr.	mn.	sec.	deg.	min.	deg.	min.	nmt	lanl	utep	uta	asl	usgs	cln	Selected	nmt	lanl	utep	uta	asl	usgs
703.	98	06	27	13	06	49.11	32	01.04	102	48.95	2.1							2.1	√					
704.	98	07	08	05	17	40.69	32	36.48	104	37.68	2.7							2.7	√					
705.	98	07	14	05	38	50.97	35	23.96	103	33.37	3.0							3.0	√					
706.	98	07	27	11	09	58.14	31	37.62	102	16.87	2.4							2.4	√					
707.	98	07	27	12	47	23.25	32	35.66	104	41.49	2.0							2.0	√					
708.	98	08	30	13	08	45.48	32	11.28	102	32.81	2.4							2.4	√					
709.	98	12	03	05	19	14.56	32	20.35	103	53.42	2.8							2.8	√					
710.	98	12	11	15	08	14.84	36	05.59	105	03.81	2.2							2.2	√					

Appendix III

Magnitude - Peak Horizontal Ground Acceleration Relationship in Probabilistic Seismic Hazard Analysis

There are two byproducts during the generation of the probabilistic seismic hazard maps for New Mexico and bordering areas, the probability-ground acceleration curves (Figure 4-10 and 4-13) and the magnitude-ground acceleration contribution plots. The probability-ground acceleration curves are frequently seen in probabilistic seismic hazard analyses and provide direct readouts between probabilities and ground accelerations for specific locations. The magnitude-ground acceleration contribution plots in this study, on the other hand, are unique to probabilistic seismic hazard analysis.

Unlike the common magnitude-distance contribution plots that provide no links between magnitudes and ground accelerations, I developed the plot so that the estimated ground accelerations for specific locations are directly linked to the magnitude contribution plots. By combining the probability-ground acceleration curves and the magnitude-ground acceleration contribution plots, the ground acceleration estimates and magnitude contribution curves can be interpolated directly from curves for given locations and probabilities. Such combination provides a perfect tool for evaluating the range of dominant magnitudes for any expected return intervals.

In fact, during the probabilistic seismic hazard analysis, a total number of 1440 probability-ground acceleration and ground acceleration-magnitude curve pairs were generated for each parameter set. In this appendix, I selected six major cities (Socorro, Albuquerque, Santa Fe, Los Alamos, Las Cruces, and Carlsbad) and two dam sites (Elephant Butte lake and Navajo Reservoir) in New Mexico and present their ground acceleration-magnitude contribution plots for a 50 year period. In addition, the magnitude contribution curves at 10% probability of exceedance for these selected sites are presented.

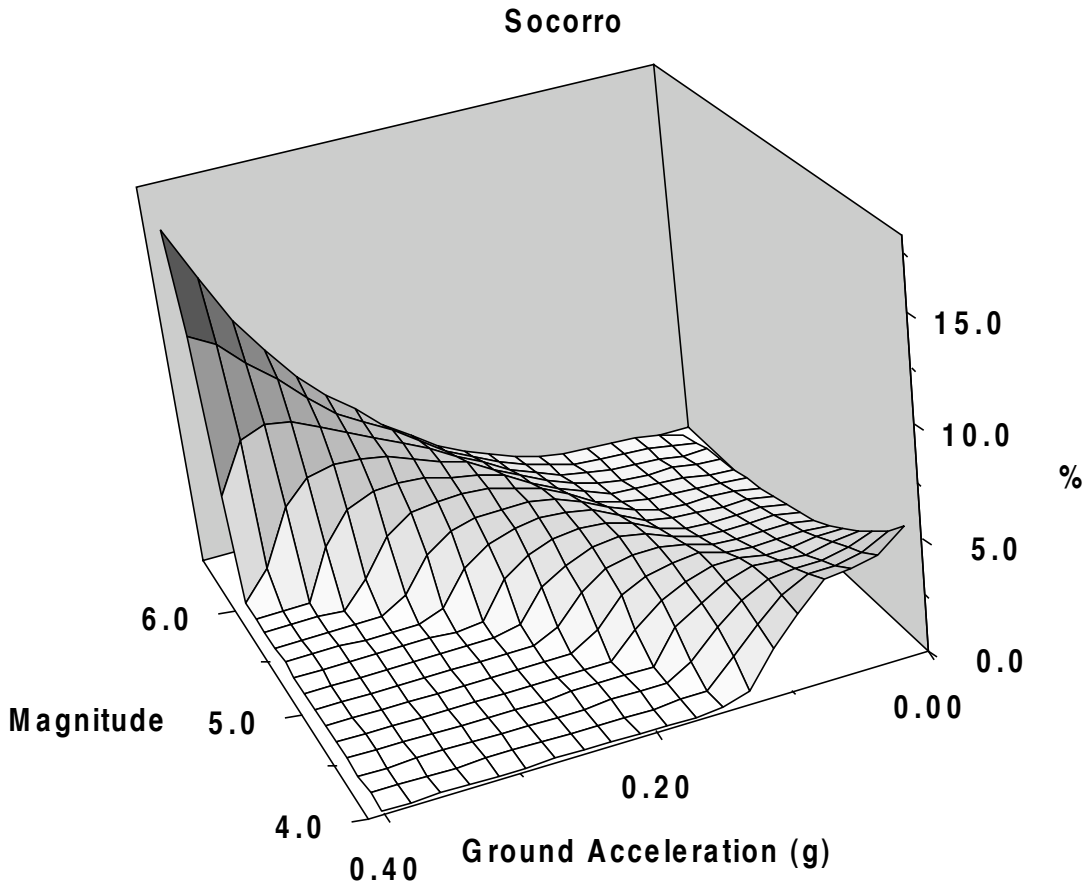

Figure III-1. Magnitude distribution percentile for the city of Socorro for ground acceleration ranging from 0.01g to 0.40g at 0.02g intervals for a 50 year period.

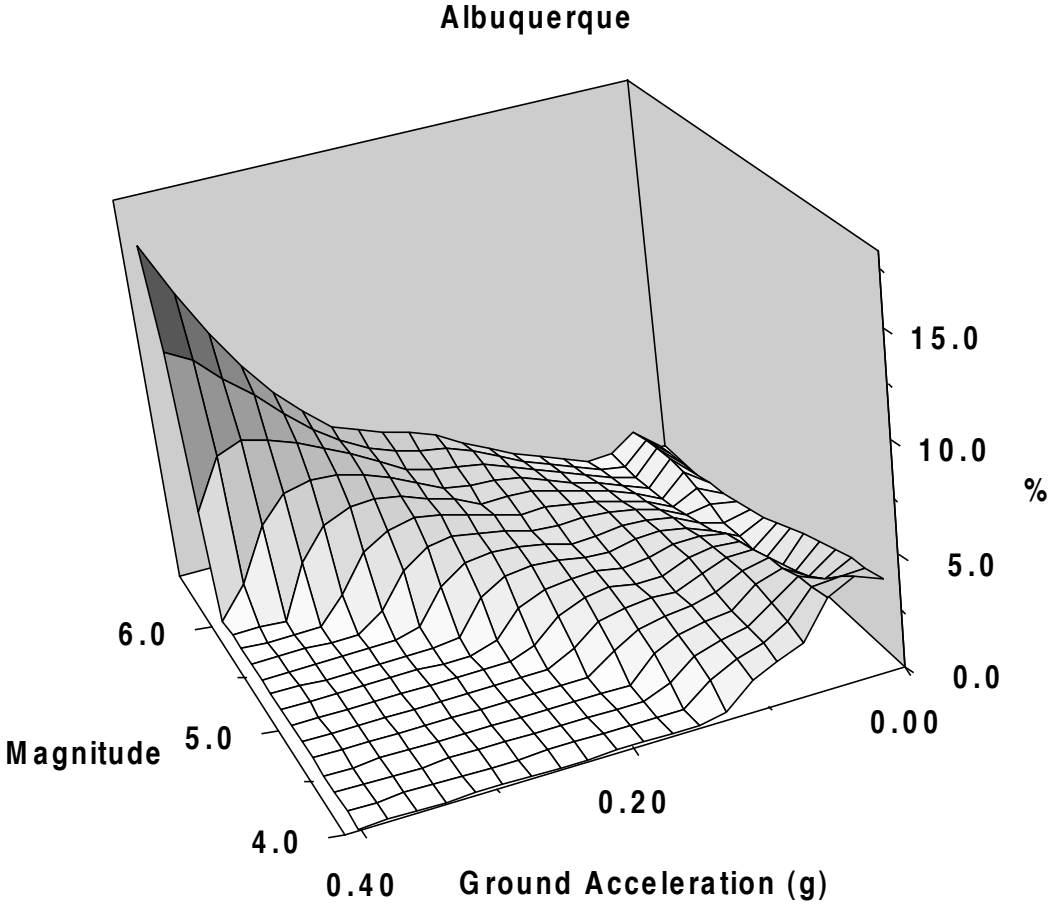

Figure III-2. Magnitude distribution percentile for the city of Albuquerque for ground acceleration ranging from 0.01g to 0.40g at 0.02g intervals for a 50 year period.

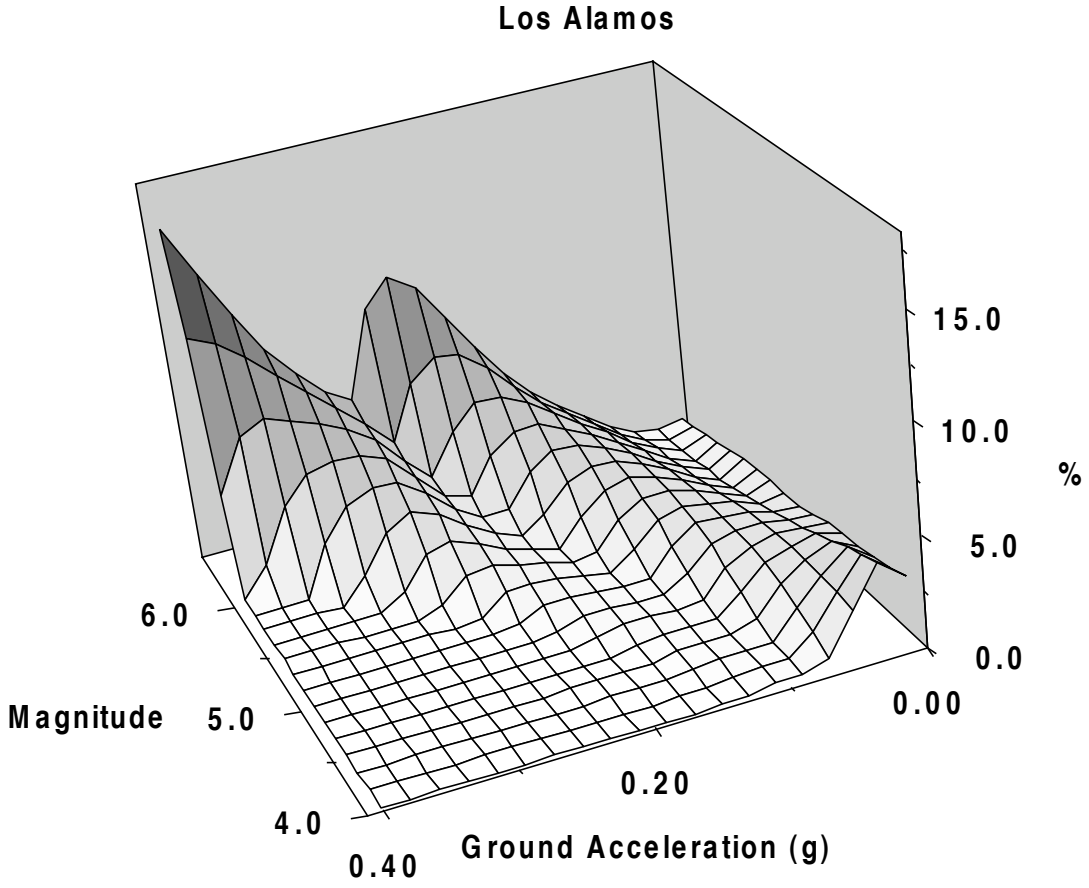

Figure III-3. Magnitude distribution percentile for the city of Los Alamos for ground acceleration ranging from 0.01g to 0.40g at 0.02g intervals for a 50 year period.

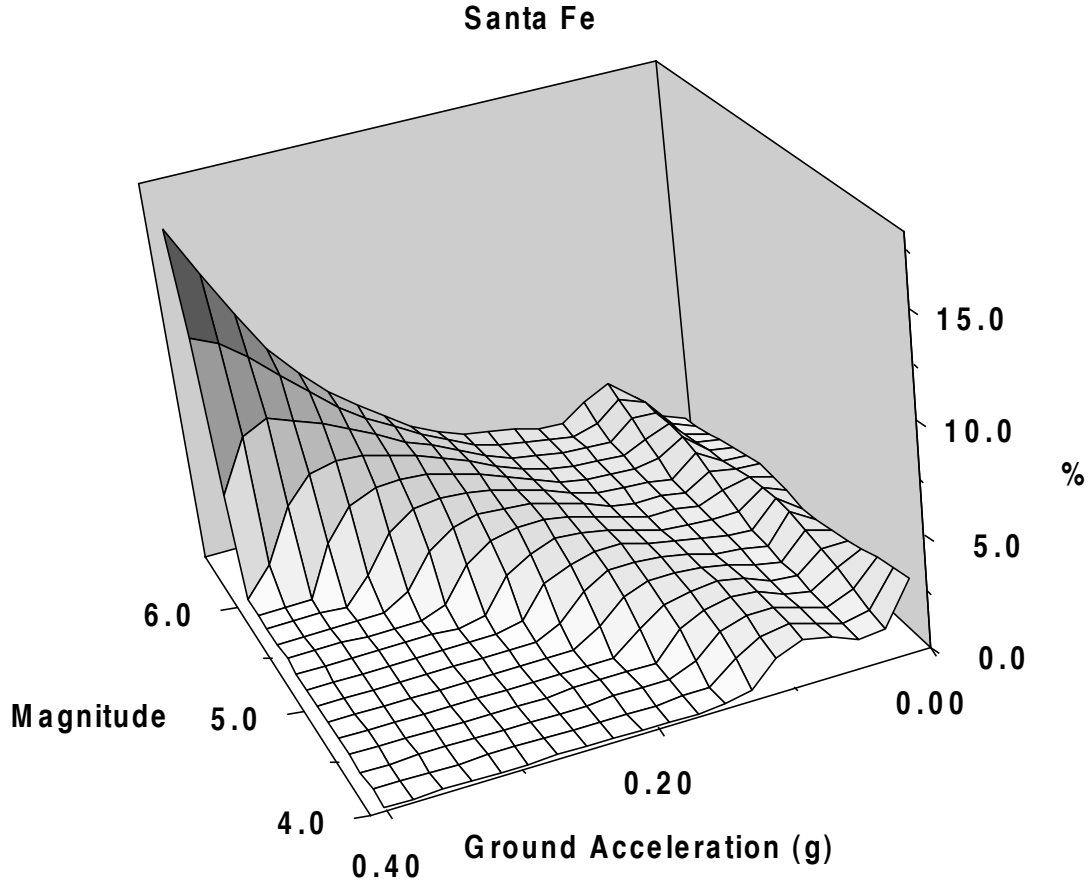

Figure III-4. Magnitude distribution percentile for the city of Santa Fe for ground acceleration ranging from 0.01g to 0.40g at 0.02g intervals for a 50 year period.

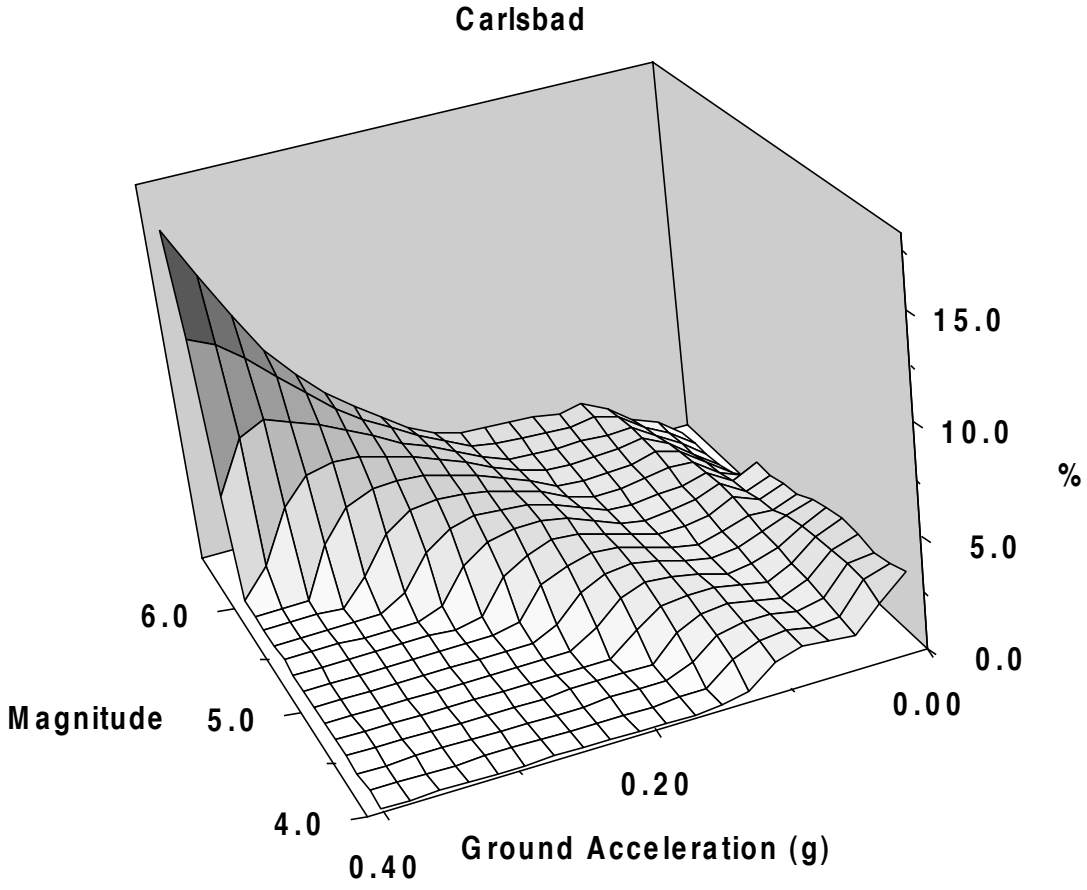

Figure III-5. Magnitude distribution percentile for the city of Carlsbad for ground acceleration ranging from 0.01g to 0.40g at 0.02g intervals for a 50 year period.

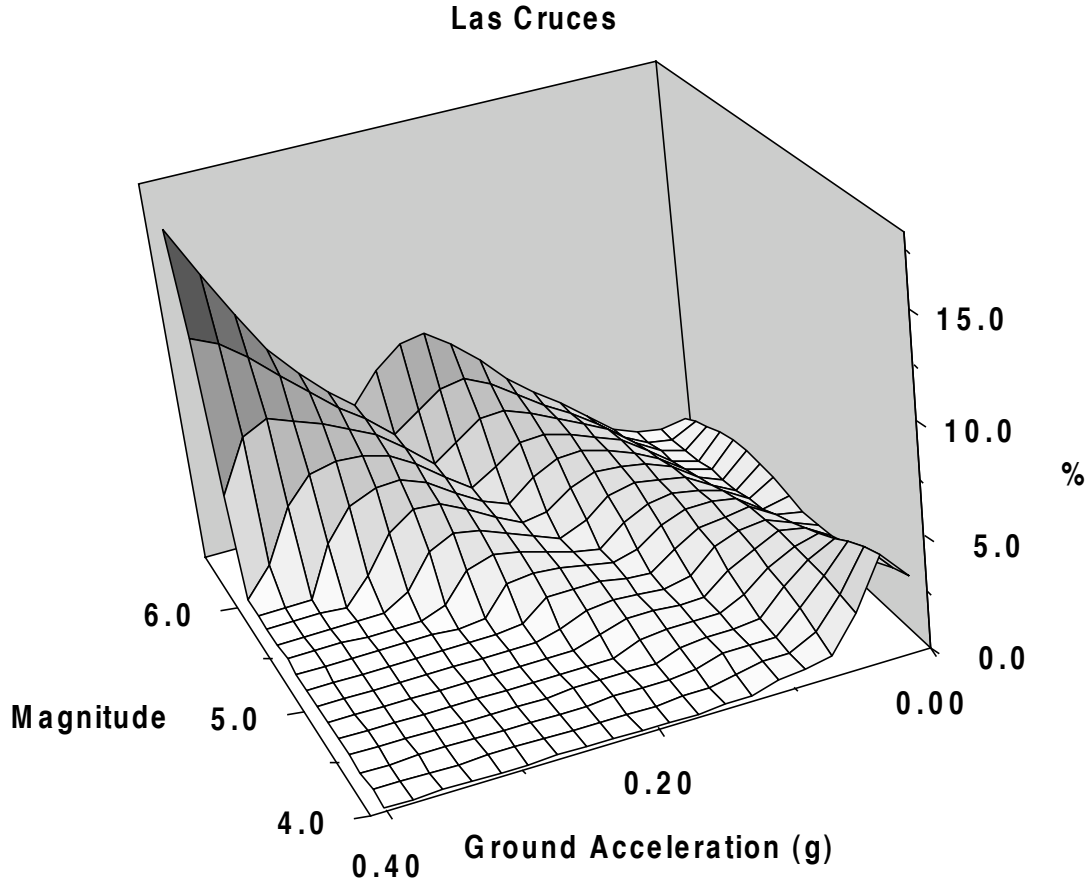

Figure III-6. Magnitude distribution percentile for the city of Los Cruces for ground acceleration ranging from 0.01g to 0.40g at 0.02g intervals for a 50 year period.

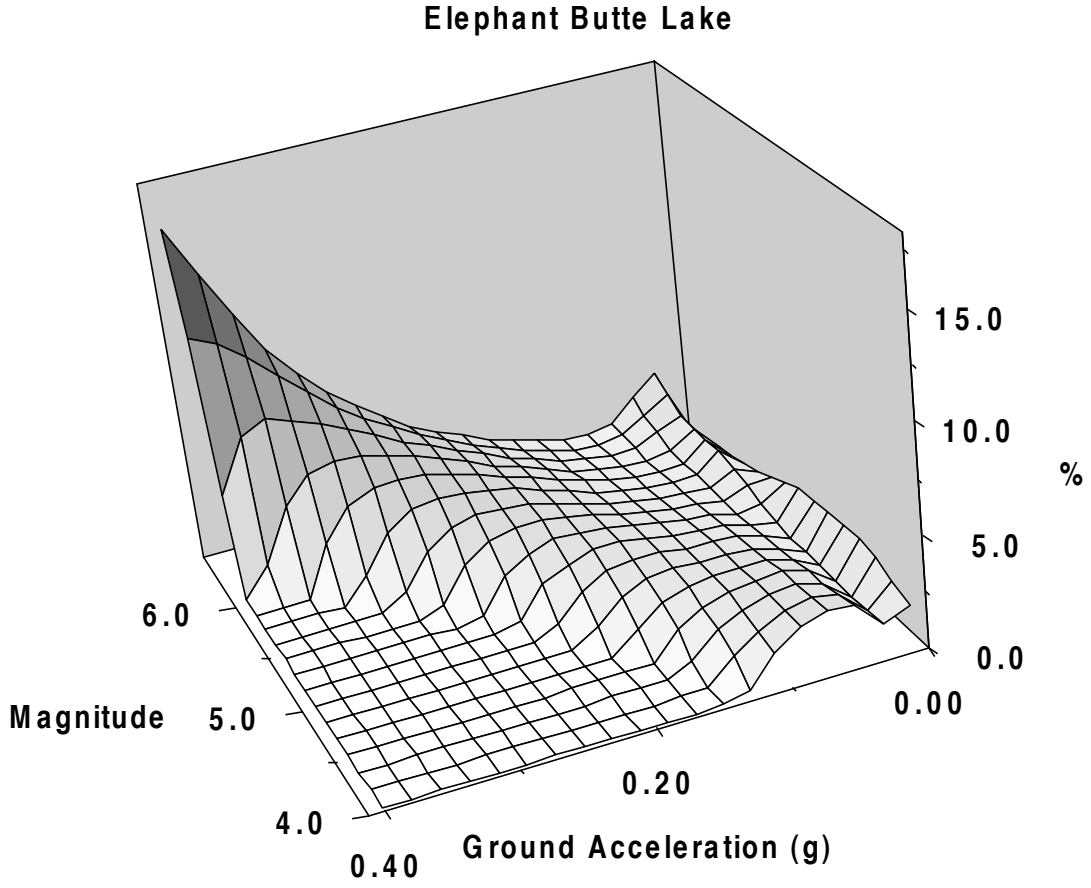

Figure III-7. Magnitude distribution percentile for the Elephant Butte Lake for ground acceleration ranging from 0.01g to 0.40g at 0.02g intervals for a 50 year period.

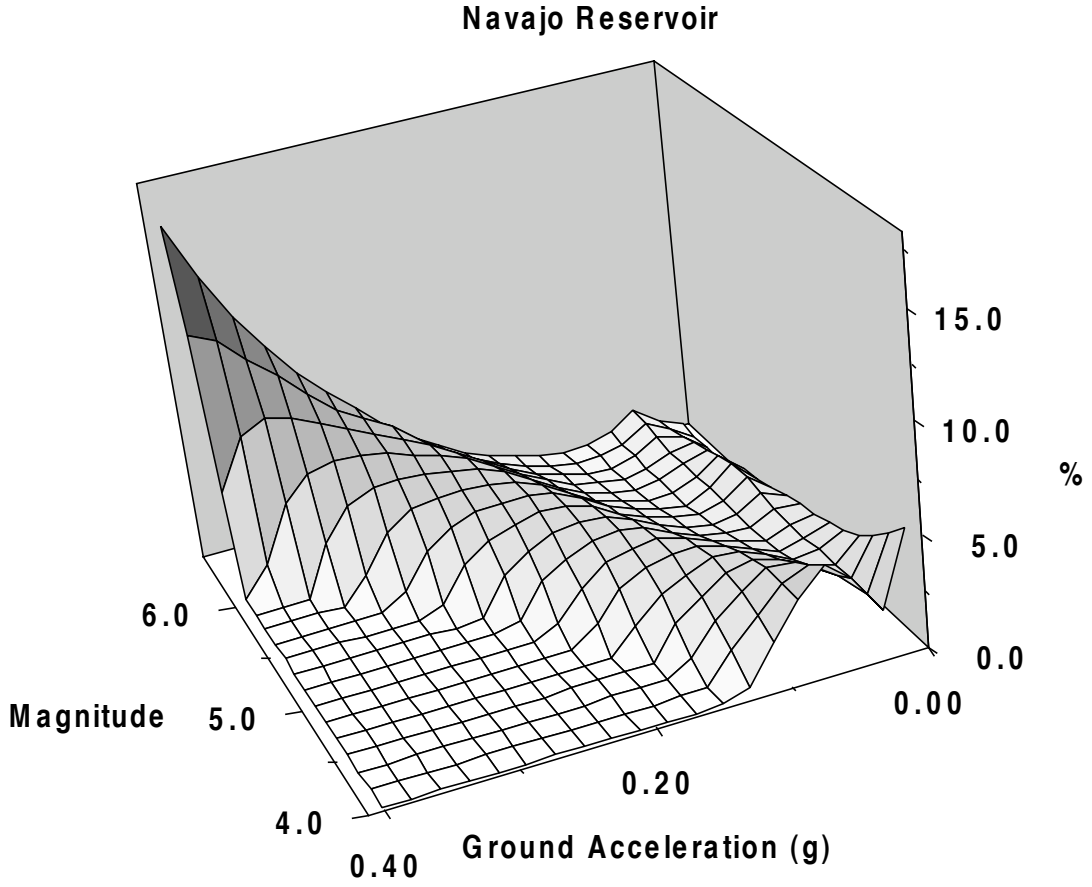

Figure III-8. Magnitude distribution percentile for the Navajo Reservoir for ground acceleration ranging from 0.01g to 0.40g at 0.02g intervals for a 50 year period.

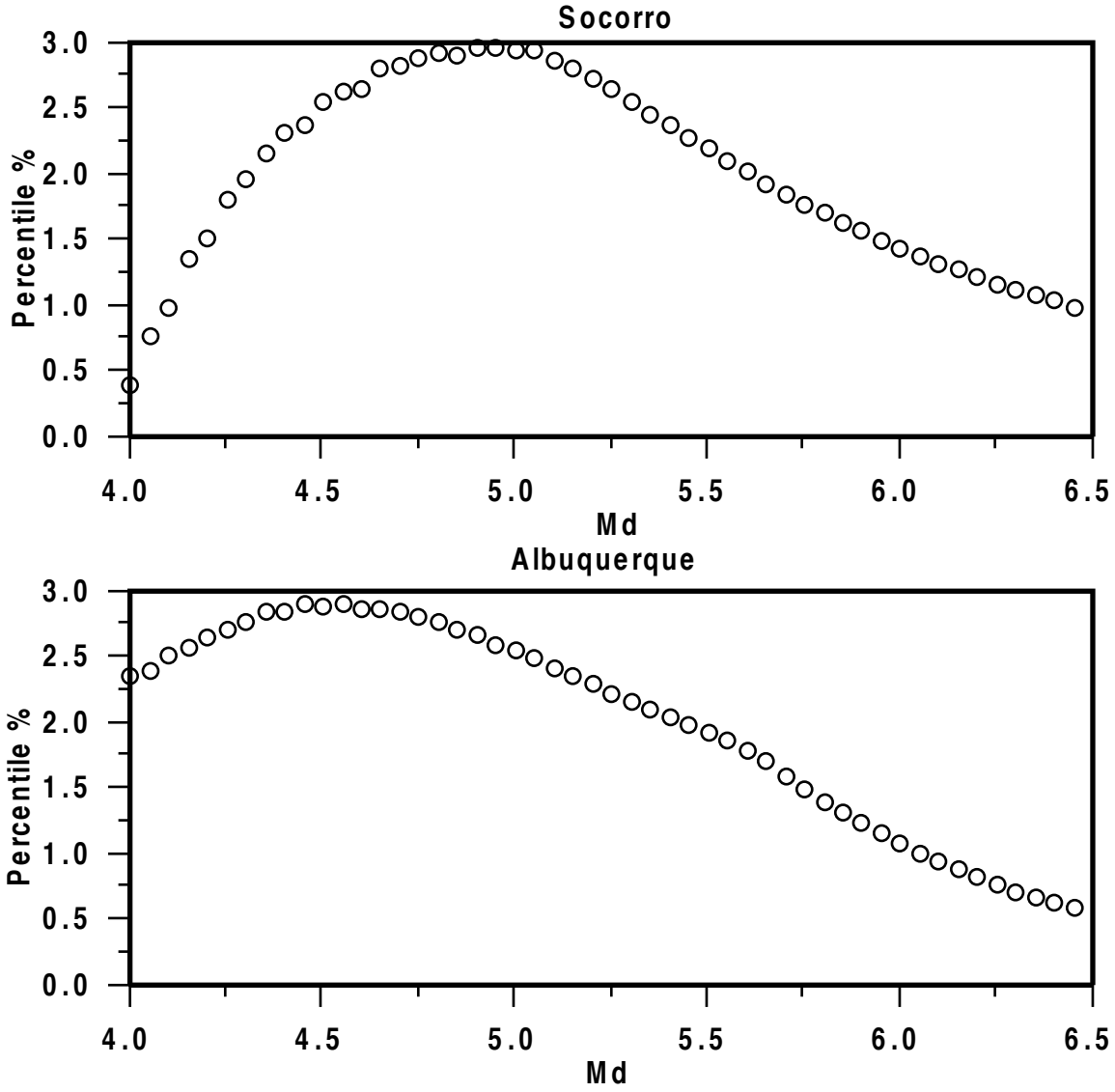

Figure III-9. Distribution of earthquakes at various magnitudes contributing to the seismic hazard estimates for both the Socorro (0.12g) and the Albuquerque (0.08g) areas at 10% probability of exceedance in a 50 year period.

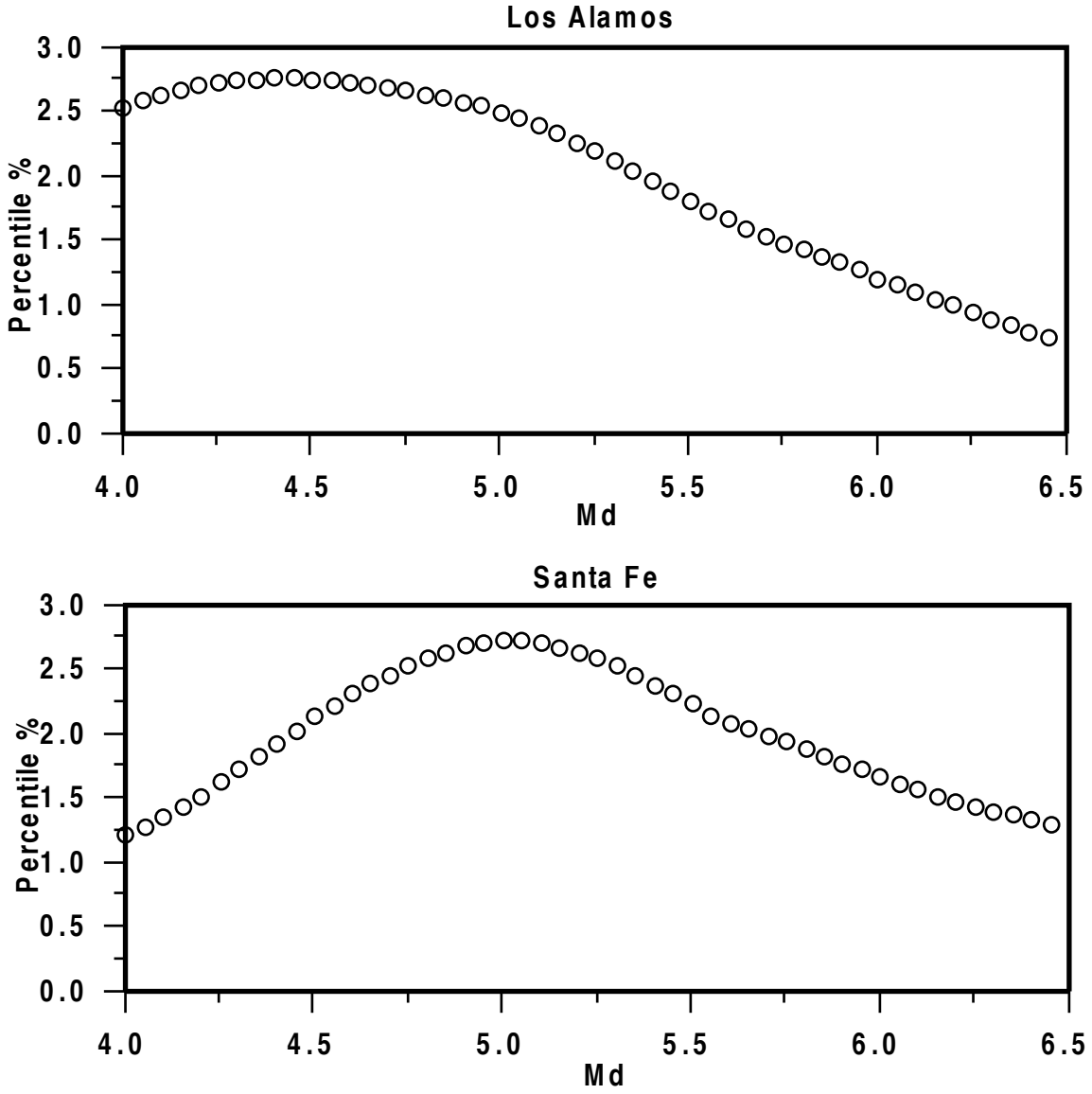

Figure III-10. Distribution of earthquakes at various magnitudes contributing to the seismic hazard estimates for both the Los Alamos (0.07g) and the Santa Fe (0.03g) areas at 10% probability of exceedance in a 50 year period.

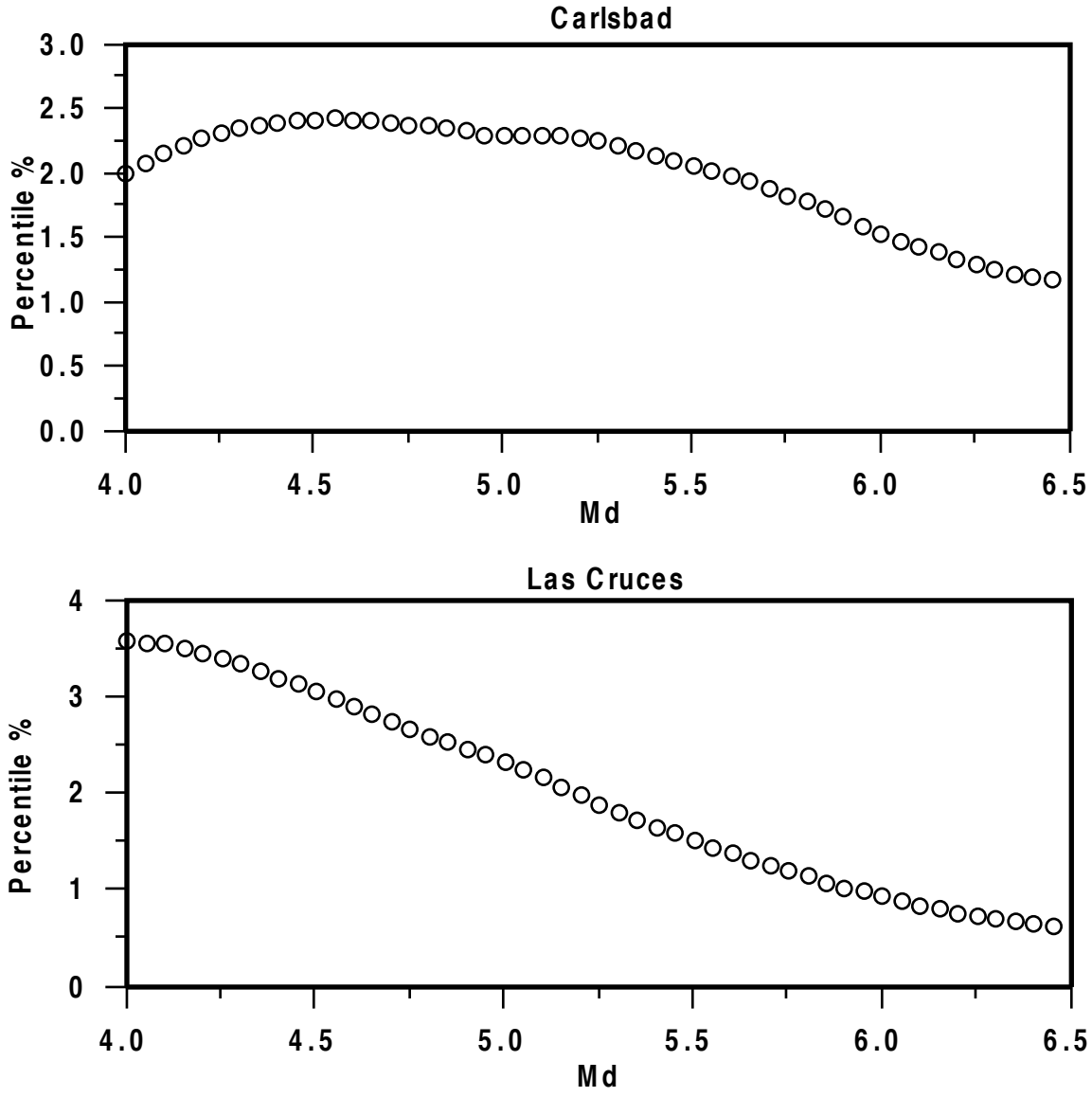

Figure III-11. Distribution of earthquakes at various magnitudes contributing to the seismic hazard estimates for both the Carlsbad (0.04g) and the Las Cruces (0.04g) areas at 10% probability of exceedance in a 50 year period.

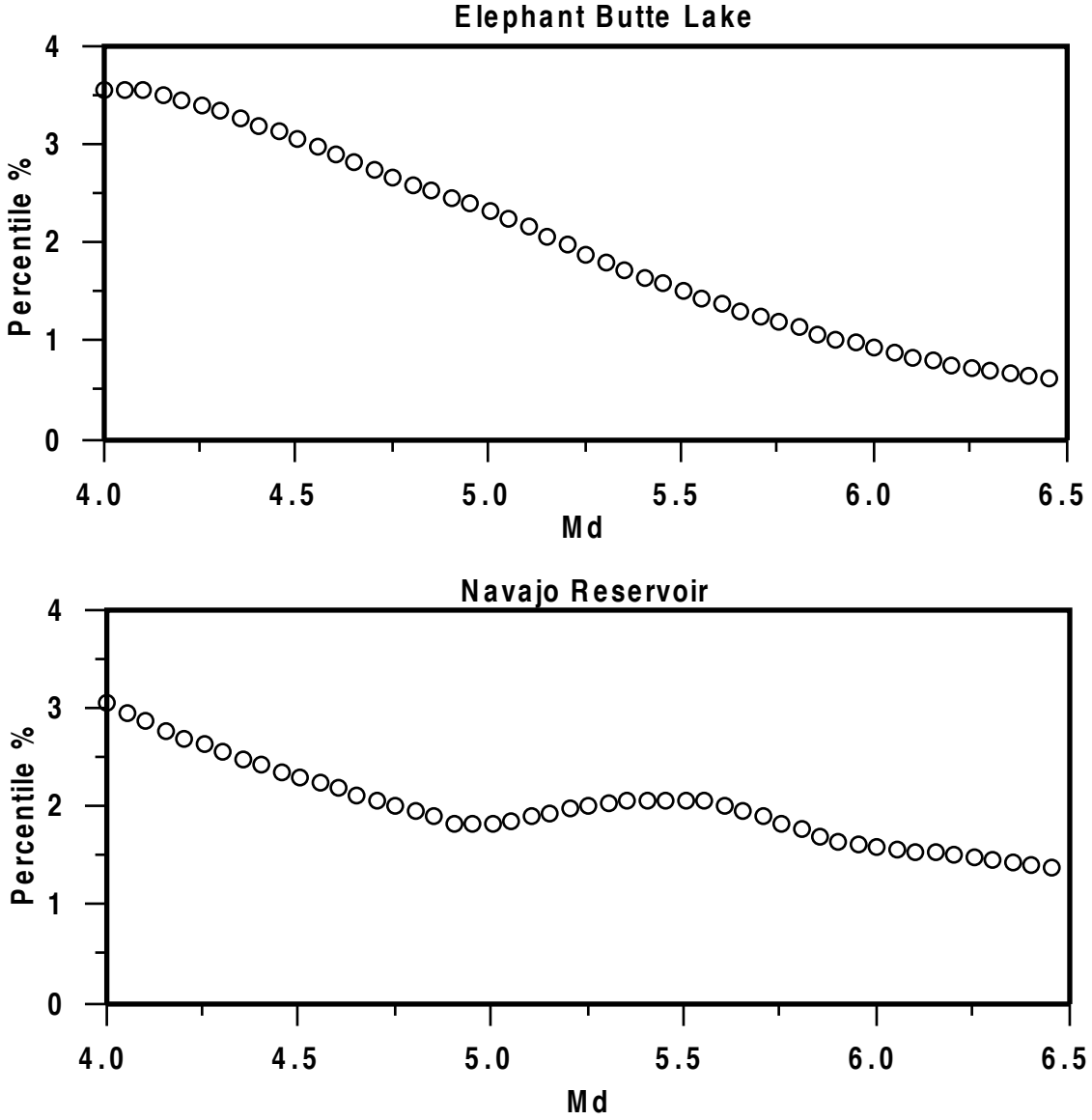

Figure III-12. Distribution of earthquakes at various magnitudes contributing to the seismic hazard estimates for both the Elephant Butte Lake (0.03g) and the Navajo Reservoir (0.04g) areas at 10% probability of exceedance in a 50 year period.

Appendix IV

Published Abstracts

This abstract was written for the Fall 1994 meeting of the American Geophysical Union and is published in EOS, **75** no. **44**.

Estimating Locations of Regional Earthquakes Using a Program Enhanced by a Fuzzy Logic Algorithm

K W Lin and A R Sanford (Both at: Geophysical Research Center, New Mexico Institute of Mining and Technology, Socorro, NM 87801; 505-835-5691; klin@griffy.nmt.edu)
H E Hartse (Los Alamos National Laboratory, MS D-443, Los Alamos, NM 87545; 505-665-8495; hans@seismo5.lanl.gov)

A new method for initial hypocenter estimation of regional earthquakes is introduced into the SEISMOS (Hartse, 1991) location program. Instead of choosing the closest seismic station as the initial epicenter, a fuzzy logic algorithm is used to estimate a preliminary epicenter. The fuzzy logic location is almost independent of crustal structure and finds only the epicentral parameters (origin time is omitted). Thus, calculating partial derivatives of travel time of specific phases with respect to epicentral parameters and the associated forward modeling process are not required.

The fuzzy logic algorithm finds a trial epicenter by checking the consistency between input phases. Four fuzzy sets are used: a travel-distance/arrival-time check of Pg pairs, a travel-distance/arrival-time check of Sg pairs, the Pg and Sg travel-time interval and the travel-time residual checksum. The Centroid defuzzification process is then applied to find the output epicenter, all fuzzy sets are parallel processed. The output epicenter also be expanded or shrunken depending on the applications. Initially, the survey area is fixed at $9x10^6$ km^2 which is divided into a grid of 1600 cells. At each subsequent iteration the survey area is reduced until the grid size is less than 4 km^2 and the final epicenter is reached. This epicenter is then used as a starting model in SEISMOS.

We have tested the fuzzy logic algorithm with synthetic and real world regional data using two seismic networks in the state of New Mexico, one in the central Rio Grande rift, the other surrounding the WIPP site in the southeast corner of the state. These tests clearly demonstrate the increase stability of Fuzzy/SEISMOS program over SEISMOS program alone. Most of the improvement is the result of avoiding local minima. By using the Fuzzy/SEISMOS program, a lower magnitude threshold for locating regional earthquakes is possible.

This abstract was written for the Spring 1995 meeting of the Seismological Society of America and is published in *Seis. Res. Letters*, **66** no. **2**.

A Seismic Anomaly in the Rio Grande Rift Near Socorro, New Mexico

Sanford A.R., and Balch, R.S., Lin, K., Geophysical Research Center and Earth and Environmental Science Department, New Mexico Institute of Mining and Technology, Socorro, NM 87801, sanford@griffy.nmt.edu

Mapping of faults in New Mexico by Machette and others indicates that nearly all surface ruptures with Holocene movement occur within the Rio Grande rift. On the other hand, instrumental monitoring of seismic activity since 1960 has generally shown levels of earthquake activity off the rift that are comparable to those within the rift. The one major exception is an area of relatively intense seismicity near Socorro, New Mexico. From historical as well as instrumental data this ~5500 km^2 area extending ~90 km north-south along the rift (from 33˚ 45' to 34˚ 35') is the most seismically active in the state. Holocene ruptures have been found in this region but none of the earthquake activity in the past 35 years appears to be associated with these faults. During this period most of the earthquakes occurred in swarms on hidden faults at depths of 2.0 to 11.0 km with 88% between 4.0 and 10.0 km. The historical record of earthquakes is also dominated by swarms, some strong. One swarm from July 1906 into early 1907 produced three shocks near magnitude 6, the three strongest earthquakes in New Mexico in the past 125 years. Since 1960 there have been 10 shocks of Md from 4.0 to 4.8 in swarms or extended sequences of earthquakes.

Geodetic measurements straddling the Socorro area seismicity (Savage *et al.*, 1985) established no significant strain accumulations in the region in the 12 year period from 1972 to 1984. One the other hand reveling of elevation benchmarks from 1911 through 1980 in the Socorro area (Larsen *et al.*, 1986) indicates surface uplift coincident with the high seismicity. The high earthquake activity and surface uplift (maximum average 1.8 mm/yr) are roughly centered over a thin (~150 m), extensive (>= 2000 km^2), horizontal layer of magma at a depth of ~19 km. We speculate that the high concentration of earthquake activity and surface uplift in the Socorro area are related to inflation of the mid-crustal magma body. Among a number of observations in possible support of this hypothesis is the existence of an seismic halo surrounding the Socorro seismicity anomaly. Inflation would produce crustal extension in the seismogenic zone above the magma body but crustal compression at the same level along the flanks of the uplift. Extension would enhance seismicity by reducing the normal stress on existing faults whereas compression would have the opposite effect and thus inhibit seismic activity.

This abstract was written for the Fall 1995 meeting of the American Geophysical Union and is published in EOS, **76** no. **44**.

Seismicity Along a Segment of a Prominent ENE Trending Topographic Lineament in New Mexico and West Texas

K W Lin, A R Sanford, I C Tsai and L H Jaksha (All at: Geophysical Research Center, New Mexico Institute of Mining and Technology, Socorro, NM 87801; 505-835-5691; klin@griffy.nmt.edu)

We are in the process of generating a seismicity map for the state of New Mexico and bordering regions, particularly West Texas, for the time period 1962 to the present. Because many epicenters have had to be determined from data obtained by small aperture arrays (<100 km), a special fuzzy-logic subroutine has been incorporated into our location program SEISMOS (Hartse, 1991) to obtain initial estimates of epicenter coordinates and thus avoid local minima. At this time the most accurate hypocenters are found using Pg and Sg arrivals, station corrections and a half space crustal model having a velocity of 6.15 km/sec and a Poisson's ratio of 0.25.

Preliminary locations have been calculated for ~1600 earthquakes with duration magnitudes greater than or equal to 1.3. For the period 1962 through 1994, seismicity was diffusely distributed throughout state with no prominent trends apparent, not even the Rio Grande rift (RGR). The most notable feature on the $M_D \geq 1.3$ seismicity map is a dense cluster of activity in the RGR near Socorro which is believed to be related to inflation of a mid-crustal magma body.

A seismicity map for earthquakes with $M_D \geq 3.0$ (~111 events) from 1962 through 1994 does reveal an interesting alignment of epicenters extending ENE from the cluster of activity near Socorro. Using a Monte Carlo technique, we have determined that this alignment cannot be accidental. The linear distribution of epicenters coincides with a prominent topographic lineation identified by Thelin and Pike (1991) on their digital shaded relief map for the conterminous U.S. The lineation extends from south-central Arizona, through New Mexico and the Texas Panhandle to the Oklahoma border. Included along its path are sections of the Gila and Salt rivers in Arizona, ENE trending basins west of the RGR in New Mexico and the course of the Canadian river in north eastern New Mexico and Texas, Panhandle. Strong historical earthquakes prior to 1962 have occurred along the Canadian river trend in West Texas.

The alignment of topographic features, the seismicity along the same trend, and the existence of a mid-crustal magma body at the intersection of the lineation and the RGR suggest a major ENE crustal flaw which because of its orientation probably predates Laramide and later structures which have northerly orientations.

This abstract was written for the Fall 1997 meeting of the American Geophysical Union and is published in EOS, **78** no. **44**.

Probabilistic Seismic Hazard Estimates for New Mexico Using Instrumental Data from 1962 through 1995

K W Lin, A R Sanford, and I C Tsai (All at: New Mexico Institute of Mining and Technology, Geophysical Research Center and Earth and Environmental Science Dept., Socorro, NM 87801; 505-835-5691; e-mail: klin@griffy.nmt.edu)

We have estimated seismic hazard throughout New Mexico based on 34 years of instrumental data collected from 1962 through 1995. After tests for completeness, our data set contained 865 earthquakes with MD ≥ 2.0; 290 within an ~6000 km2 area located in the central Rio Grande rift. This small region, designated the Socorro Seismic Anomaly (SSA), is one of the two source zones considered in the hazard analysis; the other is the remainder of the state (RNM). Dependent events were removed from the earthquake catalog using time and space windows of 7 days and 4 km for the SSA and 7 days and 25 km for the RNM. The remaining 477 independent earthquakes with MD ≥ 2.0 (133 within the SSA) were used to obtain a universal b for the entire state. For this computation, we assumed a Poisson distribution with upper and lower bound magnitudes of 6.5 and 2.0, and a magnitude bin size of 0.1.

In order to estimate spatial variations in seismic hazard, the state was subdivided into 20 km x 20 km areas. Computational errors that arise when a gridded zone contains no events were avoided by assigning a level of background seismicity for the SSA and RNM equal to 25% of the average observed in each of these two source zones. Therefore, for computation of seismic hazard, the seismicity in each 400 km2 is 75% of the observed level plus 25% of the average level for the source zone (SSA or RNM) in which it is located.

Seismic hazard estimates were obtained by combining the temporal probability of occurrence with the spatial probability of occurrence and a relation between ground acceleration and magnitude (Joyner and Fumal, 1985). Presented below is a map of our estimates of seismic hazard in New Mexico in terms of maximum horizontal ground accelerations with a 10% probability of exceedance in a 50 year period.

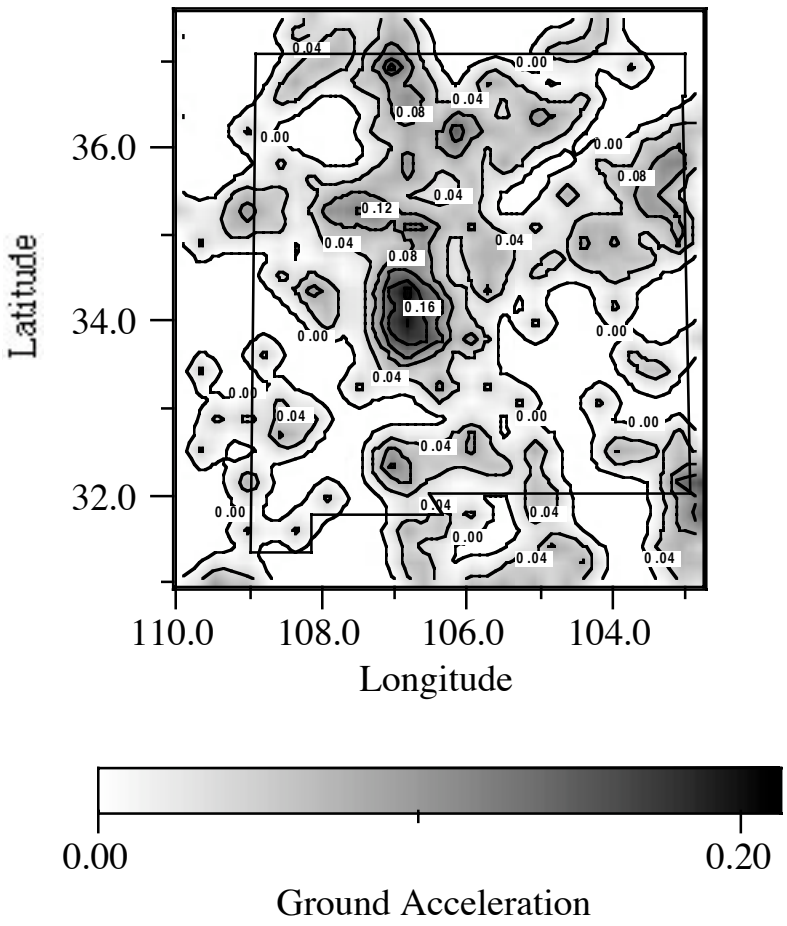
Latitude
36.0
34.0
32.0
110.0
108.0
106.0
104.0
Longitude
0.00
0.20
Ground Acceleration

This abstract was written for the Spring 1998 meeting of the Seismological Society of America and is published in *Seis. Res. Letters*, **69** no. **2**.

Some Sensitivity Studies of Probabilistic Seismic Hazard Estimates for New Mexico

Lin, K.W., Sanford A.R., and Tsai, I.C., Geophysical Research Center and Earth and Environmental Science Department, New Mexico Institute of Mining and Technology, Socorro, NM 87801, klin@griffy.nmt.edu

We have estimated seismic hazard throughout New Mexico using instrumental data collected from 1962 through 1995. Based on the distribution of seismicity, we divided the whole area into two source zones, an ~6000 km2 area located in the central Rio Grande rift which was designated as the Socorro Seismic Anomaly (SSA), and the remainder of the state (RNM). A total of 477 independent earthquakes with MD ≥ 2.0 (133 within the SSA) were used to obtain a universal b for the entire state. For this computation, we assumed a Poisson distribution with upper and lower bound magnitudes of 6.5 and 2.0, and a magnitude bin size of 0.1. We divided the state into 20 km x 20 km areas and evaluated seismic hazards on the basis of these blocks. Seismic hazard estimates were obtained by combining the temporal probability of occurrence with the spatial probability of occurrence and a relation between ground acceleration and magnitude (Joyner and Fumal, 1985). Results have been presented in the format of maximum horizontal ground accelerations at 10% probability of exceedance in a 50 year period. We have determined variations in these seismic hazard estimates arising from uncertainties in (1) the fitted slope b and (2) the maximum magnitude earthquake assumed in the recurrence relationship. The variation of the fitted slope b for the whole area, 0.6675±0.0314 (1 s.d.), resulted in minimal changes on the level of seismic hazard estimates. For example, the highest level of estimated ground acceleration for the entire area ranged only ±0.006g (1 s.d.) from a mean value of 0.212g. Changes in maximum magnitudes had larger but still moderate effects on the overall estimates of seismic hazard. The decrease in the highest level of seismic hazard obtained by reducing the maximum magnitude from 6.5 to 6.0 was -0.009g and the increase in hazard by increasing the maximum magnitude to 8.0 was +0.04g.

We have examined the effects of incorporating pre-instrumental data from 1860 through 1961 on seismic hazard estimates for the SSA. The fitted slope b derived from the pre instrumental catalog for the SSA yielded a slighter lower value, 0.6454, than that obtained from the instrumental data but within the range of the first standard deviation. The cumulative number of events N at magnitude 4.0, the starting magnitude for seismic hazard estimates, in the recurrence model also showed only ~7% changes between the two models. Thus no drastic changes in hazard estimates are expected by including pre instrumental data into the evaluation process.

This abstract was written for the Fall 1998 meeting of the American Geophysical Union and is published in EOS, **79** no. **45**.

Improving Locations of Regional Earthquakes Using a Modified *G* Matrix

K W Lin, and A R Sanford (both at: New Mexico Institute of Mining and Technology, Geophysical Research Center and Earth and Environmental Science Dept., Socorro, NM 87801; 505-835 5691; e-mail: klin@griffy.nmt.edu)

We use a modified *G* matrix containing S-P time intervals and P-P and S-S time intervals and a forward method in solving locations for regional earthquakes. Unlike the regular *G* matrix which consists of three spatial parameters (x, y, z) and one timing parameter (t), the modified *G* matrix contains only two spatial parameters (x, y) and a fixed depth (z). Locations for regional earthquakes are resolved by a grid search during the forward modelling process.

Typical problems associated with locating regional earthquakes are less accurate arrival times, less accurate velocity model and less stable *G* matrix. As a result, for a small aperture array, parameters of the epicenter (x, y) are highly dependent on the origin time parameter in the *G* matrix. Common methods like the generalized inverse method, which were originally designed for locating local earthquakes, tend to fail when no clear minima exists.

In our approach, we purposely eliminate the origin time parameter by using only relative time intervals. In the new *G* matrix, two base equations instead of one are used. The S-P time intervals constrain travel distance and P-P and S-S time intervals constrain the distribution of azimuth for an earthquake. In searching for locations of earthquakes, we first divide the modified *G* matrix based on individual time intervals and map deviations between theoretical and observed time intervals into logic space using the fuzzy logic technique. Resolutions of earthquake locations are enhanced in the logic space by applying logic operations among individual *G* matrices and the final locations are derived by search for a center of gravity in the output matrix.

Our test results indicate that the forward method is more tolerate of errors than the inverse method. For applications like the automated earthquake location process, which often contains errors in determining arrival phases, this method is likely to be beneficial.

This abstract was written for the Fall 1998 meeting of the American Geophysical Union and is published in EOS, **79** no. **45**.

Evidence for a 1400 Km Long Socorro Fracture Zone

A R Sanford and K W Lin (both at New Mexico Institute of Mining and Technology, Geophysical Research Center and Earth and Environmental Science Department, Socorro, NM 87801; 505-835-5212;e-mail: sanford@krach.nmt.edu)

We define the Socorro Fracture Zone (SFZ) as an approximately 70 km wide and 1400 km long ENE trending crustal lineament extending from southwestern Arizona through New Mexico and across the Texas Panhandle to the Oklahoma border. The observations we present in support of the existence of the SFZ are summarized below:

1. On their digital shaded relief map of the contiguous U.S., Thelin and Pike (1991) called special attention to a prominent topographic lineation that extends ENE from SW Arizona to the eastern border of the Texas Panhandle.
2. A map of instrumentally determined epicenters of earthquakes with magnitudes greater or equal to 3.0 for the period 1962 through July 1998 reveals a conspicuous band of seismicity that straddles the track of the topographic lineation from the Rio Grande Rift (RGR) near Socorro through eastern New Mexico and into the Texas Panhandle.
3. The SFZ has a gravity signature over much of its extent in low sun angle maps of Bouguer anomalies and surface deflections of the vertical; maps that have sun azimuths normal or near normal to the strike of the SFZ.
4. The SFZ intersects the RGR where its morphology undergoes a major change. To the north the rift is composed primarily of narrow NS trending basins in a right-stepping pattern. Immediately to the south of the SFZ the rift widens rather abruptly into a series of adjacent NS trending tilted basins and horst-blocks which collectively appear to require more extension than to the north.
5. West-southwest from the RGR along the track of the topographic lineation for a distance of 160 km are mapped faults with ENE and NE strikes, in marked contrast to the dominantly NS structural grain of the rift.
6. The SFZ fairly closely parallels the well-known Jemez lineament which is 150 km to the north and is defined by an ENE alignment of volcanic centers extending nearly border to border in northern New Mexico. The very large Jemez volcano is located at the intersection of the lineament and the RGR. The Socorro Magma Body, a 19 km deep, 3500 square km, mostly thin (about 150 m) magma body, is located at the intersection of the SFZ and the RGR.

This abstract was written for the Spring 1999 meeting of the Seismological Society of America and is published in *Seis. Res. Letters*, **70** no. **2**.

Historical Seismicity of New Mexico-1869 through 1998

SANFORD, A.R., LIN, K.W., JAKSHA, L.H., and TSAI, I.C. Department of Earth and Environmental Science, and Geophysical Research Center, New Mexico Institute of Mining and Technology, Socorro, NM 87801, sanford@krach.nmt.edu.

We have prepared a 30 x 32 inch map sheet with text that summarizes our investigations of the historical seismicity of New Mexico. The principal map of this document shows locations and strengths of New Mexico earthquakes obtained from instrumental data gathered from 1962 through 1998. A smaller map depicts the quality of the instrumental locations. Also presented is a seismic hazard map based on the 37 years of instrumental recording. The data base for these three maps is a New Mexico Tech catalog of over 2000 earthquakes (1962-1998) with magnitudes of 1.3 or greater. The catalog is a collation of data from New Mexico Tech (79%), Los Alamos National Laboratory (13%), U.S. Geological Survey (7%), and the University of Texas-El Paso (1%) with a major effort made to have all magnitudes tied to a single New Mexico scale based on duration. Tests made on the catalog indicate that a lower cutoff magnitude of 2.0 assures completeness of data over the entire 37 year period and therefore maps appearing on our map sheet are from a listing of 581 earthquakes of magnitude 2.0 or greater derived from the general catalog. Augmenting the three maps based solely on instrumental data is a map and table of the 30 earthquakes exceeding magnitude 4.5 from 1869 through 1998. For the period preceding 1962, reported maximum intensities were converted to magnitudes using a relation derived from New Mexico earthquakes. Procedures used in generating all the seismicity maps are presented in the text of the map sheet. Also discussed in the text are characteristics of the distribution and strength of earthquakes and the levels of risk throughout the state. Among the prominent features reviewed is a tight cluster of earthquakes in the Rio Grande rift at Socorro that occupies1.6% of the total area of the state but accounts for about 40% of the seismicity.

This dissertation is accepted on behalf of the faculty of the Institute by the following committee

Allan R. Sanford
Adviser

Richard C Gutierrez

David W. Love

Lawrence W. Teufel

October 20, 1999
Date

I release this document to New Mexico Institute of Mining and Technology.

Kaiwan Lin 10/20/99

Student's Signature Date